UNIVERSIDAD DE OVIEDO

Departamento de Ingeniería Química y Tecnología del Medio Ambiente

Programa Oficial de Doctorado en Ingeniería Química, Ambiental y Bioalimentaria

Síntesis de nanopartículas y nanocompuestos con base de almidón para bioaplicaciones / Synthesis of starch-based nanoparticles and nanocomposites for bioapplications

DIANA MORÁN TUYA

2024

RESUMEN DEL CONTENIDO DE TESIS DOCTORAL

1.- Título de la Tesis	
Español/Otro Idioma: Síntesis de nanopartículas y nanocompuestos con base de almidón para bioaplicaciones	Inglés: Synthesis of starch-based nanoparticles and nanocomposites for bioapplications

2.- Autor	
Nombre: Diana Morán Tuya	
Programa de Doctorado: Programa Oficial de Doctorado en Ingeniería Química, Ambiental y Bioalimentaria	
Órgano responsable: Centro Internacional de Postgrado	

RESUMEN (en español)

La mejora de la salud humana, animal y la preservación del Medio Ambiente son aspectos fundamentales objeto de investigación a nivel mundial. Estos han sido agrupados en el término One Health definido a inicios del año 2000 y el cual ha captado especial atención a partir del año 2020, en donde ha quedado clara la evidencia de la interdependencia entre la salud humana, animal y el ecosistema en el cual conviven. Dichos aspectos quedan recogidos en varios de los Objetivos de Desarrollo Sostenible planteados en la agenda 2030 por la Asamblea General de las Naciones Unidas y en los pilares de investigación definidos en Horizonte Europa por la Unión Europea.

En este sentido surge la necesidad del desarrollo y diseño de nanomateriales avanzados sostenibles que permiten realizar un uso más eficaz de los antibióticos o principios activos requeridos para la prevención o el tratamiento de enfermedades producidas por diferentes causas, como puede ser infecciones bacterianas, preservando a su vez el Medio Ambiente.

La infección bacteriana patógena es una de las causas de enfermedades graves en todo el mundo. Las biopelículas o biofilms son comunidades de microorganismos que crecen en cualquier superficie y pueden llegar a ser mil veces más resistentes a los antibióticos. La resistencia antimicrobiana asociada es actualmente un gran problema económico y sanitario a escala mundial y una de las mayores preocupaciones de la UE debido a los graves problemas que puede provocar en diversos entornos industriales, agrícolas o sanitarios entre otros. Es por esto por lo que la eliminación de estas bacterias y sus biopelículas es esencial para una gran cantidad de industrias.

Por otra parte, el almidón es un polisacárido ampliamente utilizado en numerosas aplicaciones debido a las atractivas propiedades que posee, tales como su biocompatibilidad, biodegradabilidad, bajo coste, además de que se trata de un polímero natural, renovable y se puede encontrar fácilmente en la naturaleza.

En este contexto, el objetivo de esta tesis doctoral plantea el diseño de nanomateriales basados en almidón susceptibles de ser utilizados en diversas bioaplicaciones. La encapsulación de compuestos activos en sistemas coloidales de tamaño controlado permitirá, por un lado, que se dirijan de manera controlada al sitio de interés, evitando así afectos secundarios, al tiempo que se preservan las propiedades tanto físicas como químicas del compuesto, aumentando así su efectividad.

Por esto, se sintetizaron nanopartículas de almidón (SNPs) empleando distintos métodos de síntesis y utilizando almidones con distinto origen botánico. Un aspecto muy importante a tener en cuenta es el control sobre el tamaño y la forma final de las partículas, ya que, en función de la aplicación en la que vayan a ser utilizadas se requerirá un tamaño u otro.

El primer paso fue encontrar los parámetros óptimos de síntesis con los cuales se pudieran obtener SNPs esféricas. Se compararon los métodos de nanoprecipitación y microemulsion (ME) para las síntesis y se estudiaron la velocidad de inyección, la proporción entre fase orgánica y acuosa, así como el efecto de la proporción de amilosa y amilopectina en el almidón, entre otros. Por otro lado, también se analizó la viabilidad de crear nanocompuestos híbridos de almidón conteniendo nanopartículas magnéticas mediante el método de ME. Previamente se estudiaron diferentes formulaciones para la preparación de microemulsiones agua en aceite (W/O) variando la proporción entre fase orgánica y acuosa y la concentración de los co-estabilizantes. Las mejores formulaciones se utilizaron para sintetizar de manera simultánea SNPs y nanopartículas de óxido de hierro con propiedades superparamagnéticas.

Una vez seleccionados los parámetros óptimos y el método de síntesis para preparar SNPs de tamaño controlado, se estudió como podrían afectar ciertas modificaciones químicas de los almidones a la forma y el tamaño final de las SNPs. En este caso se sintetizaron SNPs con almidones de amaranto, quinoa y arroz modificados por un lado con anhidrido octenil succínico (OSA) y por otro con ácidos grasos de cadena corta (SCFA), en ambos casos con distintos grados de modificación. Todas las SNPs obtenidas fueron caracterizadas en términos de morfología, tamaño, monodispersidad, estructura molecular y cristalinidad.

Finalmente, se evaluó la eficiencia de inhibición de bacterias susceptibles de crear biopelículas estudiando el efecto antimicrobiano de distintos compuestos cargados en las SNPs. Por un lado, se sintetizaron SNPs cargadas con vainillina y se determinó su eficacia contra *Escherichia coli* (*E. coli*) y por otro se sintetizaron nanopartículas hibridas de almidón y plata (Ag-SNPs) determinando su eficacia contra *E. coli,* así como contra *Staphylococcus aureus* (*S. aureus*).

RESUMEN (en Inglés)

The improvement of human and animal health and the preservation of the environment are key areas of research worldwide. These have been grouped under the term One Health, defined at the beginning of the year 2000 and which has attracted special attention since 2020, where the interdependence between human and animal health and the ecosystem where they coexist has become clear. These aspects are included in many of the Sustainable Development goals set out in the 2030 Agenda by the United Nations General Assembly and in the research pillars defined in Horizon Europe by the European Union.

In this sense, there is a need to develop and design sustainable advanced nanomaterials that allow a more effective use of antibiotics or active ingredients required for the prevention or treatment of diseases caused by various reasons, such as bacterial infections, while preserving the environment.

Pathogenic bacterial infections are a major cause of serious disease worldwide. Biofilms are communities of microorganisms that grow on any surface and can become thousands of times more resistant to antibiotics. Associated antimicrobial resistance is currently a major global health and economic problem and a major concern for the EU because of the serious problems it can cause in many industrial, agricultural, healthcare and other settings. Therefore, the elimination of these bacteria and their biofilms is essential for a wide range of industries.

On the other hand, starch is a polysaccharide that is widely used in many applications due to its attractive properties such as biocompatibility, biodegradability, low cost and the fact that it is a natural, renewable polymer that is readily found in nature.

In this context, the aim of this thesis is to design starch-based nanomaterials that can be used in different bioapplications. The encapsulation of agents in colloidal systems of controlled size will allow them to be targeted to the site of interest in a controlled manner, thus avoiding side effects, while at the same time preserving the physical and chemical properties of the compound, thus increasing its efficacy.

Therefore, starch nanoparticles (SNPs) have been synthesized using different synthesis methods and starches of different botanical origin. A very important point to consider is the control over the size and final shape of the particles, as one size or another will be required depending on the application in which they will be used.

The first step was to find the optimal synthesis parameters to obtain spherical SNPs. Nanoprecipitation and microemulsion (ME) methods were compared for the syntheses, and the injection rate, the ratio of organic to aqueous phase and the effect of the ratio of amylose to amylopectin in the starch were studied, among others.

On the other hand, the feasibility of preparing hybrid starch nanocomposites containing magnetic nanoparticles by the ME method was also investigated. Previously, different formulations for the preparation of water in oil (W/O) microemulsions were studied by varying the ratio between organic and aqueous phases and the concentration of co-stabilisers. The best formulations were used for the simultaneous synthesis of SNPs and iron oxide nanoparticles with superparamagnetic properties.

Once the optimal parameters and synthesis method for preparing size-controlled SNPs had been selected, the effect of certain chemical modifications of the starch on the final shape and size of the SNP was investigated. In this case, SNPs were synthesised with amaranth, quinoa and rice starches modified with octenyl succinic anhydride (OSA) and short chain fatty acids (SCFA), in each case with different degrees of modification. All the SNPs obtained were properly characterized in terms of morphology, size, monodispersity, molecular structure and crystallinity.

Finally, the inhibition efficacy of bacteria susceptible to biofilm formation was evaluated by studying the antimicrobial activity of different compounds loaded on the SNPs. On the one hand, vanillin-loaded SNPs were synthesized and their efficacy against *Escherichia coli* (*E. coli*) was determined, and on the other hand, hybrid starch-silver nanoparticles (Ag-SNPs) were synthesized and their efficacy against *E. coli* and *Staphylococcus aureus* (*S. aureus*) was determined.

SR. PRESIDENTE DE LA COMISIÓN ACADÉMICA DEL PROGRAMA DE DOCTORADO EN INGENIERÍA QUÍMICA, AMBIENTAL Y BIOALIMENTARIA

Agradecimientos

En primer lugar, quiero expresar mi mas profundo agradecimiento a mis directoras de tesis, Gemma y María, han sido mis guías no solo durante estos años de tesis, si no desde que decidí hacer el TFG con ellas. No tengo palabras para expresar las mujeres maravillosas que son y lo que me han enseñado a lo largo de los años. Confiaron y apostaron por mi desde el primer momento y las admiro por todo el trabajo duro que realizan y todo lo que han conseguido. También me fascina su bonita amistad y la admiración que tienen la una por la otra.

Gracias también a mi grupo de investigación NANOBIOMEM dirigido por Carmen Blanco López, con una mención especial a Esther y Alberto por ayudarme en todo lo que pudieron siempre que les preguntaba.

Quisiera expresar mi gratitud a Gerardo Palazzo por abrirme las puertas de su grupo durante mi estancia de tres meses en la Universidad de Bari en Italia, y en especial a mi amiga Helena, que supervisó en todo momento mi trabajo allí y fue una suerte poder tenerla durante ese tiempo. También quiero agradecer a Rafael Gavara por acogerme en su grupo de investigación del Instituto de Agroquímica y Tecnología de Alimentos (IATA), aunque fuera una estancia breve fue una experiencia muy gratificante, gracias a Grace, Carol, Lauri y todos los demás compañeros con los que pude compartir ese mes.

A mi Clarita, recuerdo nuestra primera conversación “hola, ¿puedo subir a verte y me dices cómo sintetizas las SNPs?”. La verdad que echando la vista atrás ya no recuerdo un día que no hayamos estado mano a mano, en las buenas y en las malas, porque habrá sido por dramas con el almidón… Siempre nos hemos considerado como MM y GG, un equipo, es tan fácil complementarnos la una a la otra, ella mi química y yo su ingeniera, yo con soluciones “chanchulleras” y ella tan analítica y buscando razones a todo.

A Ro, aunque este último año haya sido difícil verla ya que vive corriendo por los pasillos (confieso que a mi tampoco se me da mal) y si tienes suerte ves un destello morado a lo lejos. Siempre ha estado para mí desde el primer día que empezó sus prácticas. Es de esas personas que dejaría todo lo que está haciendo si necesitas ayuda, aunque eso implique salir más tarde y llegar a su casa a las mil.

Gracias a toda la gente que he conocido durante estos años, desde los técnicos del departamento (mención especial a Cris por todo lo que me ayudo este último año) hasta las personas de la cafetería, con todos ellos al final terminé entablando una bonita amistad con el paso de los años. También a Sandra, la forastera de la primera planta que un día decidió comer con nosotras y que, aunque solo compartiéramos el ratito de la comida cada día, se convirtió en una amiga con la que poder contar.

Al que más tengo que agradecer es a mi padre, sin él no estaría donde estoy, literalmente, recuerdo cuando le pedí consejo sobre la elección de mi TFG y me dijo “esas nanopartículas de almidón tienen futuro, vete a por ellas” y ya ves donde hemos llegado, ¡¡vaya si tenían futuro!! Mi papá siempre ha sido mi mayor inspiración y aunque no haya podido estar presente en muchas ocasiones, siempre conseguía sacar un ratito para escuchar mis dramas o mis logros. Siempre me decía que no entendía nada de lo que le contaba, pero él aún así me escuchaba emocionado o me aconsejaba como buenamente podía.

También a mis abuelitos, aunque nunca terminaron de entender lo que hacía y mi abuela me sigue preguntando a día de hoy que como me van los exámenes, se que siempre me han apoyado en todo, y que, aunque mi abuelito no va a poder verme oficialmente como doctora, se que haya donde esté está muy orgulloso de mí.

Mi Senén, a él intenté arrastrarle al mundo de las nanopartículas y durante un ratito si que lo conseguí, pero no hubo manera de retenerlo. Aún así él ha sido el que más cambios de humor ha tenido que soportar, porque chico sacar una tesis adelante no es fácil y menos mal que él sabía cómo manejarme. Gracias también a su familia por todo el apoyo que me dan siempre en esto y en todo lo demás.

Creo que es importante agradecerme también a mi misma, por haber trabajado tantísimo para llegar hasta aquí y sobretodo, por haberlo conseguido.

Cierro esta etapa con lágrimas en los ojos, agradecida por todo lo aprendido y abro la puerta a lo que esté por venir, con miedo e incertidumbre, pero con muchas, muchas ganas.

INDEX OF CONTENTS

Resumen

La mejora de la salud humana, animal y la preservación del Medio Ambiente son aspectos fundamentales objeto de investigación a nivel mundial. Estos han sido agrupados en el término One Health definido a inicios del año 2000 y el cual ha captado especial atención a partir del año 2020, en donde ha quedado clara la evidencia de la interdependencia entre la salud humana, animal y el ecosistema en el cual conviven. Dichos aspectos quedan recogidos en varios de los Objetivos de Desarrollo Sostenible planteados en la agenda 2030 por la Asamblea General de las Naciones Unidas y en los pilares de investigación definidos en Horizonte Europa por la Unión Europea.

En este sentido surge la necesidad del desarrollo y diseño de nanomateriales avanzados sostenibles que permiten realizar un uso más eficaz de los antibióticos o principios activos requeridos para la prevención o el tratamiento de enfermedades producidas por diferentes causas, como puede ser infecciones bacterianas, preservando a su vez el Medio Ambiente.

La infección bacteriana patógena es una de las causas de enfermedades graves en todo el mundo. Las biopelículas o biofilms son comunidades de microorganismos que crecen en cualquier superficie y pueden llegar a ser mil veces más resistentes a los antibióticos. La resistencia antimicrobiana asociada es actualmente un gran problema económico y sanitario a escala mundial y una de las mayores preocupaciones de la UE debido a los graves problemas que puede provocar en diversos entornos industriales, agrícolas o sanitarios entre otros. Es por esto por lo que la eliminación de estas bacterias y sus biopelículas es esencial para una gran cantidad de industrias.

Por otra parte, el almidón es un polisacárido ampliamente utilizado en numerosas aplicaciones debido a las atractivas propiedades que posee, tales como su biocompatibilidad, biodegradabilidad, bajo coste, además de que se trata de un polímero natural, renovable y se puede encontrar fácilmente en la naturaleza.

En este contexto, el objetivo de esta tesis doctoral plantea el diseño de nanomateriales basados en almidón susceptibles de ser utilizados en diversas bioaplicaciones. La encapsulación de compuestos activos en sistemas coloidales de tamaño controlado permitirá, por un lado, que se dirijan de manera controlada al sitio de interés, evitando así afectos secundarios, al tiempo que se preservan las propiedades tanto físicas como químicas del compuesto, aumentando así su efectividad.

Por esto, se sintetizaron nanopartículas de almidón (SNPs) empleando distintos métodos de síntesis y utilizando almidones con distinto origen botánico. Un aspecto muy importante a tener en cuenta es el control sobre el tamaño y la forma final de las partículas, ya que, en función de la aplicación en la que vayan a ser utilizadas se requerirá un tamaño u otro.

El primer paso fue encontrar los parámetros óptimos de síntesis con los cuales se pudieran obtener SNPs esféricas. Se compararon los métodos de nanoprecipitación y microemulsión (ME) para las síntesis y se estudiaron la velocidad de inyección, la proporción entre fase orgánica y acuosa, así como el efecto de la proporción de amilosa y amilopectina en el almidón, entre otros.

Por otro lado, también se analizó la viabilidad de crear nanocompuestos híbridos de almidón conteniendo nanopartículas magnéticas mediante el método de ME. Previamente se estudiaron diferentes formulaciones para la preparación de microemulsiones agua en aceite (W/O) variando la proporción entre fase orgánica y acuosa y la concentración de los co-estabilizantes. Las mejores formulaciones se utilizaron para sintetizar de manera simultánea SNPs y nanopartículas de óxido de hierro con propiedades superparamagnéticas.

Una vez seleccionados los parámetros óptimos y el método de síntesis para preparar SNPs de tamaño controlado, se estudió como podrían afectar ciertas modificaciones químicas de los almidones a la forma y el tamaño final de las SNPs. En este caso se sintetizaron SNPs con almidones de amaranto, quinoa y arroz modificados por un lado con anhidrido octenil succínico (OSA) y por otro con ácidos grasos de cadena corta (SCFA), en ambos casos con distintos grados de modificación. Todas las SNPs obtenidas fueron caracterizadas en términos de morfología, tamaño, monodispersidad, estructura molecular y cristalinidad.

Finalmente, se evaluó la eficiencia de inhibición de bacterias susceptibles de crear biopelículas estudiando el efecto antimicrobiano de distintos compuestos cargados en las SNPs. Por un lado, se sintetizaron SNPs cargadas con vainillina y se determinó su eficacia contra *Escherichia coli* (*E. coli*) y por otro se sintetizaron nanopartículas hibridas de almidón y plata (Ag-SNPs) determinando su eficacia contra *E. coli,* así como contra *Staphylococcus aureus* (*S. aureus*).

Abstract

The improvement of human and animal health and the preservation of the environment are key areas of research worldwide. These have been grouped under the term One Health, defined at the beginning of the year 2000 and which has attracted special attention since 2020, where the interdependence between human and animal health and the ecosystem where they coexist has become clear. These aspects are included in many of the Sustainable Development goals set out in the 2030 Agenda by the United Nations General Assembly and in the research pillars defined in Horizon Europe by the European Union.

In this sense, there is a need to develop and design sustainable advanced nanomaterials that allow a more effective use of antibiotics or active ingredients required for the prevention or treatment of diseases caused by various reasons, such as bacterial infections, while preserving the environment. Pathogenic bacterial infections are a major cause of serious disease worldwide. Biofilms are communities of microorganisms that grow on any surface and can become thousands of times more resistant to antibiotics. Associated antimicrobial resistance is currently a major global health and economic problem and a major concern for the EU because of the serious problems it can cause in many industrial, agricultural, healthcare and other settings. Therefore, the elimination of these bacteria and their biofilms is essential for a wide range of industries.

On the other hand, starch is a polysaccharide that is widely used in many applications due to its attractive properties such as biocompatibility, biodegradability, low cost and the fact that it is a natural, renewable polymer that is readily found in nature.

In this context, the aim of this thesis is to design starch-based nanomaterials that can be used in different bioapplications. The encapsulation of agents in colloidal systems of controlled size will allow them to be targeted to the site of interest in a controlled manner, thus avoiding side effects, while at the same time preserving the physical and chemical properties of the compound, thus increasing its efficacy.

Therefore, starch nanoparticles (SNPs) have been synthesized using different synthesis methods and starches of different botanical origin. A very important point to consider is the control over the size and final shape of the particles, as one size or another will be required depending on the application in which they will be used.

The first step was to find the optimal synthesis parameters to obtain spherical SNPs. Nanoprecipitation and microemulsion (ME) methods were compared for the syntheses, and the injection rate, the ratio of organic to aqueous phase and the effect of the ratio of amylose to amylopectin in the starch were studied, among others.

On the other hand, the feasibility of preparing hybrid starch nanocomposites containing magnetic nanoparticles by the ME method was also investigated. Previously, different formulations for the preparation of water in oil (W/O) microemulsions were studied by varying the ratio between organic and aqueous phases and the concentration of co-stabilisers. The best formulations were used for the simultaneous synthesis of SNPs and iron oxide nanoparticles with superparamagnetic properties.

Once the optimal parameters and synthesis method for preparing size-controlled SNPs had been selected, the effect of certain chemical modifications of the starch on the final shape and size of the SNP was investigated. In this case, SNPs were synthesised with amaranth, quinoa and rice starches modified with octenyl succinic anhydride (OSA) and short chain fatty acids (SCFA), in each case with different degrees of modification. All the SNPs obtained were properly characterized in terms of morphology, size, monodispersity, molecular structure and crystallinity.

Finally, the inhibition efficacy of bacteria susceptible to biofilm formation was evaluated by studying the antimicrobial activity of different compounds loaded on the SNPs. On the one hand, vanillin-loaded SNPs were synthesized and their efficacy against *Escherichia coli* (*E. coli*) was determined, and on the other hand, hybrid starch-silver nanoparticles (Ag-SNPs) were synthesized and their efficacy against *E. coli* and *Staphylococcus aureus* (*S. aureus*) was determined.

1. INTRODUCTION

CHAPTER 1 - Introduction

1.1. Background

In the last decades, scientific research has made significant progress in the development of novel and efficient materials with nanotechnological applications, as well as in the acquisition of new sustainable products from renewable raw materials [1].

In this respect, the considerable versatility of starch makes it a potential candidate for the development of highly efficient and value-added biomaterials in many fields, particularly for the delivery of active compounds in the biomedical field. This is because starch-based materials can be easily adapted to many applications by using them as templates into which specific compounds are introduced [2]. For this reason, starch nanoparticles (SNPs) are considered to be novel and promising sustainable biomaterials for use in many bioapplications [3].

Starch is one of the most widely used polymers due to its unique properties such as biodegradability and biocompatibility with the environment, it is also a natural and renewable source, and it is low cost. It is considered as the second most abundant biomass material in nature after cellulose and can be found as a primary source of energy storage in the form of carbohydrate in all chlorophyll-containing plants [4].

The molecular structure of starch is mainly composed of two molecules of different nature, amylose and amylopectin, both of which are composed of glucose units, although the latter is generally more abundant. Amylose is an amorphous linear molecule composed mainly of glucose units linked by α-(1-4) linkages [5], although some molecules are slightly branched by α-(1-6) linkages [6], so most starches are a mixture of linear and branched amyloses. Amylopectin is a crystalline and highly branched molecule and α-(1-4) and α-(1-6) linkages can be found in the glucose units. Figure 1.1 shows a schematic representation of these two molecules.

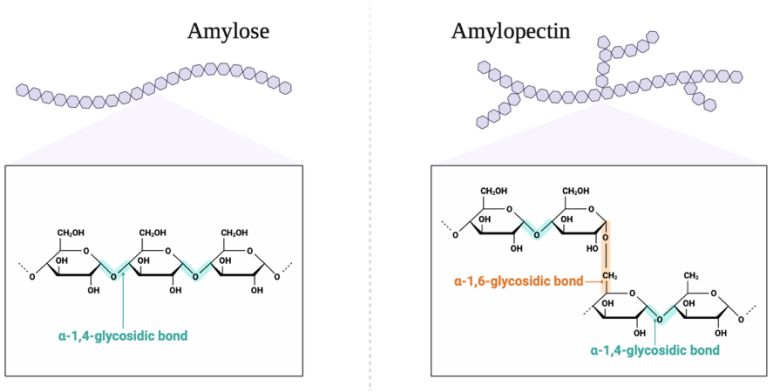

Figure 1.1. *Molecular structure of amylose and amylopectin, the main components of starch. Created with Biorender*

In addition to the major components, starch granules may also contain minor components such as proteins, lipids or phosphate groups found in low amount. The presence of these secondary components, together with the amylose/amylopectin ratio and the relationship between them, defines the resulting physical properties [5, 6].

In terms of granular structure, starch granules are partially crystalline and produce X-ray diffraction patterns that can be classified as type A, B or C. The difference between them is based on the double helix packing of which the starch granules are composed. Type A crystallinity consists of a highly packed structure with water molecules between each double helix structure, whereas type B crystallinity has a less packed structure with water molecules in a central cavity formed by six double helixes as can be seen in Figure 1.2.

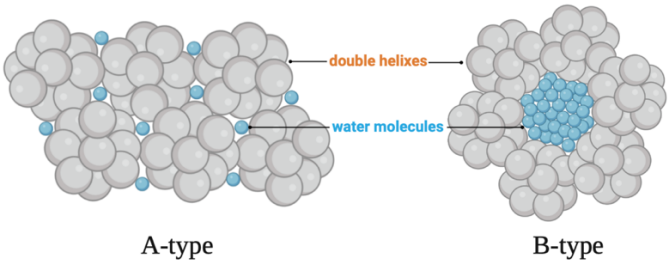

Figure 1.2. *Diagram for packing configuration of double helixes and water molecules in starch granules A-type and B-type. Created with Biorender*

On the other hand, type C crystallinity is considered a mixture of types A and B, as its X-ray diffraction pattern is a combination of them, with type A around the granule and type B inside [1].

Finally, there is also a V-type crystallinity pattern which results from complexes formed between the amylose and other possible substances such as fatty acids, alcohols or emulsifiers [7].

Nowadays, the field of nanoparticles is experiencing a huge expansion in terms of scientific research due to their potential applications in many sectors such as medicine, food packaging or cosmetics, among others. Depending on their nature, nanoparticles can be classified into many categories such as organic, inorganic, combined organic/inorganic or surface modified nanoparticles [8]. However, biomaterial-based nanoparticles, such as polysaccharides, lipids, proteins, minerals and surfactants, are of increasing interest [9]. In this sense, SNPs are of particular interest because of the properties of starch as mentioned above. SNPs are obtained by breaking down starch granules using many synthesis methods.

In general, there are two ways to obtain nanoparticles, depending on the raw material, called top-down and bottom-up approaches. The top-down approach refers to all the synthesis methods in which nanoparticles are obtained from a voluminous material or with a size of microns that is divided or aggregated from a material with nanometric size. Some common top-down approaches are lithography, laser ablation or hydrolysis. On the other hand, the bottom-up approach includes the processes in which primary nuclei of small size are formed by the assembly of atoms or molecules by thermodynamic means [3]. In this case, microemulsion (ME) and nanoprecipitation methods stand out. Figure 1.3 shows a schematic representation of obtaining nanoparticles using the top-down and bottom-up approaches.

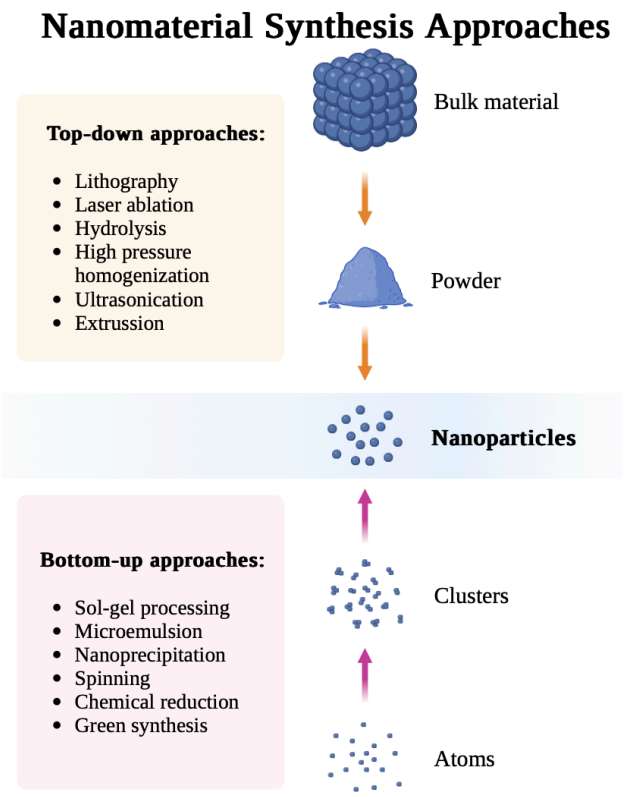

Figure 1.3. *Schematic representation of the top-down and bottom-up approaches to nanoparticles obtention. Created with Biorender*

In recent decades, SNPs have attracted much attention due to their unique properties and wide range of applications. SNPs have found novel applications in many food systems, being used as food additives [1] or food flavor binders [10], reinforcing materials in nanocomposites [11, 12], emulsion stabilizers [13-16]. At the same time, SNPs can also be used as plastic fillers [17, 18], implant materials [19] or in wastewater treatment [20].

However, among the many applications of SNPs, their use in bioapplications should be highlighted. SNPs are considered as a good carrier to improve the controlled release of many drugs and at the same time they have many applications in fields as diverse as medicine, cosmetics, biotechnology or food industry. Therefore, it can be concluded that SNPs are a safe and efficient tool for the delivery and controlled release of various biocompounds.

References

[1] D. Le Corre, J. Bras, and A. Dufresne, "Starch nanoparticles: A review," *Biomacromolecules*, vol. 11, no. 5. pp. 1139–1153, May 10, 2010. doi: 10.1021/bm901428y.

[2] R. Sarder *et al.*, "Copolymers of starch, a sustainable template for biomedical applications: A review," *Carbohydr Polym*, vol. 278, p. 118973, Feb. 2022, doi: 10.1016/j.carbpol.2021.118973.

[3] H. Y. Kim, S. S. Park, and S. T. Lim, "Preparation, characterization and utilization of starch nanoparticles," *Colloids and Surfaces B: Biointerfaces*, vol. 126. Elsevier, pp. 607–620, Feb. 01, 2015. doi: 10.1016/j.colsurfb.2014.11.011.

[4] Q. Sun, H. Fan, and L. Xiong, "Preparation and characterization of starch nanoparticles through ultrasonic-assisted oxidation methods," *Carbohydr Polym*, vol. 106, pp. 359–364, Jun. 2014, doi: 10.1016/j.carbpol.2014.02.067.

[5] S. Pérez and E. Bertoft, "The molecular structures of starch components and their contribution to the architecture of starch granules: A comprehensive review," *Starch - Stärke*, vol. 62, no. 8, pp. 389–420, Jul. 2010, doi: 10.1002/star.201000013.

[6] A. Buléon, P. Colonna, V. Planchot, and S. Ball, "Starch granules: structure and biosynthesis," *Int J Biol Macromol*, vol. 23, no. 2, pp. 85–112, Aug. 1998, doi: 10.1016/S0141-8130(98)00040-3.

[7] J. A. Putseys, L. Lamberts, and J. A. Delcour, "Amylose-inclusion complexes: Formation, identity and physico-chemical properties," *J Cereal Sci*, vol. 51, no. 3, pp. 238–247, May 2010, doi: 10.1016/j.jcs.2010.01.011.

[8] H. Bouwmeester, P. Brandhoff, H. J. P. Marvin, S. Weigel, and R. J. B. Peters, "State of the safety assessment and current use of nanomaterials in food and food production," *Trends Food Sci Technol*, vol. 40, no. 2, pp. 200–210, Dec. 2014, doi: 10.1016/j.tifs.2014.08.009.

[9] S. Kumari, B. S. Yadav, and R. B. Yadav, "Synthesis and modification approaches for starch nanoparticles for their emerging food industrial applications: A review," *Food Research International*, vol. 128, p. 108765, Feb. 2020, doi: 10.1016/j.foodres.2019.108765.

[10] T. A. Tari and R. S. Singhal, "Starch-based spherical aggregates: stability of a model flavouring compound, vanillin entrapped therein," *Carbohydr Polym*, vol. 50, no. 4, pp. 417–421, Dec. 2002, doi: 10.1016/S0144-8617(02)00055-3.

[11] Y. Chen, X. Cao, P. R. Chang, and M. A. Huneault, "Comparative study on the films of poly(vinyl alcohol)/pea starch nanocrystals and poly(vinyl alcohol)/native pea starch," *Carbohydr Polym*, vol. 73, no. 1, pp. 8–17, Jul. 2008, doi: 10.1016/j.carbpol.2007.10.015.

[12] K. R. Rajisha, H. J. Maria, L. A. Pothan, Z. Ahmad, and S. Thomas, "Preparation and characterization of potato starch nanocrystal reinforced natural rubber nanocomposites," *Int J Biol Macromol*, vol. 67, pp. 147–153, Jun. 2014, doi: 10.1016/j.ijbiomac.2014.03.013.

[13] B. P. Binks and C. P. Whitby, "Silica Particle-Stabilized Emulsions of Silicone Oil and Water: Aspects of Emulsification," *Langmuir*, vol. 20, no. 4, pp. 1130–1137, Feb. 2004, doi: 10.1021/la0303557.

[14] M. V. Tzoumaki, T. Moschakis, and C. G. Biliaderis, "Mixed aqueous chitin nanocrystal–whey protein dispersions: Microstructure and rheological behaviour," *Food Hydrocoll*, vol. 25, no. 5, pp. 935–942, Jul. 2011, doi: 10.1016/j.foodhyd.2010.09.004.

[15] A. Yusoff and B. S. Murray, "Modified starch granules as particle-stabilizers of oil-in-water emulsions," *Food Hydrocoll*, vol. 25, no. 1, pp. 42–55, Jan. 2011, doi: 10.1016/j.foodhyd.2010.05.004.

[16] C. Li, Y. Li, P. Sun, and C. Yang, "Starch nanocrystals as particle stabilisers of oil-in-water emulsions," *J Sci Food Agric*, vol. 94, no. 9, pp. 1802–1807, Jul. 2014, doi: 10.1002/jsfa.6495.

[17] E. Kristo and C. Biliaderis, "Physical properties of starch nanocrystal-reinforced pullulan films," *Carbohydr Polym*, vol. 68, no. 1, pp. 146–158, Mar. 2007, doi: 10.1016/j.carbpol.2006.07.021.

[18] H. Angellier, J.-L. Putaux, S. Molina-Boisseau, D. Dupeyre, and A. Dufresne, "Starch Nanocrystal Fillers in an Acrylic Polymer Matrix," *Macromol Symp*, vol. 221, no. 1, pp. 95–104, Jan. 2005, doi: https://doi.org/10.1002/masy.200550310.

[19] W. Thielemans, M. N. Belgacem, and A. Dufresne, "Starch Nanocrystals with Large Chain Surface Modifications," *Langmuir*, vol. 22, no. 10, pp. 4804–4810, May 2006, doi: 10.1021/la053394m.

[20] M. Labet, W. Thielemans, and A. Dufresne, “Polymer Grafting onto Starch Nanocrystals,” *Biomacromolecules*, vol. 8, no. 9, pp. 2916–2927, Sep. 2007, doi: 10.1021/bm700468f.

1.2. Objectives

Starch-based nanomaterials are emerging tools used in many bioapplications. Therefore, the aim of this work is to develop sustainable and effective formulations based on Starch Nanoparticles (SNPs) with controlled size that can be used as nanocarriers for active compounds with antimicrobial activity. The detailed objectives that have been set for its development are presented below.

- Synthesis and characterization of controlled-size SNPs by nanoprecipitation and ME methods.
- Synthesis of superparamagnetic starch nanocomposites and characterization of their morphology and magnetic properties.
- Synthesis and characterization of controlled-size SNPs modified with Short Chain Fatty Acids (SCFA) from different botanical sources.
- Synthesis and characterization of controlled-size SNPs modified with Octenyl Succinic Anhydride (OSA) from different botanical sources.
- Encapsulation of vanillin in OSA-modified SNPs and evaluation of the antimicrobial activity.
- Synthesis and characterization of starch-silver hybrid nanoparticles (hybrid Ag-SNPs) and evaluation of the antimicrobial activity.

1.3. Thesis structure

This thesis is divided into 6 chapters, each with its corresponding subchapters, and each chapter has a short introduction about the topic developed.

Chapter 1 presents the background for which this thesis was developed, and the objectives intended to be achieved (subchapters 1.1 and 1.2 respectively). Subchapter 1.4 presents different methods for the synthesis of SNPs and also describes different methods for the encapsulation of active compounds, differentiating between direct and indirect loading. In addition, subchapter 1.5 provides information on recent studies using starch as an antimicrobial loading agent.

Chapter 2 is divided into three subchapters in which the synthesis of SNPs will be discussed in more detail, each with a brief introduction. Subchapter 2.1 corresponds to a preliminary study in which two different methods for the synthesis of SNPs, nanoprecipitation and ME, were developed. The optimal synthesis conditions were selected by modifying the main parameters involved in the synthesis, such as injection rate, dissolution time, stirring rate, organic/aqueous phase ratio, as well as the effect of amylose and amylopectin content in the starch. Subchapter 2.2 dealt with the synthesis of SNPs by the ME method, where the proportion and composition of the aqueous phase, the organic phase and the amounts of stabiliser, co-stabiliser and type of precipitant used were optimised. Furthermore, nanocomposites of SNPs and Iron Oxide Nanoparticles (IONPs) were synthesised under the selected optimal conditions. Finally, subchapter 2.3 deals with the synthesis of SNPs modified with SCFA of different chain lengths.

Chapter 3 focuses on the application of SNPs as carriers for compounds with antimicrobial activity and is divided into two subchapters, each with a brief introduction. In subchapter 3.1, the feasibility of SNPs as nanocarriers of vanillin, a well-known antimicrobial compound, was investigated. However, prior to this, the synthesis and characterization of SNPs modified with OSA at different percentages of OSA was carried out. Nanoprecipitation method was used for synthesis and native and highest % OSA starches were used to synthesize vanillin-loaded SNPs and evaluate their antimicrobial activity against *E. coli*. In subchapter 3.2, SNPs were used as matrix and stabilizer for silver nanoparticles (AgNPs). Hybrid Ag-SNPs were obtained and characterized by a method combining nanoprecipitation and autoclaving. At last, the antimicrobial activity of the formulations was tested against *E. coli* and *S. aureus* both in solid medium and in microdilution method.

Chapter 4 provides the main conclusions of the results obtained in each of the previous chapters and chapter 5 gathers the bibliography. Finally, chapter 6 is dedicated to the appendices, appendix A.1 contains the list of figures, appendix A.2 the list of tables and appendix A.3 the list of abbreviations.

1.4. Synthesis of starch nanoparticles and their applications for bioactive compound encapsulation

- **Summary**

In recent years, SNPs have attracted growing attention due to their unique properties as a sustainable alternative to common nanomaterials since they are natural, renewable and biodegradable. SNPs can be obtained by the breakdown of starch granules through different techniques which include both physical and chemical methods. The final properties of the SNPs are strongly influenced by the synthesis method used as well as the operational conditions, where a controlled and monodispersed size is crucial for certain bioapplications. SNPs are considered to be a good vehicle to improve the controlled release of many bioactive compounds in different research fields due to their high biocompatibility, potential functionalization, and high surface/volume ratio. Their applications are frequently found in medicine, cosmetics, biotechnology, or the food industry, among others. Both the encapsulation properties as well as the releasing processes of the bioactive compounds are highly influenced by the size of the SNPs. In this review, a general description of the different types of SNPs (whole and hollow) synthesis methods is provided as well as on different techniques for encapsulating bioactive compounds, including direct and indirect methods, with application in several fields. Starches from different botanical sources and different bioactive compounds are compared with respect to the efficacy in vitro and in vivo. Applications and future research trends on SNPs synthesis have been included and discussed.

- **Introduction**

Starch is a natural, renewable, and biodegradable polymer produced by many plants as a source of stored energy. It is the second most abundant biomass material in Nature. It is a carbohydrate storage product found in all chlorophyll-containing plants, such as corn, potato, rice, wheat, barley, etc. The predominant model for starch is a concentric semicrystalline multiscale structure that allows the production of new nanoelements: (i) starch nanocrystals resulting from the disruption of amorphous domains from semicrystalline granules by acid hydrolysis and (ii) starch nanoparticles produced from gelatinized starch [1]. The starch industry extracts and refines starches by wet grinding, sieving, and drying. If the starch is used as extracted from the plant it is called

"native starch", while if it undergoes one or more modifications (either enzymatic, chemical, or physical) to reach specific properties it is called "modified starch" [1]. Currently, the development and evolution of synthesis methods and instrumental techniques allow us to take advantage of the possibilities offered by new materials, whose physical and chemical properties are on the border between those exhibited by atoms and those of matter on a larger scale. These materials are known as nanoparticles [2, 3]. Today the nanoparticles field is experiencing a great expansion in scientific research thanks to its potential for application in sectors such as medicine, cosmetics, and food, among other areas.

Encapsulation is a process in which small particles or droplets are surrounded by a coating or embedded in a homogeneous or heterogeneous matrix. The adsorption of bioactive compounds on the carrier is accomplished through weak chemical interactions such as hydrogen bonding and Van der Waals forces. The choice of bioactive compound loading method depends on the size of the molecule to be encapsulated and its hydrophilic/lipophilic character [4].

At the same time, the loading method used for bioactive compounds also affects the release. The efficacy and the effect of these loading methods on the release characteristics of the loaded bioactive compounds have been previously studied to some extent [5].

Starch-based carriers are widely used in the encapsulation and control release of bioactive compounds for applications in food and pharmaceutical formulations due to their high biocompatibility and their small size which offers a high surface/volume ratio and high surface/weight ratio when hollow SNPs are synthesized [6-8]. However, there is little research on the delivery of bioactive compounds using starch-based nanoparticles [9, 10]. Moreover, even the majority of the review articles focus on the methods frequently used for fabrication of the SNPs, while reports on the encapsulation methods on SNPs are scarce. For the broader application of starch-based nanoparticles as carrier for bioactive compounds, it is important to investigate the loading and release properties of starch nanoparticles using model bioactive compounds.

In this review, different techniques for the synthesis of SNPs are described and the different size ranges obtained in each case are reviewed. Some recent novel developed techniques, such as ultrasound and high-pressure homogenization, are included. The SNPs sizes obtained were dependent on the selected synthesis method as well as the type of the starch used as the natural raw

material (e.g., corn starch, banana starch, potato starch, etc.) and also the possible modifications (e.g., chemical modification, amylose/amylopectin content modification, etc.). Different types of SNPs synthesized using different parameters are reviewed. Hollow particles or coated particles prepared by novel methods, such as the sacrificial template method, are also included. Also, a revision of the advantages and disadvantages that polymeric NPs present compared to NPs synthesized with other type of materials was made (Table 1.1).

Moreover, special attention has been paid to the encapsulation of bioactive compounds as one of the main bioapplications of SNPs. Two main different types of encapsulation methods were described depending on whether the bioactive compounds were encapsulated (direct or indirect). The effect of the type of starch selected for the encapsulation of bioactive compounds has been revised. Finally, applications SNPs loaded with several bioactive compounds were described and their efficacy was discussed when tested in vitro or in vivo. Moreover, present and future trends on the synthesis of loaded SNPs were described.

1.4.1. SNPs Preparation Methods

SNPs are obtained from the breakdown of the starch granules using different methods, which can be classified into two processes, top-down and bottom-up depending on the material used for the synthesis [11, 12] as it can be seen in Figure 1.4.

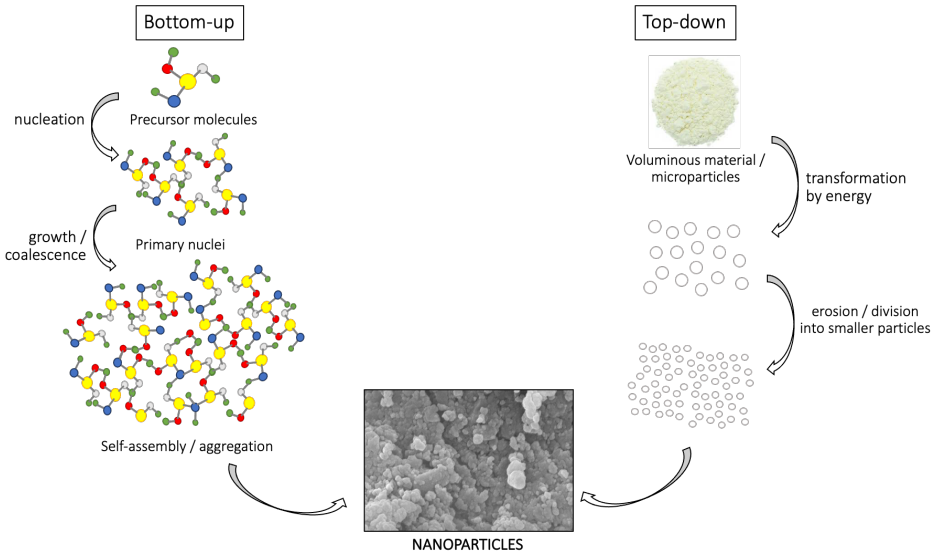

Figure 1.4. *Top-down and bottom-up processes for the synthesis of the SNPs.*

The top-down processes include all methods of synthesis where the size of the SNPs could be obtained from a voluminous material or microparticles that are eroding or being reduced to reach the structure of interest. The bottom-up processes cover all the synthesis procedures in which the SNPs are obtained from the assembly of molecules or macro-molecules in the form of small primary nuclei that are growing. These synthesis methods are described below, and shown in Tables 1.2 and 1.3, where the type of starch employed, and the resulting particle size obtained are noted.

Nanoprecipitation

Nanoprecipitation process involves the successive addition of a dilute solution of polymer to a solvent which leads to the polymer precipitation on the nanoscale. This method is essentially based on the deposition or displacement of the polymer in the interface followed by the displacement of the solvent from the lipophilic solution [13]. A schematic representation of this nanoprecipitation method is shown in Figure 1.5.

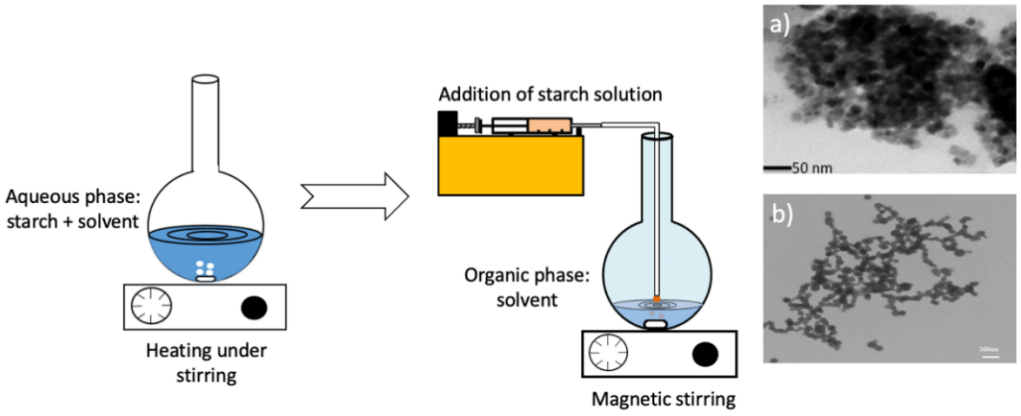

Figure 1.5. *Synthesis of SNPs through nanoprecipitation method and TEM micrographs of corn SNPs (a) [14] and (b) [15]. Reprinted from [14] with permission from Elsevier. Copyright (2015).*

One of the most common solvents used by many authors is acetone which leads to the precipitation of the starch in the form of nanoparticles when it is added dropwise from an aqueous phase where it was previously dissolved. Najafi et al. prepared SNPs using acetylated corn starch and optimized the reaction of native starch using acetic anhydride and acetic acid with low and high degrees of substitution (DS). A size range of 221–324 nm was obtained by studying different DS levels and water/acetone ratios [16]. In 2018, Acevedo-Guevara et al. used native and acetylated starch obtained from green bananas for the synthesis of SNPs by a nanoprecipitation method where they

also used acetone as the solvent. Both systems presented similar results, obtaining a size of 135 nm when the native starch was used and 190 nm when the acetylated starch was used. In turn, to understand the size difference of the SNPs, they studied the size of the starch granules. A slight aggregation in the acetylated banana starch granules was observed which was due to the increase in the intermolecular hydrogen bonds starch granules and water which could explain the difference size observed in the nanoparticles with both starches [17]. Similar studies were carried out by Nieto-Suaza et al. who also used native and acetylated banana starches for the synthesis of the SNPs. As in the previous case, larger particle sizes (198 nm) were obtained when acetylated starch was used, while using native starch, sizes of 141 nm were obtained [18].

Another common solvent used in nanoprecipitation method is absolute ethanol. In some cases, it is added dropwise to a deionized water solution containing the dissolved starch or vice versa. In recent studies, Fu et al. synthesized NPs from corn starch and amylose by this method. They observed that most of the corn SNPs were spheres with some aggregates obtaining particles from dozens of nanometres up to 500 nm. On the other hand, the amylose NPs presented irregular shapes which were smaller than the previous ones. The diffraction patterns in both NPs presented two peaks, the smaller one had practically the same position for both, however, the position of main peak turned out to be slightly different suggesting higher sizes for the corn SNPs compared to the amylose NPs. Nevertheless, both NPs presented a V-type crystalline structure. Finally, the average size of the starch particles obtained was 350 nm while that for the amylose particles was 250 nm [19]. Nyoo Putro et al. reported a method that combined nanoprecipitation methods with acid hydrolysis resulting in SNPs with different crystallinity. The acid hydrolysis method produced SNPs with high relative crystallinity, whereas the ethanol preparation method resulted in SNPs with low crystallinity. In order to vary the hydrophilicity of the starch, SNPs were also modified by using different cationic, anionic, and nonionic surfactants. The morphology observed before the modification was flaky for SNPs obtained by the hydrolysis and spherical for the nanoprecipitation ones. Significant changes were not observed after the modification with cationic and anionic surfactants for both methods. However, when nonionic surfactant was used, a significant change was observed appearing as different adsorption mechanisms on the SNPs surface in both cases. Smaller particle sizes were obtained when the acid hydrolysis method was used with particle sizes approximately between 82 and 92 nm, while sizes between 158 and 180 nm were observed when nanoprecipitation was used [20].

On the other hand, as it was aforementioned, starch can also be added in the aqueous phase in the form of short glucan chain powder dissolved into deionized water and subsequently be mixed with an ethanolic solution added dropwise leading to the starch precipitation. In the study carried out by Qiu et al., native waxy maize debranched by pullulanase was used to obtain short linear glucans to synthesize SNPs. Short glucan chains were linear and had a low degree of polymerization compared to the native starch and contributed to a more compact structure formation. Finally, particles with an average particle size of 84 nm were obtained [15]. Liu et al. also synthesized SNPs through a modified solvent displacement method using waxy corn starch which was altered into short linear glucans obtaining a particle size range between 40 and 50 nm but apparent aggregation was observed [21].

Besides, the aqueous phase, in addition to distilled water, may also contain other chemical compounds as sodium hydroxide or dimethyl sulfoxide (DMSO) mixed with the starch solution allowing its precipitation by adding absolute ethanol dropwise. El-Naggar et al. synthesized crosslinked corn SNPs by a nanoprecipitation method using a mixture of distilled water and sodium hydroxide as the dispersed phase, sodium tripolyphosphate (STPP) as a crosslinking agent in the presence of Tween 80 as a surfactant. Crosslinkers can enhance the granule stability with new covalent bonds which allows to increase the desired stability conditions [22]. Different amounts of the crosslinking agent were studied, and it was observed that the greater the amount of STPP, the greater the particle sizes. In any case, none of the experiments exceeded particle sizes of 68 nm [14]. In recent studies, Gutierrez et al. also synthesized SNPs using the nanoprecipitation method by modifying main operating parameters. Maize starch was dissolved into an aqueous phase containing sodium hydroxide in the presence or absence of urea since it was recently reported that the interactions between sodium hydroxide and urea improve the solubility of the polymers as sodium hydroxide breaks the hydrogen bonds of the starch and urea prevents self-association of the starch molecules [23]. Then, in order to precipitate the starch in the form of SNPs 1 mL of the starch solution was added into absolute ethanol as the organic phase. Also, the effect of the addition of a cationic surfactant, Cetyl Trimethyl Ammonium Bromide (CTAB) into the aqueous phase was studied. As a result, SNPs from 59 nm to 118 nm were obtained, registering the higher values when surfactant was added into the aqueous phase. The result of this study showed that the total amount of SNPs obtained was greater for urea-containing formulations and fewer agglomeration were observed for an aqueous solution with 8% (*w*/*v*) NaOH and 10% (*w*/*v*) urea [24].

Abidin et al. also prepared oxidized starch nanoparticles (oxy-SNPs) modifying the native starch by liquid-phase oxidation using H_2O_2 as the oxidant, followed by chemical dissolution and solvent-free precipitation. Starch was dispersed in ethanol and DMSO was added until the starch was gelatinized and dissolved in the DMSO, then the precipitation of the SNPs was carried out by mixing the starch solution with ethanol. The final size of the oxy-SNPs was confirmed in a scale range of approximately 178 nm [25].

Emulsion/Microemulsion

This process consists of the formation of an emulsion through two phases, an aqueous solution containing the dissolved polymer and an organic solvent that is immiscible or partially immiscible in water. Subsequently, the two phases are emulsified with intense agitation which can be carried out by means of a mechanical homogenizer such as microfluidization or ultrasonic homogenization. The presence of a surfactant is required to stabilize the emulsion. The droplets formed due to the agitation act as nanoreactors that produce the controlled precipitation of the starch in the form of nanoparticles inside. A graphic representation of this method is depicted in Figure 1.6.

Microemulsions can also be used to form SNPs, which typically lead to the formation of smaller and more uniform particles [26]. In this case, an intense agitation to form the microemulsions is not necessary since they form spontaneously with very little energy input.

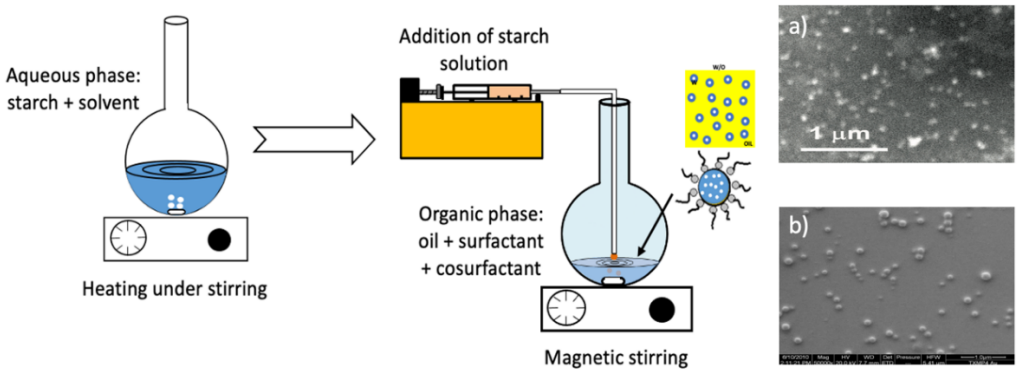

Figure 1.6. Synthesis of SNPs through emulsion/microemulsion method and SEM micrographs of (a) corn *SNPs [27] and (b) potato SNPs [28].*

In 2017, Nor Syahida and Subash synthesized SNPs by a W/O ME method where they dissolved corn starch in alkaline urea solution with different starch concentrations and further precipitated in

ethanolic emulsion system using Tween 20 as surfactant and sunflower oil by adding the starch solution dropwise into the microemulsion system. The SNPs produced this way were uniform in shape and size, due to homogeneous solution obtaining sizes of 40 nm. However, smaller sizes were obtained when the lowest starch concentrations were used [27]. Gutierrez et al. also carried out the formation of a W/O microemulsion to synthesize spherical SNPs. Maize starch was dissolved into an aqueous phase with sodium hydroxide and urea and then 1 mL of this solution was added into an organic phase under constant stirring. This organic phase was formed by oil (soybean and sunflower), a surfactant (Tween 20 and Span 60) with different concentrations, and absolute ethanol as a co-stabilizer. This method led to sizes from 35 nm to 147 nm with a higher particle formation capacity and without the presence of large agglomerates. The final SNPs size was not influenced by the type of oil used in the microemulsion formulation; however, smaller sizes were obtained by the use of very hydrophilic surfactants (Tween 20) [24].

Dandekar et al. synthesized SNPs from hydrophobic starch derivative, propyl- potato starch through an emulsion-diffusion technique. This technique differs from the conventional microemulsion in the way that a W/O emulsion is formed within a partially water-soluble solvent and subsequently water is added to the system which causes the diffusion of the solvent towards the external phase, resulting in the formation of nanoparticles [29]. It has numerous advantages such as high performance and encapsulation efficiency (EE), reproducibility, and scalability. The authors studied different nonionic surfactants and their effect on the SNPs size and homogeneity. Best results were obtained when polyvinyl alcohol (PVA) was used as a surfactant obtaining a low particle size and the most homogeneous formulation. Finally, the lowest particle size obtained was 245.5 nm, which was achieved with a drug: starch ratio of 1:5 [30]. Alp et al. also used an emulsion-diffusion method to synthesize corn SNPs obtaining a particle size of 180 nm in the aqueous solution. Starch was dissolved in DMSO as the organic phase and a mixture of PVA and distilled water was used as the aqueous phase. The droplets obtained on the biphasic system were precipitated in the form of SNPs when DMSO was diffused by the addition of distilled water to the system [31]. Similarly, Santander-Ortega et al. synthesized SNPs with a W/O emulsion-diffusion method using two different propyl-starch derivatives with high degrees of substitution (1.05 and 1.45) and an unmodified starch polymer. The inclusion of propyl groups would allow a good solubility in low-risk organic solvents and the incorporation of PVA into the formulation improved the hydrodynamic size distribution of nanoparticles. SNPs synthesized with propyl starch

derivatives showed a spherical shape with a narrow size distribution with a size range of approximately 150-183 nm, where the largest size was obtained with the highest degree of substitution (DS). However, in the case of unmodified starch, the formation of SNPs could not be observed [28].

Emulsion Cross-Linking

Recently, the synthesis of SNPs by an emulsion-crosslinking technique has been reported. This technique involves mixing of an aqueous phase which contains cross-linking agents with another phase that contains dissolved starch. The mixture is then added into an oily or organic phase with the presence of emulsifying agents as can be seen in Figure 1.7. Through this W/O emulsion, small particles are generated by cross-linking reaction within the aqueous droplets. However, the particles obtained from this emulsion cross-linking approach are relatively large and, on the microscale, [32, 33].

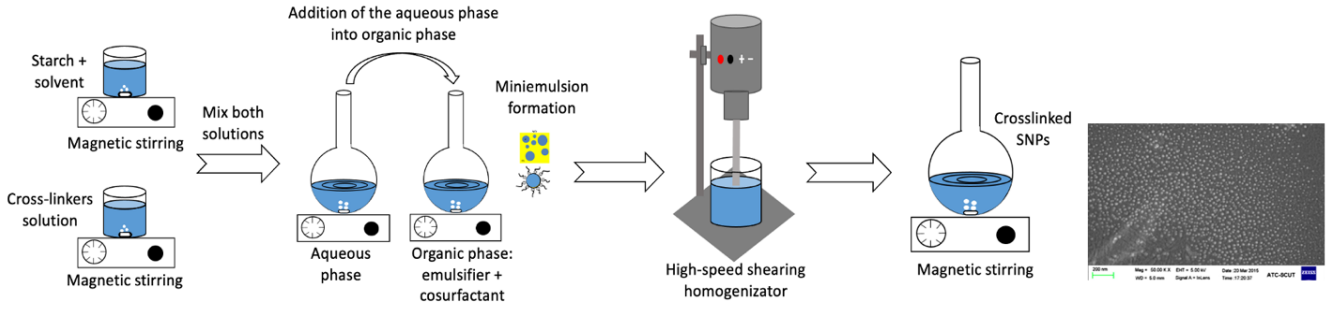

Figure 1.7. *Synthesis of SNPs through emulsion cross-linking method and SEM micrograph of SNPs. Reprinted from [34] with permission from Elsevier. Copyright (2016).*

To reduce the size of these particles, the emulsion should contain nanoscale droplets, which means use a miniemulsion (also called nanoemulsions) instead of an emulsion [35]. Ding et al. used retrograded starch (RS III) to synthesize SNPs through a high-speed shearing emulsification method using N,N'-methylenediacrylamide (MBAA) as the cross-linking agent and $NaHSO_3$ as an inducing agent in the aqueous phase which contained the dissolved starch in a potassium hydroxide solution. The oil phase was formed by mixing cyclohexane with a mixture of Span 80 and Tween 80 at an 84:16 proportion. The aqueous phase was added to the oil phase in order to form the microemulsion which was homogenized by a high-shear homogenizer to break the droplets and form the nanoemulsion. A small particle size distribution was obtained, and the average size was

approximately 287 nm. The stability of the particles was studied, and it was shown that these nanoparticles were stable in neutral and alkaline pH or in low NaCl concentration [36].

Dialysis

The dialysis technique involves the dissolution of the biopolymer in an organic solvent. The solution is placed inside a dialysis bag, which is immersed in a liquid that is miscible with the organic solvent, but the biopolymer is insoluble in it. Due to the progressive displacement phenomenon between the organic solvent and the external liquid through the dialysis bag in which the biopolymer is not soluble, it is possible to achieve supersaturation of the biopolymer solution located inside the dialysis bag and therefore, the biopolymer will be gradually aggregated due to the change in the polarity caused by the environment where it is found [37, 38]. This process is schematized in Figure 1.8.

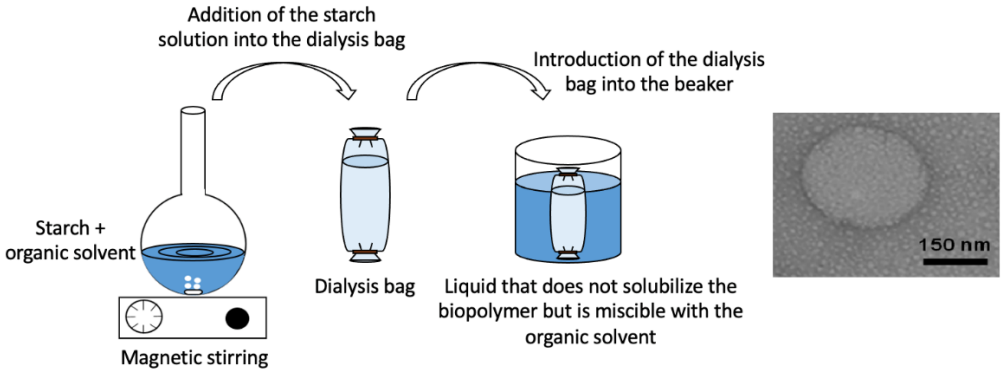

Figure 1.8. *Synthesis of SNPs through dialysis method and TEM micrograph of potato SNPs [39].*

Some advantages of the dialysis method are the control of the aggregation rate, the modulation of the particle size, and the simplicity and versatility of the technology [40]. Delsarte et al. reported the synthesis of the SNPs through a dialysis method using potato starch modified with OSA and 1,4-butane sultone (BS). The critical aggregation concentration (CAC) was initially studied to investigate the possible formation of colloidal aggregates of OSA-BS starch. The results suggested a modification on the morphology of the polymer when its concentration increases stipulating that under the CAC of the OSA-BS starch presented an aggregate formed with a dense core and a swollen cover, which was consistent with the higher mobility of the remaining OSA. Beyond CAC, the molecular structure self-assembled in uniform aggregate with collapsed chains. TEM images revealed the presence of different sizes of nanoparticles with diameters between 5 and 200 nm [39].

Xu et al. also reported this method for the synthesis of SNPs using cholesterol-modified oxidized starch and imidazole. Most of the SNPs exhibited homogeneous sphere shapes as well as good dispersibility with mean diameters of 212 nm [41].

Sacrificial Template

This method is especially used for the synthesis of hollow or porous particles. Up until now, hollow nanoparticles (HNPs) have been prepared by creating a void space inside of a solid precursor through a variety of physical and chemical techniques, such as the sacrificial template method, nozzle reactor processes, emulsion polymerization, and phase separation [42]. Among these, the hard templating strategy is the simplest and most widely used method [43, 44]. This approach typically consists of coating the outer surface of a material that will act as a template with a polymeric material, in this case starch, and subsequently, the material used as a template will be removed until a hollow particle is obtained [45-47] as it can be seen in Figure 1.9.

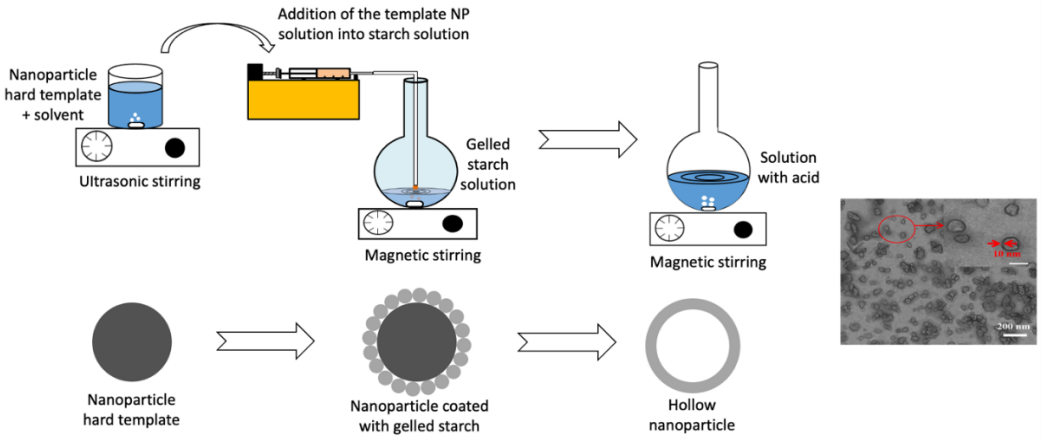

Figure 1.9. *Synthesis of SNPs through sacrificial template method and TEM micrograph of pea, mung, bean, potato, and corn hollow SNPs [48].*

For this purpose, it is necessary to add a suspension containing the particles that will act as a template to a solution in which the gelled starch is found, which will lead to the precipitation of the starch and its deposition on the template particles. Finally, a change in the medium is produced, such as a change in pH or temperature that will cause the dissolution of the material that acts as the template, thus producing the hollow SNPs. The final conditions of the hollow particles are limited by the size and shape of the starting template, while the thickness of the coating material is determined by its coating process. In 2017, Yang et al. reported this method for the synthesis of hollow SNPs using gelled starch as the shell where different concentrations of $CaCO_3$ as hard

templates were used. SNPs with diameters ranging from 30 to 300 nm and a shell thickness of 5–10 nm were obtained [48].

Ball Milling

Ball milling is one of the reliable techniques to produce nanoparticles without the aid of additives or the requirement of a final dehydration step to recover the nanoparticles. Over the years, the ball milling process has been explored for the nanoreduction of different polymeric materials including starch [49], cellulose [50] and protein-based polymers [51] for different applications. This process can be conducted in dry (without solvents) or wet (with solvents) conditions. The milling occurs due to mechanical friction between the grinding media, such as balls of the same or various sizes, and the ground material. The container and the grinding balls are typically made of the same, super hard material (zirconia, corundum, or stainless steel). Mechanical energy is provided to the system by the rotary motion of the bowl, as in the case of a planetary ball mill. Wet ball milling is also considered to be a green chemistry approach, as it does not require high temperatures (energy saving) and consumes minimal quantities of solvents [52]. A schematic representation of the ball milling method is shown in Figure 1.10.

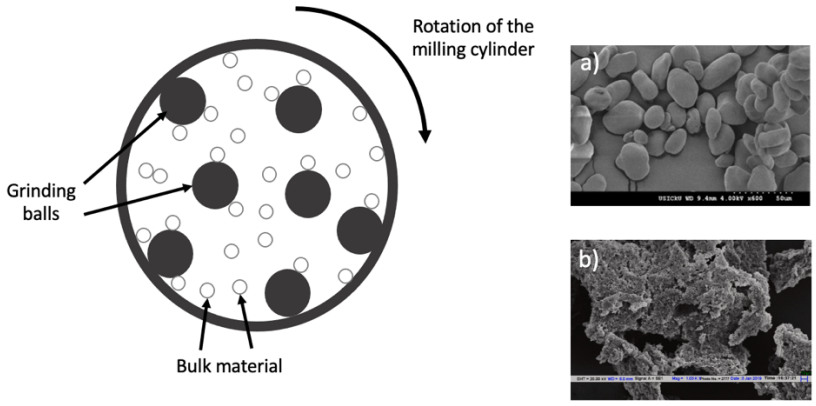

Figure 1.10. *Synthesis of SNPs through ball milling method and SEM micrographs of (a) water chestnut SNPs [53] (reprinted with permission from Elsevier. Copyright (2019)) and (b) lotus stem, horse and water chestnut [54] (reprinted with permission from Elsevier. Copyright (2021)).*

This process is a cost-efficient and environmentally friendly physical processing method that has been proven capable of changing starch properties [55, 56]. In 2019, Ahmad et al. carried out a study synthesizing water chestnuts SNPs by a physical method of ball milling. SNPs were obtained by reducing the starch size with a planetary ball for 5 h and finally, the average particle size

obtained after the milling process was 271 nm [53]. In recent studies, Ahmad et al. also synthesized SNPs through a ball milling method using a mixture of starches (lotus stem, horse, and water chestnut) to create nanocapsules for bioactive compounds encapsulation. SNPs were obtained in the same way as their previous study with a planetary ball for 5 h. For this study, higher hydrodynamic particle sizes were obtained, being the smallest for the horse chestnut starch with a particle size of 420 nm approximately and with a PdI of 32% what indicated a narrow size distribution [54].

Ultrasound with or without Acid Hydrolysis

This method consists of a precipitation process that involves the addition of a solution in which the starch is diluted into an aqueous phase in the presence of ultrasound homogenization that reduces the size of the particles formed due to the breaking of the starch covalent bonds as a result of the shear forces or the mechanical effects produced by the collapse of microbubbles that form sound waves [57-59].

However, this method has been applied together with acid hydrolysis since the combination of physical and chemical processes produces nanoparticles with more desired properties [60]. This technique is simple and convenient in terms of safety, cost and can give better yield with desired particle size.

Acid hydrolysis is a process that can be conveniently divided into three stages based on the reaction rates involved: rapid stage, slow stage, and very slow stage [61]. A series of steps is typically required to produce SNPs using the acid hydrolysis process: (i) the starch is mixed with the acid; (ii) this mixture is heated for a certain time with constant stirring; (iii) the resulting suspension is washed with distilled water by successive centrifugation until neutralization is achieved and (iv) the suspension is refrigerated for a specified time [62]. The main disadvantages of this method are the low recovery yield, slow reaction rate, and tendency for particle aggregation to occur [63].

Both processes, with and without acid hydrolysis are presented in Figures 1.11 a,b respectively.

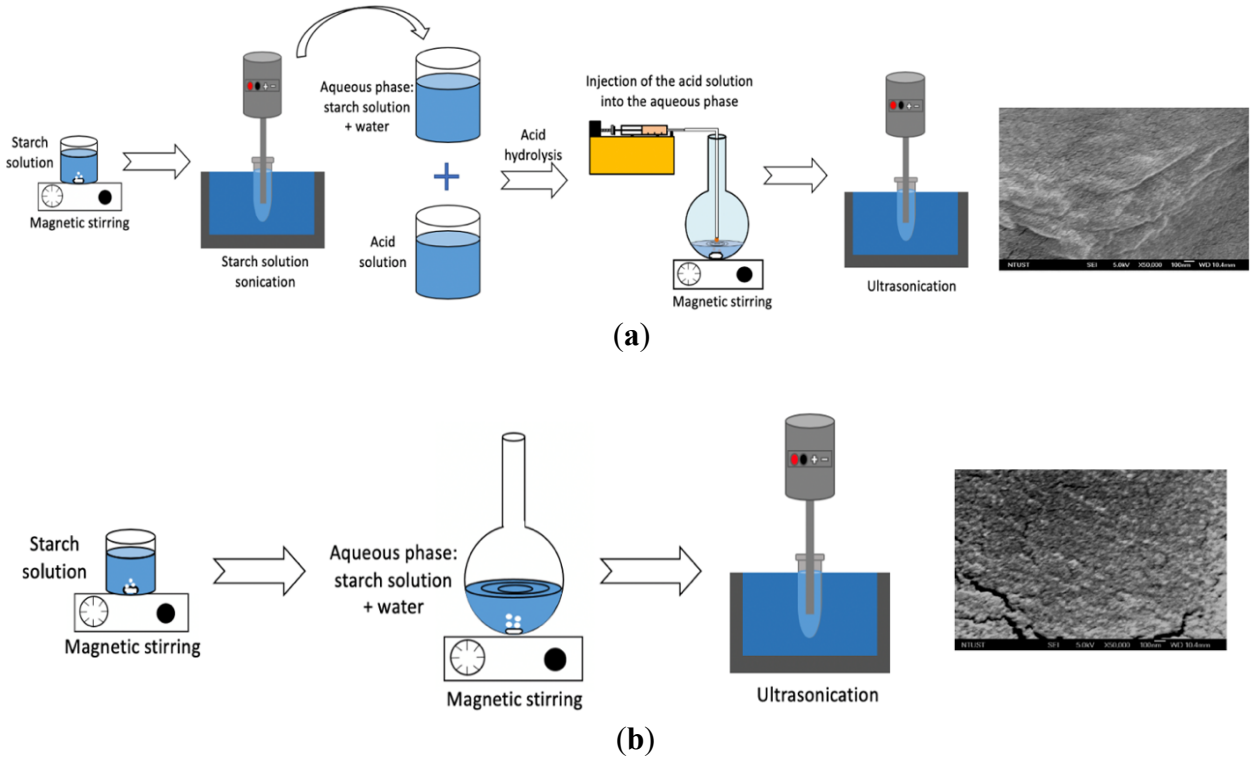

Figure 1.11. *Synthesis of SNPs through ultrasound method: (a) with acid hydrolysis; (b) without acid hydrolysis and SEM micrograph of corn and potato SNPs [64].*

In 2019, Shabana et al. reported the synthesis of SNP from potato starch using an ultrasound-assisted method with and without acid hydrolysis. The ultrasound-assisted acid hydrolyzed starch exfoliates the native starch and modifies the structural arrangement, in this acid treatment, the amorphous nature of the starch becomes crystalline. A solution of corn and potato starch was prepared and sonicated and subsequently treated with dilute sulfuric acid. The hydrolysis of those of the SNPs was carried out by diluting part of the starch solution in distilled water and subsequently concentrated H_2SO_4 was added dropwise and sonicated until the addition of dilute sulfuric acid was completed. To neutralize this solution, a solution of NaOH and distilled water was added. Finally, particle sizes of 42 nm were obtained when the acid hydrolyzed ultrasound approach was used while sizes of 80 nm were obtained when only the ultrasound was used [64].

Ultrasonic Atomization

Ultrasonic atomization is a promising way to generate liquid microdroplets through the use of ultrasonic energy. In the droplet formation mechanism, two major hypotheses have been suggested to explain the thin vibrating liquid film disintegration during ultrasonic atomization comprising

capillary waves, and cavitation mechanism [65]. Capillary waves consist of an ordered mesh-like structure with the same number of ridges and valleys per unit area [66]. In the common model of ultrasonic atomization, droplets detach from the crests of the stationary capillary waves and in the cavitation mechanism, cavitation bubbles are formed on the vibrating surface due to the application of ultrasonic waves. During the collapse of these cavities, generated hydraulic shocks initiate the segregation of the liquid film and consequently result in the ejection of the droplets [67]. This process is shown in Figure 1.12.

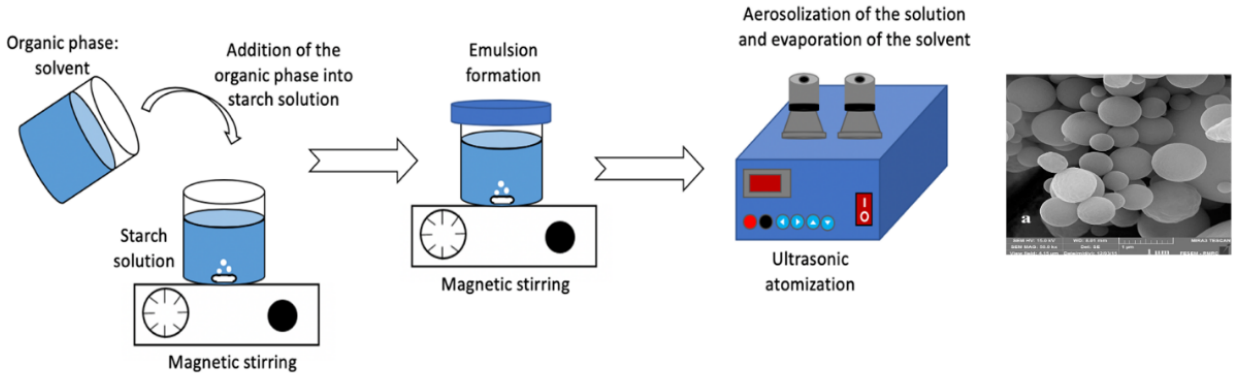

Figure 1.12. *Synthesis of SNPs through ultrasonic atomization method and FE-SEM micrograph of SNPs. Reprinted from [68] with permission from Elsevier. Copyright (2019).*

Recently, Shahgholian and Rajabzadeh developed a bovine serum albumin (BSA) based SNP synthesis method by an ultrasonic atomization procedure using an ultrasonic piezoelectric oscillator. An integrated apparatus was designed for the manufacturing of aerosol solutions, as well as for the drying and collection of the resulting SNPs, and finally, the formation of spherical SNPs with a uniform smooth surface and particle sizes ranging from 200 to 800 nm had resulted [68].

High-Speed Jet

Recently, a physical technology has been developed based on a high-speed jet treatment which is a novel combination with high pressure and speed and a model of liquid-solid impact [69]. It is basically consisted of a piston chamber in which crude suspension is drawn in through downward stroke. The suspension passes through a small, fixed nozzle that produces a high-speed jet during the upstroke. Before colliding with the target, the jet circulates through a pipe and then it is cooled by a recirculating flow of coolant from the rupture chamber walls. However, it is suggested that the high-speed jet is an intense mechanical treatment that can affect the size and the gelatinization properties of starch [70]. The schematization of this process is shown in Figure 1.13 above.

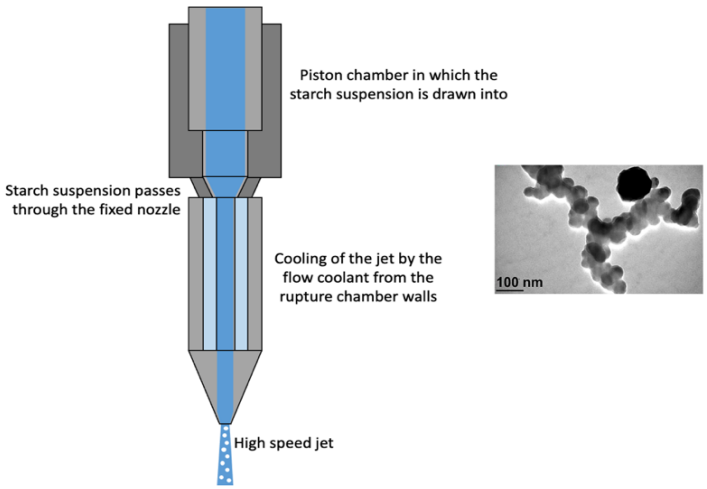

Figure 1.13. *Synthesis of SNPs by high-speed jet method and TEM micrograph of tapioca SNPs. Reprinted from [71] with permission from Elsevier. Copyright (2020).*

In a recent study Xia et al. synthesized SNPs from tapioca starch using this physical method. Before the high-speed jet treatment, the native starch was treated with a vibrating superfine mill with different micronization periods to improve the polymer solubility and after 60 min of micronization, the optimum pretreated material was achieved. Next, the pretreated starch was mixed with distilled water and stirred at room temperature and then, the suspension was treated with a high-speed jet at different pressures followed by vacuum filtering and finally dried for 24 h. Particle size decreased after the high-speed jet treatment and an increase in the pressure produced a more uniform SNPs size achieving the smallest sizes (55.3 nm) with 240 MPa of pressure [71].

Nanoparticles have been used as vehicles for the delivery of bioactive compounds for several applications in food, cosmetic and pharmaceutical formulations. Frequently, in order to obtain more effective materials with large surface area per unit of mass, hollow nanoparticles are prepared. The most common materials used for hollow nanoparticle preparation are polymers. Starch is a natural polymer that has attracted interest for its use as raw material for covering already prepared nanoparticles of several other metal materials. However, their individual use for SNPs preparation has increased during the last decade. SNPs present both advantages and disadvantages with respect to the other type of nanoparticles which are made with other materials, such as polymers, metals, or silica, as summarized in Table 1.1 [72-75].

Table 1.1. *Advantages and disadvantages of SNPs versus other types of nanoparticles.*

Advantages	**Disadvantages**

- Starch nature makes it a non-toxic material with high biocompatibility and non-hazardous to human health	
- Starch is biodegradable, renewable, and abundant in nature	- Native starch present poor tolerance to a broad range of processing conditions (temperature, pressure, pH) limiting its applications in the food industry
- Starch can be easily modified due to the presence of a large number of hydroxyl groups on its main components (amylose and amylopectin)	- Native starches present low solubility and retrogradation which restricts their functional properties
- SNPs present greater surface area per mass	- Modification of starch usually requires the use of solvents that could produce a final product with undesired conditions
- Versatility: a large number of different types of starch and the physical and chemical methods used to prepare SNPs makes it possible to obtain nanoparticles with diverse crystallinity and different sizes	

1.4.2. Encapsulation Methods

SNPs have attracted a lot of attention due to their unique properties that are different from those of their source material (native starch granules). One of the main applications of SNPs is the encapsulation of bioactive compounds [27, 76]. Encapsulation is defined as the technology by which active compounds are confined within a polymer matrix. This technique creates a microenvironment in the capsule that is capable of controlling the interactions between the interior and the exterior [77]. Encapsulation can be divided into direct and indirect encapsulation depending on how the synthesis method is performed as it will be discussed below. Table 1.2 summarizes all the parameters discussed in this section for the SNPs direct encapsulation.

Direct Encapsulation

This type of encapsulation refers to when both the synthesis of the SNPs and the encapsulation of the active compound are carried out simultaneously.

Table 1.2. *Examples of recent studies of SNPs synthesis methods and encapsulation of different compounds through direct encapsulation.*

Preparation Method	Type of Starch	Particle Size (nm)	Encapsulated Compound	Evaluation Method	Applications	Tested On	EE (%)	References
Microemulsion	Corn	40	Penicillin/streptomycin	Disk diffusion	Anti-bacterial, harmful pathogenic organisms	*S. pyogenes* and *E. coli*	/	[27]
Nanoprecipitation	Acetylated corn	221–324	Ciprofloxacin	UV-vis	Medical	/	21–90	[16]
Nanoprecipitation	Native and acetylated green banana	135–190	Curcumin	UV-vis	Drug and nutraceutical delivery	SIG, SIF in vitro	85–90	[17]
Nanoprecipitation	Corn	21–68	Diclofenac sodium	UV-vis	Medical	Rat skin in vitro	73–91	[14]
Nanoprecipitation	Lotus stem, horse chestnut and chestnut	323–615	Catechin	UV-vis	Functional foods	In vitro digestion	48–57	[57]
Nanoprecipitation	Corn + pullulanase	84	Essential oils	UV	Cosmetics, food preservation, antibacterial	In vitro dialysis	72–87	[15]
Emulsion-diffusion	Corn	180	CG-1521	Crystal violet assays	Breast cancer therapy and other tumors	MCF-7 breast cancer cells in vitro	/	[31]
Nanoprecipitation	Insoluble porous corn	/	Paclitaxel	HPLC	Anti-cancer	Rats through oral administration	71–74	[78]
Nanoprecipitation	Corn	283	Triphala churna	UV-vis	Pharmaceutical	*S. dysenteriae*, *S. aureus* and *S. Typhi* in vitro	92	[79]

Nanoprecipitation	/	45	Vitamin E	UV-vis	Wound dressing	SF-PVA Aloe Vera nanofibers in vitro	92	[80]
Emulsion-diffusion	Corn + OSA	375–617	Conjugated linoleic acid	Gravimetry	Controlled release, functional foods, cosmetics	Gastrointestinal rat tract in vivo	97	[81]
Dialysis	/	212	Curcumin	UV-vis	Anti-cancer	Human lung cancer cell A549	82	[41]
Emulsion-diffusion	Corn	150–183	Testosterone, flufenamic ac., caffeine	HPLC	Transdermal delivery	Human skin undergone abdominal plastic surgery	80–95	[28]
Ultrasonic atomization	/	200–800	Curcumin	UV-vis	Bioactive encapsulation	SIG, SIF	64–92	[68]
Nanoprecipitation	Banana + Aloe Vera	141–198	Curcumin	UV-vis	Food packaging	Highly hydrophilic/lipophilic foods	82–92	[18]
Emulsion-diffusion	Potato	245.5	Docetaxel	HPLC	Anti-cancer	Caco-2 cells	82	[30]
Nanoprecipitation	Corn	250–350	Lutein	/	Food, medicine, feed	/	/	[19]
Nanoprecipitation	Quinoa	283–871	Piroxicam	UV/vis	Pharmaceutical	In vitro dialysis	84	[82]
Ultrasounds	Quinoa and maize	107–222	Rutin	Spectrophotometry	Functional foods	Simulated salivary juice	63–67	[72]

Nanoprecipitation Starch Sources

The most common synthesis method used for direct encapsulation is through nanoprecipitation method. Many authors use this method for the encapsulation of different active compounds and also, different types of starches can be used, where corn starch is the most common of them.

Corn Starch

In recent studies, acetylated corn starch was formulated with high and low DS where the antibiotic-loaded SNPs were prepared by a nanoprecipitation process by Najafi et al. Acetylated starch with different DS was dissolved and mixed with the antibiotic (ciprofloxacin) in acetone as the organic phase. Subsequently, distilled water was added into the solution containing the polymer under stirring until the acetone was completely evaporated [16]. In the same way, El-Naggar et al. synthesized diclofenac sodium (DFS) loaded cross-linked corn SNPs by modified nanoprecipitation method. The aqueous phase contained corn starch dispersed in distilled water containing NaOH under continuous high-speed homogenization. Tween 80 was dissolved in distilled water containing different amounts of the drug was added dropwise to the starch solution under a high rate of homogenization and then distilled water containing different amounts of the crosslinking agent (sodium tripolyphosphate) was added to the solution. The resulting DS encapsulated crosslinked SNPs were subsequently precipitated with absolute ethanol and further purified by centrifugation and washing two times with absolute ethanol/water to remove unreacted compounds and finally with absolute ethanol [14]. Other authors reported the loading of *Triphala churna* in corn SNPs following the graft copolymerization method, which consists of loading the drug in gelatinized starch. This is accomplished by heating starch in NaOH solution. Thereafter, the gelatinized starch and the drug were mixed, and acetone is added dropwise under constant stirring for the conversion of the solubilized starch into SNPs [79]. Also, some authors used native waxy corn starch that was debranched with pullulanase to obtain short linear glucans for the synthesis of SNPs for encapsulation of essential oils (EO). The debranched starch was precipitated in presence of an excess of absolute alcohol and washed with aqueous dimethyl sulfoxide solution. The starch was dispersed in deionized water and then autoclaved. Synthesis and encapsulation were carried out by precipitating the dissolved EO in hot ethanol into the starch solution under constant stirring [15]. The loading of drugs in porous starch nanoparticles was also studied by Wang et al. in 2019. The paclitaxel used as the drug was completely dissolved in acetone and then

insoluble porous corn starch (starch treated with α-amylase and glucoamylase in weak acid) was added under stirring. Subsequently, the porous starch adsorbed with the paclitaxel acetone solution was added to deionized water containing hydroxypropyl methyl cellulose and then stirred. At the same time, the load of paclitaxel in porous starch was also studied as a control group [78]. Fu et al. also synthesized lutein-loaded SNPs in order to find a better dispersibility of lutein in water and its stability against chemical oxidation. Corn starch or amylose was mixed with deionized water at different concentrations. These solutions were heated under continuous stirring until the starch was gelatinized. Subsequently, half of an ethanol solution containing lutein was added dropwise. After cooling the mixture to room temperature, the same volume of the ethanol and lutein solution was added again, and the precipitate obtained was washed with ethanol. In this study, an oxidation rate of 25% for the pure lutein encapsulated in SNPs was obtained [19].

Banana Starch

Nieto-Suaza et al. reported the development and characterization of composite films made from starch and aloe vera gel incorporated with curcumin-loaded starch nanoparticles from native and acetylated banana starch using a nanoprecipitation method. Starch was dispersed in a curcumin-acetone solution under magnetic stirring and then water was added dropwise with constant stirring. The resulting suspension was stirred at room temperature until the acetone was completely vaporized. The obtained SNPs were washed several times with ethanol to remove any excess of curcumin, to be used in the preparation of composite films [18].

Mixture of Starches

A mixture of different types of starches can be also used in the synthesis of the SNPs. In recent studies, Ahmad et al. used starches from lotus stem, horse chestnut, and water chestnut for catechin nanoencapsulation. The starch mixture was then hydrolyzed in NaOH solution which was subsequently replaced with distilled water. The catechin was dissolved in ethanol and added dropwise into the hot starch solution under constant stirring to initiate precipitation. To increase the EE and reduce the size of the SNPs, the solution was subjected to an ultrasound process using a fixed probe sonicator [57].

Microemulsion Starch Sources

Another common method used for the SNPs synthesis is the ME method. Also, corn starch is one of the most common starches used in this synthesis method.

Corn Starch

In 2017 Nor Syahida and Subash produced antibiotic-loaded SNPs by an ethanolic microemulsion system. An aqueous phase was formulated containing corn starch in an alkaline urea solution. Meanwhile, the organic phase was composed of sunflower oil, ethanol, Tween 20 as an emulsifying agent, and the antibiotic solution in different quantities (streptomycin and penicillin were used). A small volume of the aqueous phase was pumped into the solution containing the antibiotic under constant stirring. Finally, the nanoparticles were washed twice with ethanol to remove unincorporated components [27]. Alp et al. also used corn starch for the synthesis of SNPs by the ME method for delivery of the histone deacetylase inhibitor CG-1521 in breast cancer. A mixture of starch and the drug dissolved in DMSO was used as the organic phase, while PVA dissolved in distilled water was used as the aqueous phase. The starch solution was added to the aqueous phase with a homogenizer under nitrogen at room temperature. Finally, SNPs were formed when DMSO was diffused by adding distilled water followed by stirring and the SNPs loaded with the drug were washed with distilled water [31]. In addition, SNPs loaded with conjugated linoleic acid (CLA) were synthesized by an emulsion method where Yang et al. used modified OSA waxy maize starch as the polymeric precursor of the SNPs and xanthan gum (XG) as a complex carrier to protect it. The aqueous phase consisted of the OSA starch and XG with different mass ratios kept under stirring and the organic phase contained the CLA. The emulsion was homogenized using a high shear mixer and passed twice through a high-pressure homogenizer. Finally, CLA-loaded SNPs were obtained by spray drying [81]. Also, Santander-Ortega et al. studied the capacity of SNPs as a drug delivery system using three different model drugs, flufenamic acid, testosterone, and caffeine. In this study, the organic phase was consisted of the corn starch derivative that was dissolved in ethyl acetate. This solution was added to an aqueous phase with different percentages of PVA obtaining a biphasic system that was emulsified with a high-speed homogenizer. Subsequently, highly purified water was added to force the complete diffusion of the organic solvent into the aqueous phase. The resulting SNPs were obtained when the organic solvent was completely evaporated [28].

Potato Starch

Dandekar et al. used potato starch for nanoparticles mediated delivery of docetaxel through the ME method. The docetaxel in ethanol and the potato starch in ethyl acetate were prepared and mixed homogeneously. These two solutions were mixed to obtain the organic phase that was poured into an aqueous solution of PVA and subsequently the mixture was emulsified with the help of a high-speed homogenizer. To facilitate the complete diffusion of the organic phase in the aqueous phase, purified water was added to increase the volume. Finally, the organic phase was completely evaporated [30].

Finally, when it comes to bioactive compounds, curcumin is one of the most studied due to its chemopreventive and therapeutic properties against many tumors [83]. Shahgholian et al. studied synthesized BSA based SNPs for encapsulation of curcumin using an ultrasonic atomization method for the synthesis of the SNPs. BSA binary compounds including BSA/capsule starch, BSA/national starch, BSA/chitosan were applied as carriers of the model drug. Curcumin was dissolved in ethanol and this solution was added to the aqueous biopolymer solution with stirring in a sealed beaker to form a thick emulsion. A high-frequency piezoelectric oscillator aerosolized the solution and the generated atomized droplets were blown through the hot glass drying chamber where the solvent was evaporated. The BSA SNPs loaded with curcumin were finally collected in the stainless-steel electrostatic collector [68]. Also, SNPs loaded with curcumin were synthesized using oxidized starch and simultaneously modified with cholesterol and imidazole (Cho-Imi-OS) by a simple dialysis method previously used by Xu et al. Cho-Imi-OS was dissolved in DMSO under stirring at high temperature in an oil bath. The model drug was dissolved in DMSO, and this was added dropwise to the starch solution under constant stirring. Then the mixture was transferred to a dialysis bag and dialyzed against phosphate buffer solution (PBS). Finally, the SNPs were washed with deionized water [41].

Indirect Encapsulation

In this case, the encapsulation is carried out just after the synthesis of the SNPs. Table 1.3 summarizes all the parameters discussed in this section for the indirect encapsulation of the SNPs.

Table 1.3. *Examples of recent studies of SNPs synthesis methods and encapsulation of different compounds through indirect encapsulation.*

Preparation Method	Type of Starch	Particle Size (nm)	Encapsulated Compound	Evaluation Method	Applications	Tested On	EE (%)	References
Dialysis	Potato + BS + OSA	5–200	Benzo[a]pyrene	Fenton reaction	Environmentally treatments	/	95	[39]
Sacrificial template	Pea, mung bean, corn and potato	30–300	Doxorubicin hydrochloride	UV-vis	Cancer therapy	AML12 and HepG2 cells in vitro	97.6	[48]
Ball milling	Water chestnut	271	Pediococcus acidolactici	Enumeration on MRS agar	Food applications	SIG, SIF	73	[53]
Microemulsion cross-linking	/	287	5-Fluorouracil	HPLC	Medical	Dialysis in a simulated digestive environment in vitro	49	[36]
Ultrasound w/ or w/o acid hydrolysis	Potato and corn	40/80	L-ascorbic acid and oxalic acid	HPLC	Food packaging, drug delivery, barrier coatings	/	/	[64]
Emulsion cross-linking	/	/	Ciprofloxacin	UV	/	Dialysis	52–94	[5]
Microemulsion cross-linking	/	94	Methylene blue	UV-vis	Medical	/	51–79	[34]
Acid hydrolysis /nanoprecipitation	Potato	82–180	Paclitaxel	UV-vis	Oral drug delivery	Mouse bone marrow cells	57–96	[20]
Microemulsion cross-linking	/	40–400	5-Aminosalicylic acid	UV-vis	Drug controlled release	Human HeLa cancer cells in vitro	/	[84]
Nanoprecipitation	Corn	140	Curcumin	UV-vis	Gastrointestinal tissue disorders	/	/	[85]

Nanoprecipitation	Corn	40–50	Polyphenols	UV-vis	Food applications	SIG, SIF	60–70	[21]
Nanoprecipitation	Corn	178	Urea	UV-vis	Dialysate regeneration system	/	95	[25]
High-speed jet	Tapioca	55.3–120	Myricetin	/	Food formulations	SIG, SIF in vitro	/	[71]
Ultrasounds and crystallization	Maize	351–468	Tangeretin	UV-vis	Food, pharmaceutical and cosmetic industries	Human microenvironments in vitro	74–83	[86]
Ball milling	Lotus stem, horse chestnut and water chestnut	419–797	Resveratrol	Spectrophotometry	Food and pharmaceutical sector	SIG, SIF digestion	76–81	[54]
Ultrasound and nanoprecipitation	Maize	65–390	Ardisia compressa anthocyanins	Differential pH method	Biodegradable food packaging or antioxidant additives	/	45–52	[87]

The most common methods used for the synthesis of SNPs before the encapsulation in the indirect encapsulation method, similar to the direct encapsulation method, are based on nanoprecipitation and also microemulsion crosslinking. At the same time, in addition to the SNPs synthesis method, the phase where the model drug is dissolved before the encapsulation may vary.

Bioactive Compound Dissolved in an Aqueous Solution

One of the most common procedures followed by many authors is to dissolve the drug in an aqueous solution. Liu et al. carried out a study on SNPs as carriers for polyphenols where the SNPs were synthesized through a simple nanoprecipitation method. Four types of polyphenols were used: catechin, epicatechin, epigallocatechin-3-gallate, and proanthocyanidins, dissolved in water. The loaded SNPs were prepared by adsorption experiments and incubated in tubes containing different volumes of polyphenol for different periods of time under constant shaking. Once these times were exceeded, the SNPs were washed three times with water [21]. Also, in 2018, Ding et al. prepared retrograded starch (RS III) nanoparticles for application as a wall material for colon-specific drug delivery by high-speed shearing emulsification using MBAA as the crosslinking agent. The retrograde SNPs were added to 5-fluorouracil (5-FU) aqueous solutions which is one of the common drugs for the treatment of colon cancer and finally, the 5-FU concentration was determined using high-performance liquid chromatography (HPLC) in order to obtain the loading capacity (LC) and the EE [36]. In addition, Shi et al. studied two different methods for drug loading: coating and adsorption method. Also, ciprofloxacin was used as the model drug since it is a commonly used antibiotic. The loading of the model drug through the coating method was carried out at the same time as the SNPs synthesis (direct encapsulation) by adding the ciprofloxacin into the emulsion aqueous phase containing the starch and the crosslinking agent. Nevertheless, through the adsorption method SNPs were dispersed into an aqueous solution containing the drug and the adsorption was allowed for 12 h. At last, in both cases, the concentration of ciprofloxacin was determined using UV spectrophotometry. Finally, compared to the coating method, the release of ciprofloxacin from the SNPs was faster when the adsorption method was used [5]. 5-Aminosalicylic acid (5-ASA), which is an anti-inflammatory agent used primarily to treat inflammatory bowel diseases, was used as a model drug to investigate drug loading and controlled release behaviour of crosslinked SNPs synthesized by a ME crosslinking method. SNPs were dispersed in boiled aqueous solution containing the drug with shaking for several days.

Subsequently, they were centrifuged and lyophilized to obtain the drug-loaded SNPs in order to determine the drug loading content [84]. Delsarte et al. prepared SNPs from OSA starch and 1,4-butane sultone (OSA-BS SNPs) by using the water dialyzed method for its use to solubilize benzo[a]pyrene (BaP) as a result of the degradation by Fenton process. The drug was introduced in dichloromethane solution and after the solvent evaporation, the starch aqueous solution was added at different concentrations. The results showed that the BaP was almost completely degraded, after the encapsulation and Fenton oxidation, which is a very promising result for developing an environmentally friendly treatment [39]. In a recent study Shabana et al. synthesized SNPs from modified potato starch using ultrasound-assisted and acid hydrolyzed ultrasound-assisted methods. Next, modified SNPs were coated with antioxidants since they improve food properties during its shelf-life. Two types of antioxidants (L-ascorbic acid and oxalic acid) were added to the SNPs solution and sonicated for half an hour. The antioxidant-laden starch pellet was collected and dried in an incubator [64]. Also, Wang et al. prepared SNPs based on the W/O ME method using epichlorohydrin as the crosslinking agent to investigate their drug loading and release properties with methylene blue (MB) as a model drug. SNPs were suspended in a glucose aqueous solution with different amounts of MB and the suspensions were then shaken at different temperatures and for different periods of time. Subsequently, the solutions were centrifuged, and 1 mL of each supernatant was extracted and diluted to a certain volume to determine the drug loading extent and EE [34].

Bioactive Compound Dissolved in Phosphate Buffer Solution

Another procedure followed by some authors is to dissolve the model drug into PBS since it maintains the required pH in the solution. Yang et al. encapsulated doxorubicin hydrochloride (DOX-HCl) into hollow SNPs that were synthesized through a hard template sacrifice process using gelled pea, mung bean, potato, and corn starches as the coat. A mixture of SNPs and DOX was dissolved in PBS and the solution was stirred for one day in the dark to fully charge the model drug. The suspension was centrifuged and washed with PBS to rule out DOX-HCl adsorbed on the surfaces of the SNPs [48]. In addition, oxidized starch nanoparticles (oxy-SNPs) were synthesized for urea adsorption in a recent study by Abidin et al. Urea solutions with different concentrations in PBS were prepared to maintain a neutral pH. SNPs were added to a flask containing the urea solution and the mixture was stirred for one day under ambient conditions. This study confirmed

the hypothesis that the oxy-SNPs presented significantly more active sites for the urea union than the typical oxy-starch [25].

Bioactive Compound Dissolved in an Organic Solution

The drug can also be dissolved into an organic phase. It could be both, into an organic solvent and also into an emulsion or an oily phase which will form an emulsion. In a recent study, Nyoo Putro et al. compared the drug LC of SNPs synthesized through nanoprecipitation and acid hydrolysis, in order to know which method may result in a higher LC. Also, different types of surfactants (CTAB, SDS, and Tween 20) were used to modify the SNPs and obtain the highest drug loading. The drug used in this study was paclitaxel, which was dissolved in ethanol at different concentrations, and mixed with the SNPs under stirring. The concentration of unbound paclitaxel was analyzed using UV-Vis spectrophotometry and the characterization of paclitaxel concentration was carried out by mixing drug solution with a mixture of PBS and ethanol [20]. Sufi-Maragheh et al. reported the use of amphiphilic crosslinked SNPs as a stabilizer for Pickering emulsion formulation which was then used for curcumin encapsulation. SNPs were prepared through the alkali freezing method followed by crosslinking by citric acid. The crosslinked SNPs were then dispersed in water at different contents and sonicated followed by the addition of an oil phase containing the curcumin dissolved at room temperature to the aqueous phase in order to form the solid particle-stabilized oil-in-water emulsions [85]. Ahmad et al. carried out a comparative study with native starch and SNPs synthesized through a ball milling mechanical method for the encapsulation of probiotic bacterial cells (*Pediococcus acidolactici*). A phase containing the starch dispersed in Milli-Q water was prepared and subsequently emulsified with the addition of vegetable oil and surfactant. This mixture was homogenized and the cell culture containing the bacteria was added under slow agitation. The study concluded that SNPs were not the optimal distribution vehicles for probiotics, making native starch a better alternative for this application [53].

1.4.3. Applications

SNPs are considered a good vehicle to improve the controlled release of many bioactives. Encapsulated bioactives have numerous applications in different fields such as medicine, cosmetics, biotechnology, or the food industry among others. In addition to Tables 1.2 and 1.3

where different applications of encapsulated bioactive compounds are summarized, a general schematic representation of different applications is shown below in Figure 1.14.

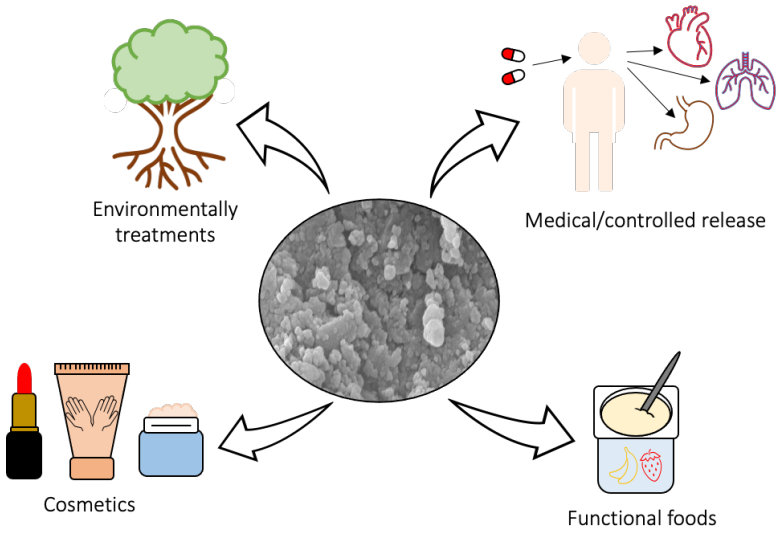

Figure 1.14. *Schematic representation of different fields in which SNPs can be used.*

Medical Applications

One of the main medical applications in which SNPs could be used is cancer therapy. In a recent study, Alp et al. demonstrated the advantages offered by the encapsulation of antitumor agents in polymeric nanoparticles for improving the solubility of the drug while protecting against rapid systemic metabolism to increase the time of exposure and reducing the toxicity. To measure the effectiveness of the encapsulated drug, the authors conducted tests with MCF-7 breast cancer cells. The data demonstrated that the encapsulation of CG-1521 in the SNPs improved the therapeutic efficacy against MCF-7 cells and suggested that this encapsulation technology may be useful for other hormone-dependent cancers [31].

Yang et al. also performed in vitro experiments with synthesized and antibiotic-loaded SNPs. They evaluated normal liver cells (AML12) and liver hepatocellular cells (HepG2) using MTT assays where it was revealed that SNPs had excellent biocompatibility for normal cells and hepatocellular cells. However, the free drug showed greater antitumor efficacy than particles charged to HepG2 cells due to direct contact with cancer cells, although loaded SNPs showed to release the drug more slowly. On the other hand, they also demonstrated that the viability of AML12 cells was greater than that of HepG2 cells for the different concentrations of the antibiotics studied [48].

Wang et al. also demonstrated the efficacy of SNPs as drug delivery systems. Experiments were carried out in rats by oral administration of the drug or the drug-loaded SNPs as well as the drug directly on the starch and blood samples were collected for the analysis. The mean values obtained for the residence time of the particles were not significantly different from those of the raw paclitaxel. It was concluded that the preparation method of SNPs had a very significant effect on the bioavailability of paclitaxel and that the improving effect for SNPs was better than when the drug directly loaded on starch. Therefore, the preparation of SNPs is an effective way to improve the bioavailability of paclitaxel [78].

Recently, Xu et al. evaluated the cellular absorption capacity of SNPs using a human lung cancer cell line A549 using curcumin as a control group. Cytotoxicity tests were carried out using free curcumin, which showed limited efficacy against cancer cells. Compared to free curcumin, the SNPs showed an inhibitory effect on cancer cells and the results indicated that these particles as drug-bearing material were not cytotoxic at the required concentrations and could be a promising drug delivery system for the lung cancer cells, acting as an effective vehicle to target and administer medications to the tumor site [41].

Dandekar et al. also demonstrated the safety and efficacy of drug-loaded SNPs as an effective but safe anticancer treatment through cellular cytotoxicity assays using Caco-2 cells. The efficacy of the free drug was studied, and both were analyzed at equimolar concentration. The authors performed the tests during the exponential growth phase of the cells in order to provide an unequivocal indication of any type of cellular toxicity. The effect of the drug on cancer cells was, in turn, compared to that of non-cancer cells using the same test conditions. Finally, the possibility and efficacy of propyl starch to encapsulate and control the release of hydrophobic anticancer agents such as docetaxel in nanocarriers were confirmed [30].

In a most general medical field of application, some authors also carried out tests to determine the functioning of SNPs loaded with drugs to verify their functionality as drug delivery vehicles. El-Naggar et al. conducted a histological pathology study on rat skin to confirm whether the formulation was tolerated without symptoms of skin irritation. They coated the skin of rats was with the gel having DFS as the drug which was loaded in the cross-linked SNPs and the results were compared with control where the skin of the rats was not coated. Finally, the study revealed that the SNPs loaded with the drug did not show any harmful effect on the skin of the rats and that

therefore they could be considered as a good vehicle for treat rheumatoid disorders and other chronic inflammatory diseases [14].

Food Applications

Among food applications, Ahmad et al. recently studied the release of catechin from SNPs to retain the properties of the bioactive compound throughout simulated gastric and intestinal conditions. The SNPs protected catechin against the hostile gastric environment and helped to retain its bioactive properties during the in vitro digestion process [57]. Ahmad et al. also performed in vitro studies on the viability of probiotic-loaded SNPs. The study was carried out under simulated gastrointestinal and processing conditions, using both gastric juice and simulated intestinal fluid. However, in this case, it was concluded that SNPs are not good vehicles for probiotics since it was shown that the particles were too small to encapsulate the probiotic cells within them and, therefore, they were immediately released into the simulated gastric or intestinal solutions that lead to cell death due to the harsh conditions of these environments [53]. In another study carried out by Nieto-Suaza et al. recently, different food simulators were used to evaluate curcumin release profiles, where some intended to simulate highly hydrophilic foods and others intended to simulate highly lipophilic foods. The authors concluded that the released curcumin was favored in lipophilic substances and can be controlled by reducing the polarity of the SNPs [18]. Also, Liu et al. investigated the in vitro release of SNPs loaded with polyphenols in simulated gastric and intestinal juices. This study showed sustained release profiles of polyphenols from SNPs and suggested that SNPs may be promising and effective nanocarriers to protect bioactive compounds against sensitive environments and control their release [21].

1.4.4. Future Research Perspectives

Among the methods mentioned in previous sections, there are other types of preparation methods for NPs that have been explored recently from which promising results were obtained, such as enzymatic hydrolysis, which has been used to produce SNPs for application as stabilizers of Pickering emulsions [88, 89]. Recrystallization is another physical method to prepare SNPs with a clear environmental advantage since it does not use solvents during the preparation process, it is based on a molecular reassociation during a cooling or drying process to produce starch gel [90]. In addition, ultrasound as a unique technique, has been used to produce SNPs combined with other

conventional techniques [91]. Plasma had also been used as a preparation technique for SNPs providing a promising method to develop SNPs with low crystallinity [92].

During the last years, SNPs preparation methods have been focused on the use of green technology which could reduce or even eliminate the use of organic solvents that could have negative effects on further SNPs applications or even reduce their potential applications. Moreover, the reduction of the use of solvents will have a positive effect from an environmental point of view.

Moreover, in recent years, the interest in SNPs has been increased since apart from the mentioned applications such as Pickering emulsions preparation, other applications are being investigated with some preliminary promising results [6]. The treatment of tumor cells by targeted delivery is one major potential for the SNPs since they present a large area/volume ratio which makes them suitable for the delivery of bioactive compounds as well as drugs. Moreover, the molecular structure of the main compounds of starch allows to easily attach many types of proteins, bioactive compounds, or antibodies which will be a promising approach for specific delivery and avoiding systemic effects [93]. Hence, starch not only presents a promising alternative as nanostructured systems but also present clear advantages as therapeutic systems [94]. Also, another promising application of SNPs is in DNA precipitation where SNPs interact with DNA and result in precipitation in an ethanol solution at room temperature [95].

Furthermore, the emerging applications of SNPs include their use for sensor development. Filter paper has been coated with pyrene modified SNPs and tested as a fluorescence quenching sensor platform. Nitroaromatic compounds were detected with good limits of detection and selectivity over non-nitrated aromatics, amines, and aromatic ketones [96]. Also, in recent studies, nanocomposites prepared with potato starch and ZnS quantum dots were used as a sensor for Pb^{2+} and Cu^{2+} ions. The detection was based on the decreased emission intensity of the photoluminescent spectral bands [97].

Even with the numerous advantages and applications of SNPs, their production is poorly industrialized on a large scale. As it is the case of the other types of NPs, for which the techno-economic production analysis has been described in other works [98], the first step will be the collection of information from the laboratory experiments to identify the main streams and processes. Further pilot plant experiments should be designed in order to have data related to the

scale-up production, energy requirements, and raw material required. Further major unit operations are needed to be defined and designed, as well as main process streams.

1.4.5. Conclusions

Currently, the field of nanoparticles is experiencing a great expansion in terms of scientific research due to its great potentials as nanocarriers in different bioapplications in fields as medicine, cosmetics, or food. SNPs offer a clear advantage compared to the other types of nanoparticles due to their high biocompatibility and versatility since there is a wide range of potential synthesis methods that allow the controlling of the final shape properties such as and size and size distribution.

SNPs have been synthesized through different synthesis methods using starches from several sources. Usually, both the synthesis method and the type of starch will affect the final properties of the nanoparticles, as well as their capacity for encapsulation. Maize starch is one of the most commonly used for SNPs synthesis both individually or in combination with other starches, such as potato, pea, or mung bean, which has shown to led to small particle sizes. Both nanoprecipitation and ME methods allow obtaining SNPs with target small sizes.

SNPs have been used to encapsulate bioactive compounds for controlled release in different biomedical applications such as drug administration, enzyme inhibition process, and even DNA precipitation.

The EE of the bioactive compounds did not vary significantly when the encapsulation was performed directly or indirectly and therefore, it was concluded that the encapsulation method does not influence the amount of bioactive compound encapsulated in the SNPs. Nevertheless, the type of starch selected has shown to have a major influence since higher encapsulation efficiencies were obtained when maize starch was used for the SNPs synthesis with both encapsulation methods.

It has been demonstrated through in vivo and in vitro experiments that SNPs are a good vehicle for the controlled release of bioactive compounds and the use of these loaded SNPs are promising agents to encapsulate drugs and antitumor agents that could be used in therapy. However, there is still not enough research performed on the characterization of the SNPs for in vivo drug delivery formulations which is necessary to study the possible interactions with the human body and their

consequences in order to determine how SNPs will adversely affect human health in short and long terms.

The main disadvantage of SNPs is that their synthesis process is not scaled up yet. Even some pilot plant processes have been designed for SNPs preparation, there is still further research necessary to develop more novel methods that will allow obtaining large-scale production of SNPs with control on the final particle size. Moreover, the studies found regarding the preparation of SNPs containing encapsulated bioactive compounds have not yet been industrialized and future research is necessary in order to obtain satisfactory bioactive or drug-loaded SNPs on a large scale.

- **References**

[1] D. Le Corre, J. Bras, and A. Dufresne, "Starch nanoparticles: A review," *Biomacromolecules*, vol. 11, no. 5. pp. 1139–1153, May 10, 2010. doi: 10.1021/bm901428y.

[2] S. Bel Haaj, A. Magnin, C. Pétrier, and S. Boufi, "Starch nanoparticles formation via high power ultrasonication," *Carbohydr Polym*, vol. 92, no. 2, pp. 1625–1632, Feb. 2013, doi: 10.1016/j.carbpol.2012.11.022.

[3] M. N. Tahir *et al.*, "Facile synthesis and characterization of monocrystalline cubic ZrO2 nanoparticles," *Solid State Sci*, vol. 9, no. 12, pp. 1105–1109, Dec. 2007, doi: 10.1016/j.solidstatesciences.2007.07.033.

[4] J. Salonen *et al.*, "Mesoporous silicon microparticles for oral drug delivery: Loading and release of five model drugs," *Journal of Controlled Release*, vol. 108, no. 2–3, pp. 362–374, Nov. 2005, doi: 10.1016/j.jconrel.2005.08.017.

[5] A. Shi, D. Li, H. Liu, B. Adhikari, and Q. Wang, "Effect of drying and loading methods on the release behavior of ciprofloxacin from starch nanoparticles," *Int J Biol Macromol*, vol. 87, pp. 55–61, Jun. 2016, doi: 10.1016/j.ijbiomac.2016.02.038.

[6] A. Caldonazo, S. L. Almeida, A. F. Bonetti, R. E. L. Lazo, M. Mengarda, and F. S. Murakami, "Pharmaceutical applications of starch nanoparticles: A scoping review," *International Journal of Biological Macromolecules*, vol. 181. Elsevier B.V., pp. 697–704, Jun. 30, 2021. doi: 10.1016/j.ijbiomac.2021.03.061.

[7] P. H. Campelo, A. S. Sant'Ana, and M. T. Pedrosa Silva Clerici, "Starch nanoparticles: production methods, structure, and properties for food applications," *Current Opinion in Food Science*, vol. 33. Elsevier Ltd, pp. 136–140, Jun. 01, 2020. doi: 10.1016/j.cofs.2020.04.007.

[8] A. Jayakumar *et al.*, "Starch-PVA composite films with zinc-oxide nanoparticles and phytochemicals as intelligent pH sensing wraps for food packaging application," *Int J Biol Macromol*, vol. 136, pp. 395–403, Sep. 2019, doi: 10.1016/j.ijbiomac.2019.06.018.

[9] A. K. Jain, R. K. Khar, F. J. Ahmed, and P. V. Diwan, "Effective insulin delivery using starch nanoparticles as a potential trans-nasal mucoadhesive carrier," *European Journal of Pharmaceutics and Biopharmaceutics*, vol. 69, no. 2, pp. 426–435, Jun. 2008, doi: 10.1016/j.ejpb.2007.12.001.

[10] R. Jain *et al.*, "Enhanced cellular delivery of idarubicin by surface modification of propyl starch nanoparticles employing pteroic acid conjugated polyvinyl alcohol," *Int J Pharm*, vol. 420, no. 1, pp. 147–155, Nov. 2011, doi: 10.1016/j.ijpharm.2011.08.030.

[11] R. Wang, "The chemistry of nanomaterials - C. N. R. Rao, A. M□ller, A. K. Cheetham (eds), Wiley-VCH Verlag GmbH & Co. KGaA, Weinheim 2004. ISBN 3-527-30686-2, 741 pages," *Colloid Polym Sci*, vol. 283, no. 2, pp. 234–234, Dec. 2004, doi: 10.1007/s00396-004-1140-1.

[12] S. B. Sant, "Nanoparticles: From Theory to Applications," *Materials and Manufacturing Processes*, vol. 27, no. 12, pp. 1462–1463, Dec. 2012, doi: 10.1080/10426914.2012.663137.

[13] H. Y. Kim, S. S. Park, and S. T. Lim, "Preparation, characterization and utilization of starch nanoparticles," *Colloids and Surfaces B: Biointerfaces*, vol. 126. Elsevier, pp. 607–620, Feb. 01, 2015. doi: 10.1016/j.colsurfb.2014.11.011.

[14] M. E. El-Naggar, M. H. El-Rafie, M. A. El-sheikh, G. S. El-Feky, and A. Hebeish, "Synthesis, characterization, release kinetics and toxicity profile of drug-loaded starch nanoparticles," *Int J Biol Macromol*, vol. 81, pp. 718–729, Nov. 2015, doi: 10.1016/j.ijbiomac.2015.09.005.

[15] C. Qiu *et al.*, "Preparation and characterization of essential oil-loaded starch nanoparticles formed by short glucan chains," *Food Chem*, vol. 221, pp. 1426–1433, Apr. 2017, doi: 10.1016/j.foodchem.2016.11.009.

[16] S. H. Mahmoudi Najafi, M. Baghaie, and A. Ashori, "Preparation and characterization of acetylated starch nanoparticles as drug carrier: Ciprofloxacin as a model," *Int J Biol Macromol*, vol. 87, pp. 48–54, Jun. 2016, doi: 10.1016/j.ijbiomac.2016.02.030.

[17] L. Acevedo-Guevara, L. Nieto-Suaza, L. T. Sanchez, M. I. Pinzon, and C. C. Villa, "Development of native and modified banana starch nanoparticles as vehicles for curcumin," *Int J Biol Macromol*, vol. 111, pp. 498–504, May 2018, doi: 10.1016/j.ijbiomac.2018.01.063.

[18] L. Nieto-Suaza, L. Acevedo-Guevara, L. T. Sánchez, M. I. Pinzón, and C. C. Villa, "Characterization of Aloe vera-banana starch composite films reinforced with curcumin-loaded starch nanoparticles," *Food Structure*, vol. 22, Oct. 2019, doi: 10.1016/j.foostr.2019.100131.

[19] Y. Fu, J. Yang, L. Jiang, L. Ren, and J. Zhou, "Encapsulation of Lutein into Starch Nanoparticles to Improve Its Dispersity in Water and Enhance Stability of Chemical Oxidation," *Starch/Staerke*, vol. 71, no. 5–6, May 2019, doi: 10.1002/star.201800248.

[20] J. N. Putro, S. Ismadji, C. Gunarto, F. E. Soetaredjo, and Y. H. Ju, "A study of anionic, cationic, and nonionic surfactants modified starch nanoparticles for hydrophobic drug loading and release," *J Mol Liq*, vol. 298, Jan. 2020, doi: 10.1016/j.molliq.2019.112034.

[21] C. Liu *et al.*, "Adsorption mechanism of polyphenols onto starch nanoparticles and enhanced antioxidant activity under adverse conditions," *J Funct Foods*, vol. 26, pp. 632–644, Oct. 2016, doi: 10.1016/j.jff.2016.08.036.

[22] J. Singh, L. Kaur, and O. J. McCarthy, "Factors influencing the physico-chemical, morphological, thermal and rheological properties of some chemically modified starches for food applications-A review," *Food Hydrocolloids*, vol. 21, no. 1. pp. 1–22, Jan. 2007. doi: 10.1016/j.foodhyd.2006.02.006.

[23] S. F. Chin, S. C. Pang, and S. H. Tay, "Size controlled synthesis of starch nanoparticles by a simple nanoprecipitation method," *Carbohydr Polym*, vol. 86, no. 4, pp. 1817–1819, Oct. 2011, doi: 10.1016/j.carbpol.2011.07.012.

[24] G. Gutiérrez, D. Morán, A. Marefati, J. Purhagen, M. Rayner, and M. Matos, "Synthesis of controlled size starch nanoparticles (SNPs)," *Carbohydr Polym*, vol. 250, Dec. 2020, doi: 10.1016/j.carbpol.2020.116938.

[25] M. N. Z. Abidin *et al.*, "Highly adsorptive oxidized starch nanoparticles for efficient urea removal," *Carbohydr Polym*, vol. 201, pp. 257–263, Dec. 2018, doi: 10.1016/j.carbpol.2018.08.069.

[26] S. F. Chin, A. Azman, and S. C. Pang, "Size controlled synthesis of starch nanoparticles by a microemulsion method," *J Nanomater*, vol. 2014, 2014, doi: 10.1155/2014/763736.

[27] N. S. Ismail and S. C. B. Gopinath, "Enhanced antibacterial effect by antibiotic loaded starch nanoparticle," *Journal of the Association of Arab Universities for Basic and Applied Sciences*, vol. 24, no. 1, pp. 136–140, Oct. 2017, doi: 10.1016/j.jaubas.2016.10.005.

[28] M. J. Santander-Ortega *et al.*, "Nanoparticles made from novel starch derivatives for transdermal drug delivery," *Journal of Controlled Release*, vol. 141, no. 1, pp. 85–92, Jan. 2010, doi: 10.1016/j.jconrel.2009.08.012.

[29] S.-W. Choi, H.-Y. Kwon, W.-S. Kim, and J.-H. Kim, "Thermodynamic parameters on poly(D,L-lactide-co-glycolide) particle size in emulsification-diffusion process," 2002. [Online]. Available: www.elsevier.com/locate/colsurfa

[30] P. Dandekar *et al.*, "A Hydrophobic Starch Polymer for Nanoparticle-Mediated Delivery of Docetaxel," *Macromol Biosci*, vol. 12, no. 2, pp. 184–194, Feb. 2012, doi: 10.1002/mabi.201100244.

[31] E. Alp, F. Damkaci, E. Guven, and M. Tenniswood, "Starch nanoparticles for delivery of the histone deacetylase inhibitor CG-1521 in breast cancer treatment," *Int J Nanomedicine*, vol. 14, pp. 1335–1346, 2019, doi: 10.2147/IJN.S191837.

[32] Y. yuan Fang *et al.*, "Preparation of crosslinked starch microspheres and their drug loading and releasing properties," *Carbohydr Polym*, vol. 74, no. 3, pp. 379–384, Nov. 2008, doi: 10.1016/j.carbpol.2008.03.005.

[33] O. Franssen and W. E. Hennink, "A novel preparation method for polymeric microparticles without the use of organic solvents," 1998.

[34] X. Wang, H. Chen, Z. Luo, and X. Fu, "Preparation of starch nanoparticles in water in oil microemulsion system and their drug delivery properties," *Carbohydr Polym*, vol. 138, pp. 192–200, Mar. 2016, doi: 10.1016/j.carbpol.2015.11.006.

[35] A. M. Shi, D. Li, L. J. Wang, B. Z. Li, and B. Adhikari, "Preparation of starch-based nanoparticles through high-pressure homogenization and miniemulsion cross-linking: Influence of various process parameters on particle size and stability," *Carbohydr Polym*, vol. 83, no. 4, pp. 1604–1610, Feb. 2011, doi: 10.1016/j.carbpol.2010.10.011.

[36] Y. Ding, Q. Lin, and J. Kan, "Development and characteristics nanoscale retrograded starch as an encapsulating agent for colon-specific drug delivery," *Colloids Surf B Biointerfaces*, vol. 171, pp. 656–667, Nov. 2018, doi: 10.1016/j.colsurfb.2018.08.007.

[37] L. Chronopoulou, I. Fratoddi, C. Palocci, I. Venditti, and M. V. Russo, "Osmosis based method drives the self-assembly of polymeric chains into micro-and nanostructures," *Langmuir*, vol. 25, no. 19, pp. 11940–11946, Oct. 2009, doi: 10.1021/la9016382.

[38] J. P. Rao and K. E. Geckeler, "Polymer nanoparticles: Preparation techniques and size-control parameters," *Progress in Polymer Science (Oxford)*, vol. 36, no. 7. Elsevier Ltd, pp. 887–913, 2011. doi: 10.1016/j.progpolymsci.2011.01.001.

[39] I. Delsarte, F. Delattre, C. Rafin, and E. Veignie, "Investigations of benzo[a]pyrene encapsulation and Fenton degradation by starch nanoparticles," *Carbohydr Polym*, vol. 186, pp. 344–349, Apr. 2018, doi: 10.1016/j.carbpol.2018.01.037.

[40] H. Namazi, F. Fathi, and A. Dadkhah, "Hydrophobically modified starch using long-chain fatty acids for preparation of nanosized starch particles," *Scientia Iranica*, vol. 18, no. 3 C, pp. 439–445, 2011, doi: 10.1016/j.scient.2011.05.006.

[41] Y. Xu *et al.*, "pH-Responsive nanoparticles based on cholesterol/imidazole modified oxidized-starch for targeted anticancer drug delivery," *Carbohydr Polym*, vol. 233, Apr. 2020, doi: 10.1016/j.carbpol.2020.115858.

[42] S. D. Steichen, M. Caldorera-Moore, and N. A. Peppas, "A review of current nanoparticle and targeting moieties for the delivery of cancer therapeutics," *European Journal of Pharmaceutical Sciences*, vol. 48, no. 3. Elsevier B.V., pp. 416–427, Feb. 14, 2013. doi: 10.1016/j.ejps.2012.12.006.

[43] J. Hu, M. Chen, X. Fang, and L. Wu, "Fabrication and application of inorganic hollow spheres," *Chem Soc Rev*, vol. 40, no. 11, pp. 5472–5491, 2011, doi: 10.1039/C1CS15103G.

[44] J. Qi *et al.*, "Multi-shelled hollow micro-/nanostructures," *Chem Soc Rev*, vol. 44, no. 19, pp. 6749–6773, 2015, doi: 10.1039/C5CS00344J.

[45] T. Nakashima and N. Kimizuka, "Interfacial synthesis of hollow TiO2 microspheres in ionic liquids," *J Am Chem Soc*, vol. 125, no. 21, pp. 6386–6387, May 2003, doi: 10.1021/ja034954b.

[46] X. Sun, J. Liu, and Y. Li, "Use of Carbonaceous Polysaccharide Microspheres as Templates for Fabricating Metal Oxide Hollow Spheres," *Chemistry – A European Journal*, vol. 12, no. 7, pp. 2039–2047, Feb. 2006, doi: https://doi.org/10.1002/chem.200500660.

[47] Y. Yin, Y. Lu, B. Gates, and Y. Xia, "Template-assisted self-assembly: A practical route to complex aggregates of monodispersed colloids with well-defined sizes, shapes, and structures," *J Am Chem Soc*, vol. 123, no. 36, pp. 8718–8729, Sep. 2001, doi: 10.1021/ja011048v.

[48] J. Yang *et al.*, "Fabrication and characterization of hollow starch nanoparticles by gelation process for drug delivery application," *Carbohydr Polym*, vol. 173, pp. 223–232, Oct. 2017, doi: 10.1016/j.carbpol.2017.06.006.

[49] L. Dai, C. Li, J. Zhang, and F. Cheng, "Preparation and characterization of starch nanocrystals combining ball milling with acid hydrolysis," *Carbohydr Polym*, vol. 180, pp. 122–127, Jan. 2018, doi: 10.1016/j.carbpol.2017.10.015.

[50] S. Deng, R. Huang, M. Zhou, F. Chen, and Q. Fu, "Hydrophobic cellulose films with excellent strength and toughness via ball milling activated acylation of microfibrillated cellulose," *Carbohydr Polym*, vol. 154, pp. 129–138, Dec. 2016, doi: 10.1016/j.carbpol.2016.07.101.

[51] K. Ramadhan and T. J. Foster, "Effects of ball milling on the structural, thermal, and rheological properties of oat bran protein flour," *J Food Eng*, vol. 229, pp. 50–56, Jul. 2018, doi: 10.1016/j.jfoodeng.2017.10.024.

[52] L. Protesescu, S. Yakunin, O. Nazarenko, D. N. Dirin, and M. V. Kovalenko, "Low-Cost Synthesis of Highly Luminescent Colloidal Lead Halide Perovskite Nanocrystals by Wet Ball Milling," *ACS Appl Nano Mater*, vol. 1, no. 3, pp. 1300–1308, Mar. 2018, doi: 10.1021/acsanm.8b00038.

[53] M. Ahmad, A. Gani, F. Hamed, and S. Maqsood, "Comparative study on utilization of micro and nano sized starch particles for encapsulation of camel milk derived probiotics (Pediococcus acidolactici)," *LWT*, vol. 110, pp. 231–238, Aug. 2019, doi: 10.1016/j.lwt.2019.04.078.

[54] M. Ahmad and A. Gani, "Ultrasonicated resveratrol loaded starch nanocapsules: Characterization, bioactivity and release behaviour under in-vitro digestion," *Carbohydr Polym*, vol. 251, Jan. 2021, doi: 10.1016/j.carbpol.2020.117111.

[55] N. Li, M. Niu, B. Zhang, S. Zhao, S. Xiong, and F. Xie, "Effects of concurrent ball milling and octenyl succinylation on structure and physicochemical properties of starch," *Carbohydr Polym*, vol. 155, pp. 109–116, Jan. 2017, doi: 10.1016/j.carbpol.2016.08.063.

[56] H. Lin, L. Z. Qin, H. Hong, and Q. Li, "Preparation of Starch Nanoparticles via High-Energy Ball Milling," *Journal of Nano Research*, vol. 40, pp. 174–179, 2016, doi: 10.4028/www.scientific.net/JNanoR.40.174.

[57] M. Ahmad, P. Mudgil, A. Gani, F. Hamed, F. A. Masoodi, and S. Maqsood, "Nano-encapsulation of catechin in starch nanoparticles: Characterization, release behavior and bioactivity retention during simulated in-vitro digestion," *Food Chem*, vol. 270, pp. 95–104, Jan. 2019, doi: 10.1016/j.foodchem.2018.07.024.

[58] N. M. C. Da Silva, P. R. C. Correia, J. I. Druzian, F. M. Fakhouri, R. L. L. Fialho, and E. C. M. C. De Albuquerque, "PBAT/TPS Composite Films Reinforced with Starch Nanoparticles Produced by Ultrasound," *Int J Polym Sci*, vol. 2017, 2017, doi: 10.1155/2017/4308261.

[59] Y. Chang, X. Yan, Q. Wang, L. Ren, J. Tong, and J. Zhou, "High efficiency and low cost preparation of size controlled starch nanoparticles through ultrasonic treatment and precipitation," *Food Chem*, vol. 227, pp. 369–375, Jul. 2017, doi: 10.1016/j.foodchem.2017.01.111.

[60] M. A. El-Sheikh, "New technique in starch nanoparticles synthesis," *Carbohydr Polym*, vol. 176, pp. 214–219, Nov. 2017, doi: 10.1016/j.carbpol.2017.08.033.

[61] H. Angellier, J.-L. Putaux, S. Molina-Boisseau, D. Dupeyre, and A. Dufresne, "Starch Nanocrystal Fillers in an Acrylic Polymer Matrix," *Macromol Symp*, vol. 221, no. 1, pp. 95–104, Jan. 2005, doi: https://doi.org/10.1002/masy.200550310.

[62] D. C. Aldao, E. Šárka, P. Ulbrich, and E. Menšiková, "Starch nanoparticles – Two ways of their preparation," *Czech Journal of Food Sciences*, vol. 36, no. 2, pp. 133–138, 2018, doi: 10.17221/371/2017-CJFS.

[63] X. Ma, R. Jian, P. R. Chang, and J. Yu, "Fabrication and characterization of citric acid-modified starch nanoparticles/plasticized-starch composites," *Biomacromolecules*, vol. 9, no. 11, pp. 3314–3320, Nov. 2008, doi: 10.1021/bm800987c.

[64] S. Shabana, R. Prasansha, I. Kalinina, I. Potoroko, U. Bagale, and S. H. Shirish, "Ultrasound assisted acid hydrolyzed structure modification and loading of antioxidants on potato starch nanoparticles," *Ultrason Sonochem*, vol. 51, pp. 444–450, Mar. 2019, doi: 10.1016/j.ultsonch.2018.07.023.

[65] F. Barreras, H. Amaveda, and A. Lozano, "Transient high-frequency ultrasonic water atomization," *Exp Fluids*, vol. 33, no. 3, pp. 405–413, 2002, doi: 10.1007/s00348-002-0456-1.

[66] K. A. Ramisetty, A. B. Pandit, and P. R. Gogate, "Investigations into ultrasound induced atomization," *Ultrason Sonochem*, vol. 20, no. 1, pp. 254–264, 2013, doi: 10.1016/j.ultsonch.2012.05.001.

[67] B. Avvaru, M. N. Patil, P. R. Gogate, and A. B. Pandit, "Ultrasonic atomization: Effect of liquid phase properties," *Ultrasonics*, vol. 44, no. 2, pp. 146–158, Feb. 2006, doi: 10.1016/j.ultras.2005.09.003.

[68] N. Shahgholian and G. Rajabzadeh, "Preparation of BSA nanoparticles and its binary compounds via ultrasonic piezoelectric oscillator for curcumin encapsulation," *J Drug Deliv Sci Technol*, vol. 54, Dec. 2019, doi: 10.1016/j.jddst.2019.101323.

[69] W. Xia *et al.*, "Advanced technology for nanostarches preparation by high speed jet and its mechanism analysis," *Carbohydr Polym*, vol. 176, pp. 127–134, Nov. 2017, doi: 10.1016/j.carbpol.2017.08.072.

[70] W. Xia *et al.*, "Effect of high speed jet on the physical properties of tapioca starch," *Food Hydrocoll*, vol. 49, pp. 35–41, Jul. 2015, doi: 10.1016/j.foodhyd.2015.03.010.

[71] W. Xia, B. Zheng, T. Li, F. Lian, Y. Lin, and R. Liu, "Fabrication, characterization and evaluation of myricetin adsorption onto starch nanoparticles," *Carbohydr Polym*, vol. 250, Dec. 2020, doi: 10.1016/j.carbpol.2020.116848.

[72] M. K. Remanan and F. Zhu, "Encapsulation of rutin using quinoa and maize starch nanoparticles," *Food Chem*, 2020, doi: 10.1016/j.foodchem.2020.128534.

[73] T. M. T. Vo *et al.*, "Rice starch coated iron oxide nanoparticles: A theranostic probe for photoacoustic imaging-guided photothermal cancer therapy," *Int J Biol Macromol*, vol. 183, pp. 55–67, Jul. 2021, doi: 10.1016/j.ijbiomac.2021.04.053.

[74] R. Chang *et al.*, "Fabrication and characterization of hollow starch nanoparticles by heterogeneous crystallization of debranched starch in a nanoemulsion system," *Food Chem*, vol. 323, p. 126851, Sep. 2020, doi: 10.1016/j.foodchem.2020.126851.

[75] M. Ahmad, A. Gani, F. A. Masoodi, and S. H. Rizvi, "Influence of ball milling on the production of starch nanoparticles and its effect on structural, thermal and functional properties," *Int J Biol Macromol*, vol. 151, pp. 85–91, May 2020, doi: 10.1016/j.ijbiomac.2020.02.139.

[76] C. Qiu, C. Wang, C. Gong, D. J. McClements, Z. Jin, and J. Wang, "Advances in research on preparation, characterization, interaction with proteins, digestion and delivery systems of starch-based nanoparticles," *International Journal of Biological Macromolecules*, vol. 152. Elsevier B.V., pp. 117–125, Jun. 01, 2020. doi: 10.1016/j.ijbiomac.2020.02.156.

[77] M. Borgogna, B. Bellich, L. Zorzin, R. Lapasin, and A. Cesàro, "Food microencapsulation of bioactive compounds: Rheological and thermal characterisation of non-conventional gelling system," *Food Chem*, vol. 122, no. 2, pp. 416–423, Sep. 2010, doi: 10.1016/j.foodchem.2009.07.043.

[78] L. Wang *et al.*, "Loading paclitaxel into porous starch in the form of nanoparticles to improve its dissolution and bioavailability," *Int J Biol Macromol*, vol. 138, pp. 207–214, Oct. 2019, doi: 10.1016/j.ijbiomac.2019.07.083.

[79] P. Nallasamy, T. Ramalingam, T. Nooruddin, R. Shanmuganathan, P. Arivalagan, and S. Natarajan, "Polyherbal drug loaded starch nanoparticles as promising drug delivery system: Antimicrobial, antibiofilm and neuroprotective studies," *Process Biochemistry*, vol. 92, pp. 355–364, May 2020, doi: 10.1016/j.procbio.2020.01.026.

[80] S. A. Kheradvar, J. Nourmohammadi, H. Tabesh, and B. Bagheri, "Starch nanoparticle as a vitamin E-TPGS carrier loaded in silk fibroin-poly(vinyl alcohol)-Aloe vera nanofibrous dressing," *Colloids Surf B Biointerfaces*, vol. 166, pp. 9–16, Jun. 2018, doi: 10.1016/j.colsurfb.2018.03.004.

[81] J. Yang *et al.*, "Conjugated linoleic acid loaded starch-based emulsion nanoparticles: In vivo gastrointestinal controlled release," *Food Hydrocoll*, vol. 101, Apr. 2020, doi: 10.1016/j.foodhyd.2019.105477.

[82] M. Bhatia and S. Rohilla, "Formulation and optimization of quinoa starch nanoparticles: Quality by design approach for solubility enhancement of piroxicam," *Saudi Pharmaceutical Journal*, vol. 28, no. 8, pp. 927–935, Aug. 2020, doi: 10.1016/j.jsps.2020.06.013.

[83] R. K. Maheshwari, A. K. Singh, J. Gaddipati, and R. C. Srimal, "Multiple biological activities of curcumin: A short review," in *Life Sciences*, Mar. 2006, pp. 2081–2087. doi: 10.1016/j.lfs.2005.12.007.

[84] J. Yang, Y. Huang, C. Gao, M. Liu, and X. Zhang, "Fabrication and evaluation of the novel reduction-sensitive starch nanoparticles for controlled drug release," *Colloids Surf B Biointerfaces*, vol. 115, pp. 368–376, Mar. 2014, doi: 10.1016/j.colsurfb.2013.12.007.

[85] P. Sufi-Maragheh, N. Nikfarjam, Y. Deng, and N. Taheri-Qazvini, "Pickering emulsion stabilized by amphiphilic pH-sensitive starch nanoparticles as therapeutic containers," *Colloids Surf B Biointerfaces*, vol. 181, pp. 244–251, Sep. 2019, doi: 10.1016/j.colsurfb.2019.05.046.

[86] Y. Hu, Y. Qin, C. Qiu, X. Xu, Z. Jin, and J. Wang, "Ultrasound-assisted self-assembly of β-cyclodextrin/debranched starch nanoparticles as promising carriers of tangeretin," *Food Hydrocoll*, vol. 108, Nov. 2020, doi: 10.1016/j.foodhyd.2020.106021.

[87] A. A. Escobar-Puentes, A. García-Gurrola, S. Rincón, A. Zepeda, and F. Martínez-Bustos, "Effect of amylose/amylopectin content and succinylation on properties of corn starch nanoparticles as encapsulants of anthocyanins," *Carbohydr Polym*, vol. 250, Dec. 2020, doi: 10.1016/j.carbpol.2020.116972.

[88] C. Qiu *et al.*, "A review of green techniques for the synthesis of size-controlled starch-based nanoparticles and their applications as nanodelivery systems," *Trends in Food Science and Technology*, vol. 92. Elsevier Ltd, pp. 138–151, Oct. 01, 2019. doi: 10.1016/j.tifs.2019.08.007.

[89] X. Lin, S. Sun, B. Wang, B. Zheng, and Z. Guo, "Structural and physicochemical properties of lotus seed starch nanoparticles," *Int J Biol Macromol*, vol. 157, pp. 240–246, Aug. 2020, doi: 10.1016/j.ijbiomac.2020.04.155.

[90] C. Guida, A. C. Aguiar, and R. L. Cunha, "Green techniques for starch modification to stabilize Pickering emulsions: a current review and future perspectives," *Current Opinion in Food Science*, vol. 38. Elsevier Ltd, pp. 52–61, Apr. 01, 2021. doi: 10.1016/j.cofs.2020.10.017.

[91] A. F. K. Minakawa, P. C. S. Faria-Tischer, and S. Mali, "Simple ultrasound method to obtain starch micro- and nanoparticles from cassava, corn and yam starches," *Food Chem*, vol. 283, pp. 11–18, Jun. 2019, doi: 10.1016/j.foodchem.2019.01.015.

[92] R. Chang *et al.*, "Green preparation and characterization of starch nanoparticles using a vacuum cold plasma process combined with ultrasonication treatment," *Ultrason Sonochem*, vol. 58, p. 104660, Nov. 2019, doi: 10.1016/j.ultsonch.2019.104660.

[93] R. Singh, "Nanotechnology based therapeutic application in cancer diagnosis and therapy," *3 Biotech*, vol. 9, p. 415, 1940, doi: 10.1007/s13205-019-1940-0.

[94] J. Yang *et al.*, "The inhibition effect of starch nanoparticles on tyrosinase activity and its mechanism," *Food Funct*, vol. 7, no. 12, pp. 4804–4815, 2016, doi: 10.1039/C6FO01228K.

[95] A. C. F. Ip, T. H. Tsai, I. Khimji, P. J. J. Huang, and J. Liu, "Degradable starch nanoparticle assisted ethanol precipitation of DNA," *Carbohydr Polym*, vol. 110, pp. 354–359, Sep. 2014, doi: 10.1016/j.carbpol.2014.04.007.

[96] S. Patel, J. Seet, L. Li, and J. Duhamel, "Detection of Nitroaromatics by Pyrene-Labeled Starch Nanoparticles," *Langmuir*, vol. 35, no. 40, pp. 13145–13156, Oct. 2019, doi: 10.1021/acs.langmuir.9b02371.

[97] G. Khachatryan and K. Khachatryan, "Starch based nanocomposites as sensors for heavy metals – detection of Cu2+ and Pb2+ ions," *Int Agrophys*, vol. 33, no. 1, pp. 121–126, Feb. 2019, doi: 10.31545/intagr/104414.

[98] C. Abbati De Assis *et al.*, "Techno-Economic Assessment, Scalability, and Applications of Aerosol Lignin Micro- and Nanoparticles," *ACS Sustain Chem Eng*, vol. 6, no. 9, pp. 11853–11868, Sep. 2018, doi: 10.1021/acssuschemeng.8b02151.

1.5. Starch-based materials as delivery systems for antimicrobial compounds

- **Summary**

Antimicrobial resistance is becoming a problem that needs to be eradicated as it can have serious consequences for public health. To this end, the use of natural sources with antimicrobial properties is proposed as a substitute for conventional synthetic antimicrobials avoiding their potential adverse health effects due to their non-toxicity and safety. On the other hand, to improve the properties of these compounds in terms of controlled release and targeted delivery, it is essential to incorporate them into a matrix, which in turn will also improve their physical instability and bioactivity. Starch stands out as a versatile and promising material for the development of matrices loaded with antimicrobial compounds. Its ability to form films and coatings makes it an attractive option for applications in various industries, such as food and biomedical. Moreover, starch offers additional advantages, such as biocompatibility, renewability and low cost, positioning it as an ideal candidate for improving the efficacy and sustainability of controlled release and active packaging systems. This review provides information on recent studies using starch as a bulking agent for antimicrobial compounds including an overview of the different types of antimicrobials available, as well as their loading methods and applications.

- **Introduction**

Antimicrobial resistance is one of the greatest emerging threats to global public health, and it is estimated that it could lead to the loss of millions of lives as well as significant clinical and economic consequences. One of the lessons learned from the COVID-19 pandemic is that solutions must be found to minimize future pandemic episodes and for early detection of pathogens. Early detection and/or intervention is essential to eliminate unwanted microbial contamination.

In this context, inorganic particles, organic biocomposites and sustainable nanoformulations are considered as one of the most effective alternatives to conventional antibiotics to combat multiresistance. One of the alternatives proposes the substitution of conventional nanomaterials by natural-based sources with similar properties and antimicrobial targeting, with the advantage that these materials have no harmful side effects for humans or the environment [1].

Generally, antimicrobial compounds are organic materials, including enzymes, polymers and organic acids, and inorganic materials, which may include metal oxides or metal nanoparticles [2]. However, the physical instability and bioactivity of some compounds can be a problem, so incorporating them into a matrix is a practical and effective approach to solve this. In turn, it will also favour their controlled delivery and release over time, regardless of their nature, provided that the appropriate carrier is chosen, and the protection of the compound will also benefit its safety and efficacy [3].

In this sense, there are several studies on the use of starch as a bulking agent for these antibacterial compounds [4-6]. It is widely known for having numerous advantages: natural, renewable, biodegradable, biocompatible and cost-effective, as well as being the second most abundant biomass material in nature and very easy to obtain as it is found in all chlorophyll-containing plants.

Therefore, this review brings together information on the latest advances in the release of compounds with antimicrobial activity using starch as a stabilizing agent. It includes an overview of the different types of antimicrobial agents that exist according to their nature (natural, synthetic and semi-synthetic) and describes some of the recent work in which they have been used. Some of the loading systems that exist are reviewed, describing the different antimicrobial loading matrices that can be used, with particular interest in starch-based films, as well as the most commonly used methods for obtaining them (casting and extrusion methods). Finally, the applications in which these fillers can be used are mentioned, with particular interest in food packaging applications. All this information can also be seen in Table 1.4.

1.5.1. Types of antimicrobial agents

Antimicrobial compounds can be classified according to their nature, chemical structure, mechanism of action, pharmacological effects and spectrum of activity [7].

In terms of their mechanism of action, the main targets of these compounds against bacteria are the inhibition of cell wall synthesis, protein synthesis, nucleic acid synthesis and cell membrane function. All these processes play a key role in bacterial growth [8]. Another mechanism would be to block key metabolic pathways [9], which would be chemotherapeutics.

In terms of pharmacological effects, there are two types of compounds: those that induce bacterial cell death, such as some types of peptides [8], are called bactericidal compounds. On the other hand, those that stop cell activity and bacterial growth without causing cell death, such as sulphonamides [7], are called bacteriostatic compounds.

Depending on their spectrum of activity, they can be classified as broad-spectrum or narrow-spectrum compounds. The former are able to act against a wide range of bacteria at the same time, whereas narrow-spectrum compounds are only able to act against one type of gram-positive or gram-negative bacteria. Although, contrary to what one might think, the latter would differ from the former as they are considered to be much more specific [10].

In terms of their nature, they can be divided into three categories: natural, synthetic and semi-synthetic. In this sense, natural compounds would be those derived from the plant or animal world, synthetic compounds would be those produced in a laboratory and semi-synthetic compounds would be those derived from a natural compound and modified in a laboratory. The following is a breakdown of some of the most commonly used in the last few years and they can be found in Table 1.4.

Table 1.4. *Latest advances in the release of compounds with antimicrobial activity using starch as a stabilizing agent, types of carriers, active compounds, loading methods and final applications.*

Carrier	Antimicrobial agent	Nature of compound	Loading method	Target microorganism[1]	Antimicrobial activity test	Application	References
PLA/starch films	Pomegranate peel	Natural	Extrusion	*S. aureus*	Agar diffusion 10.4-33.2 mm	Food packaging	[11]
Starch-epichlorohydrin-N-ethylpiperazine polymer	N-etilpiperazina	Synthetic	One-pot method	*S. aureus, E. coli, M. smegmatis* and antifungic activity against *C. albicans*	Agar diffusion 8-13 mm / optical density method / resazurin assay	Wound dressing or textile applications	[12]
Starch/PVA films	Ethyl lauroyl arginate	Semi-synthetic	Electrostatic interactions	*E. coli, S. aureus* and *S. putrefaciens*	Agar diffusion 7.1-20.8 mm	Active packaging films	[13]
Starch/PBAT blown films	Quaternary ammonium salts	Synthetic	Extrusion blowing	*S. aureus* and *E. coli*	Agar diffusion	Packaging	[14]
SNPs	Phenolic compounds from green propolis	Natural	Antisolvent precipitation	*L. monocytogenes*	Microdilution assay	Natural ingredients	[15]
Starch/PBAT blown films	ε-polylysine hydrochloride and organically modified nanomontmorillonites	Natural	Extrusion blowing	*S. aureus* and *E. coli*	Microdilution assay	Packaging	[16]
Taro starch, nisin and sodium alginate-based biodegradable films	Nisin	Natural	Casting	*L. monocytogenes*	Agar diffusion 2.42 mm	Food packaging	[17]

Hydroxypropyl methyl cellulose/carboxy methylstarch/succinic acid film	Gallic acid	Natural	Casting	*S. aureus* and *E. coli*	Plate counting	Wound dressing	[18]
Rice husk fiber-reinforced starch film	Benzalkonium chloride	Synthetic	Casting	*S. aureus, B. subtilis, K. pneumoniae* and *E. coli*	Agar diffusion 0.6-16 mm	Food, cosmetics and pharmaceutical packaging	[19]
Bentonite-reinforced starch-gelatin bioplastic	Quercetin	Natural	Casting	*E. coli, P. aeruginosa, C. albicans* and *S. aureus*	Agar diffusion 10-22 mm	Food packaging and pharmaceutical applications	[20]
PBAT/thermoplastic starch films	Cinnamon essential oil	Natural	Melting blending and extrusion casting	*E. coli, S. aureus* and *S. putrefaciens*	Plate counting	Food packaging	[21]
Thermoplastic starch	Natural rosin	Natural	Melt mixing and extrusion casting	*S. aureus*	Agar diffusion	Food packaging, biomedical and agricultural fields	[22]
Starch	AgNPs	Semi-synthetic	Dissolution and mixing	*S. aureus, S. typhi enterica, E. coli and P. aeruginosa*	Agar diffusion / microdilution / bio-TEM assay / fluorescent staining	Clinical biomedicine	[23], [24]
Starch/PVA films	Basil leaf extract	Natural	Solvent casting	*S. aureus* and *E. coli*	Microdilution assay	Food packaging	[24]
Cassava starch/glycerol films	Quitosan and oregano essential oil	Natural	Casting	*Z. bailii*	Microdilution assay	Biodegradable active packaging	[25]

Carboxymethyl chitosan and carboxymethyl starch films	Date seed extract	Natural	Dissolution and drying	*E. coli, S. typhimuruim, S. aureus, L. monocytogenes, R. oryzae* and *A. niger*	Agar diffusion 14-25 mm	Food packaging	[26]
Starch/PVA films	Tea polyphenols	Natural	Electrospinning	*S. aureus* and *E. coli*	Agar diffusion 12-15.9 mm	Food packaging	[27]
Pickering emulsions	Satureja khuzestanica essential oil	Natural	High-speed homogenization	*S. aureus* and *S. enterica*	Agar diffusion 16-20.5 mm / microdilution assay	Food industry	[28]
Hydroxypropyl starch/PVA films	Zinc oxide NPs	Semi-synthetic	Solvent casting	*E. coli, S. aureus, A. niger, A. flavus, P. expansum* and *F. oxysporum*	Agar diffusion 9-22 mm	Food packaging	[29]
SNPs	Vanillin	Natural	Nanoprecipitation	*E. coli*	Agar diffusion	Bioapplications	[30]
Solanum tuberosum tuber-driven starch-mediated of cerium oxide NPs	Cerium oxide NPs	Semi-synthetic	Green-hydrothermal synthesis	*S. aureus* and *E. coli*	Agar diffusion 11-17 mm	Environmental pollution	[31]
Plasticized starch-based film	Quitosan NPs	Natural	Ultrasound	*S. aureus* and *E. coli*	Plate counting / agar diffusion	Food packaging	[32]
Thermoplastic starch with chlorhexidine gluconate and epoxy resin	Chlorhexidine gluconate	Synthetic	Casting	*S. aureus, B. cereus, A. oryzae, R. oligosporus,* and *S. cerevisiae*	Agar diffusion	Medicine, agriculture and packaging	[33]

Thermoplastic starch	Tannin	Natural	Extrusion injection moulding	*S. aureus*	Agar diffusion	Biomedical, food packaging and agriculture	[34]

[1]Shown those with positive results.

Natural antimicrobial compounds

Natural compounds can come from a variety of sources, including plants, animals, microorganisms and minerals.

Among plant-origin compounds, one of the most commonly used are EO. These are volatile and aromatic compounds extracted from various plants and have been used for centuries for their medicinal, anti-inflammatory, analgesic and antiviral properties [35].

In a recent study, Tian et al. prepared films containing cinnamon essential oil (CEO) to determine their antibacterial activity and release behaviour. CEO is a volatile EO extracted from the bark, twigs, leaves, fruits and other parts of cinnamon and is widely used in the food, cosmetic and medical industries for its antibacterial, antioxidant and anticancer properties. It has also been studied for the development of packaging films [21].

In 2023, Hernandez, Ludueña and Flores investigated the use of oregano EO for the development of antimicrobial edible films due to its hydrophobic nature and significant antioxidant and antimicrobial properties. One of its major constituents, carvacrol, is a phenolic compound that has been widely used in the development of edible films. The authors suggest that the use of this EO for the constitution of active films could promote improvements in their mechanical, barrier and solubility properties [25]. In this context, Amrani et al. used EO from Satureja khuzestanica, an endemic plant that contains significant amounts of carvacrol, making it highly suitable for use as an antimicrobial agent in the food industry [28].

On the other hand, phenolic compounds found in many plants, are another widely used natural compound. Polyphenols are a group of micronutrients found in many medicinal plants. They are known for their antioxidant properties, their abundance in our diet and their possible use in the prevention of various degenerative or cardiovascular diseases. They consist of one or more hydroxyl groups attached to an aromatic ring (phenolic group) and many are found in edible plants [36]. Phenolic compounds are classified according to the number of phenolic rings and the structural elements linking them [37]. They are divided into phenolic acids, flavonoids, tannins and lignans, each with different mechanisms of action. They can also be divided into two groups according to their solubility in organic solvents: extractable phenolic compounds and non-

extractable phenolic compounds. The main difference is that the former can be easily removed from foods by extraction with organic solvents and/or water and stirring, whereas the latter cannot be extracted with organic solvents or solvent/water mixtures alone [38].

Recent studies have demonstrated the use of propolis, a natural resin produced by bees that exhibits a wide range of biological activities, by extracting its phenolic compounds and evaluating its antimicrobial and antioxidant properties [15]. The use of vanillin as an antimicrobial agent, which is the main component of vanilla extract and gives it its characteristic aroma and flavour, has also recently been demonstrated [30]. Gallic acid is also a natural phenolic compound found in many plants and fruits with broad antimicrobial and antioxidant activity [18], as are tea polyphenols (TP), which are of increasing interest in the field of food processing and storage, as they may not only maintain food quality and extend shelf life but may also inhibit deterioration of the packaging film [27]. Finally, quercetin is a flavonoid that is also widely used for its anti-inflammatory, antioxidant and antibacterial activities and is readily found in fruits, vegetables, wine and tea [20].

Eventually, the use of fruit or plant extracts, e.g. pomegranate peel (PGP), which contains several bioactive compounds (including phenolic compounds) and has shown positive results against bacterial growth in food packaging, is also known [11]. The use of basil leaf extracts in packaging with antimicrobial agents based on PVA/starch films has also been described [24], and date extract has also been used due to its high content of bioactive compounds with antimicrobial activity and potential use in food packaging applications [26].

Chitosan is one of the most widely used animal origin antimicrobials. It is a polysaccharide obtained mainly from the shells of some crustaceans and is known for its film-forming capacity, mechanical properties and antimicrobial activity [25]. It is a biodegradable, biocompatible and non-toxic chitin derivative that can also be physically modified, thus offering a wide range of forms to be developed [39]. Chitosan nanoparticles have gained attention as a substitute for reinforcements in biocomposites, water treatment, textile industry, food packaging and coating [32]. Recently, Babaee et al. successfully synthesized starch nanocomposites containing chitosan nanoparticles. The aim was to evaluate the loading influence of chitosan nanoparticles on the physico-mechanical, biodegradation and antimicrobial properties of starch nanocomposites. The authors concluded that chitosan-loaded starch films have excellent potential for use as active food packaging [32].

On the other hand, antimicrobial peptides are produced by almost all living organisms, from bacteria to plants and animals [40]. They are part of the natural immunity of both vertebrates (fish, mammals and amphibians) and invertebrates (insects and marine animals) [41]. Many peptides show a broad spectrum of activity against gram-negative and gram-positive bacteria, fungi, viruses and parasites. These peptides and their derivatives would therefore represent a new class of antimicrobial compounds [40]. Some mammals, such as the mouse, have a large number of antimicrobial peptides, including defensins and cathelicidins, each with a distinct and specific mode of action [40]. Lysozyme is a polypeptide that is part of the immune system of most mammals and has good antimicrobial activity [42]. It is also found in large amounts in egg white [43]. Finally, portamine is an antimicrobial peptide used as a natural food preservative and found in several types of fish [44].

Among the compounds derived from microorganisms, bacteriocins stand out. These are antibacterial peptides synthesized ribosomally by bacteria [45] and can be active against other bacteria of the same species (narrow spectrum) or against bacteria of different species (broad spectrum) [40]. On the other hand, the use of probiotics is not new, as they have been used since ancient times for their numerous health benefits. Their clinical benefits have been extensively studied, highlighting their use in the prevention of gastrointestinal diseases, in *Helicobacter pylori* eradication therapies or in the dental field, both for the prevention of periodontal diseases and caries [46].

Eventually, metal-based compounds are also currently being used to combat antimicrobial resistance. Copper and silver are some of the most commonly used to prevent and treat infections [47], but the use of arsenic, lithium, platinum or gold derivatives and selenium has also been highlighted [48].

Synthetic antimicrobial compounds

Synthetic antimicrobials are used as chemical preservatives to control food spoilage and extend shelf life. However, their use is being discouraged due to their negative health effects, and natural antimicrobials have attracted attention for their safety and non-toxicity [44]. Some of these recently used are quaternary ammonium salts [14], N-ethylpiperazine [12], benzalkonium chloride [19] or chlorhexidine gluconate [33].

Semi-synthetic antimicrobial compounds

Finally, semi-synthetics are those derived from natural compounds. Qiao et al. recently used ethyl lauroyl arginate (LAE) to develop antimicrobial starch films with PVA using electrostatic interactions between nanocellulose and LAE. LAE is a synthetic derivative of lauric acid, arginine and ethanol that has potent antimicrobial activity and is considered a safe food additive because it can be rapidly metabolized in the body to lauric acid and arginine [13].

On the other hand, the use of metals reduced to the nanoescale is also very common. Previous works have already demonstrated the advantages of nanoparticles over their raw material [30, 49, 50]. Some recent examples are silver NPs [23], cerium oxide NPs [31] or zinc oxide NPs [29], all known for their antibacterial activity.

1.5.2. Loading agents for antimicrobial compounds

Controlled release systems aim to deliver the right amount of an active compound at the right time and place. The compound is released gradually over time at a rate that is controlled by the delivery system. Nanomedicine proposes that delivery systems identify, target and selectively release their charge in a controlled way in response to a stimulus, either internal (pH, presence of enzymes or a change in redox potential) or external (light, temperature, magnetic field). The materials used in the design of delivery systems can be classified into organic nanostructures, which include polymeric materials that can be used to build nanospheres, nanocapsules or micelles, among others, and inorganic nanostructures, which would be nanoparticles of metal oxides, mesoporous silica or carbon nanotubes [51].

Polymeric nanoparticles have attracted considerable interest in many biomedical and controlled-release applications. Some polymers, such as polylactic acid (PLA) [11], chitosan [32] or starch [30], have been used as bulking agents for active compounds. In this sense, the use of starch as a bulking agent is highlighted due to its numerous advantages, such as improving the solubility and stability of compounds, as well as reducing their toxicity and adverse effects, in addition to all the advantages that starch itself possesses (low cost, biocompatible, natural and renewable among others) [52].

Types of antimicrobial carriers

Different types of matrices have been proposed as bulking agents, including nanoparticles, microcapsules, hydrogels, coatings, films, etc., the choice of which will depend on the type of application in which they will be used. Some of these different matrices used as carriers of active compounds are shown in Table 1.4.

In recent years, films have become one of the most widely used matrices for carrying antimicrobial compounds. Recently, Li et al. developed a PLA/starch composite packaging material functionalized with PGP as antimicrobial compound. They developed the films both in the presence and absence of starch and determined the antimicrobial capacity of the films against *S.aureus*. The authors concluded that the presence of starch acted not only as a filler, but also as a controlled release agent for the bioactive compounds contained in PGP, as larger inhibition zones were observed in the presence of starch, even at lower PGP concentrations [11]. In the same context and following on from natural antimicrobial agents, Chen et al. also developed films of high amylose starch with PVA, which improves the mechanical properties of starch and loaded with TP for active antimicrobial packaging. The formed film showed superior antimicrobial activity against *S. aureus* by disrupting its cell wall and cytomembrane and degrading existing DNA fragments [27]. Qiao et al. developed starch and PVA films too, but in this case loaded with LAE, a semi-synthetic compound designed to be released in a controlled manner through electrostatic interactions with nanocellulose. They showed that the addition of nanocellulose slowed down the release of LAE, and that it decreased as the amount of LAE increased. The authors carried out antimicrobial activity tests against *E. coli, S. aureus and S. putrefaciens*, and the films showed higher antimicrobial activity against Gram-positive (*S. aureus*) than Gram-negative (*S. putrefaciens, E. coli*) bacteria [13].

Mixed films of starch combined with poly(butylene adipate-co-terephthalate) (PBAT) are also available. PBAT is a biodegradable synthetic copolyester that improves the poor mechanical properties of starch [16]. However, PBAT also has certain limitations when used alone, such as a slow degradation rate under natural conditions and its high cost [21]. Combining the two therefore makes it possible to compensate for the limitations of each. Gao et al. developed antimicrobial films composed of PBAT and starch loaded with ε-polylysine hydrochloride. They used different organically modified nanomontmorillonites (OMMT) as reinforcements and their combination with ε-polylysine hydrochloride showed synergistic antimicrobial effects. The authors concluded

that the obtained films have the necessary potential to be used in the field of antimicrobial packaging [16]. In turn, Tian et al. also developed films composed of thermoplastic starch and PBAT, but this time loaded with CEO. The authors investigated the effect of starch concentration and films with a higher amount of starch showed higher CEO retention and better antimicrobial activity against *E. coli, S. aureus* and *S. putrefaciens*. At the same time, the rate and amount of CEO release also increased with increasing starch content, indicating that the release behaviour could be regulated by the starch content present in the films [21].

Nanoparticles are also a good matrix as a carrier for antimicrobial compounds. Santos Alves et al. synthesized nanoparticles of native starch from cassava and potato as a carrier and stabilizer for phenolic compounds obtained from green propolis. The obtained SNPs had a wide size range and loading efficiency (LE) of 65-73%, and also showed positive results in terms of antimicrobial activity against *L. monocytogenes* [15]. Morán et al. also synthesized size-controlled SNPs with starches of different botanical origin, which could be used as bulking agents. The authors evaluated the antimicrobial activity of vanillin-loaded SNPs against *E. coli* using the agar-well diffusion method and demonstrated their inhibitory capacity [30].

Antimicrobial loading methods

As developed above, films are one of the most widely used matrices as antimicrobial carriers. The methods frequently used to produce these antimicrobial loaded films are casting and extrusion.

In general, the extrusion process consists of mixing all the materials together in a high-speed mixer. To balance all the components, the mixtures are stored in sealed polyethylene bags at room temperature for 24 hours and then passed through a twin-screw extruder. The extruded material is cooled with air and cut into pellets, which are fed into a single-screw blown film extruder. It should be noted that it is important to control the blowing and take-up ratio to ensure the desired film thickness [14, 16]. A graphical representation of this method is shown in Figure 1.15 below.

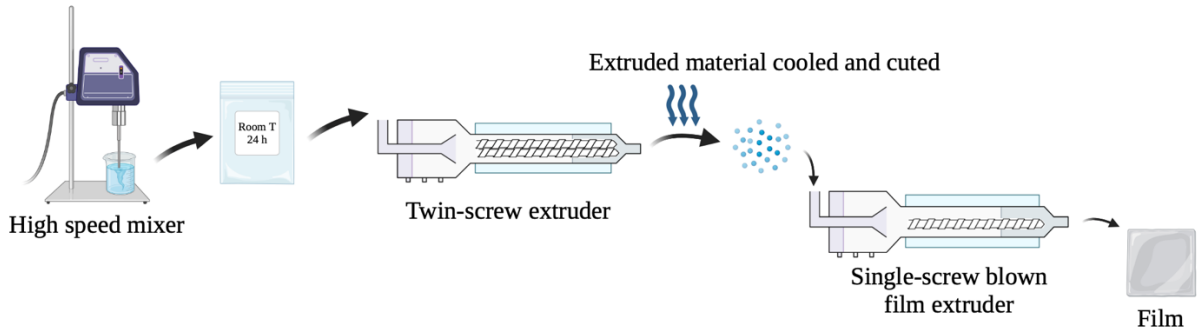

Figure 1.15. *Schematic representation of the extrusion process. Created in Biorender.com*

Gao et al. used this method in some of their last works. In each work, they synthesized blown starch films with PBAT but loaded with different antimicrobials. In both, the extrusion parameters were the same but in one they mixed all the components together with the glycerine to form the film [16] and in the other they mixed the components and then added a mixture of glycerine and citric acid at low speed from an upper feed port. Citric acid was used as a cross-linking agent to improve the compatibility between starch and PBAT, as it has ester groups that graft onto the starch chains [14]. The rest of the process was the same in both works.

Li et al. also used an extrusion method to form starch and PLA films. The authors used one-step extrusion techniques that combine material composition and extrusion to reduce PLA degradation during extrusion. In this case, the single-screw extruder was connected to the twin-screw extruder at one end and to a film die at the other end, allowing continuous material compounding and film extrusion [11].

Another common method for develop starch-based films is the casting method. Basically, the method consists of forming a solution containing all the components that will form the film, pouring it into a cast and evaporating the solvent under controlled conditions of temperature and humidity. This process is schematized in Figure 1.16.

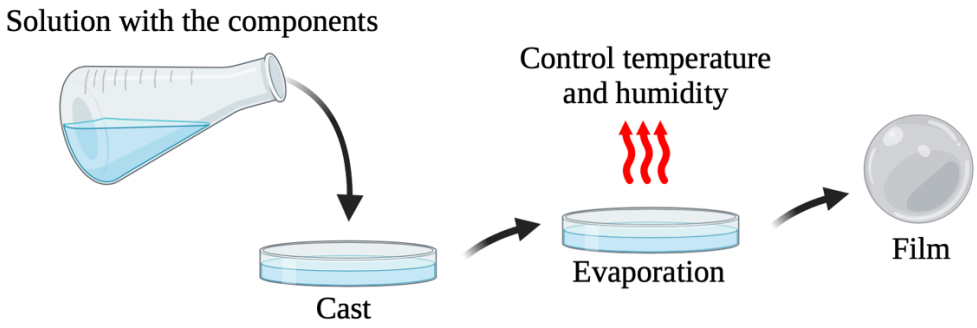

Figure 1.16. *Schematic representation of the casting method. Created in Biorender.com*

Guevara-Carrión et al. used this method to develop biodegradable films based on taro starch, nisin and sodium alginate and to study their antimicrobial activity. They prepared the film-forming solution by dissolving starch in water at high temperature and then adding glycerol and sodium alginate, which improves the low mechanical properties of starch. Then, they added nisin, the antimicrobial compound, and cooled the solution. Finally, the film was formed by pouring the solution into Petri dishes and leaving them in a dehydrator for 12 h at 41°C [17]. Pitpisutkul and Prachayawarakorn also used the casting method to develop porous antimicrobial hydroxypropylmethylcellulose and carboxymethylstarch (HP/CMS) films containing gallic acid as an antimicrobial agent for use as wound dressings. They also used glycerol as a plasticiser and succinic acid as a cross-linking agent. Unloaded and loaded films were prepared, and in both cases the components were mixed and dispersed in hot water for complete dissolution. Those containing the antimicrobial were allowed to cool before adding the gallic acid solution, which was mixed at room temperature. Finally, the samples were poured into polypropylene trays, dried and these dried films were preheated to 110°C to complete cross-linking [18].

1.5.3. Applications of starch-based matrices as antimicrobial carriers

As described, starch is a good candidate for use as a carrier for compounds with antimicrobial activity, either alone or in combination with other compounds. Table 1.4 also provides a summary of the different applications in which these active compound-loaded matrices can be used such as biomedical, cosmetics or agricultural applications.

However, food packaging is one of the major applications where these active compound-loaded matrices are most commonly used. In a recent study, Gao et al. developed starch/PBAT blown films containing two types of commercial quaternary ammonium salts. Their research covered both

the physicochemical properties, antimicrobial activity and meat preservation ability of the film. They carried out a preliminary meat preservation experiment by vacuum sealing the samples and storing them in a dark cold room at temperatures between 0 and 4°C. They determined the total viable count (TVC) and lactic acid bacteria (LAB) on different days of storage and statistical analysis showed that film type, storage time and their interaction significantly affected these values. This indicated that, within a given storage period, an excellent meat preservation effect could be obtained if suitable packaging materials loaded with quaternary ammonium salts were chosen, and that these films could be a promising alternative to traditional plastic packaging [14].

Following this application, Guevara-Carrión et al. also developed biodegradable films based on taro starch, nisin and sodium alginate and characterized their antimicrobial effect on chicken meat by counting viable cells, also over different time periods. Samples with film inhibited bacterial growth during 15 days of refrigerated storage, while samples without film or with film but without the presence of the antimicrobial showed exponential bacterial growth and natural degradation was observed after 6 days [17, 21].

Tian et al. also developed PBAT/thermoplastic starch films using CEO as the antimicrobial compound and investigated their use in sea bass packaging. The packaged samples were stored in a refrigerator at 4°C and relevant indicators such as colour and TVC were analyzed. The results showed that films containing CEO could inhibit protein degradation and microbial growth in sea bass. In turn, the higher the amount of thermoplastic starch in the films, the greater the inhibitory effect [21].

In 2023, Varghese et al. developed antimicrobial active packaging based on PVA/starch films incorporating basil leaf extracts as an antimicrobial agent. The developed films were tested in the storage of green chillies for 7 days by keeping the bags fully sealed at room temperature. After 7 days, the change in appearance and quality was observed and it was shown that chillies packed in the biocomposite films with basil extract achieved better freshness retention compared to those packed in pure films which had lost weight and discoloured [24].

1.5.4. Conclusions

Antimicrobial resistance is a major threat to global public health that requires innovative and sustainable solutions.

The diversity of antimicrobial compounds and their different mechanisms of action, pharmacological effects and nature offer a wide field of study and application in the fight against microbial infections and antimicrobial resistance. A wide variety of compounds are available, ranging from natural compounds such as EO or plant extracts to synthetic and semi-synthetic compounds such as metal particles and modified polymers.

Controlled release systems offer an effective way to deliver active compounds gradually and selectively into the body. These systems allow precise release in response to internal or external stimuli, which can improve therapeutic efficacy and reduce unwanted side effects.

In addition, the role of starch as a bulking agent in these systems is highlighted due to its many advantages, such as its biocompatibility, renewability and ability to enhance the stability and solubility of active compounds. This suggests that starch could be a promising option in the design of controlled release systems for a variety of biomedical and pharmaceutical applications.

The choice of a suitable matrix for the delivery of antimicrobial compounds depends on several factors, such as the type of application, the desired properties of the final product and the specific compounds being used. Films and nanoparticles offer versatile and effective options for the development of packaging materials and other products with enhanced antimicrobial properties. Starch-based films, in combination with other biodegradable materials, can significantly improve the shelf life of food by inhibiting bacterial growth and natural degradation. These films loaded with antimicrobial agents have been shown to be a promising alternative to traditional plastic packaging for food preservation. The incorporation of natural ingredients, such as basil leaf extracts or EO, provides a more sustainable and environmentally friendly solution for food packaging.

Therefore, it can be concluded that starch-based controlled release systems of antimicrobial compounds are a promising tool in the fight against microbial infections and antimicrobial resistance and offer a variety of options for the development of new treatments and applications in the biomedical and public health fields.

- **References**

[1] D. Morán *et al.*, "Sustainable antibiofilm self-assembled colloidal systems," *Frontiers in Soft Matter*, vol. 2, Nov. 2022, doi: 10.3389/frsfm.2022.1041881.

[2] X. Hou, H. Wang, Y. Shi, and Z. Yue, "Recent advances of antibacterial starch-based materials," *Carbohydr Polym*, vol. 302, p. 120392, Feb. 2023, doi: 10.1016/j.carbpol.2022.120392.

[3] M. Zanetti *et al.*, "Use of encapsulated natural compounds as antimicrobial additives in food packaging: A brief review," *Trends Food Sci Technol*, vol. 81, pp. 51–60, Nov. 2018, doi: 10.1016/j.tifs.2018.09.003.

[4] J. B. Pires *et al.*, "Starch extraction from avocado by-product and its use for encapsulation of ginger essential oil by electrospinning," *Int J Biol Macromol*, vol. 254, p. 127617, Jan. 2024, doi: 10.1016/j.ijbiomac.2023.127617.

[5] Y. Fang, J. Fu, C. Tao, P. Liu, and B. Cui, "Mechanical properties and antibacterial activities of novel starch-based composite films incorporated with salicylic acid," *Int J Biol Macromol*, vol. 155, pp. 1350–1358, Jul. 2020, doi: 10.1016/j.ijbiomac.2019.11.110.

[6] L. Zhu, H. Luo, Z.-W. Shi, C. Lin, and J. Chen, "Preparation, characterization, and antibacterial effect of bio-based modified starch films," *Food Chem X*, vol. 17, p. 100602, Mar. 2023, doi: 10.1016/j.fochx.2023.100602.

[7] D. F. Pancu *et al.*, "Antibiotics: Conventional Therapy and Natural Compounds with Antibacterial Activity—A Pharmaco-Toxicological Screening," *Antibiotics*, vol. 10, no. 4, p. 401, Apr. 2021, doi: 10.3390/antibiotics10040401.

[8] H. Ullah and S. Ali, "Classification of Anti-Bacterial Agents and Their Functions," in *Antibacterial Agents*, InTech, 2017. doi: 10.5772/intechopen.68695.

[9] K. M. Percival, "Antibiotic Classification and Indication Review for the Infusion Nurse," *Journal of Infusion Nursing*, vol. 40, no. 1, pp. 55–63, Jan. 2017, doi: 10.1097/NAN.0000000000000207.

[10] J. Acar, "Broad- and narrow-spectrum antibiotics: an unhelpful categorization," *Clinical Microbiology and Infection*, vol. 3, no. 4, pp. 395–396, Aug. 1997, doi: 10.1111/j.1469-0691.1997.tb00274.x.

[11] Y. Li *et al.*, "Antimicrobial packaging materials of PLA/starch composites functionalized by pomegranate peel," *J Taiwan Inst Chem Eng*, vol. 156, p. 105371, Mar. 2024, doi: 10.1016/j.jtice.2024.105371.

[12] S. Kanth, Y. Malgar Puttaiahgowda, and A. Kulal, "Synthesis, characterization, and antimicrobial activities of a starch-based polymer," *Carbohydr Res*, vol. 532, p. 108900, Oct. 2023, doi: 10.1016/j.carres.2023.108900.

[13] J. Qiao, Y. Dong, C. Chen, and J. Xie, "Development and characterization of starch/PVA antimicrobial active films with controlled release property by utilizing electrostatic interactions between nanocellulose and lauroyl arginate ethyl ester," *Int J Biol Macromol*, vol. 261, p. 129415, Mar. 2024, doi: 10.1016/j.ijbiomac.2024.129415.

[14] S. Gao *et al.*, "Starch/poly (butylene adipate-co-terephthalate) blown films contained the quaternary ammonium salts with different N-alkyl chain lengths as antimicrobials," *Food Chem*, vol. 436, p. 137650, Mar. 2024, doi: 10.1016/j.foodchem.2023.137650.

[15] M. J. dos Santos Alves *et al.*, "Starch nanoparticles containing phenolic compounds from green propolis: Characterization and evaluation of antioxidant, antimicrobial and digestibility properties," *Int J Biol Macromol*, vol. 255, p. 128079, Jan. 2024, doi: 10.1016/j.ijbiomac.2023.128079.

[16] S. Gao, X. Zhang, J. Jiang, W. Wang, and H. Hou, "Starch/poly(butylene adipate-co-terephthalate) blown antimicrobial films based on ε-polylysine hydrochloride and different nanomontmorillonites," *Int J Biol Macromol*, vol. 253, p. 126609, Dec. 2023, doi: 10.1016/j.ijbiomac.2023.126609.

[17] M. G. Carrión, M. A. R. Corripio, J. V. H. Contreras, M. R. Marrón, G. M. Olán, and A. S. H. Cázares, "Optimization and characterization of taro starch, nisin, and sodium alginate-

based biodegradable films: antimicrobial effect in chicken meat," *Poult Sci*, vol. 102, no. 12, p. 103100, Dec. 2023, doi: 10.1016/j.psj.2023.103100.

[18] V. Pitpisutkul and J. Prachayawarakorn, "Porous antimicrobial crosslinked film of hydroxypropyl methylcellulose/carboxymethyl starch incorporating gallic acid for wound dressing application," *Int J Biol Macromol*, vol. 256, p. 128231, Jan. 2024, doi: 10.1016/j.ijbiomac.2023.128231.

[19] V. Srivastava, S. Singh, and D. Das, "Rice husk fiber-reinforced starch antimicrobial biocomposite film for active food packaging," *J Clean Prod*, vol. 421, p. 138525, Oct. 2023, doi: 10.1016/j.jclepro.2023.138525.

[20] H. Mubarak Aldawsari *et al.*, "Development and evaluation of quercetin enriched bentonite-reinforced starch-gelatin based bioplastic with antimicrobial property," *Saudi Pharmaceutical Journal*, vol. 31, no. 12, p. 101861, Dec. 2023, doi: 10.1016/j.jsps.2023.101861.

[21] Y. Tian, Q. Lei, F. Yang, J. Xie, and C. Chen, "Development of cinnamon essential oil-loaded PBAT/thermoplastic starch active packaging films with different release behavior and antimicrobial activity," *Int J Biol Macromol*, vol. 263, p. 130048, Apr. 2024, doi: 10.1016/j.ijbiomac.2024.130048.

[22] X. Zhang, H. Ma, W. Qin, B. Guo, and P. Li, "Antimicrobial and improved performance of biodegradable thermoplastic starch by using natural rosin to replace part of glycerol," *Ind Crops Prod*, vol. 178, p. 114613, Apr. 2022, doi: 10.1016/j.indcrop.2022.114613.

[23] K. Saravanakumar *et al.*, "Synthesis, characterization, and cytotoxicity of starch-encapsulated biogenic silver nanoparticle and its improved anti-bacterial activity," *Int J Biol Macromol*, vol. 182, pp. 1409–1418, Jul. 2021, doi: 10.1016/j.ijbiomac.2021.05.036.

[24] S. A. Varghese, H. Pulikkalparambil, S. M. Rangappa, J. Parameswaranpillai, and S. Siengchin, "Antimicrobial active packaging based on PVA/Starch films incorporating basil leaf extracts," *Mater Today Proc*, vol. 72, pp. 3056–3062, 2023, doi: 10.1016/j.matpr.2022.09.062.

[25] M. S. Hernández, L. N. Ludueña, and S. K. Flores, "Citric acid, chitosan and oregano essential oil impact on physical and antimicrobial properties of cassava starch films," *Carbohydrate Polymer Technologies and Applications*, vol. 5, p. 100307, Jun. 2023, doi: 10.1016/j.carpta.2023.100307.

[26] N. Zidan *et al.*, "Active and smart antimicrobial food packaging film composed of date palm kernels extract loaded carboxymethyl chitosan and carboxymethyl starch composite for prohibiting foodborne pathogens during fruits preservation," *Eur Polym J*, vol. 197, p. 112353, Oct. 2023, doi: 10.1016/j.eurpolymj.2023.112353.

[27] L. Chen *et al.*, "Encapsulation of tea polyphenols into high amylose corn starch composite nanofibrous film for active antimicrobial packaging," *Int J Biol Macromol*, vol. 245, p. 125245, Aug. 2023, doi: 10.1016/j.ijbiomac.2023.125245.

[28] M. Amrani, S. Pourshamohammad, M. Tabibiazar, H. Hamishehkar, and M. Mahmoudzadeh, "Antimicrobial activity and stability of Satureja khuzestanica essential oil pickering emulsions stabilized by starch nanocrystals and bacterial cellulose nanofibers," *Food Biosci*, vol. 55, p. 103016, Oct. 2023, doi: 10.1016/j.fbio.2023.103016.

[29] A. H. Hashem, M. E. El-Naggar, A. M. Abdelaziz, S. Abdelbary, Y. R. Hassan, and M. S. Hasanin, "Bio-based antimicrobial food packaging films based on hydroxypropyl starch/polyvinyl alcohol loaded with the biosynthesized zinc oxide nanoparticles," *Int J Biol Macromol*, vol. 249, p. 126011, Sep. 2023, doi: 10.1016/j.ijbiomac.2023.126011.

[30] D. Morán *et al.*, "Bio-based starch nanoparticles with controlled size as antimicrobial agents nanocarriers," *React Funct Polym*, vol. 198, p. 105881, May 2024, doi: 10.1016/j.reactfunctpolym.2024.105881.

[31] H. Siddiqui *et al.*, "Solanum tuberosum tuber-driven starch-mediated green-hydrothermal synthesis of cerium oxide nanoparticles for efficient photocatalysis and antimicrobial activities," *Chemosphere*, vol. 352, p. 141418, Mar. 2024, doi: 10.1016/j.chemosphere.2024.141418.

[32] M. Babaee, F. Garavand, A. Rehman, S. Jafarazadeh, E. Amini, and I. Cacciotti, "Biodegradability, physical, mechanical and antimicrobial attributes of starch nanocomposites containing chitosan nanoparticles," *Int J Biol Macromol*, vol. 195, pp. 49–58, Jan. 2022, doi: 10.1016/j.ijbiomac.2021.11.162.

[33] N. Thajai *et al.*, "Antimicrobial thermoplastic starch reactive blend with chlorhexidine gluconate and epoxy resin," *Carbohydr Polym*, vol. 301, p. 120328, Feb. 2023, doi: 10.1016/j.carbpol.2022.120328.

[34] H. Ma, W. Qin, B. Guo, and P. Li, "Effect of plant tannin and glycerol on thermoplastic starch: Mechanical, structural, antimicrobial and biodegradable properties," *Carbohydr Polym*, vol. 295, p. 119869, Nov. 2022, doi: 10.1016/j.carbpol.2022.119869.

[35] N. El Hachlafi *et al.*, "Tetraclinis articulata (Vahl) Mast. essential oil as a promising source of bioactive compounds with antimicrobial, antioxidant, anti-inflammatory and dermatoprotective properties: In vitro and in silico evidence," *Heliyon*, vol. 10, no. 1, p. e23084, Jan. 2024, doi: 10.1016/j.heliyon.2023.e23084.

[36] C. Manach, A. Scalbert, C. Morand, C. Rémésy, and L. Jiménez, "Polyphenols: food sources and bioavailability," *Am J Clin Nutr*, vol. 79, no. 5, pp. 727–747, May 2004, doi: 10.1093/ajcn/79.5.727.

[37] M. M. Vuolo, V. S. Lima, and M. R. Maróstica Junior, "Phenolic Compounds," in *Bioactive Compounds*, Elsevier, 2019, pp. 33–50. doi: 10.1016/B978-0-12-814774-0.00002-5.

[38] C. Carboni Martins, R. C. Rodrigues, G. Domeneghini Mercali, and E. Rodrigues, "New insights into non-extractable phenolic compounds analysis," *Food Research International*, vol. 157, p. 111487, Jul. 2022, doi: 10.1016/j.foodres.2022.111487.

[39] R. de Sousa Victor, A. Marcelo da Cunha Santos, B. Viana de Sousa, G. de Araújo Neves, L. Navarro de Lima Santana, and R. Rodrigues Menezes, "A Review on Chitosan's Uses as Biomaterial: Tissue Engineering, Drug Delivery Systems and Cancer Treatment," *Materials*, vol. 13, no. 21, p. 4995, Nov. 2020, doi: 10.3390/ma13214995.

[40] G. Maróti, A. Kereszt, É. Kondorosi, and P. Mergaert, "Natural roles of antimicrobial peptides in microbes, plants and animals," *Res Microbiol*, vol. 162, no. 4, pp. 363–374, May 2011, doi: 10.1016/j.resmic.2011.02.005.

[41] F. A. Santos *et al.*, "Systematic review of antiprotozoal potential of antimicrobial peptides," *Acta Trop*, vol. 236, p. 106675, Dec. 2022, doi: 10.1016/j.actatropica.2022.106675.

[42] S. Varahan, V. S. Iyer, W. T. Moore, and L. E. Hancock, "Eep Confers Lysozyme Resistance to Enterococcus faecalis via the Activation of the Extracytoplasmic Function Sigma Factor SigV," *J Bacteriol*, vol. 195, no. 14, pp. 3125–3134, Jul. 2013, doi: 10.1128/jb.00291-13.

[43] T. Silvetti, S. Morandi, M. Hintersteiner, and M. Brasca, "Use of Hen Egg White Lysozyme in the Food Industry," in *Egg Innovations and Strategies for Improvements*, Elsevier, 2017, pp. 233–242. doi: 10.1016/B978-0-12-800879-9.00022-6.

[44] F. Saeed, M. Afzaal, T. Tufail, and A. Ahmad, "Use of Natural Antimicrobial Agents: A Safe Preservation Approach," in *Active Antimicrobial Food Packaging*, IntechOpen, 2019. doi: 10.5772/intechopen.80869.

[45] S. D. Todorov and L. M. T. Dicks, "Bacteriocin production by Pediococcus pentosaceus isolated from marula (Scerocarya birrea)," *Int J Food Microbiol*, vol. 132, no. 2–3, pp. 117–126, Jun. 2009, doi: 10.1016/j.ijfoodmicro.2009.04.010.

[46] Y. L. P. López, R. Torres-Rosas, and L. Argueta-Figueroa, "Mecanismos de acción de los probióticos en la inhibición de microorganismos cariogénicos," *Revista Médica Clínica Las Condes*, vol. 34, no. 3, pp. 216–223, May 2023, doi: 10.1016/j.rmclc.2023.03.010.

[47] N. K. Monych and R. J. Turner, "Multiple Compounds Secreted by *Pseudomonas aeruginosa* Increase the Tolerance of *Staphylococcus aureus* to the Antimicrobial Metals Copper and Silver," *mSystems*, vol. 5, no. 5, Oct. 2020, doi: 10.1128/mSystems.00746-20.

[48] S. Ramos-Inza, D. Plano, and C. Sanmartín, "Metal-based compounds containing selenium: An appealing approach towards novel therapeutic drugs with anticancer and antimicrobial

effects," *Eur J Med Chem*, vol. 244, p. 114834, Dec. 2022, doi: 10.1016/j.ejmech.2022.114834.

[49] G. Gutiérrez, D. Morán, A. Marefati, J. Purhagen, M. Rayner, and M. Matos, "Synthesis of controlled size starch nanoparticles (SNPs)," *Carbohydr Polym*, vol. 250, Dec. 2020, doi: 10.1016/j.carbpol.2020.116938.

[50] D. Morán, G. Gutiérrez, M. C. Blanco-López, A. Marefati, M. Rayner, and M. Matos, "Synthesis of Starch Nanoparticles and Their Applications for Bioactive Compound Encapsulation," *Applied Sciences*, vol. 11, no. 10, p. 4547, May 2021, doi: 10.3390/app11104547.

[51] Y. Rojas-Aguirre, K. Aguado-Castrejón, and I. González-Méndez, "La nanomedicina y los sistemas de liberación de fármacos: ¿la (r)evolución de la terapia contra el cáncer?," *Educación Química*, vol. 27, no. 4, pp. 286–291, Oct. 2016, doi: 10.1016/j.eq.2016.07.002.

[52] J. Yang, Y. Huang, C. Gao, M. Liu, and X. Zhang, "Fabrication and evaluation of the novel reduction-sensitive starch nanoparticles for controlled drug release," *Colloids Surf B Biointerfaces*, vol. 115, pp. 368–376, Mar. 2014, doi: 10.1016/j.colsurfb.2013.12.007.

2. SYNTHESIS OF STARCH NANOPARTICLES

CHAPTER 2 – Synthesis of starch nanoparticles

Introduction

In this chapter, different strategies for the synthesis of SNPs are summarised. Starches of different botanical origin and starches modified with SCFA were used. The synthesis of SNPs was carried out following two commonly used bottom-up methods, nanoprecipitation and ME. These methods are characterized by their simplicity, as they do not require extensive equipment, large amounts of reagents or energy. At the same time, they allowed easy control of both the final size and shape of the particles.

The chapter is divided into three subchapters. The first deals with finding the optimal conditions for the synthesis of SNPs by varying the main operating parameters such as injection rate, dissolution time, stirring rate and organic/aqueous phase ratio. In this study, maize starches with different amylose and amylopectin contents were used, so that the effect of the amylose/amylopectin ratio was also evaluated. The syntheses were carried out by both nanoprecipitation and ME methods and the results were compared. The size and shape of the SNPs were characterized by dynamic light scattering (DLS) and scanning electron microscopy (SEM). X-ray powder diffraction (XRPD) and Fourier transform infrared spectroscopy (FTIR) analysis were used to determine the crystallinity and molecular structure of the granules and SNPs, respectively.

In the second work, SNPs were synthesized by the W/O ME method using native maize starch. Different formulations were used to prepare the microemulsions and, the proportion and composition of the aqueous phase, the organic phase and the amounts of stabilizer, co-stabilizer and type of precipitant used were optimized. Again, SNPs were characterized for size and shape by DLS and SEM, and the crystallinity of SNPs and starch granules by XRPD. Furthermore, the best selected formulations were used to obtain starch-based superparamagnetic nanocomposites by simultaneous synthesis of SNPs and IONPs. The nanocomposites were characterized by their size, shape and crystallinity in the same way as the SNPs, and their magnetic properties were also analyzed.

The last subchapter deals with the feasibility of producing SCFA-modified SNPs. In recent years, modified starches with SCFA have attracted a great deal of interest, as they are known to have many benefits for human intestinal health. In this work, acetylated, propionylated and butyrylated starches from quinoa and rice with different degrees of modification were used and the nanoprecipitation method with optimal synthesis conditions was applied. The same characterizations as in the previous work were carried out and FTIR was used to determine whether the DS was affected by the synthesis method.

2.1. Synthesis of controlled size starch nanoparticles (SNPs)

- **Summary**

SNPs are a promising choice for the strategic development of new renewable and biodegradable nanomaterials for novel biomedical and pharmaceutical applications when loaded with antibiotics or with anticancer agents as target drug delivery systems. The final properties of the SNPs are strongly influenced by the synthesis method and conditions being a controlled and monodispersed size crucial for these applications.

The aim of this work was to synthesize controlled size SNPs through nanoprecipitation and ME methods by modifying main operating parameters regarding the effect of amylose and amylopectin ratio in maize starches. SNPs were characterized by size and shape.

SNPs from 59 to 118 nm were obtained by the nanoprecipitation method, registering the higher values when surfactant was added to the aqueous phase. ME method led to 35-147 nm sizes observing a higher particle formation capacity. The composition of the maize used influenced the final particle size and shape.

2.1.1. Introduction

Nanoparticles are a promising choice for the strategic development of new drug delivery systems with novel applications in food, cosmetics and healthcare [1]. Starch is a non-allergenic abundant polysaccharide in nature, renewable and biodegradable making it an ideal candidate as a component of green bio-formulations. The starch model is described as a concentric semi-crystalline multistate structure that can be involved in the production of new nano-elements. Starch

nanoparticles are often referred to as starch nanocrystals. Some authors stated that the disruption of amorphous domains of semi-crystalline granules by acid hydrolysis will produce starch nanocrystals, while gelatinized starch will create SNPs [2] that may include amorphous matrices. However, other authors reported that it becomes almost impossible to clarify the terms starch nanocrystals and starch nanoparticles since both terms have been used to refer to the crystalline parts of starch remaining after hydrolysis or other physical treatments and suggest the general term SNPs is applied to describe the elements that have at least one dimension in the nanoscale [1].

The preparation of SNPs may be classified in two main different processes, bottom-up and top-down depending on the precursor material employed on the synthesis. In top-down processes, nanoparticles can be produced from structure and size refinement through a breakdown of larger voluminous materials or microparticles while in a bottom-up process, nanoparticles can be prepared from a buildup of atoms or molecules in a controlled manner in the form of small primary cores that is regulated by thermo-dynamic means such as self-assembly [1].

Another classification for top-down processes may be done according to the number of steps required to prepare the final SNPs involving simple or hybrid processes. Some of the most common top-down simple methods that have been known to produce SNPs are acid or enzymatic hydrolysis [3, 4]. Hydrolysis involves long periods of time with low yields and resulting SNPs normally present more crystalline regions in starch granules since they are more resistant to the acid hydrolysis than the amorphous regions. LeCorre et al. investigated the influence of the botanic origin of starch on the final crystallinity of SNPs prepared using acid hydrolysis using an X-ray diffraction analysis. This study demonstrated that the most important parameter in determining the degree of crystallinity of SNPs was the amylose content in starch while no differences were observed when starches with different botanical origins but with similar amylose content were compared [2].

On the other hand, physical treatments, such as high-pressure homogenization [5], ultrasonication [6] or extrusion [7] involve shorter periods of time with higher yields but it is difficult to control crystal destruction. Hybrid top-down processes have also been used with satisfactory results when a combination of both enzymatic and acid hydrolysis has been used for the preparation of SNPs since it was reported that the SNP preparation could be done within a reduced time by using the combined procedure [8]. There are also several studies in which hydrolysis was combined with a

post-physical treatment of ultrasonication as final refinement [9, 10]. However, ultrasonication may change the X-ray diffraction pattern of starch reducing crystallinity for longer periods of time.

Regarding bottom-up processes the most common methods of SNPs preparation are the ME [11-13] and nanoprecipitation methods [12, 14-18]. The nanoprecipitation process involves the successive addition of a dilute solution of polymer to a solvent which leads to the polymer nanoprecipitation based on its interfacial deposition following the displacement of a semipolar solvent that is miscible with water. ME method involves the preparation of W/O microemulsions consisting of aqueous domains dispersed in a continuous oil phase stabilized by an interfacial film of surfactant molecules working as nanoreactors where the synthesis of the desired SNPs take place. These two approaches present many advantages since both are gentle chemical techniques with growing interest because large amounts of toxic solvents and external energy sources are avoided with efficient control of size, shape, monodispersity and composition of SNPs obtained [11, 14]. Moreover, these preparation methods are the most common ones for encapsulation purposes.

The final properties of the SNPs are strongly influenced by the synthesis method and conditions, which in turn will determine its final applications. A controlled and monodispersed size is crucial for biomedical or pharmaceutical applications [19]. There have been indications of SNPs loaded with antibiotics (e.g., penicillin, ampicillin, ciprofloxacin, citoplastin) or biocide metals, such as Ag, having bacterial inhibition properties [13, 16, 19, 20] or with anticancer agents as target drug delivery systems (doxorubicin, docetaxel) [21, 22]. However, some authors reported that the bactericidal properties were shown to be size-dependent and most effective in the 1-10 nm range [19].

Therefore, this work aimed to synthesize controlled size SNPs with the use of bottom-up nanotechnology through nanoprecipitation and ME methods by modifying main parameters involved, as injection rate, dissolution time, stirring rate, organic to aqueous phase ratio, as well as studying the effect of amylose and amylopectin ratio in maize starches. The SNPs were characterized by the size and shape using DLS and SEM. XRPD and FTIR were used to analyze the structure and crystallinity of both the granules and SNPs.

2.1.2. Materials

Milli-Q water was used for all experiments to prepare the different aqueous phases while absolute ethanol was supplied by Sigma Aldrich (USA) as the main organic phase. Urea supplied by Serva Electrophoresis GmbH and NaOH provided by Panreac were used to formulate the different aqueous phases studied.

Maize starches with three different ratios of amylose and amylopectin, normal-, high amylose-, and waxy (high amylopectin) from Cerestar-AKV I/S (Denmark), were used in the study.

CTAB was supplied by Sigma-Aldrich (USA). It is a quaternary ammonium salt, with a long alkyl group which present cationic surfactant properties with a hydrophilic-lipophilic balance (HLB) of 10. The HLB of an emulsifier is parameter that allows to classify surfactants for their lipophilic/hydrophilic character. This method is based on the proportion between the weight percentages of the hydrophilic and lipophilic groups of a surfactant molecule [23].

CTAB was used to decrease the interfacial tension between water and ethanol during the nanoprecipitation process and study their effect on the resulting final SNPs size. The molecular formula is $C_{19}H_{42}BrN$ (MW=364.46 g/mol), and it has an appearance of white or almost white crystalline powder.

Two different non-ionic surfactants, Tween® 20 and Span® 60, were used to prepare SNPs by the ME method, both were supplied by Sigma Aldrich (USA).

Tweens® or polysorbates are in simple terms ethoxylated chains. The solubility of Tweens® in aqueous solutions increases with the degree of ethoxylation. Tweens® are hydrophilic and are soluble or dispersible in water and dilute electrolytes solutions. Tween® 20 is a yellow viscous liquid, with a molecular formula of $C_{58}H_{114}O_{26}$ (MW=1227.54 g/mol) and its HLB of 16.7.

Sorbitan fatty acid esters are commercially known as Span®. All the Spans® have the structure of sorbitan (1,4-D-sorbitol anhydride) in common which is esterified with one or several fatty acids. Span® 60's HLB is 4.7 and has a molecular formula of $C_{24}H_{46}O_6$ (MW=430.62 g/mol).

Sunflower oil was purchased from the local supermarket, while soybean oil was supplied by Sigma Aldrich (USA). These two oils were used to formulate the microemulsions combined with Tween® 20 or Span® 60 as surfactants, ethanol as co-surfactant and Milli-Q water as the aqueous phase.

2.1.3. Nanoprecipitation method

Nanoprecipitation method was adapted from a method used in previous works by the nanoprecipitation of polymeric particles [24]. This process involves the successive addition of a dilute solution of dissolved starch to a solvent which leads to the starch precipitation.

First, 1% (w/v) starch solution was prepared by dissolving 0.2 g of starch into 20 mL of an aqueous phase by stirring at 80 °C for 30 or 60 min. Four different aqueous phases were tested: (i) 2 % (w/v) NaOH, (ii) 8 % (w/v) NaOH, (iii) 2 % (w/v) NaOH + 10% (w/v) urea, and (iv) 8 % (w/v) NaOH + 10 (%) (w/v) urea. Then, 1 mL of starch solution was added with a syringe pump (at injection rate: 2, 4 and 8 mL/h) into absolute ethanol (from 5 to 40 mL) under constant stirring (500 and 800 rpm).

The effect of the presence of surfactant in the aqueous phase was also studied. For these experiments 4 % (w/v) of CTAB was added to the aqueous phase.

2.1.4. Microemulsion method

ME method was based on the addition of an aqueous starch solution to an organic solvent including a surfactant while being homogenized to form a fine W/O microemulsion where nanoparticles precipitate [25].

First, 1 % (w/v) starch solution was prepared by dissolving 0.2 g of starch into 20 mL of an aqueous phase by stirring at 80 °C for 30 min. Then, 1 mL of starch solution prepared was added with a syringe pump at 4 mL/h into the organic phase (30 mL) under constant stirring (500 rpm).

The organic phase was formed by ethanol with 1 % (w/v) of oil (soybean or sunflower) and two different surfactants used as stabilizers: Tween® 20 and Span® 60 at three different concentrations being 0.1, 1 and 3% (w/v). To prepare the organic phase the surfactant and the oil were added to absolute ethanol and gently mixed for an hour. The presence of ethanol will act as co-stabilizers enhancing the spontaneous microemulsion formation [13, 14, 16].

2.1.5. SNPs characterization

Particle size distribution

Size (in number) and polydispersity index (PdI) of particles were measured by DLS using a Zetasizer Nano ZS equipment (Malvern Instruments Ltd, Malvern, UK). First, the samples were centrifuged at room temperature at 1000 rpm for 10 min. The supernatant was removed to obtain the SNPs in the form of pellets which were washed twice to remove the remains of NaOH and urea, primarily with absolute ethanol and then with Milli-Q water centrifuging again at the same conditions between each wash. Samples were measured with the 173° backscatter detector in disposable low volume cuvettes (Malvern Instruments Ltd, Malvern, UK).

Morphology and size

The shape and size of SNPs were analyzed using a JEOL JSM-6610 LV field emission SEM at an acceleration voltage of 20 kV. Samples were washed in ethanol and then dehydrated in a heater for 24 h at 80 °C. Dehydrated samples were fractured with a spatula and fragments were mounted on aluminum SEM stubs and coated with gold in Balzers SCD 004 sputter coater (Bal-Tec AG, Liechtenstein) before the analysis. The average particle size of the SNPs was determined by random measurements using ImageJ software.

X-Ray Powder Diffraction

The crystalline structure of the starch granules and the synthesized SNPs have been determined by XRPD analysis. The X-ray powder data for the samples were collected, at RT, using $CuK_{\alpha 1,2}$ radiation (λ= 1.54056 Å and 1.54439 Å) in a Bragg-Brentano reflection configuration, on PHILIPS X' PERT PRO Panalytical diffractometer in a 2θ range of 5–27°, with a step size of 0,08356.

Fourier transform infrared spectroscopy

FTIR spectra were acquired in a Fourier transform infrared spectrophotometer (Varian 620-IR, Thermo Fisher ScientificInc., U.S.A.) at room temperature. Samples, dried powder and approximately 1 mg, were directly measured, and spectra were recorded between 650 - 4000 cm−1 (medium infrared band).

2.1.6. Results and discussion

- **Nanoprecipitation method**

2.1.6.1. Screening of operating conditions

To do an initial screening of operating variables affecting the process, the injection rate was varied (2, 4 and 8 mL/h), the dissolution time (30 and 60 min) and stirring rate (500 and 800 rpm). Results are shown in Table 2.1 and Figure 2.1.

It was observed that the mean particle sizes decreased as the injection rate increased. However, it seemed that higher particle formation capacity and more spherical SNPs were obtained when the medium injection rate, i.e., 4 mL/h, was used (Sample N2 from Fig 2.1). Regarding the effect of the stirring rate, although no large differences were found on mean sizes, it was observed that SNPs were laminar in shape instead of spherical at the highest stirring rate (Sample N4 from Fig 2.1). In addition, the results showed that by increasing the aqueous phase dissolution time, a larger amount of agglomerates were produced (Sample N5 from Fig 2.1).

Taking these results into account, the operating conditions selected were 4 mL/h of injection rate, 30 minutes of aqueous phase dissolution time and 500 rpm of stirring rate.

2.1.6.2. Effect of aqueous phase formulation

Different formulations for the aqueous phase used to nanoprecipitate the SNPs were in terms of NaOH and urea solutions since it was reported in previous studies performed with cellulose and starch that the presence of NaOH breaks the intermolecular interactions and intramolecular hydrogen bonds of starch molecules, while urea plays an important role in preventing the self-association of starch molecules, which leads to greater solubility of starch powder [14, 26].

To determine the best aqueous phase formulation, experiments were carried out with each one of them using the nanoprecipitation method with an initial volume of ethanol of 20 mL as an organic phase, a constant stirring speed during the injection of 500 rpm and a pumping flow rate of 4 mL/h. These parameters were determined based on the literature as well as some preliminary experiments [11, 14]. Subsequently, the particle size and PdI were characterized by DLS, and results are shown in Table 2.1. SNPs were also observed under SEM (Figure 2.1) and the size was measured using ImageJ. In addition, shape was also observed since the shape of SNPs depends on synthesis conditions, they can be rod-like in shape, spherical or a mixture of both [14].

It was observed that SNPs were obtained with all of the aqueous phases tested. However, non-spherical shape for SNPs was obtained when 2% (w/v) NaOH solution was used (Sample N6 from Fig 2.1). The number of nanoparticles obtained was greater for urea-containing formulations, as expected. In fact, for the 8% (w/v) NaOH and 10% urea (w/v) solution, fewer agglomerates were observed obtaining an average particle size around 75.1 nm, measured on the micrographs (Sample N2 from Fig 2.1). Therefore, this formulation was selected for subsequent experiments. Size obtained with DLS was around 30 nm in number with a PdI of 0.43. This discrepancy can be explained by the fact that particle size varied in a fairly wide range (25 nm to 100 nm), which is in good agreement with the PdI obtained, but it was observed that small particles were predominated, which is consistent with the data obtained in number by the DLS technique.

2.1.6.3. Effect of ratio of organic phase versus aqueous phase

The effect of different ratios of organic: aqueous phase on the formulation of SNPs was studied since in previous studies it was observed that this ratio could affect the final shape of the SNPs [14]. The ratios tested were: 5:1, 10:1; 15:1, 20:1, 25:1, 30:1 and 40:1 using in all the experiments ethanol as the organic phase. Results are shown in Table 2.1 and SEM micrographs are shown in Figure 2.1. Spherical SNPs were observed at a ratio interval of 20:1-30:1 (Samples N2, N12 and N13 from Fig 2.1). At lower ratios, fibrous shaped SNPs were obtained while mixtures of fibers and spheres were obtained when higher ratios were used (Sample N14 from Fig 2.1). These results were in good agreement with previously reported by Chin et al.

Table 2.1. *Mean sizes and PdI of SNPs obtained by the nanoprecipitation method using normal maize starch at different operating conditions and formulations*

Sample	Type of starch	Aqueous phase (% w/v)	Flow rate (mL/h)	Stirring (rpm)	Dissolution time (min)	O:A ratio (mL/mL)	Size (nm) Number	PdI	ImageJ (nm)
N1	Normal	NaOH 8% + urea 10%	2	500	30	20:1	42.6±27.5	0.44±0.01	---[1]
N2	Normal	NaOH 8% + urea 10%	4	500	30	20:1	29.7±77.4	0.43±0.04	75.1±39.8
N3	Normal	NaOH 8% + urea 10%	8	500	30	20:1	13.9±9.03	0.46±0.01	67.2±19.9
N4	Normal	NaOH 8% + urea 10%	4	800	30	20:1	25.1±10.5	0.34±0.04	---[1]
N5	Normal	NaOH 8% + urea 10%	4	500	60	20:1	23.2±8.62	0.61±0.01	77.6±23.3
N6	Normal	NaOH 2%	4	500	30	20:1	42.8±43.1	0.32±0.06	---[1]
N7	Normal	NaOH 8%	4	500	30	20:1	15.8±4.34	0.39±0.07	66.1±12.6
N8	Normal	NaOH 2% + urea 10%	4	500	30	20:1	55.2±32.2	0.23±0.02	74.6±17.3
N9	Normal	NaOH 8% + urea 10%	4	500	30	5:1	316±56.8	0.59±0.03	---[1]
N10	Normal	NaOH 8% + urea 10%	4	500	30	10:1	34.9±9.59	0.66±0.03	---[1]
N11	Normal	NaOH 8% + urea 10%	4	500	30	15:1	34.3±10.3	0.79±0.16	---[1]
N12	Normal	NaOH 8% + urea 10%	4	500	30	25:1	23.3±6.23	0.46±0.04	63.3±33.8
N13	Normal	NaOH 8% + urea 10%	4	500	30	30:1	24.5±4.53	0.47±0.08	59.1±28.5
N14	Normal	NaOH 8% + urea 10%	4	500	30	40:1	24.4±5.77	0.39±0.08	---[1]
N15	Waxy	NaOH 8% + urea 10%	4	500	30	20:1	22.3±24.4	0.37±0.05	63.1±22.6
N16	Waxy	NaOH 8% + urea 10%	4	500	30	30:1	26.2±3.83	0.43±0.03	58.8±15.6
N17	High amylose	NaOH 8% + urea 10%	4	500	30	20:1	29.3±16.7	0.44±0.03	73.6±20.5
N18	High amylose	NaOH 8% + urea 10%	4	500	30	30:1	16.4±6.70	0.48±0.01	72.6±12.2
N19	Normal	NaOH 8% + urea 10% + 4%CTAB	4	500	30	20:1	126±40.8	0.47±0.12	---[1]

N20	Normal	NaOH 8% + urea 10% + 4%CTAB	4	500	30	30:1	56.7±8.95	0.42±0.04	---[1]
N21	Waxy	NaOH 8% + urea 10% + 4%CTAB	4	500	30	20:1	50.3±8.63	0.61±0.12	---[1]
N22	Waxy	NaOH 8% + urea 10% + 4%CTAB	4	500	30	30:1	36.6±8.15	0.45±0.05	117±47.1
N23	High amylose	NaOH 8% + urea 10% + 4%CTAB	4	500	30	20:1	> 500	0.63±0.10	65.6±21.3
N24	High amylose	NaOH 8% + urea 10% + 4%CTAB	4	500	30	30:1	> 300	0.53±0.03	64.3±13.8

[1] Non spherical SNPs

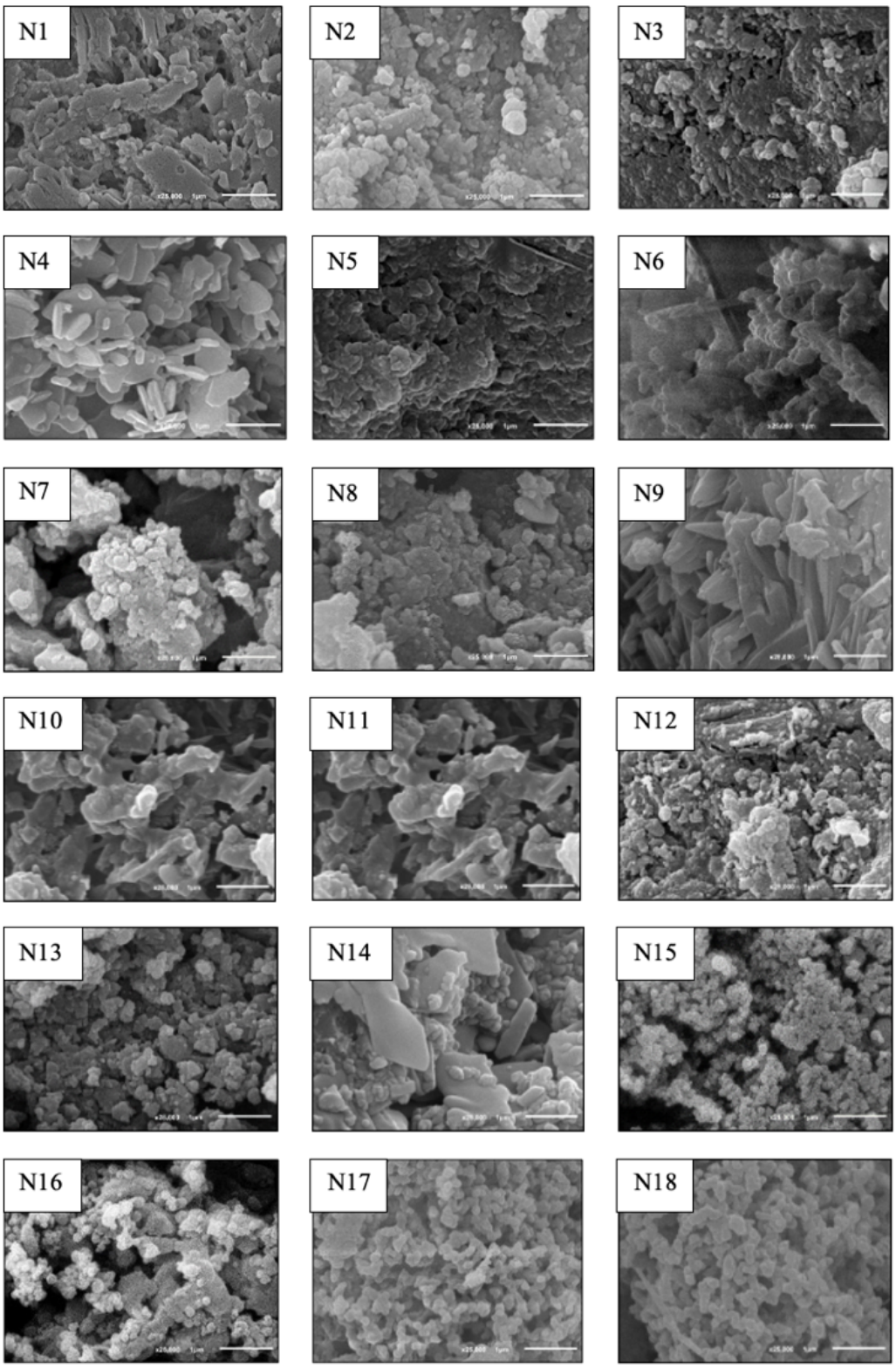

Figure 2.1. *SEM micrographs of SNPs obtained by the nanoprecipitation method using different operating conditions and different formulations by nanoprecipitation method.*

2.1.6.4. Effect of amylose/amylopectin content

Three maize starches were used to investigate the effect of amylose/amylopectin content on the SNPs size formation. The results are presented in Table 2.1 and Figure 2.1. Samples N2 and N13 are referred to normal maize starch, samples N15 and N16 to waxy maize starch and samples N17 and N18 to high amylose maize starch. Smaller particle sizes were obtained when the waxy starch was used, obtaining an average size measured with ImageJ of 63.1 nm and with a 20:1 ratio organic: aqueous phase. When the ratio was 30:1 an average size of 58.8 nm was obtained. While when the starch with high amylose content was used, SNPs average size was 73.6 nm for a 20:1 ratio and 72.6 nm when a 30:1 ratio was used.

By looking at the pictures, normal maize seemed to give two different distributions of particle sizes. For waxy starch, the particles seem to be smaller and tender to cluster, while for high amylose, the particles seem to be more rod-like and forming kind of a pearl string. When comparing this to the molecular structure of the different starches, normal starch contains both amylose and amylopectin which means the presence of two different sized molecules with different structures, waxy is highly branched molecule and amylose is a long chain molecule with just a few branches. Therefore, how the SNPs are organized in these images seems to be correlated with the structure of the pure starch molecules of the intact granules when comparing them.

2.1.6.5. Effect of surfactant addition

The effect of surfactant addition on the mean particle sizes of SNPs formed was studied since surfactants can interfere with the interfacial tension between the organic and the aqueous phase during the nanoprecipitation process. For this purpose, the best organic: aqueous phase ratios were used (20:1 and 30:1) to synthesize SNPs using CTAB for the three types of starches studied as it was demonstrated in previous studies that led to smaller sizes [14]. The main results obtained are shown in Table 2.1 and Figure 2.2 (samples from N19 to N24).

No differences in shape were observed when normal maize starch was used in presence of CTAB (Figure 2.2, samples N19 and N20). However, SNPs obtained with waxy starch in the presence of CTAB led to a mixture of spherical particles and rod-shaped particles (Figure 2.2, samples N21 and N22) while for starch with high amylose content, spherical particles predominated (Figure 2.2,

samples N23 and N24). In general, when comparing sizes in number for the three types of starches they were smaller without the presence of surfactant (Table 2.1). Moreover, non-spherical particles were observed under SEM for waxy and normal starches. However, for high amylose SNPs size was reduced around 8-9 nm probably caused by the interactions between high amylose starch molecules and CTAB surfactant that could improve starch SNPs stability by reducing particle agglomeration. It has been demonstrated in previous studies that interactions between amylose and amylopectin with CTAB seemed to be similar but with small differences probably caused by the different structure [27, 28].

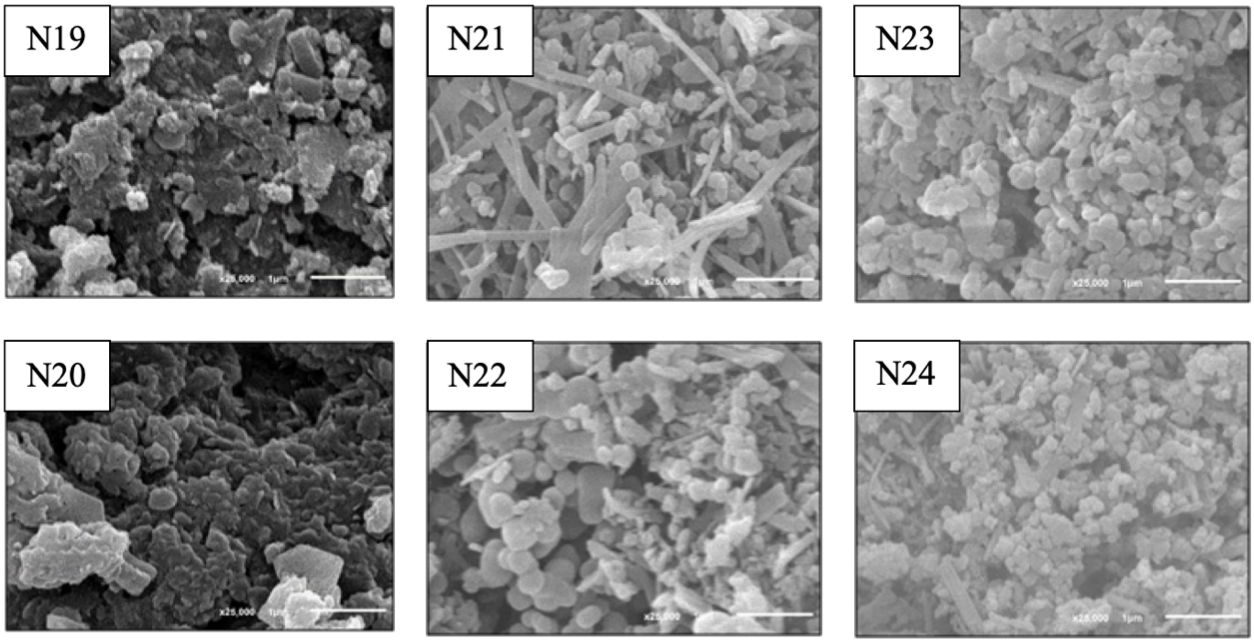

Figure 2.2. *SEM micrographs of SNPs obtained by the nanoprecipitation method using an aqueous phase consisting of 8% (w/v) NaOH and 10% (w/v) solution and 4 % (w/v) of CTAB using starches with different amylose/amylopectin content and different organic:aqueous phase ratios.*

- **Microemulsion method**

2.1.6.6. Effect of microemulsion formulation

The results obtained are shown in Table 2.2 and Figure 2.3.

Table 2.2. *Mean sizes and PdI of SNPs obtained by ME method using an aqueous phase consisting of 8 % (w/v) NaOH and 10 % (w/v) solution with normal starch and different type of oil (1 % w/v) and surfactants as well as different concentrations of surfactant.*

Sample	Type of starch	Oil	Surfactant (% w/v)	Size (nm) Number	PdI	ImageJ (nm)
M1	Normal	Soybean oil	0.1%T20	62.3±11.4	0.55±0.03	59.9±14.4
M2	Normal	Sunflower oil	0.1%T20	41.8±3.85	0.56±0.07	59.6±16.2
M3	Normal	Soybean oil	0.1%S60	66.3±26.7	0.52±0.04	81.2±15.1
M4	Normal	Sunflower oil	0.1%S60	46.8±5.33	0.54±0.03	63.9±17.5
M5	Normal	Soybean oil	1% T20	31.0±59.9	0.74±0.04	46.4±14.9
M6	Normal	Sunflower oil	1 % T20	58.1±12.8	0.72±0.05	61.7±14.7
M7	Normal	Soybean oil	1% S60	60.4±14.7	0.67±0.09	64.6±15.1
M8	Normal	Sunflower oil	1% S60	51.5±13.8	0.69±0.11	49.6±9.25
M9	Normal	Soybean oil	3% T20	56.5±13.8	0.53±0.09	43.8±11.8
M10	Normal	Sunflower oil	3% T20	53.4±17.3	0.54±0.01	52.9±11.5
M11	Normal	Soybean oil	3% S60	112±50.3	0.39±0.04	120±44.5
M12	Normal	Sunflower oil	3% S60	61.1±38.8	0.37±0.04	---[1]

[1] Non spherical SNPs

For 1% (w/v) oil spherical particles were obtained in all cases with the same average particle size of 60 nm (sample M1) measured with ImageJ, for the formulations containing 0.1% (w/v) Tween 20 and either soybean or sunflower oil. On the other hand, formulations with 0.1% (w/v) Span 60 gave rise to larger SNPs for both oils tested. This differences in size could be attributed to the different hydrophilicity of the different types of the surfactants used what could modify the interactions between starch particles. Tween 20 is more hydrophilic than Span 60, and would interact stronger with starch molecules, and therefore smaller SNPs could be precipitated. A similar trend was observed by other authors when two surfactants with different HLB were tested [14].

Increasing the amount of surfactant to a 1% (w/v), a decrease of around 10-20 nm was observed in the SNP sizes for both surfactants and oil used. This could be explained by the fact that at higher surfactant concentrations microemulsions with smaller droplet size could be obtained producing at the same time a decrease in the resulting SNPs formed. Following formulations used by other authors, it was observed that 3% seemed to be enough to stabilize the interface during SNPs formation and controlling the size [11].

On the other hand, a different trend was found when Span 60 was used since a large increase in the average particle size was observed, with values up to 120 nm (sample M11), when soybean oil was used while particles that did not present spherical form, as shown in Figure 2.3 (sample M12), were obtained with the formulation with sunflower oil.

It can be observed that, compared to results obtained by the nanoprecipitation method, particle formation capacity obtained by ME method seemed to be higher in all cases.

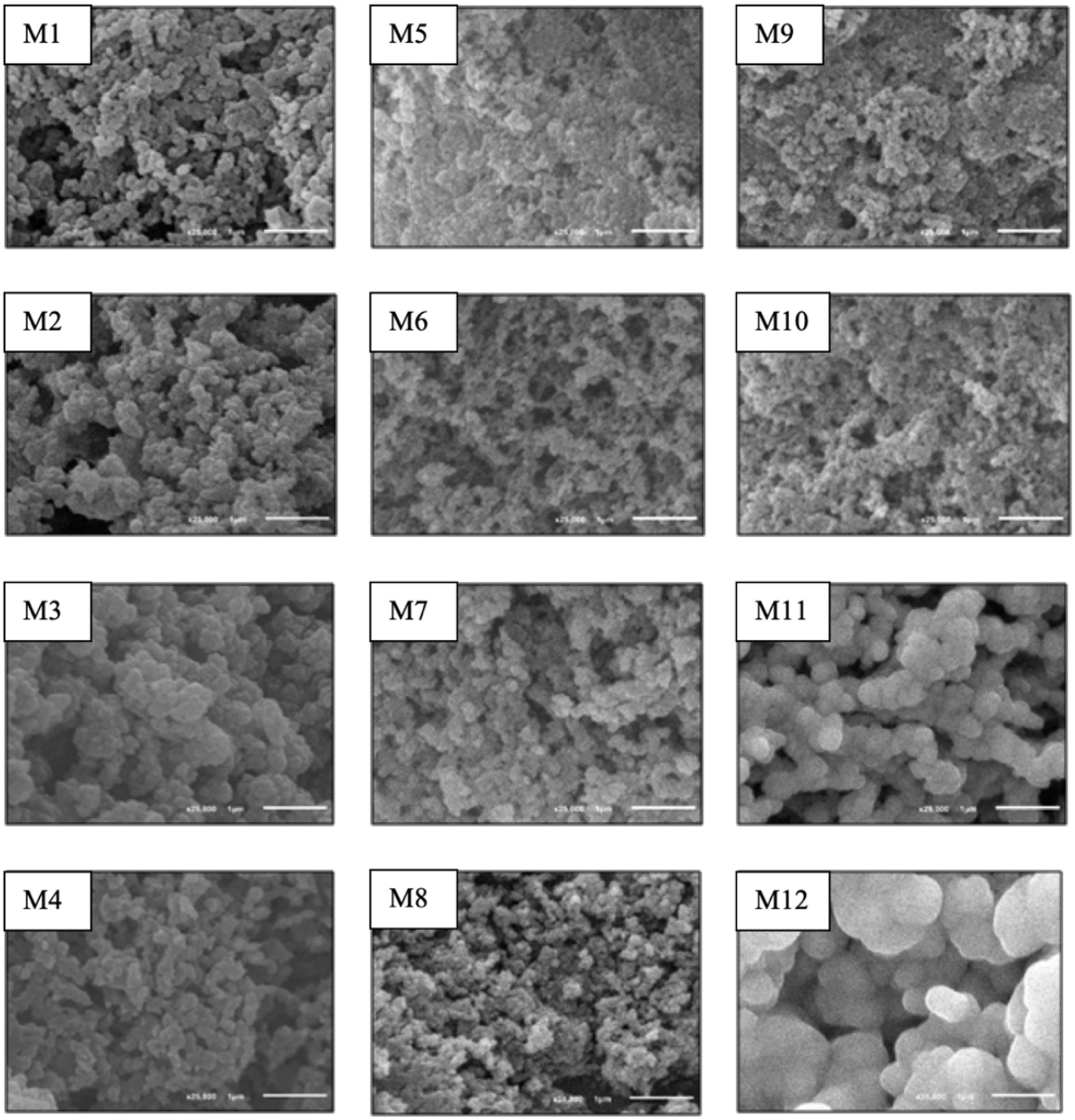

Figure 2.3. *SEM micrographs of SNPs obtained by ME method using an aqueous phase consisting of 8 % (w/v) NaOH and 10 % (w/v) solution and different type of oil (1 %) and surfactants (0.1, 1 or 3 % w/v).*

2.1.6.7. Effect of amylose and amylopectin content

All results are shown in Table 2.3, Figure 2.4 and Figure 2.5. Sizes obtained with waxy and high amylose starches with ME method presented higher dependence to the microemulsion formulation than the ones obtained with normal starch, being high amylose starch the one that present more variations on the SNPs size registered in all formulations tested.

Table 2.3. *Mean sizes and PdI of SNPs obtained by ME method using an aqueous phase consisting of 8 % (w/v) NaOH and 10 % (w/v) solution with waxy and high amylose starch and different concentrations of surfactant at 1 % (w/v) sunflower/soybean oil content and 30:1 ratio of organic to aqueous phase.*

Sample	Type of starch	Oil	Surfactant (%w/v)	Size (nm) Number	PdI	ImageJ (nm)
M13	Waxy	Soybean oil	0.1% T20	22.9±9.21	0.43±0.01	38.9±11.7
M14	Waxy	Sunflower oil	0.1% T20	24.6±10.1	0.40±0.01	---[1]
M15	Waxy	Soybean oil	0.1% S60	38.5±20.9	0.37±0.03	84.3±16.4
M16	Waxy	Sunflower oil	0.1% S60	48.7±63.7	0.24±0.01	78.4±14.8
M17	Waxy	Soybean oil	1% T20	38.8±20.8	0.36±0.05	---[1]
M18	Waxy	Sunflower oil	1% T20	30.9±15.5	0.38±0.04	---[1]
M19	Waxy	Soybean oil	1% S60	44.9±13.1	0.61±0.10	84.8±23.4
M20	Waxy	Sunflower oil	1% S60	52.8±15.1	0.49±0.08	62.6±28.3
M21	Waxy	Soybean oil	3% T20	36.9±17.9	0.27±0.01	46.5±12.7
M22	Waxy	Sunflower oil	3% T20	38.1±14.1	0.33±0.01	---[1]
M23	Waxy	Soybean oil	3% S60	81.5±24.3	0.62±0.11	---[1]
M24	Waxy	Sunflower oil	3% S60	59.2±24.1	0.39±0.04	---[1]
M25	High amylose	Soybean oil	0.1% T20	61.7±8.80	0.69±0.16	75.4±17.8
M26	High amylose	Sunflower oil	0.1% T20	90.8±23.4	0.99±0.01	106±26.5
M27	High amylose	Soybean oil	0.1% S60	65.3±8.29	0.79±0.27	54.5±13.2
M28	High amylose	Sunflower oil	0.1% S60	82.5±35.3	0.62±0.08	114±49.7
M29	High amylose	Soybean oil	1% T20	67.2±28.6	0.58±0.05	55.4±11.1
M30	High amylose	Sunflower oil	1% T20	73.6±10.6	0.80±0.09	40.9±10.5
M31	High amylose	Soybean oil	1% S60	78.3±10.9	0.89±0.14	134±32.2
M32	High amylose	Sunflower oil	1% S60	72.1±34.5	0.65±0.16	147±28.8
M33	High amylose	Soybean oil	3% T20	107±26.3	0.49±0.05	34.8±10.1
M34	High amylose	Sunflower oil	3% T20	54.2±57.3	0.46±0.08	---[1]

M35	High amylose	Soybean oil	3% S60	113±67.2	0.26±0.01	129±28.2
M36	High amylose	Sunflower oil	3% S60	77.9±41.9	0.68±0.12	---[1]

[1] Non spherical SNPs

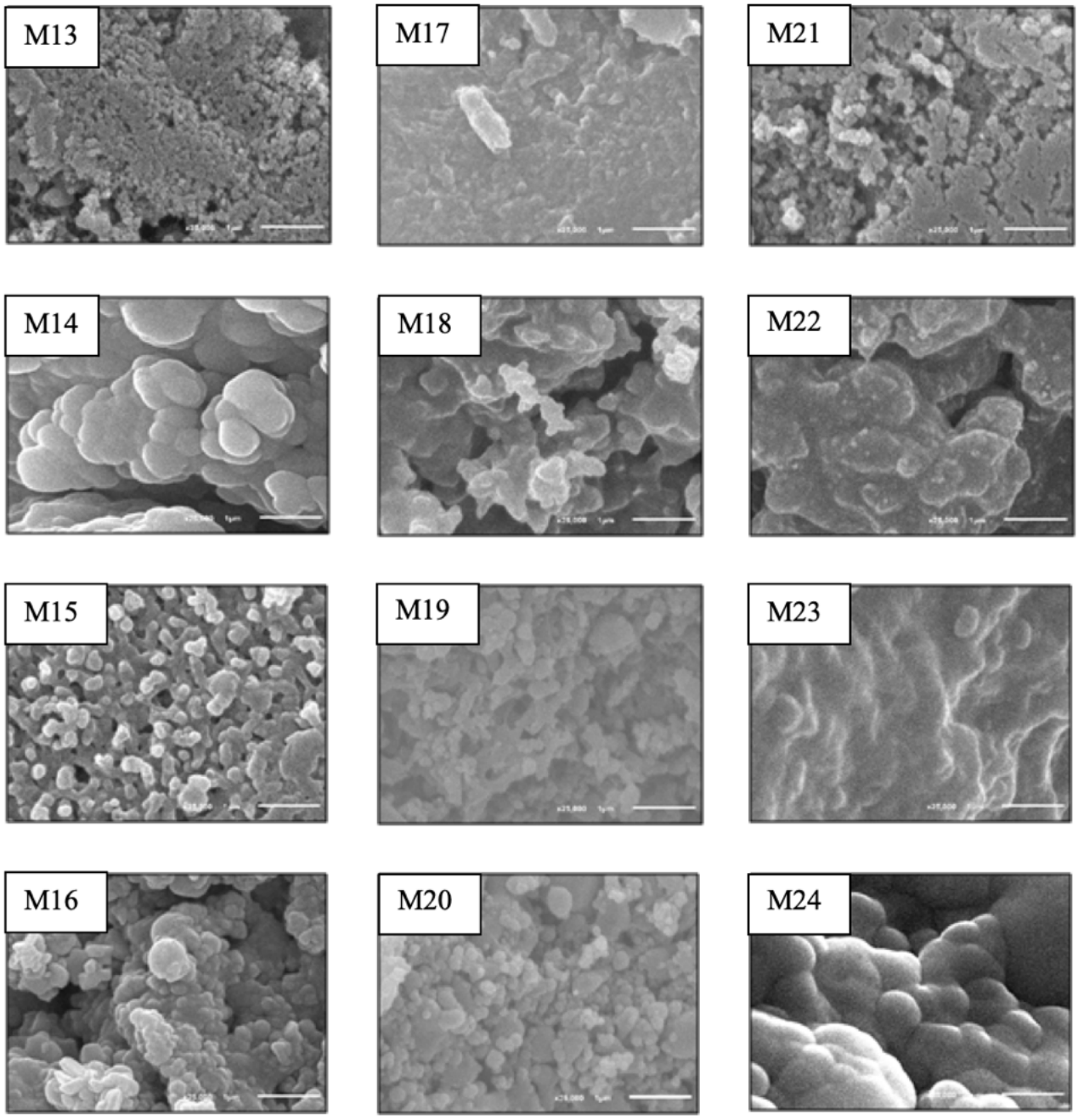

Figure 2.4. *SEM micrographs of waxy SNPs obtained by ME method using an aqueous phase consisting of 8% (w/v) NaOH and 10% (w/v) solution, waxy starch and different type of oil (1%) and surfactants (0.1, 1 or 3%).*

Best results were obtained at lower surfactant concentrations. Comparing both types of starch used smaller average size, 38.9 nm, measured with ImageJ, was obtained when 0.1% (w/v) surfactant of Tween 20 was used for waxy starch when using soybean oil (sample M13) while a mean size of 75.4 nm was obtained for high amylose starch (sample M25). The opposite trend was found with Span 60 when the same oil was used since the sizes obtained were 84.3 nm and 54.5 nm when waxy (sample M15) and high amylose (sample M27) starches were used respectively.

Using sunflower oil, the average size was 106 nm when 0.1% (w/v) Tween 20 was used with high amylose starch (sample M26) while non spherical particles were obtained when using waxy starch. When the surfactant was used with Span 60 at the same concentration the average sizes was 78.4 nm for the waxy starch (sample M16) and 114 nm using high amylose starch (sample M28). Furthermore, when the amount of the surfactant was increased to 1% (w/v), particles were not formed for Tween 20 and waxy starch with both types of oil. However, using 1% (w/v) Span 60 the average size obtained was 84.8 nm (sample M19) and 62.6 nm (sample M20) when soybean and sunflower oil were used respectively.

When high amylose starch was used, a smaller average size was obtained (55.4 nm) (sample M29) with soybean oil and 1% (w/v) Tween 20 and 134 nm (sample M31) for 1% (w/v) Span 60. A similar trend was found when sunflower oil was used with the same type of starch with the average size of 40.9 nm (M30) for 1% (w/v) Tween 20 while particles with a size of 147 nm (sample M32) were obtained with the Span 60. This is an indication that Span 60 presents a negative effect on high amylose SNPs formation as was the case for normal starch.

At soybean oil and 3% (w/v) Tween 20 concentration, an average size of 34.8 nm was obtained for high amylose starch (sample M33) and 46.5 nm with waxy starch (sample M21).

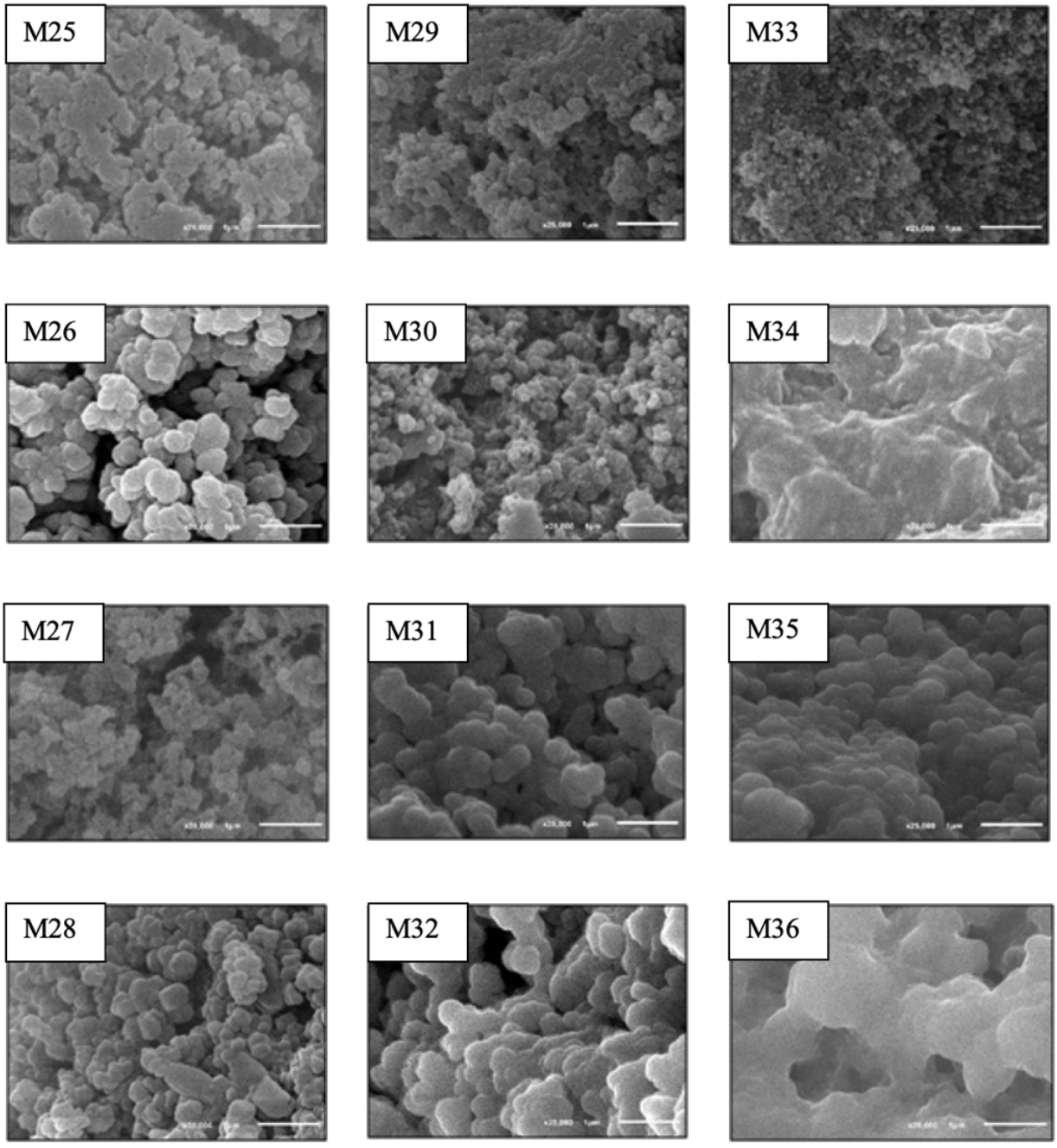

Figure 2.5. *SEM micrographs of high amylose SNPs obtained by ME method using an aqueous phase consisting of 8 % (w/v) NaOH and 10 % (w/v) solution, waxy starch and different type of oil (1 %) and surfactants (0.1, 1 or 3 % w/v).*

Results obtained with the rest of the formulations containing 3% (w/v) Span 60 did not show spherical shape but aggregates which means that SNPs were not formed completely what could be caused because of using a high volume of a hydrophobic surfactant, probably caused by interactions between the hydrocarbon chains.

2.1.6.8. XRPD and FTIR analysis

The three types of granules used in this study were analyzed by FTIR as well as the resulting SNPs prepared with each type of granules by the two methods of preparation used (nanoprecipitation and ME), using the operational conditions that led best results, being in total 9 samples analyzed.

The FTIR spectra depicted in Figure 2.6 shows almost identical characteristic bands for the three types of starch granules studied. The strong absorption peak was observed around 3280–3243 cm^{-1} which is attributed to is attributed to overlapping of stretching bands of the different -OH groups. Similar results were obtained by other authors [29, 30].

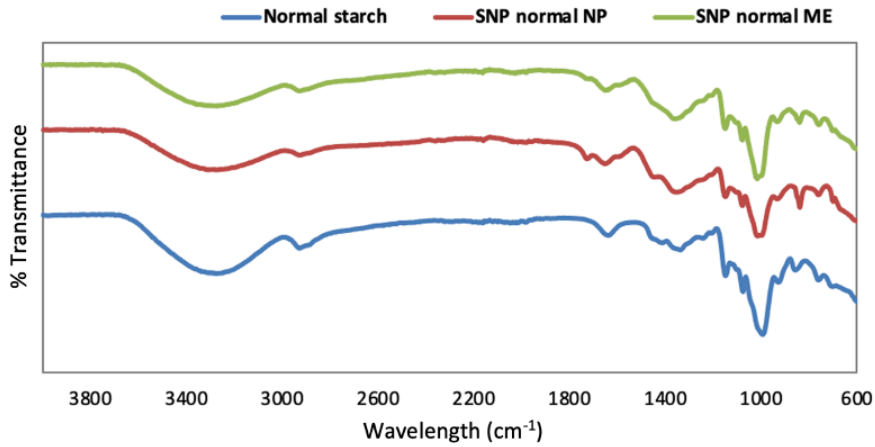

(A) Normal starch granules and nanoparticles: N2 and M1

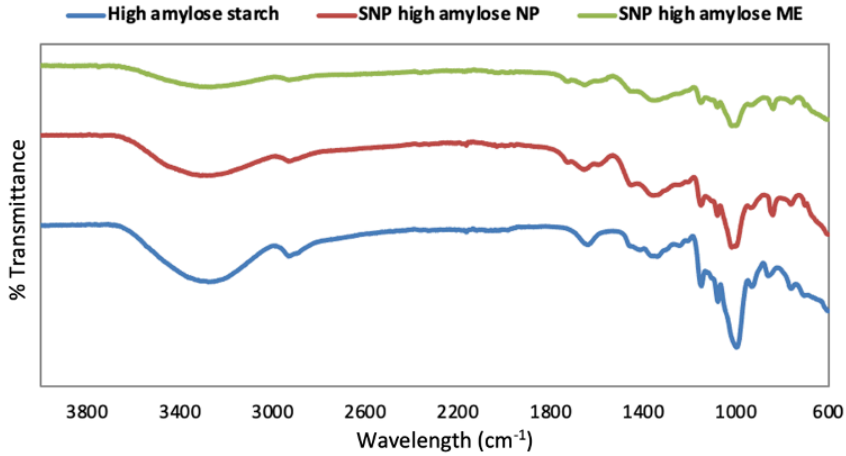

(B) High amylose starch granules and nanoparticles: N17 and M30

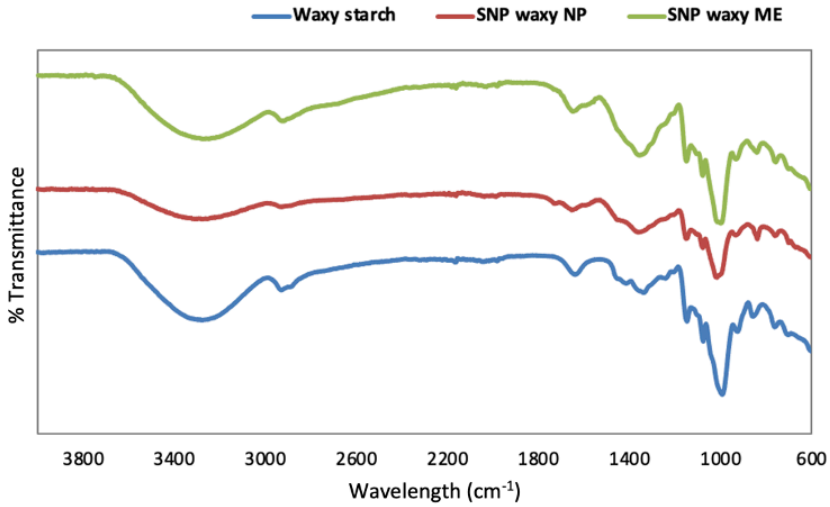

(C) Waxy starch granules and nanoparticles: N15 and M20

Figure 2.6. *FTIR curves of normal, waxy and high amylose starches and the resulting SNPs synthesized at optimum conditions. ME: Microemulsion method; nanop: Nanoprecipitation method.*

However, Ahmad et al. also reported that the peaks of O–H stretching shifted to higher wavelength range for SNPs, obtained by alkalization and sonication processes, what was attributed to the loss of the crystalline structure and exposure of -OH groups of the starch molecule to the preparation process [29]. Moreover, in the FTIR images obtained in that study it can be observed how the intensity of the absorption peaks within that wavelength is much less pronounced for the SNPs. A similar trend was observed for SNPs obtained by nanoprecipitation and ME methods for the three types of starches.

The absorption peak observed at 2927 cm^{-1} can be explained by -CH_2 stretching vibrational modes bands while the peaks observed at the wavelengths of 1147, 1078 and 990 cm^{-1} are associated with the stretching vibration of the C-O bond, C-O-H and C-O-C groups in the glucose ring, respectively. The absorption peak at 1643 cm^{-1} can be due to the presence of bound water in starch. This is in good agreement with previous studies [29, 31].

FTIR spectroscopy can also be used to determine the crystallinity of starch by characterizing the changes that occur in the semi crystalline and amorphous domains within starch granules [29]. The high peak intensity obtained at 995 cm^{-1} that possess shoulder at the wavenumber of 1018 cm^{-1} and 1047 cm^{-1} indicated amorphous character and crystalline order of starch. No differences were observed when comparing the spectra within this range for normal maize starch granules and SNPs produced by both methods of preparation. However, for high amylose starch a less pronounced peak was observed when SNPs were obtained by the ME method. Similar trend was found when comparing the spectra obtained with waxy starch regarding a different absorption with SNPs obtained by nanoprecipitation. Therefore, the type of starch used, and the method of preparation selected for the synthesis of SNPs could produce some changes in the physico-chemical structure of the resulting nanoparticles.

The same samples were analyzed by XRPD in order to observe the crystalline structure of the granules and the spectra are shown in Figure 2.7.

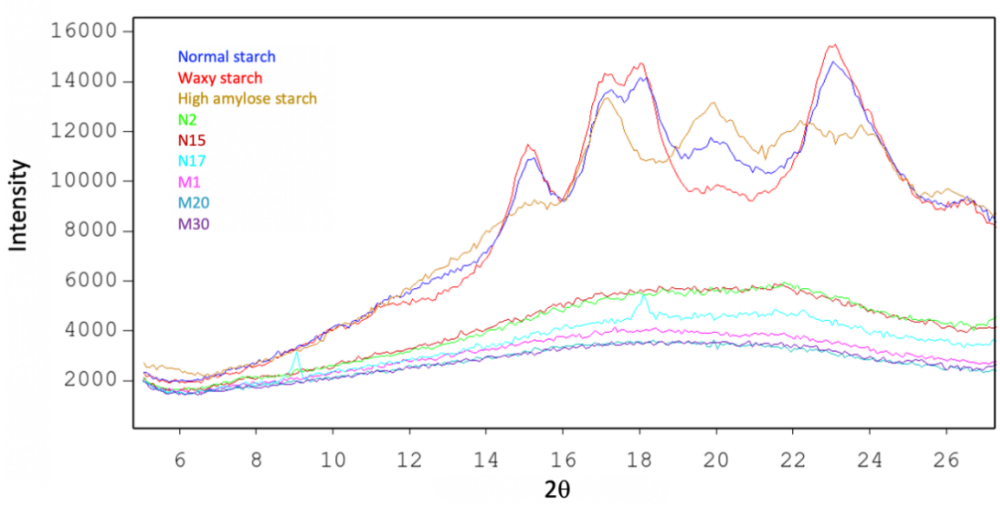

Figure 2.7. *XRPD spectra of normal, waxy and high amylose starches and the resulting SNPs synthesized at optimum conditions. ME: Microemulsion method (samples M1, M20 and M30); nanop: Nanoprecipitation method (samples N2, N15 and N17).*

The A-type X-ray diffractions patterns were observed for normal and waxy maize starch granules with peaks at Bragg angles (2θ) at 15°, 17°, 18° and 23°. High amylose starch exhibited B+V type crystalline pattern displaying the peaks at 17.1°, 19.9°, 22.3° and 24.9°. These results are in good agreement with previous studies [32].

On the other hand, major peak diffraction did not exist for all SNPs analyzed appearing the whole structure like amorphous. Similar results were reported by other authors [33]. Moreover, it was also reported that low X-ray crystallinity is not necessarily related to poorly ordered starch molecules but may be the result of small size crystallite in the granules [34]. Therefore, the small size of the SNPs reported in the manuscript could explain the XRD spectra obtained.

2.1.7. Conclusions

Nanoprecipitation method allowed to produce maize SNPs in the range 58-73 nm, at optimum conditions, while by the use of ME method sizes between 35-147 nm were registered, obtaining the smaller sizes when waxy maize starch was used in both techniques. The type of oil used for microemulsion formulation did not present a high influence on the SNPs size, but the type of surfactant was a key factor, as a general trend smaller sizes were obtained by the use of very hydrophilic surfactants. Comparing both methods of preparation, higher particle formation capacity was observed by ME method with a more monodispersed and discrete appearance without

the presence of large agglomerates. Therefore, controlled size SNPs could be obtained by this ME method selecting the appropriate formulation and starch type.

References

[1] H. Y. Kim, S. S. Park, and S. T. Lim, "Preparation, characterization and utilization of starch nanoparticles," *Colloids and Surfaces B: Biointerfaces*, vol. 126. Elsevier, pp. 607–620, Feb. 01, 2015. doi: 10.1016/j.colsurfb.2014.11.011.

[2] D. Le Corre, J. Bras, and A. Dufresne, "Starch nanoparticles: A review," *Biomacromolecules*, vol. 11, no. 5. pp. 1139–1153, May 10, 2010. doi: 10.1021/bm901428y.

[3] J. Kim, D. Park, and S. Lim, "Fragmentation of Waxy Rice Starch Granules by Enzymatic Hydrolysis," *Cereal Chem*, vol. 85, no. 2, pp. 182–187, Mar. 2008, doi: 10.1094/CCHEM-85-2-0182.

[4] J.-L. Putaux, S. Molina-Boisseau, T. Momaur, and A. Dufresne, "Platelet Nanocrystals Resulting from the Disruption of Waxy Maize Starch Granules by Acid Hydrolysis," *Biomacromolecules*, vol. 4, no. 5, pp. 1198–1202, Sep. 2003, doi: 10.1021/bm0340422.

[5] D. Liu, Q. Wu, H. Chen, and P. R. Chang, "Transitional properties of starch colloid with particle size reduction from micro- to nanometer," *J Colloid Interface Sci*, vol. 339, no. 1, pp. 117–124, Nov. 2009, doi: 10.1016/j.jcis.2009.07.035.

[6] S. Bel Haaj, A. Magnin, C. Pétrier, and S. Boufi, "Starch nanoparticles formation via high power ultrasonication," *Carbohydr Polym*, vol. 92, no. 2, pp. 1625–1632, Feb. 2013, doi: 10.1016/j.carbpol.2012.11.022.

[7] D. Song, Y. S. Thio, and Y. Deng, "Starch nanoparticle formation via reactive extrusion and related mechanism study," *Carbohydr Polym*, vol. 85, no. 1, pp. 208–214, Apr. 2011, doi: 10.1016/j.carbpol.2011.02.016.

[8] D. LeCorre, E. Vahanian, A. Dufresne, and J. Bras, "Enzymatic Pretreatment for Preparing Starch Nanocrystals," *Biomacromolecules*, vol. 13, no. 1, pp. 132–137, Jan. 2012, doi: 10.1021/bm201333k.

[9] H.-Y. Kim, J.-A. Han, D.-K. Kweon, J.-D. Park, and S.-T. Lim, "Effect of ultrasonic treatments on nanoparticle preparation of acid-hydrolyzed waxy maize starch," *Carbohydr Polym*, vol. 93, no. 2, pp. 582–588, Apr. 2013, doi: 10.1016/j.carbpol.2012.12.050.

[10] H.-Y. Kim, D. J. Park, J.-Y. Kim, and S.-T. Lim, "Preparation of crystalline starch nanoparticles using cold acid hydrolysis and ultrasonication," *Carbohydr Polym*, vol. 98, no. 1, pp. 295–301, Oct. 2013, doi: 10.1016/j.carbpol.2013.05.085.

[11] S. F. Chin, A. Azman, and S. C. Pang, "Size controlled synthesis of starch nanoparticles by a microemulsion method," *J Nanomater*, vol. 2014, 2014, doi: 10.1155/2014/763736.

[12] S. F. Chin, S. N. A. Mohd Yazid, and S. C. Pang, "Preparation and Characterization of Starch Nanoparticles for Controlled Release of Curcumin," *Int J Polym Sci*, vol. 2014, pp. 1–8, 2014, doi: 10.1155/2014/340121.

[13] N. S. Ismail and S. C. B. Gopinath, "Enhanced antibacterial effect by antibiotic loaded starch nanoparticle," *Journal of the Association of Arab Universities for Basic and Applied Sciences*, vol. 24, pp. 136–140, Oct. 2017, doi: 10.1016/j.jaubas.2016.10.005.

[14] S. F. Chin, S. C. Pang, and S. H. Tay, "Size controlled synthesis of starch nanoparticles by a simple nanoprecipitation method," *Carbohydr Polym*, vol. 86, no. 4, pp. 1817–1819, Oct. 2011, doi: 10.1016/j.carbpol.2011.07.012.

[15] X. Ma, R. Jian, P. R. Chang, and J. Yu, "Fabrication and characterization of citric acid-modified starch nanoparticles/plasticized-starch composites," *Biomacromolecules*, vol. 9, no. 11, pp. 3314–3320, Nov. 2008, doi: 10.1021/bm800987c.

[16] S. H. Mahmoudi Najafi, M. Baghaie, and A. Ashori, "Preparation and characterization of acetylated starch nanoparticles as drug carrier: Ciprofloxacin as a model," *Int J Biol Macromol*, vol. 87, pp. 48–54, Jun. 2016, doi: 10.1016/j.ijbiomac.2016.02.030.

[17] H. Saari, C. Fuentes, M. Sjöö, M. Rayner, and M. Wahlgren, "Production of starch nanoparticles by dissolution and non-solvent precipitation for use in food-grade Pickering emulsions," *Carbohydr Polym*, vol. 157, pp. 558–566, Feb. 2017, doi: 10.1016/j.carbpol.2016.10.003.

[18] Y. Tan, K. Xu, L. Li, C. Liu, C. Song, and P. Wang, "Fabrication of Size-Controlled Starch-Based Nanospheres by Nanoprecipitation," *ACS Appl Mater Interfaces*, vol. 1, no. 4, pp. 956–959, Apr. 2009, doi: 10.1021/am900054f.

[19] S. V. Kumar, A. P. Bafana, P. Pawar, A. Rahman, S. A. Dahoumane, and C. S. Jeffryes, "High conversion synthesis of <10 nm starch-stabilized silver nanoparticles using microwave technology," *Sci Rep*, vol. 8, no. 1, p. 5106, Mar. 2018, doi: 10.1038/s41598-018-23480-6.

[20] S. Likhitkar and A. K. Bajpai, "Magnetically controlled release of cisplatin from superparamagnetic starch nanoparticles," *Carbohydr Polym*, vol. 87, no. 1, pp. 300–308, Jan. 2012, doi: 10.1016/ j.carbpol.2011.07.053.

[21] P. Dandekar *et al.*, "A Hydrophobic Starch Polymer for Nanoparticle-Mediated Delivery of Docetaxel," *Macromol Biosci*, vol. 12, no. 2, pp. 184–194, Feb. 2012, doi: 10.1002/mabi.201100244.

[22] S. Xiao *et al.*, "Preparation of folate-conjugated starch nanoparticles and its application to tumor-targeted drug delivery vector," *Chinese Science Bulletin*, vol. 51, no. 14, pp. 1693–1697, Jul. 2006, doi: 10.1007/s11434-006-2039-7.

[23] G. W. C., "Calculation of HLB values of non-ionic surfactants," *Am Perfumer Essent Oil Rev*, vol. 65, pp. 26–29, 1955, Accessed: May 14, 2024. [Online]. Available: https://cir.nii.ac.jp/crid/1572261549150924416.bib?lang=ja

[24] A. P. Mathew and A. Dufresne, "Morphological Investigation of Nanocomposites from Sorbitol Plasticized Starch and Tunicin Whiskers," *Biomacromolecules*, vol. 3, no. 3, pp. 609–617, May 2002, doi: 10.1021/bm0101769.

[25] C. Qiu, C. Wang, C. Gong, D. J. McClements, Z. Jin, and J. Wang, "Advances in research on preparation, characterization, interaction with proteins, digestion and delivery systems of starch-based nanoparticles," *International Journal of Biological Macromolecules*, vol. 152. Elsevier B.V., pp. 117–125, Jun. 01, 2020. doi: 10.1016/j.ijbiomac.2020.02.156.

[26] H. Jin, C. Zha, and L. Gu, "Direct dissolution of cellulose in NaOH/thiourea/urea aqueous solution," *Carbohydr Res*, vol. 342, no. 6, pp. 851–858, May 2007, doi: 10.1016/j.carres.2006.12.023.

[27] H. Lundqvist, A.-C. Eliasson, and G. Olofsson, "Binding of hexadecyltrimethylammonium bromide to starch polysaccharides. Part II. Calorimetric study," *Carbohydr Polym*, vol. 49, no. 2, pp. 109–120, Aug. 2002, doi: 10.1016/S0144-8617(01)00326-5.

[28] H. Lundqvist, "Binding of hexadecyltrimethylammonium bromide to starch polysaccharides. Part I. Surface tension measurements," *Carbohydr Polym*, vol. 49, no. 1, pp. 43–55, Jul. 2002, doi: 10.1016/S0144-8617(01)00299-5.

[29] M. Ahmad, A. Gani, ifra Hassan, Q. Huang, and H. Shabbir, "production and characterization of starch nanoparticles by mild alkali hydrolysis and ultra-sonication process," 2020, doi: 10.1038/s41598-020-60380-0.

[30] L. Acevedo-Guevara, L. Nieto-Suaza, L. T. Sanchez, M. I. Pinzon, and C. C. Villa, "Development of native and modified banana starch nanoparticles as vehicles for curcumin," *Int J Biol Macromol*, vol. 111, pp. 498–504, May 2018, doi: 10.1016/j.ijbiomac.2018.01.063.

[31] C. Qiu, Y. Qin, S. Zhang, L. Xiong, and Q. Sun, "A comparative study of size-controlled worm-like amylopectin nanoparticles and spherical amylose nanoparticles: Their characteristics and the adsorption properties of polyphenols," *Food Chem*, vol. 213, pp. 579–587, Dec. 2016, doi: 10.1016/j.foodchem.2016.07.023.

[32] Q. Lin *et al.*, "Fabrication of debranched starch nanoparticles via reverse emulsification for improvement of functional properties of corn starch films," *Food Hydrocoll*, vol. 104, p. 105760, Jul. 2020, doi: 10.1016/j.foodhyd.2020.105760.

[33] Y. Ding, Q. Lin, and J. Kan, "Development and characteristics nanoscale retrograded starch as an encapsulating agent for colon-specific drug delivery," *Colloids Surf B Biointerfaces*, vol. 171, pp. 656–667, Nov. 2018, doi: 10.1016/j.colsurfb.2018.08.007.

[34] E. Aytunga, A. Arık Kibar, İ. Gönenç, and F. Us, "Gelatinization of waxy, normal and high amylose corn starches", *the journal of food*, May 2009.

2.2. Synthesis of controlled-size starch nanoparticles and superparamagnetic starch nanocomposites by microemulsion method

- **Summary**

This subchapter deals with the synthesis of SNPs by the W/O ME method. Different formulations were tested by varying key synthesis parameters such as the proportion and composition of the aqueous phase, the organic phase and the amounts of stabiliser, co-stabiliser and type of precipitant used. The size, morphology, monodispersity and crystallinity of the SNPs were evaluated. Moreover, the ME method was also used to develop starch-based superparamagnetic nanocomposites. SNPs and IONPs were simultaneously synthesized with the previously selected optimal systems and their morphology and magnetic properties were evaluated.

2.2.1. Introduction

Starch is a natural, renewable, biodegradable, and biocompatible polysaccharide and it is the main source of carbohydrate storage in plants [1]. From the chemical point of view, it is a polymer composed by two polysaccharides, amylose and amylopectin, both made up of by glucose units. SNPs are considered one of the most promising novel sustainable biomaterials for use in many different biotechnological applications. SNPs are obtained from starch granules through different physical and chemical techniques and both the synthesis method, and the operating conditions influence their final properties for different further applications.

Several physicochemical methods have been reported to produce SNPs. Some of them are high-pressure nanoemulsification, crosslinking, ME or nanoprecipitation, among others [2-7]. The ME method is a soft chemistry technique with a growing interest is a soft chemistry alternative with a growing interest as it does not require sophisticated equipment, hazardous reagents or extreme conditions. Moreover, efficient control of the size, shape, monodispersity and composition of SNPs can be achieved [5]. Microemulsions are an alternative and novel approach for the SNPs synthesis, as their composition and structure can be optimized to achieve the desired characteristics of the SNPs [8]. W/O microemulsions consist of small water droplets (dispersed or internal phase) dispersed in an oily phase (continuous, external or dispersing phase), where surfactants and co-

surfactants are present to stabilize the interphase. The small water domains formed within the microemulsions can be used as nanoreactors where the starch precipitates as SNPs [8].

Nanotechnology is opening new horizons at the biomedical field and optical, electronic, chemical and mechanical applications [9]. Magnetic nanoparticles have been studied for drug delivery, enzyme immobilization [10] and different biotechnological purposes [11]. They are composed of pure metals, metal alloys and metal oxides [12]. IONPs, in particular, are frequently used due their minimal toxicity and excellent physico-chemical properties such as the superparamagnetism, and their biocompatibility and stability in aqueous solutions [13-15].

The feasibility of producing loaded magnetic iron oxide-impregnated SNPs by a synthesis based on an emulsion crosslinking method has been reported. These nanocomposites are attractive as possible and potential drug carriers for magnetically directed drug delivery [16].

Our research group has developed a ME method to produce size-tuned iron oxide nanoparticles with superparamagnetic properties [17]. In the present study, the main objective was to adapt and optimize this ME method to produce controlled-size SNPs, and then use it to carry out the simultaneous synthesis of both types of nanoparticles (SNPs and IONPs). Thus, one of the most remarkable research advances of this work is to demonstrate the versatility of using the ME method to synthesize sustainable nanoparticles of different nature with slight modifications in the W/O microemulsion formulation prepared for this purpose, and also the ability to nanoprecipitate them simultaneously. Therefore, the hypothesis of this study is that by optimizing the formulation of the W/O microemulsion used for the precipitation of nanoparticles, as well as the formulation of the precipitating agent, it is possible to simultaneously synthesize controlled-size starch nanoparticles and iron oxide nanoparticles with superparamagnetic properties to develop sustainable novel nanocomposites, which will demonstrate that the proposed ME method is an innovative technology for the design and development of new and novel nanomaterials.

Thus, in this work, controlled-size SNPs were synthesized by the W/O ME method using different formulations for the microemulsions preparation and optimizing the proportion and composition of the aqueous phase, the organic phase and the amounts of stabilizer, co-stabilizer, and the type of precipitating agents used. The synthesized SNPs were characterized in terms of shape and size by DLS and SEM. XRPD was used to analyze the crystallinity of both the granules and resulting

SNPs. Nanocomposites of SNPs and IONPs have been synthesized by the ME method, and their morphology and magnetic properties have been studied.

2.2.2. Materials

CTAB ($C_{19}H_{42}BrN$, M_W = 364.46 g/mol), was supplied as a white powder by Sigma-Aldrich (USA). This is a quaternary ammonium salt, with long alkyl and detergent activity. In this cationic surfactant, the hydrophilic part is positively charged, and its HLB value is 10. 1-Butanol was supplied by Sigma Aldrich (USA) and was used as a co-stabilizer in the microemulsion. 1-Hexanol, supplied by Alfa Aesar (USA), acts as the organic phase in the microemulsion as it has a longer alkyl chain than that of 1-butanol.

Milli-Q water was used to prepare the solutions to be used in the synthesis and for the subsequent washing of the nanoparticles. Absolute ethanol supplied by Sigma Aldrich (USA) was also used to wash the nanoparticles.

Maize starch with 0.25% moisture and a branching (α-1,4)/(α-1,6) ratio of 15.2 was purchased from Cerestar-AKV I/S (Denmark). It was presented as a white powder insoluble in water at room temperature.

NaOH (M_W = 39.997 g/mol) was supplied by Panreac AppliChem (Spain) and used was used as a precipitating agent for the SNPs synthesis, as well as for the formulation of the aqueous phases. Urea (M_W = 60.056 g/mol), was supplied by Serva Electrophoresis GmbH (Germany). This reagent is presented as white crystalline powder and due to its dipole moment, it is soluble in water and in alcohol. In this work it was also used for the formulation of the aqueous phases.

Ammonia 30% (NH_3, M_W = 17.03 g/mol) was used as a precipitating agent in order to alkalinize the aqueous solution containing the starch and the iron salts and precipitate them in the form of nanoparticles. It was provided by Panreac AppliChem (Spain). Ferric chloride hexahydrate ($FeCl_3 \cdot 6\ H_2O$, M_W = 270.30 g/mol), a very hygroscopic yellow-orange crystalline solid, was supplied by Panreac AppliChem (Spain). Ferrous chloride tetrahydrate ($FeCl_2 \cdot 4\ H_2O$, M_W = 198.81 g/mol) was supplied by J.T. Baker (USA). It is a light green solid, soluble in water and with a high tendency to oxidize to ferric chloride. Both the ferric and the ferrous chloride were used in an

aqueous solution as precursors for the production of magnetite. Hydrochloric acid 38% (HCl), was supplied by Sigma-Aldrich (Germany) and it was used to prepare the aqueous solution of iron salts.

- **Methods**

ME method was adapted from a previous works for synthesis of superparamagnetic nanoparticles [17]. The obtention of the SNPs by this ME method can be achieved in two steps: (i) preparation of the microemulsion systems and (ii) synthesis of the SNPs by adding the precipitating agent.

2.2.3. Preparation of the microemulsions

Microemulsions formulated in this work were W/O type, i.e., water droplets dispersed into an oily phase. To obtain a W/O microemulsion, the oily phase contained the organic solvent, alcohol as co-stabilize and surfactant as stabilizer. The surfactant and alcohol molecules are arranged as reverse micelles, which means that the water-soluble hydrophilic heads point towards the inner part of the droplets, while the hydrophobic tails point towards the outside, where the organic solvent is found.

Subsequently, this organic phase was in contact with an aqueous phase in which the biopolymer was dissolved, and this quickly diffused towards the hydrophilic regions of the micelles, giving rise to the formation of nanometric hydrophilic regions rich in biopolymer, with diameters generally less than 100 nm. This small water regions that will later act as templates for the SNPs formation can be called nanoreactors [8].

To obtain the microemulsions, a series of steps must be followed, as detailed below.

Preparation of the aqueous phase

First, 1% (w/v) starch solution was prepared by dissolving 0.2 g of starch into 20 mL of a solvent system. Three different solvents were tested: (i) Milli-Q water, (ii) 8% (w/v) NaOH, and (iii) 8% (w/v) NaOH + 10% (w/v) urea. This starch solution was kept under a 1000 rpm constant stirring at 80°C for 30 min until the starch was fully dissolved, obtaining a completely homogeneous solution. These synthesis parameters were selected based on a previous work [18].

Microemulsions formulation

In order to formulate the microemulsions, an organic solution consisting of a mixture of CTAB (surfactant that acts as a stabilizer), 1-butanol (co-stabilizer) and 1-hexanol (organic phase) was prepared. A 3:2 mass ratio of surfactant to co-stabilizer was kept constant in all formulations. 1-butanol is distributed mainly between the interfacial layer and the organic phase, acting as a co-stabilizer in the interfacial layer and as a co-solvent in the organic phase [19].

Different microemulsion formulations were studied. In order to determine the appropriate composition for SNPs preparation, a microemulsion stability region must first be determined by the titration method in a ternary diagram [17]. Figure 2.8 shows the six optimal microemulsion formulations selected from previous studies for the present work (M1, M2, M3, M4, M5 and M6).

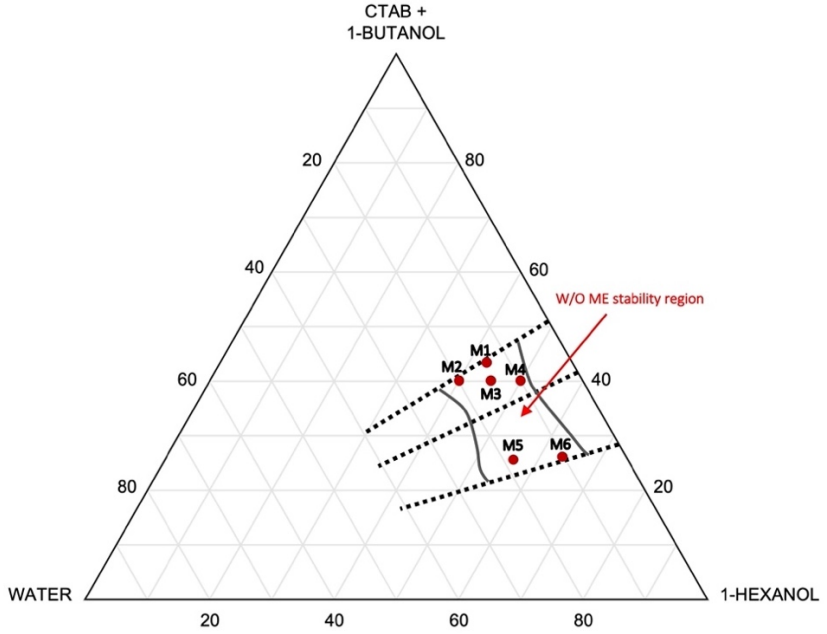

Figure 2.8. *Ternary diagram of the CTAB-butanol-hexanol-water system with the composition of the microemulsions studied for the SNPs synthesis (M1 to M6).*

Once the six best formulations for obtaining the microemulsions were identified, the surfactant and the co-stabilizer were added to the organic phase by weighing. Subsequently, this mixture was kept under high agitation for 10 min until a homogeneous solution was obtained. Afterwards, the aqueous phase prepared above was added, and the mixture was gently stirred to promote homogenization and hence microemulsion formation. Due to the small size of the aqueous droplets formed (values less than 1 micron), light can pass through them, so microemulsion formation was evident once the solution became totally translucent. Table 2.4 gathers the compositions of the different reagents of each microemulsion formulation.

Table 2.4. *Microemulsion composition of the six formulations selected within the microemulsion stability region for the SNPs synthesis.*

Microemulsion system	Microemulsion composition (g)			
	CTAB	1-Butanol	1-Hexanol	Aqueous phase
M1	5	4	9	3
M2	5	3	8	4
M3			9	3
M4			10	2
M5	3	2	11	4
M6			13	2

2.2.4. Synthesis of the SNPs

SNPs were obtained by adding a solution containing a precipitating agent (an organic solvent) to the previously prepared microemulsion which causes the starch to precipitate in the form of nanoparticles inside the water droplets of the microemulsion. Two precipitating agents were tested: (i) 12% (w/v) NaOH + ethanol, and (ii) pure ethanol. For the preparation of the NaOH solution, it was necessary to stir the mixture at 500 rpm for 24 h at room temperature due to the low solubility of NaOH in ethanol with respect to its solubility in water.

Once the precipitating solution was ready, it was added dropwise to the microemulsion system, keeping the mixture under constant high stirring at all times. SNPs formation was noted visually as small white aggregates appeared in the solution as drops were added. As soon as these aggregates appeared, the addition of the drops was stopped since the SNPs were formed. A scheme of this process is shown at Figure 2.9.

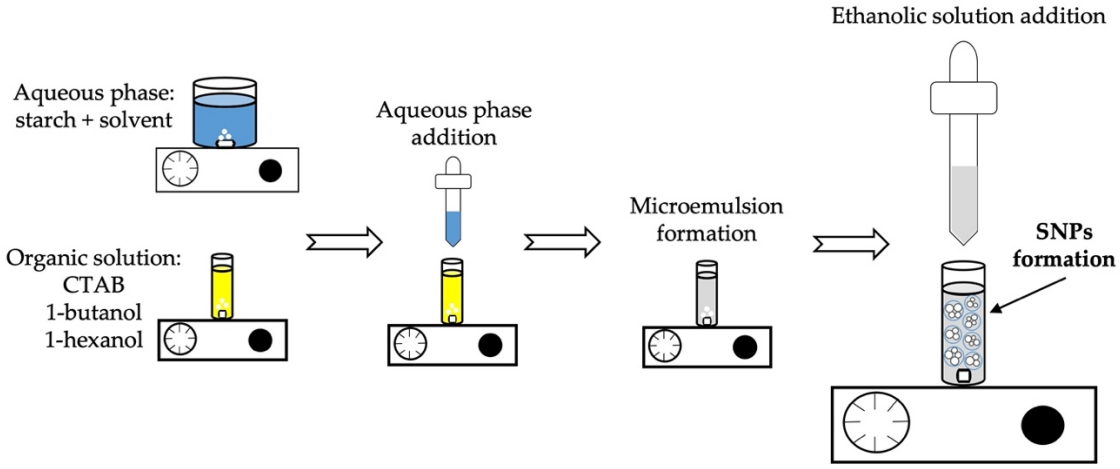

Figure 2.9. *Scheme of the SNPs synthesis process by the ME method.*

Once the SNPs were obtained and prior to their characterization, samples had to be carefully washed to remove the excess of stabilizers or solvents. First, samples were centrifuged at room temperature for 10 min at 10000 rpm and the supernatant was removed to obtain the particles as pellets, which were then washed six times with alternate washes of ethanol and 50%-50% mixtures of absolute ethanol and Milli-Q water, centrifuging again under the same conditions between each washing step.

2.2.5. Synthesis of the starch superparamagnetic nanocomposites

The same ME method was followed for the obtention of composites SNPs-IONPs. However, in this case, the aqueous phase consisted of a mixture of solutions of starch and iron salts. A 2.5% (w/v) starch solution was prepared by dissolving 0.5 g of starch into 20 mL of Milli-Q water under 1000 rpm constant stirring at 80°C for 30 min. In turn, a 50 mL solution with a molar ratio of iron salts Fe^{2+}/Fe^{3+} of 0.5 was prepared, containing 0.01 M of HCl to prevent further oxidation of the Fe^{2+}. When both solutions were completely dissolved, they were mixed and kept at 1000 rpm constant stirring at 80°C for 30 min. Once prepared, the final solution was allowed to cool until room temperature was reached. Finally, it was added to the CTAB-1-butanol-1-hexanol system to form the microemulsion, as for the SNPs synthesis. The same 6 microemulsion systems were also studied in this case.

The SNP-IONPs composites were achieved by adding the precipitating agent (30% (v/v) ammonia solution) dropwise to the microemulsion under high stirring. The synthesis of the nanoparticles was now visually detected by the appearance of a mixture of a black precipitate and white

nanoparticles. Therefore, at that moment, the addition of ammonia was stopped. The solution was left under magnetic stirring for 2 h and then washed several times with distilled water assisted by a permanent magnet.

2.2.6. SNPs characterization

Particle size distribution

An approximate idea of the hydrodynamic size (in number) and PdI of the particles was obtained by DLS using a Zetasizer Nano ZS equipment (Malvern Instruments Ltd, Malvern, UK). Samples were measured with the 173° backscatter detector in low volume disposable cuvettes (Malvern Instruments Ltd, Malvern, UK).

Morphology and size

The final size and shape of the SNPs were analyzed using a JEOL JSM-5600 field emission SEM at an acceleration voltage of 20 kV. Samples were dried in a stove for 24 h at 80°C. Once dehydrated, they were fractured with a spatula and deposited on a double-sided adhesive tape on a copper substrate. They were coated with a gold thin film in Balzers SCD 005 sputtering device (Bal-Tec AG, Liechtenstein) prior to the analysis to prevent the electric charge built-up under the electron beam in the microscope. The average particle size of the SNPs was determined by random measurements on the images using ImageJ software.

Furthermore, the final size and shape of the superparamagnetic SNPs were analyzed using a transmission electron microscope (TEM) (JEOL-2000 EX-II). An aliquot of an aqueous suspension of the samples was placed into a copper-grid supported transparent carbon foil and analyzed. The average particle size was also determined by using ImageJ software.

X-Ray Powder Diffraction

XRPD was used to determine the crystalline structure of the synthesized SNPs as well as the starch granules. The powder X-ray diffraction data for the samples were collected at RT, using CuKα1.2 radiation (λ = 1.54056 Å and 1.54439 Å) in a Bragg-Brentano reflection configuration, on a Philips Panalytical X'Pert Pro diffractometer in a 2θ range of 5-27°, with a step size of 0.08356. The estimation of the crystalline domain sizes of the SNPs was obtained using the FullProf program.

Magnetic characterization

An EV9 vibrating sample magnetometer (VSM) equipped with an electromagnet producing fields up to ±2.2 T was used to obtain the magnetization curves of the superparamagnetic SNPs and IONPs at room temperature (298.15 K). Powder samples were analyzed, by using 0.05 T field steps, and the results were normalized to the magnetic phase.

2.2.7. Results and discussion

- **Starch nanoparticles (SNPs)**

2.2.7.1. Particle size distribution, size and morphology

As explained in sections 2.2.3 and 2.2.4, the synthesis of the SNPs was carried out under different synthesis conditions, studying different microemulsion systems (M1 to M6) and different ethanolic solutions. The purpose was to optimize the method and to achieve the precipitation of the starch in the form of nanoparticles.

Results for the morphological characterization for each system are shown at Table 2.5. The particle size distributions and the PdI were obtained by DLS, and the shape of the particles (spherical or non-spherical) by SEM.

The protocol was the same for each case: first SNPs were synthesized (different compositions), after the washing steps, they were characterized by DLS and finally, they were dried and characterized by SEM. All the experiments were performed in triplicate (at least) in order to evaluate their reproducibility.

Table 2.5. *Main sizes of SNPs obtained by the ME method with the different microemulsion systems studied.*

Sample	Aqueous phase (%w/v)	Precipitating agent (%w/v)	Size (nm)	PdI	Spherical shape
M1-A	Starch + Milli-Q	NaOH 12% + ethanol	165±19	0.75±0.03	Yes
M1-B	Starch + Milli-Q	Ethanol	-[1]	-[1]	-[1]
M1-C	Starch + NaOH 8%	Ethanol	21±3	0.49±0.06	No
M1-D	Starch + NaOH 8% + urea	Ethanol	43±5	0.60±0.06	No

M2-A	Starch + Milli-Q	NaOH 12% + ethanol	40±3	0.81±0.18	Yes
M2-B	Starch + Milli-Q	Ethanol	-[1]	-[1]	-[1]
M2-C	Starch + NaOH 8%	Ethanol	29±4	0.27±0.05	No
M2-D	Starch + NaOH 8% + urea	Ethanol	43±10	0.55±0.06	No
M3-A	Starch + Milli-Q	NaOH 12% + ethanol	34±10	0.77±0.12	Yes
M3-B	Starch + Milli-Q	Ethanol	-[1]	-[1]	-[1]
M3-C	Starch + NaOH 8%	Ethanol	31±4	0.54±0.10	Yes
M3-D	Starch + NaOH 8% + urea	Ethanol	38±6	0.55±0.09	No
M4-A	Starch + Milli-Q	NaOH 12% + ethanol	-[1]	-[1]	-[1]
M4-B	Starch + Milli-Q	Ethanol	-[1]	-[1]	-[1]
M4-C	Starch + NaOH 8%	Ethanol	28±5	0.48±0.07	No
M4-D	Starch + NaOH 8% + urea	Ethanol	48±3	0.58±0.14	Yes
M5-A	Starch + Milli-Q	NaOH 12% + ethanol	36±7	0.98±0.04	Yes
M5-B	Starch + Milli-Q	Ethanol	-[1]	-[1]	-[1]
M5-C	Starch + NaOH 8%	Ethanol	66±13	0.47±0.01	Yes
M5-D	Starch + NaOH 8% + urea	Ethanol	47±4	0.61±0.09	Yes
M6-A	Starch + Milli-Q	NaOH 12% + ethanol	40±4	0.64±0.15	Yes
M6-B	Starch + Milli-Q	Ethanol	-[1]	-[1]	-[1]
M6-C	Starch + NaOH 8%	Ethanol	24±3	0.42±0.02	Yes
M6-D	Starch + NaOH 8% + urea	Ethanol	58±17	0.52±0.09	No

[1] No DLS available.

Looking at the DLS size results in Table 2.5, a first conclusion can be reached: the smallest particle sizes were reached when NaOH was present in the aqueous phase, obtaining relatively small sizes both in presence and absence of urea (samples C and D of each system) in most of the cases studied. For each formulation tested, particle sizes were smaller in the absence of urea, except for the M5 microemulsion system where the smallest sizes were obtained when both NaOH and urea were present in the aqueous phase with the starch. However, when samples were analyzed by SEM, only five of them presented a spherical shape (M3-C, M4-D, M5-C, M5-D and M6-C) but most of them shown agglomerates.

When NaOH acted as the precipitating agent (sample A of each system), small particle sizes were obtained by DLS (M2-A, M3-A, M5-A and M6-A), except for samples M1-A and M4-A which

presented large particles and no particles, respectively. It is important to point out that M1, M4 and M6 represent the formulations with lower water content compared to the other systems. When M2-A, M3-A, M5-A and M6-A samples were analyzed by SEM, all of them showed a spherical shape, although some agglomerates were observed in M2-A sample. However, the size was also measured with ImageJ software for all formulations tested. A size range between 12 nm and 47 nm was obtained for M2-A sample. For M3-A sample a size range between 27 nm and 74 nm was obtained. In spite of the higher sizes than the previous ones, the particles presented less aggregates and a greater number of particles was obtained. The same effect was observed with sample M5-A, where the amount of particles obtained was also higher, and the size range varied from 24 nm to 51 nm. Finally, large spherical particles were obtained for sample M6-A, in contrast with the small sizes expected with the DLS results: the size range for the SNPs varied from 64 nm to 180 nm and some particle aggregates were observed, also indicating in this case that the formulations that correspond to the stability region with less water content indicate is not suitable to form uniform SNPs.

Taking into account these sizes obtained, it can be concluded that the best results were achieved when an aqueous phase containing 1% (w/v) starch dissolved in Milli-Q water was used in combination with a precipitant solution containing NaOH (12% (w/v) NaOH in ethanol). Low aspect ratio particles were thus obtained (samples A). NaOH breaks the hydrogen bonds between water and starch, resulting in the disruption of the existing molecular orders within the starch granules [20], thus improving starch solubility in water [21].

At the same time, with these synthesis parameters, microemulsion systems M2, M3 and M5 showed the smallest particle sizes. The size obtained by DLS was around 40 nm for the sample M2-A, with a PdI of 0.81. This high value of the PdI can be explained by the fact that particle size varied over a fairly wide range as mentioned above (from 12 nm to 47 nm). This explains that the sample is not monodisperse, but it rather presents great variety of sizes. The same happened with the other two samples: size obtained by DLS was around 34 nm for sample M3-A, with a PdI of 0.77 but ranging from 27 nm to 74 nm; for sample M5-A, size obtained with DLS was around 36 nm with a PdI of 0.98 in an interval from 24 nm to 51 nm. The micrographs in Figure 2.10 show that small particles predominated in samples M3-A and M5-A, which is consistent with the data obtained by DLS where slightly smaller particles were observed compared to sample M2-A.

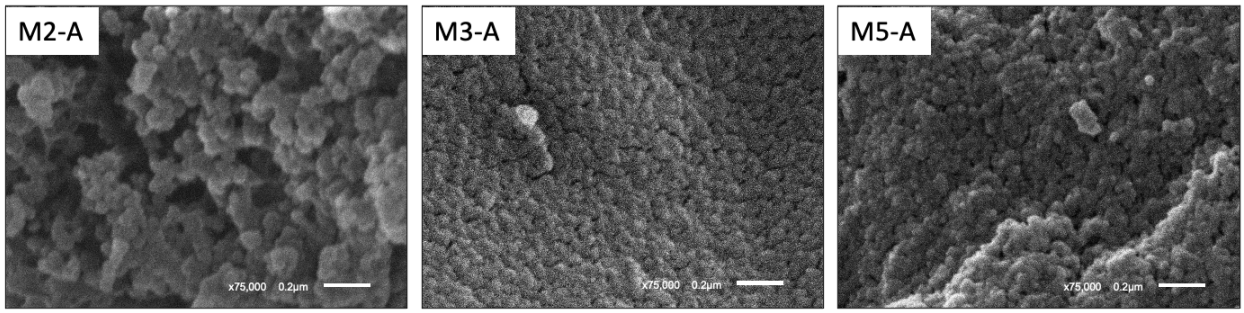

Figure 2.10. *SEM micrographs for M2-A, M3-A and M5-A systems.*

From Figure 2.10, it could be estimated that both the M2-A system, as well as the M3-A and M5-A systems were optimal the formulations to obtain small, spherical and homogeneous SNPs by the ME method. Similar results were reported by other authors (Zhou, Luo & Fu, 2014) who suggested the use of the ME method to obtain SNPs with good sphericity, small size and a narrow particle size distribution to be used as drug delivery systems.

2.2.7.2. SNPs production yield

Once the synthesis conditions and the optimal microemulsion systems were selected, SNPs production yield was determined. For this purpose, the total amount of SNPs per amount of starch added into the aqueous phase was calculated. Samples were dried in a stove, in the same way as for the SEM characterization, for 24 h at 80ºC in small flat-bottomed glass tubes.

The experiments were carried out in triplicate and finally, for each 0.2 g of starch added to the aqueous phase, 0.032 g of particles were obtained for the M2 microemulsion system, 0.020 g for the M3 system and 0.029 g for the M5 system. The production yield of SNPs obtained was 16% for the M2 system, 10% for the M3 system and 15% for the M5 system.

2.2.7.3. XRPD analysis

XRPD was applied to determine the crystalline structure of starch granules as well as that of the SNPs of the optimal formulations. The spectra are shown in Figure 2.11. Starch granules showed peaks at Bragg angles (2θ) at 15°, 17°, 18° and 23° corresponding to A-type X-ray diffraction patterns, which is in good agreement with results from previous studies [23].

Nevertheless, these starch characteristic peaks did not appear in the spectra obtained for the SNPs. This may indicate that the synthesis process affected the crystalline structure of the starch granules,

and finally all synthesized SNPs showed an amorphous crystalline structure, which is in agreement with the results obtained by other authors [24].

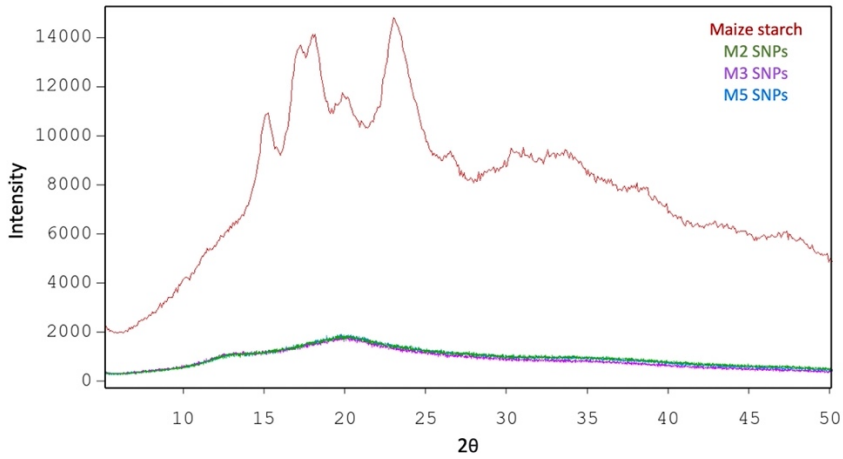

Figure 2.11. *XRPD spectra of starch granules and the resulting SNPs synthesized with the optimal formulations.*

Dufresne et al summarized the polymer nanocomposite trend as a function of the nature (crystalline or amorphous) of the matrix and its interaction with nanostructured fillers where several nanocomposites presented amorphous structure with good interaction for different fillers [25].

2.2.7.4. Starch superparamagnetic nanocomposites

Formulations M3 and M5 were used to simultaneously synthetized SNPs and IONPs and produce size-tuned starch-based superparamagnetic nanocomposites susceptible to be used for further bioapplications. It has been demonstrated in previous studies that starch-based magnetic nanocapsules have a major potential for the targeted delivery of hydrophilic bioactives through a magnetic field-generated [26]. Similar trend was observed in another study where an effectively delivery of the antitumor drug cisplatin from superparamagnetic nanoparticles of crosslinked starch impregnated was reported in the presence and absence of magnetic field via diffusion-controlled pathway [16].

Best results for the synthesized nanoparticles were obtained for these M3 and M5 systems with a size range that varied between sizes from 28 nm to 55 nm for system M3, and between 23 nm y 73 nm for system M5. The average diameters varied between 44 nm and 43 nm respectively. TEM micrographs shown in Figure 2.12 revealed the formation of low aspect ratio particles despite of certain agglomeration degree and some irregular shapes. In both micrographs, the SNPs with

IONPs can be easily identified. In turn, the properties of these SNP-IONPs composited can be compared with those of the iron salts in absence of starch (IONPs M3 and IONPs M5).

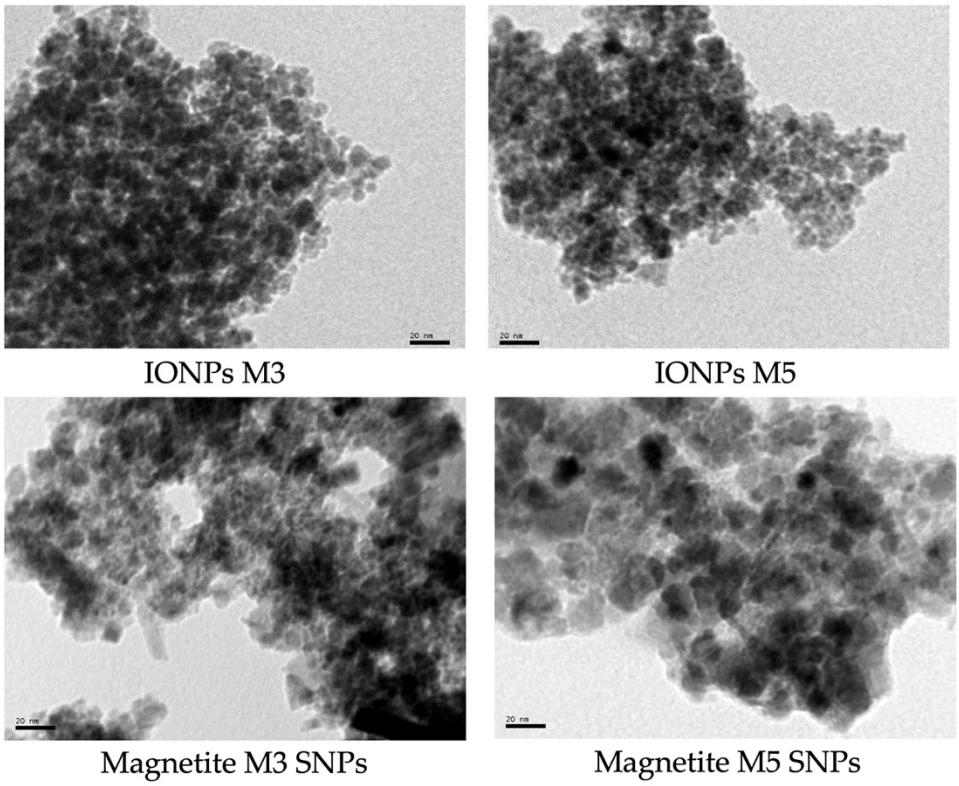

Figure 2.12. *TEM micrographs of the superparamagnetic SNPs and IONPs obtained with M3 and M5 microemulsion systems.*

In addition, Figure 2.13 shows the SEM micrographs where the different particle sizes for each system can be seen.

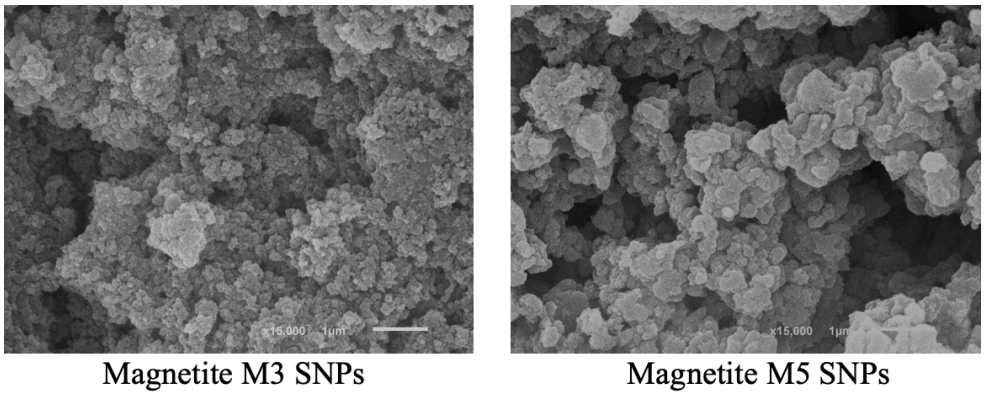

Figure 2.13. *SEM micrographs of the superparamagnetic SNPs (SNP-IONPs composites) obtained with M3 and M5 microemulsion systems.*

At the same time, magnetization studies with iron oxide SNPs were performed and compared with IONPs synthesized in absence of starch (named as magnetite samples M3 and M5). Rebodos & Vikesland, reported that, based on magnetisation loops, magnetite nanoparticles exhibited superparamagnetic-like behaviour, which was expected for particles within a small size range [27].

Figure 7 shows the magnetization (M) versus the applied magnetic field (H) curve obtained at room temperature curves for SNPs-IONPs composites (M3 magnetite + starch and M5 magnetite + starch samples) and the corresponding bare IONPs in absence of starch (M3 magnetite and M5 magnetite samples). The absence of hysteresis loop confirms the superparamagnetic behaviour of all samples analysed. The saturation magnetization of magnetite nanoparticles has been determined by setting the experimental data to the law of approach to saturation [28] and their values were 49.5 emu/g for M3 sample and 58.5 emu/g for M5 sample, being similar to those reported in a previous study where IONPs were synthesized by the ME method [17]. Similar results were also reported by Likhitar & Bajpai who obtained a saturation magnetization of about 58 emu/g [16]. However, it was noticed that, for both formulations, the iron oxide impregnated SNPs showed lower magnetization and superparamagnetic behaviour properties than their corresponding bare IONPs. This can be explained by the fact that IONPs are impregnated in a starch matrix consisting of SNPs.

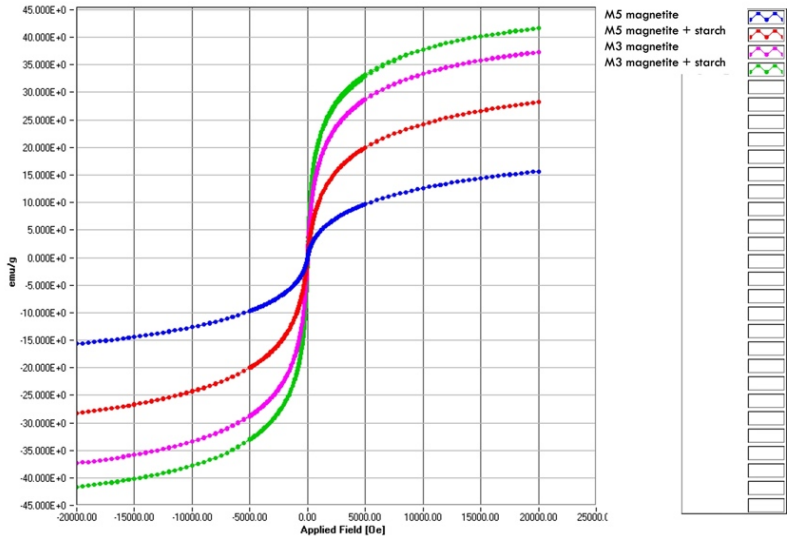

Figure 2.14. *Magnetization curves for SNPs-IONPs composites and the corresponding bare IONPs in absence of starch.*

Finally, XRPD diagrams were collected to compare the obtained nanocrystalline phases with the magnetite reference structure [29] since XRPD analysis is an important tool for determination of crystallinity of materials [30] and has also been used for previous authors to demonstrate the presence of iron oxide nanoparticles in superparamagnetic nanoparticles of crosslinked starch impregnated designed for drug delivery purposes [16]. The spectra are shown in Figure 2.15. In all the XRPD diagrams the corresponding peaks match the spectral pattern of the pure magnetite structure, named in the diagram as magnetite sample, which means that pure crystalline phases have been obtained in this work.

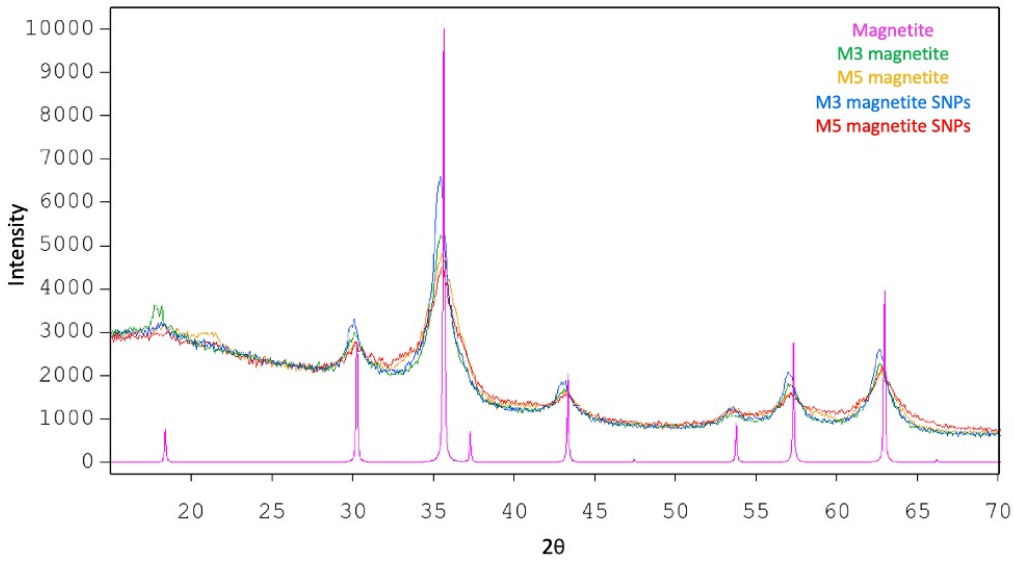

Figure 2.15. *XRPD spectra of IONPs (M3 and M5 magnetite) and SNPs-IONPs (M3 magnetite SNPs and M5 magnetite SNPs) for M3 and M5 systems.*

2.2.8. Conclusions

The synthesis of size-tuned SNPs (30-40 nm) was achieved through the use of a ME method. This was possible by controlling the ratio and composition of the reagents used in the microemulsion system (aqueous and organic phases, stabilizer and co-stabilizer), as well as the precipitating agents used.

Moreover, the versatility of the developed ME method has also been demonstrated, as iron oxide SNPs with controlled size and superparamagnetic properties were also synthesized simultaneously using this method what validates the hypothesis stated and confirms the potential of this method as an innovative technology for the design and development of new functional nanomaterials.

The synthesized size-tuned magnetic-polymeric nanocomposites are promising materials that are likely to be used for different biomedical applications, such as drug delivery nanocarriers or potential markers for theragnostic purposes.

- **References**

[1] C. Liu, K. Li, X. Li, M. Zhang, and J. Li, "Formation and structural evolution of starch nanocrystals from waxy maize starch and waxy potato starch," *Int J Biol Macromol*, vol. 180, pp. 625–632, Jun. 2021, doi: 10.1016/j.ijbiomac.2021.03.115.

[2] H. Y. Kim, S. S. Park, and S. T. Lim, "Preparation, characterization and utilization of starch nanoparticles," Feb. 01, 2015, *Elsevier*. doi: 10.1016/j.colsurfb.2014.11.011.

[3] D. Le Corre, J. Bras, and A. Dufresne, "Starch nanoparticles: A review," May 10, 2010. doi: 10.1021/bm901428y.

[4] H. Saari, C. Fuentes, M. Sjöö, M. Rayner, and M. Wahlgren, "Production of starch nanoparticles by dissolution and non-solvent precipitation for use in food-grade Pickering emulsions," *Carbohydr Polym*, vol. 157, pp. 558–566, Feb. 2017, doi: 10.1016/j.carbpol.2016.10.003.

[5] S. F. Chin, A. Azman, and S. C. Pang, "Size controlled synthesis of starch nanoparticles by a microemulsion method," *J Nanomater*, vol. 2014, 2014, doi: 10.1155/2014/763736.

[6] S. F. Chin, S. C. Pang, and S. H. Tay, "Size controlled synthesis of starch nanoparticles by a simple nanoprecipitation method," *Carbohydr Polym*, vol. 86, no. 4, pp. 1817–1819, Oct. 2011, doi: 10.1016/j.carbpol.2011.07.012.

[7] S. H. Mahmoudi Najafi, M. Baghaie, and A. Ashori, "Preparation and characterization of acetylated starch nanoparticles as drug carrier: Ciprofloxacin as a model," *Int J Biol Macromol*, vol. 87, pp. 48–54, Jun. 2016, doi: 10.1016/j.ijbiomac.2016.02.030.

[8] S. Asgari, A. H. Saberi, D. J. McClements, and M. Lin, "Microemulsions as nanoreactors for synthesis of biopolymer nanoparticles," *Trends Food Sci Technol*, vol. 86, pp. 118–130, Apr. 2019, doi: 10.1016/j.tifs.2019.02.008.

[9] M. Darroudi, M. Hakimi, E. Goodarzi, and R. Kazemi Oskuee, "Superparamagnetic iron oxide nanoparticles (SPIONs): Green preparation, characterization and their cytotoxicity effects," *Ceram Int*, vol. 40, no. 9, pp. 14641–14645, Nov. 2014, doi: 10.1016/j.ceramint.2014.06.051.

[10] H. Vaghari *et al.*, "Application of magnetic nanoparticles in smart enzyme immobilization," *Biotechnol Lett*, vol. 38, no. 2, pp. 223–233, 2016, doi: 10.1007/s10529-015-1977-z.

[11] E. M. Materón *et al.*, "Magnetic nanoparticles in biomedical applications: A review," *Applied Surface Science Advances*, vol. 6, p. 100163, Dec. 2021, doi: 10.1016/j.apsadv.2021.100163.

[12] N. Malhotra *et al.*, "Potential Toxicity of Iron Oxide Magnetic Nanoparticles: A Review," *Molecules*, vol. 25, no. 14, 2020, doi: 10.3390/molecules25143159.

[13] S. F. Medeiros *et al.*, "Synthesis and characterization of stable aqueous dispersion of functionalized double-coated iron oxide nanoparticles," *Mater Lett*, vol. 160, pp. 522–525, Dec. 2015, doi: 10.1016/j.matlet.2015.08.026.

[14] P. I. P. Soares *et al.*, "Iron oxide nanoparticles stabilized with a bilayer of oleic acid for magnetic hyperthermia and MRI applications," *Appl Surf Sci*, vol. 383, pp. 240–247, Oct. 2016, doi: 10.1016/j.apsusc.2016.04.181.

[15] V. Valdiglesias *et al.*, "Are iron oxide nanoparticles safe? Current knowledge and future perspectives," *Journal of Trace Elements in Medicine and Biology*, vol. 38, pp. 53–63, Dec. 2016, doi: 10.1016/j.jtemb.2016.03.017.

[16] S. Likhitkar and A. K. Bajpai, "Magnetically controlled release of cisplatin from superparamagnetic starch nanoparticles," *Carbohydr Polym*, vol. 87, no. 1, pp. 300–308, Jan. 2012, doi: 10.1016/ j.carbpol.2011.07.053.

[17] M. Salvador, G. Gutiérrez, S. Noriega, A. Moyano, M. C. Blanco-López, and M. Matos, "Microemulsion synthesis of superparamagnetic nanoparticles for bioapplications," *Int J Mol Sci*, vol. 22, no. 1, pp. 1–17, Jan. 2021, doi: 10.3390/ijms22010427.

[18] G. Gutiérrez, D. Morán, A. Marefati, J. Purhagen, M. Rayner, and M. Matos, "Synthesis of controlled size starch nanoparticles (SNPs)," *Carbohydr Polym*, vol. 250, Dec. 2020, doi: 10.1016/j.carbpol.2020.116938.

[19] X. Wang, H. Chen, Z. Luo, and X. Fu, "Preparation of starch nanoparticles in water in oil microemulsion system and their drug delivery properties," *Carbohydr Polym*, vol. 138, pp. 192–200, Mar. 2016, doi: 10.1016/j.carbpol.2015.11.006.

[20] S. Vijay, and S. Lalit, "Various techniques for the modification of starch and the applications of its derivatives" 2012.

[21] J. A. Han and S. T. Lim, "Structural changes in corn starches during alkaline dissolution by vortexing," *Carbohydr Polym*, vol. 55, no. 2, pp. 193–199, Jan. 2004, doi: 10.1016/j.carbpol.2003.09.006.

[22] G. Zhou, Z. Luo, and X. Fu, "Preparation and characterization of starch nanoparticles in ionic liquid-in-oil microemulsions system," *Ind Crops Prod*, vol. 52, pp. 105–110, Jan. 2014, doi: 10.1016/j.indcrop.2013.10.019.

[23] Q. Lin *et al.*, "Fabrication of debranched starch nanoparticles via reverse emulsification for improvement of functional properties of corn starch films," *Food Hydrocoll*, vol. 104, p. 105760, Jul. 2020, doi: 10.1016/j.foodhyd.2020.105760.

[24] Y. Ding, Q. Lin, and J. Kan, "Development and characteristics nanoscale retrograded starch as an encapsulating agent for colon-specific drug delivery," *Colloids Surf B Biointerfaces*, vol. 171, pp. 656–667, Nov. 2018, doi: 10.1016/j.colsurfb.2018.08.007.

[25] E. Medeiros, A. Dufresne, and W. Orts, "Starch-based nanocomposites," in *Starches*, CRC Press, 2009, pp. 205–251. doi: 10.1201/9781420080247-c9.

[26] A. C. C. Sousa *et al.*, "Starch-based magnetic nanocomposite for targeted delivery of hydrophilic bioactives as anticancer strategy," *Carbohydr Polym*, vol. 264, p. 118017, Jul. 2021, doi: 10.1016/j.carbpol.2021.118017.

[27] R. L. Rebodos and P. J. Vikesland, "Effects of Oxidation on the Magnetization of Nanoparticulate Magnetite," *Langmuir*, vol. 26, no. 22, pp. 16745–16753, Nov. 2010, doi: 10.1021/la102461z.

[28] H. Zhang, D. Zeng, and Z. Liu, "The law of approach to saturation in ferromagnets originating from the magnetocrystalline anisotropy," *J Magn Magn Mater*, vol. 322, no. 16, pp. 2375–2380, Aug. 2010, doi: 10.1016/j.jmmm.2010.02.040.

[29] N. Nakagiri, M. H. Manghnani, L. C. Ming, and S. Kimura, "Crystal structure of magnetite under pressure," *Phys Chem Miner*, vol. 13, no. 4, pp. 238–244, Jul. 1986, doi: 10.1007/BF00308275.

[30] A. K. Bajpai and R. Gupta, "Magnetically mediated release of ciprofloxacin from polyvinyl alcohol based superparamagnetic nanocomposites," *J Mater Sci Mater Med*, vol. 22, no. 2, pp. 357–369, Feb. 2011, doi: 10.1007/s10856-010-4214-2

2.3. Synthesis and characterization of controlled-size starch nanoparticles modified with Short Chain Fatty Acids

- **Summary**

In this subchapter the synthesis of controlled-size SNPs modified with SCFA by the nanoprecipitation method is described. Quinoa and rice acetylated, propionylated and butyrylated starches with different degrees of modification were used and the SNPs obtained were characterized in terms of size, shape and charge. The crystallinity of both the starch granules and the SNPs was also determined. Finally, the molecular structure of the starch granules and the synthesized SNPs were compared to determine whether the SCFA modification was affected by the synthesis.

2.4.1. Introduction

Many industries are showing special interest in the use of starch since it is a natural polymer, abundant in nature, non-toxic and also compatible with the environment due to its biodegradability [1].

In this work, two starches from different botanical sources (quinoa and rice) were studied. Quinoa is a pseudo-cereal that has recently attracted increasing interest for its nutritional value. It is high in protein, has a balanced amino acid composition, is a good source of fiber and is rich in vitamins, minerals and compounds such as polyphenols and flavonoids. The main component of quinoa grains is starch, with a content of about 60% [2].

Rice, on the other hand, is one of the most important cultivated cereals and, like quinoa, its main component is starch, with a content of about 80%. Compared to other cereal starches, rice has a higher freeze-stability, higher acid resistance and a wide range of amylose/amylopectin content. In turn, rice has higher digestibility and absorption [3].

However, some of the physico-chemical properties of native starches, such as the insolubility in water, the resistance to enzymatic hydrolysis and the instability against changes in temperature, pH and shearing forces [4] are not suitable for many applications and limit their uses [5]. Thus, starches are modified to improve their physical, chemical and functional properties. Generally,

starches can be modified through physical, chemical or enzymatic procedures. Physical methods involve thermal techniques, such as pre-gelatinization [6] or hydro-thermal treatment (e.g., annealing [7, 8] and heat/moisture treatments [9, 10]) which are the most commonly used. Other than that, non-thermal techniques are also applicable for physical treatment for instance high-pressure processing [11], micronization [12, 13], pulse electric field [14, 15] or ultrasonication [15]. In addition, enzymatic methods involve the use of enzymes by modifying some of the native starch characteristics like viscosity, solubility or gelation [16, 17].

However, chemical modification is the most preferrable starch modification technique which involves the incorporation of new functional groups into the starch molecule without affecting the morphology or size of the granules but achieving a change in the physico-chemical properties, making them good candidates for different applications [5, 18]. Instead, chemical methods change the starch molecule by including different functional groups through derivatization or decomposition reactions [5], such as acetylation [19, 20], oxidation [19, 21], acid hydrolysis [22], cross-linking [21, 23], esterification with OSA [24] and succinylation [25].

The use of hydrophobic materials and water-resistance induced by chemical modification has been widely registered in the past years. This modification takes place through a chemical reaction of a hydrophobic molecule with the hydroxyl groups present in the starch molecule. In this context, an example of starch chemical modification frequently used is esterification. Starch esters can be obtained with different reactants such as anhydride acids, OSA, dodecenyl succinic anhydride (DDSA) or fatty acids with different length chains [26].

Starch is composed of two principal molecules with different nature, linear amylose and highly branched amylopectin [27], both of them composed of glucose units [28, 29]. At the same time, these glucose units contain the hydroxyl groups on which the esterification reactions take place [30].

The amylose molecule has a hydrophobic cavity where different hydrophobic compounds can be contained, such as lipids or lipid-soluble substances [28]. In the last years, starch modified with fatty acids, especially the short-chain ones, was attracting interest due to the numerous potential applications, both in clinical and non-clinical fields [31]. Amylose-fatty acid complexes could be used as nanocarriers of many thermal and oxidation-sensitive bioactive compounds, since they

could protect sensitive substances more effectively than other conventional encapsulation techniques [32]. In the gut, SCFA are formed as products from the microbial fermentation of carbohydrates, and to a lesser extent also proteins [33].

Although starch can be completely digested by the digestive enzymes in the small intestine, there is a fraction of starch (resistant starch) that resists digestion in the small intestine and reach the large intestine, where it gets fermented by the intestinal microorganisms, resulting in the production of the SCFA [31]. SCFA are fatty acids with chains of up to six carbons, but in this sense, acetylated (C2), propionylated (C3) and butyrylated (C4) are the most relevant due to their capacity to keep the normal physiological function of the large bowel [31] besides being the most produced in the human colon [34]. Due to all their possible clinical applications SCFA have been of particular interest in the last years and the possibilities for their delivery to the colon were investigated [35, 36]. One approach is the chemical modification of resistant starch with SCFA allowing a more efficient delivery to the colon compared to free SCFA in the food, since they are protected from release and absorption in the small intestine [37, 38]. In addition, it was recently demonstrated that starch acylation has a higher potential to improve the emulsifying capacity for quinoa and rice starches that will have many future perspectives for the pharmaceutical field, food applications as prebiotics [39] or as a Pickering emulsions stabilizer [40].

On the other hand, SNPs have been the focus of a large number of studies due to their unique surface area and reactivity compared to native starch granules [41]. One of the most important medical applications in which SNPs can be used is in the treatment of cancer, where they act as an effective vehicle for targeting and delivering drugs to the tumor site [42-44]. However, control of the final particle size and shape is key to their use in such applications [45]. In addition, nanoprecipitation is a simple, one-step method that is quick and easy to perform, as it does not require sophisticated equipment, hazardous reagents or extreme conditions to carry out the synthesis.

The aim of this study was to analyze the feasibility of using starches with different botanical origin modified with SCFA of different chain length (acetylated, propionylated and butyrylated) to obtain SNPs with controlled size in an appropriate range for bioapplications. For that purpose, the nanoprecipitation method was used to synthesize SNPs using acetylated, propionylated and butyrylated starches from different botanical sources with different degrees of modification.

Therefore, by selecting the appropriate type of starch modified with a specific SCFA at a certain DS, size-controlled SCFA-SNPs can be obtained since it is a fundamental requirement depending on the final application (e.g., nanocarriers for food fortification and active release in the long bowel) in which they will be subsequently used. Starches from two different botanical sources (quinoa and rice) were used as well as different degrees of modification. The synthesized SNPs were characterized by their size, shape and charge using DLS and SEM. While XRPD and FTIR were used to analyze the structure and crystallinity of the starch granules, and the SNPs synthetized.

2.4.2. Materials

Milli-Q water was used to prepare the aqueous solutions and absolute ethanol (Sigma Aldrich, USA) was used as the organic phase to synthesize the SNPs and also to wash the nanoparticles.

Starches from two different botanical sources (quinoa and rice with 20.95% and 4.43% amylose content respectively, and moisture content of 11.4% and 10.7%, respectively) were used, both of them acetylated, propionylated and butyrylated at different degrees of modification. Starches were modified by esterification with the anhydrides at Max-Rubner Institut as Abdul Hadi, Wiege, et al., (2020), described in previous works and they are presented as a white powder insoluble in water at room temperature.

2.4.3. SNPs synthesis

SNPs synthesis was carried out by the nanoprecipitation method under optimal conditions that were obtained in previous works [47].

SNPs were obtained by the addition of 1 mL of a 1% (w/v) aqueous starch solution (0.1 g of starch into 10 mL of Milli-Q water, heated at 80ºC under a 1000 rpm constant stirring for 30 minutes) into an organic phase of 20 mL of absolute ethanol. The starch solution was added dropwise into the organic phase with a syringe pump under a 4 mL/h constant injection rate and during the injection, the organic phase was kept under a 500 rpm constant stirring.

Once SNPs were obtained, samples were washed before their characterization to remove reagent remains. Samples were centrifuged for 10 minutes at 15880×g (1000 rpm) at room temperature (18

to 22ºC) and the obtained SNPs once the supernatant and residues were removed, were washed twice under the same conditions with absolute ethanol.

2.4.4. SNPs characterization

Particle size distribution and zeta potential

The hydrodynamic size (in number) of the synthesized particles was measured by DLS using a Zetasizer Nano ZS equipment (Malvern Instruments Ltd, Malvern, UK) and refers to the diameter of the particles. Samples were measured with the 173 °C backscatter detector in disposable low-volume cuvettes (Malvern Instruments Ltd, Malvern, UK). Zeta potential was also measured with this technique in disposable folded capillary cells (DTS1070).

- **Structural analysis**

Morphology and size

JEOL JSM-5600 field emission SEM was used to analyze the final size and shape of the SNPs at an acceleration voltage of 20 kV. The samples were dried on a heating unit at 80 °C for 24 h, and the dehydrated samples were crushed and deposited on a double-sided adhesive tape placed on a copper sample holder and coated with a thin gold film in a Balzers SCD 005 sputtering device (Bal-Tec AG, Liechtenstein) prior to analysis to avoid the accumulation of electric charge under the electron beam in the microscope. The SNPs average size was determined by measuring random particles using ImageJ Fiji software and refers to the diameter of the particles.

X-Ray powder diffraction

XRPD was used to determine the crystalline structure of starch granules and the synthesized SNPs. The X-ray powder diffraction data for the samples were collected at RT, using CuKα1.2 radiation (λ = 1.54056 Å and 1.54439 Å) in a Bragg-Brentano reflection configuration, on a Philips Panalytical X'Pert Pro diffractometer in a 2θ range of 5-27°, with a step size of 0.08356. The crystalline domains of the starch granules and the SNPs were estimated using the FullProf program.

- **Chemical analysis**

Fourier transform infrared spectroscopy

FTIR was used to determine the molecular structure of the SNPs and starch granules and to check whether the DS was affected by the synthesis method. FTIR spectra were recorded in a Fourier transform infrared spectrophotometer (Varian 620-IR, Thermo Fisher Scientific Inc., U.S.A.) at room temperature. Dried powder samples of approximately 1 mg were measured directly and spectra were recorded between 650-4000 cm-1 (mid-infrared band).

SNPs production yield

In order to know the total amount of SNPs obtained in each experiment, the production yield of each starch at each DS was determined. Samples were dried on a stove for 24 h at 80ºC in small flat-bottomed glass tubes. Each experiment was performed in triplicate to ensure its reproducibility.

Statistical analysis of data

All data were expressed as mean±standard deviation of three independent experiments and statistical analysis of data (ANOVA) was performed to analyze differences between test groups. Significant differences were determined by Fischer's least significant difference (LSD) test using Microsoft Excel ($p<0.05$).

2.4.5. Results and discussion

2.4.5.1. Particle size distribution, morphology, size and zeta potential

The final size, shape and surface charge of the SNPs were analysed using DLS and SEM. SEM micrographs are shown in Figure 2.16 and Figure 2.17 for quinoa and rice SNPs, respectively. In addition, Table 2.6 presents the summary of zeta potential measurements obtained by DLS and the sizes obtained by measuring the micrographs with ImageJ Fiji software.

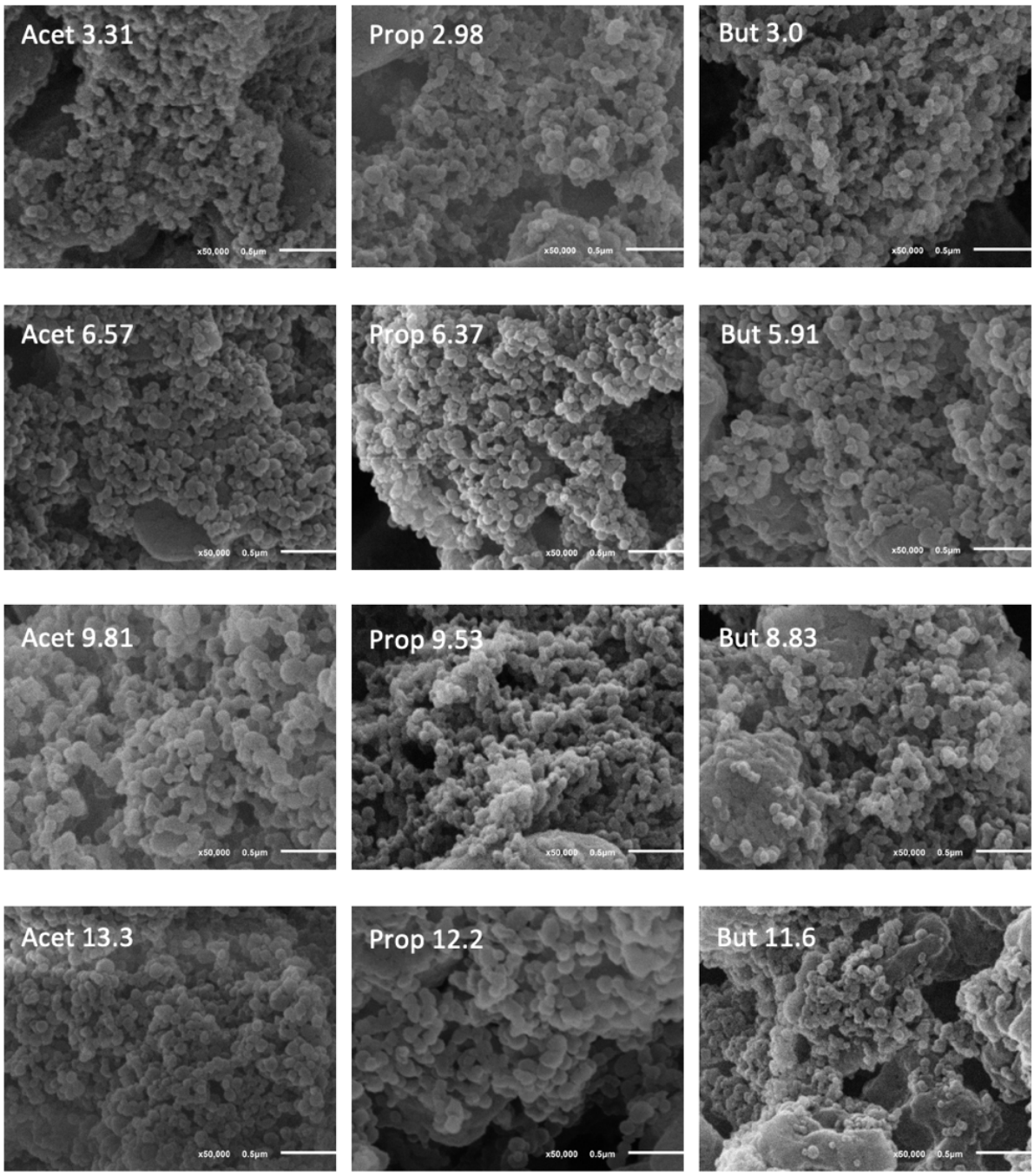

Figure 2.16. *SEM micrographs of SNPs obtained by the nanoprecipitation method using the quinoa starch (Acet=Acetate; Prop=Propionate; But=Butyrate) with different degrees of substitution.*

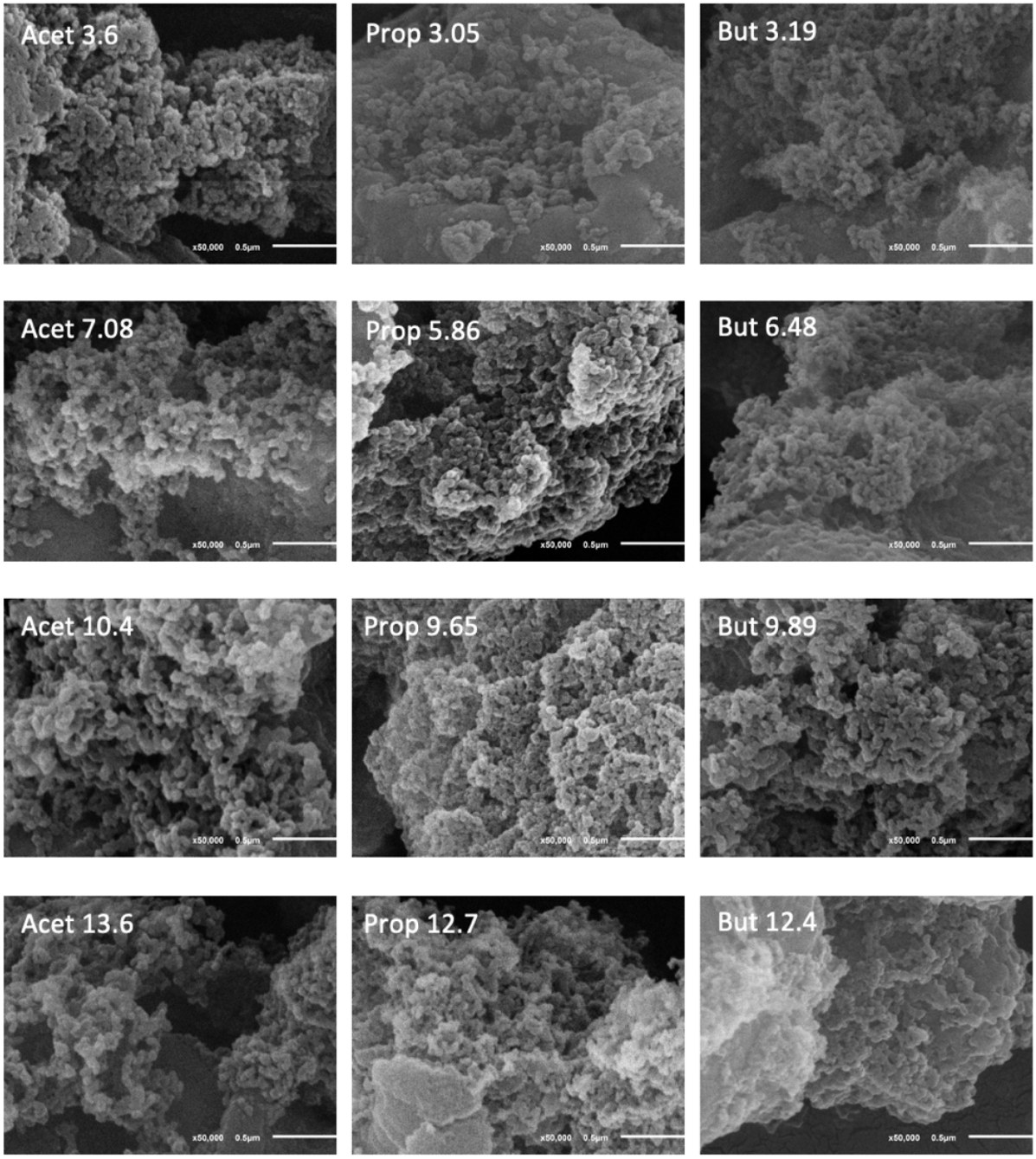

Figure 2.17. *SEM micrographs of SNPs obtained by the nanoprecipitation method using the rice starch (Acet=Acetate; Prop=Propionate; But=Butyrate) with different degrees of substitution.*

Table 2.6. *Mean sizes of SNPs obtained by ImageJ Fiji software and Zeta potential obtained by DLS for the different starches and degrees of substitution.*

Type of starch	Chain length	Degree of substitution	Zeta potential (mV)	Size (nm)
Quinoa	Acetate	3.31	-1.9±3.4	95.5±27.9
		6.57	-4.1±3.1	152±16.6
		9.81	-3.6±4.6	170±21.1
		13.3	-3.0±3.1	149±16.0
	Propionate	2.98	-2.5±2.9	158±13.3
		6.37	-1.3±3.2	136±16.9
		9.53	3.1±2.6	138±11.9
		12.2	0.4±2.7	163±18.5
	Butyrate	3.0	6.5±3.6	132±12.8
		5.91	6.6±2.9	138±13.2
		8.83	-1.0±4.9	134±10.2
		11.6	-0.8±3.3	132±11.7
Rice	Acetate	3.6	-5.4±3.7	116±13.8
		7.08	-3.7±3.2	122±12.1
		10.4	-4.4±3.8	124±10.0
		13.6	-3.0±3.7	123±9.80
	Propionate	3.05	-7.5±7.4	124±9.20
		5.86	-6.8±6.9	128±11.1
		9.65	-5.1±7.5	125±9.40
		12.7	-2.1±3.1	118±9.50
	Butyrate	3.19	-3.2±3.9	106±7.60
		6.48	-3.3±5.8	110±8.60
		9.89	-5.8±7.7	110±8.70
		12.4	-2.5±4.5	107±8.80

Data are expressed as the mean±standard deviation (n = 3). Significant differences between measurements were obtained ($p>0.05$).

In terms of particle shape, most of SNPs synthesized with quinoa starch resulted in spherical and monodispersed particles. However, in some of the experiments, it can be appreciated that a portion of SNPs are not completely formed. This phenomenon was observed for acetylated and propionylated SNPs when the lowest DS was used, and also for propionylated and butyrylated SNPs when the highest DS was used.

It also has to be noticed that looking at the mean sizes in Table 2.6 obtained with the ImageJ Fiji software, the size range is wider for the acetylated and propionylated quinoa SNPs, as for the first the smallest size was 96 nm while the largest was 170 nm, and for the propionylated, the lowest

size was 136 nm while the highest was 163 nm. This does not happen for the butyrylated SNPs since the obtained sizes with the different modifications were quite similar.

In the case of rice SNPs synthesized, sizes obtained for each chain length were quite similar between them, being, 116-124 nm for acetylated, 118-128 nm for propionylated and 106-110 nm for butyrylated SNPs, which could indicate that the modification degree did not affect the final mean particle size. Nevertheless, looking at the rice SNPs micrographs, smaller spherical particles were observed compared with quinoa starch (which is also confirmed by the sizes obtained with the software) but there are also more regions where the particles were not completely formed compared to the quinoa SNPs synthesized. At the same time, for these rice SNPs seemed like more particle agglomerates can be appreciated.

The fact that smaller sizes were obtained for rice SNPs than for quinoa SNPs could be due to the amylose content of the two starches used. Rice starch contains a much lower amount of amylose than quinoa starch (4.43% rice versus 20.95% quinoa), which means that the SCFA-amylose complexes formed in rice were smaller than in quinoa, resulting in a smaller particle size.

It has been reported that chemical modification by acetylation is highly effective for encapsulating hydrogen bond donor molecules, as an increase in the number of free hydrogen bonding sites would lead to a stronger interaction between the SNPs and the compound to be encapsulated, facilitating the uptake of more of this one [48]. Acevedo-Guevara et al. demonstrated the great potential of acetylated SNPs as curcumin delivery systems compared to native SNPs. They achieved particle sizes similar to those reported in this article (135.1 nm and 190.2 nm for native and acetylated SNPs, respectively) and in both cases high LE were achieved, although the result was slightly higher for acetylated SNPs. Something similar was described by Mahmoudi Najafi et al. who studied the encapsulation of ciprofloxacin in acetylated SNPs with different degrees of modification and concluded that the EE of the compound increased with the DS. On the other hand, there is not enough literature on the use of propionylated and butyrylated SNPs as delivery systems and more research is needed in this field to explore their potential and determine their efficacy for different bioapplications. However, a recent study was found regarding the interest of encapsulating propionic acid with nutraceutical purposes considering its health benefits related to colon-diseases [35].

The zeta potential of SNPs for the different chain lengths and modifications was close to zero, as expected for these types of nanoparticles comparing to literature [51]. Such low values of the zeta potential indicate that particles can easily form aggregates [36], since the repulsion of the particles is not large enough to prevent them from attracting each other [52]. On the other hand, the tendency of these starches to agglomerate may be due to their hydrophobic character due to the presence of fatty acids. This creates hydrophobic forces between the particles, leading to the solvation of water and hence the tendency to agglomerate [53].

This particle aggregation is easily observed in the micrographs of rice SNPs. Usually, to consider a suspension physically stable, zeta potential values should be higher than 25-30 mV [52, 54, 55]. Therefore, these SNPs should be suitable for applications where slight particle agglomeration is not an issue. For example, in a previous study by Acevedo-Guevara et al. (referenced in the manuscript) it was demonstrated the potential of acetylated SNPs as a delivery system for curcumin. They reported that although acetylation did not affect particle morphology, slight aggregation of the granules was observed, but they achieved LE and LC above 80%. Although the tendency to form agglomerates would not affect the EE, it is true that agglomeration reduces the surface area, thereby delaying the release of the encapsulated compounds, which could be considered a disadvantage for applications focused on drug release. However, the delayed release of the compound could be advantageous when a gradual release is required for certain bioapplications, such as the encapsulation of compounds that need to be released in the large bowel or the release of antimicrobial compounds used in food preservation for example.

2.4.5.2. SNPs production yield

In order to know the total amount of SNPs obtained in each experiment, the production yield of each starch and DS was determined. The production yields obtained for each 0.1 g of starch added into the aqueous phase are presented in Table 2.7.

Table 2.7. *SNPs production yield obtained for the different starches and degrees of substitution.*

Type of starch	Chain length	Degree of substitution	Production yield (%)
Quinoa	Acetate	3.31	5.0±1.0
		6.57	1.0±0.3
		9.81	12±2.7
		13.3	9.0±2.5
	Propionate	2.98	13±0.9
		6.37	17±2.6[a]
		9.53	19±1.1
		12.2	13±0.8
	Butyrate	3.0	10±1.7
		5.91	17±0.5[ab]
		8.83	13±0.7
		11.6	13±2.0
Rice	Acetate	3.6	20±3.0
		7.08	18±0.7
		10.4	18±2.3[b]
		13.6	17±1.0
	Propionate	3.05	17±2.9[b]
		5.86	17±0.8
		9.65	14±1.0
		12.7	9.5 ±0.6
	Butyrate	3.19	15±1.3
		6.48	14±0.8
		9.89	13±0.9
		12.4	13±3.1

Data are expressed as the mean±standard deviation (n = 3). No significant differences between measurements are indicated by the same superscript ($p<0.05$).

The production yields obtained were rather low, as in no case was 20% achieved. Comparing acetylated, propionylated and butyrylated quinoa starch, the lowest production yields were obtained for the acetylated one, especially for the 6.57% modification degree where just a production yield of 1% was obtained. For propionylated and butyrylated SNPs, a higher amount of particles was obtained compared to the previous one, being 19% the highest production yield for the propionylated and 17% for the butyrylated SNPs. It can be concluded that, for this quinoa

starch, the highest production yields of SNPs can be obtained when modification degrees are between 5.9-9.5% of modification using propionate or butyrate as short-chain fatty acid.

Regarding rice SNPs, acetylated rice starch reaches higher production yields contrary to quinoa starch. Also, for the four modification degrees studied, a higher yield was obtained with the smallest one (3.6%) with a production yield of 20%, being also the maximum yield registered. A maximum yield of 17% was obtained for the propionylated, for both the 3.05 % and 5.86% modification degrees. On the other hand, butyrylated rice SNPs exhibited the highest production yield that was obtained at the lowest modification degree, being the maximum yield obtained in this case 15%. So, for rice starch, it can be concluded that to obtain a higher production yields, lower modification degrees, than for the quinoa ones, are required. In the case of rice SNPs, the chain length seems to affect the production yield, since it decreases with increasing chain length.

It would have been expected that starches with a higher DS and a higher fatty acid chain would have resulted in a higher yield, as their higher hydrophobicity would favour precipitation, and their lower solubility would also result in less loss of material during washing. For quinoa it can be seen that the yield for propionate and butyrate was generally slightly higher than for acetate, although there is no clear trend with the DS. However, this tendency was not observed in the case of the rice SNPs.

2.4.5.3. XRPD analysis

In order to know the crystalline structure, the two different starches used as well as the SNPs obtained with each one, were analyzed with XRPD and the obtained spectrum can be seen in Figure 2.18.

It can be observed that for both starch granules and SNPs a crystalline structure was obtained. Starch granules presented an A-type crystalline structure since its characteristic peaks were found at 15º, 17º, 18º and 23º regarding Bragg angles (2θ) which is in accordance with previous studies [47, 56, 57]. Also, another characteristic peak at 20º was observed both for starch granules and SNPs, which fit the model of a V-type pattern. This type of pattern describes the interactions that amylose molecules of starch can have with other molecules, such as fatty acids [57, 58]. According to previous studies, this peak confirms the formation of an amylose inclusion complex [59, 60]

where the amylose double helices transform into a single helix and in its hydrophobic cavity hydrocarbon chain of the ligand can reside [58], i.e., of fatty acid in our case.

Every case presents similar results for starch granules, however, an increase in the intensity for the lowest modification quinoa acetate starch granules (3.31%) and for the propionate granules with a 9.53% of modification was noticed. Regarding the SNPs spectra, acetylated starches presented higher intensity when midrange degrees of modification was used. In turn, there was a strong drop in peak intensity for the highest modification of the quinoa acetylate. For the propionylated SNPs, spectra shown a higher peak intensity for the lowest modification (2.98% for quinoa and 3.05% for rice) in both cases. However, for the butyrylated starches, the opposite trend was observed since the higher peak intensity was obtained for the higher modification (11.6% for quinoa and 12.4% for rice), being this very pronounced specially for rice starch. It should also be noted that all the SNPs spectra obtained with the unmodified starches are practically the same, since the intensity obtained is much lower compared to the modified starches.

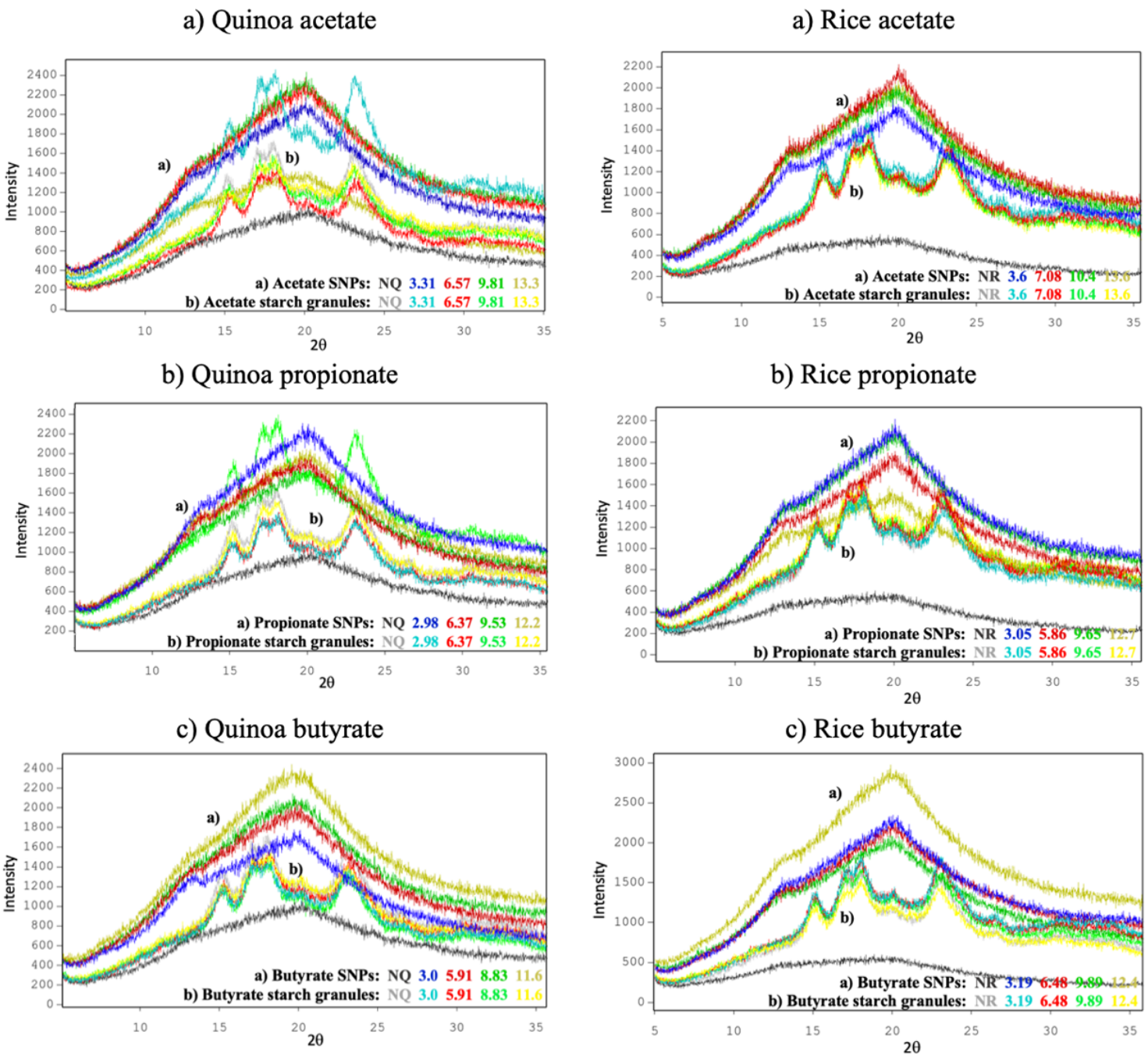

Figure 2.18. *Left column: XRPD spectra of the quinoa starch and the resulting SNPs synthesized. (a) Acetate; (b) Propionate; (c) Butyrate. Right column: XRPD spectra of the rice starch and the resulting SNPs synthesized. (a) Acetate; (b) Propionate; (c) Butyrate.*

2.4.5.4. FTIR spectrometry

FTIR technique allows to know the molecular changes that the compound of interest has encountered according to the changes in the intensity and broadness of the obtained bands. As well,

it allows us to know the changes that have occurred due to chemical treatments and to check the effectiveness of these [31].

Similar spectra were obtained for both starch granules and the SNPs as can be seen in Figure 2.19, indicating the preservation of starch chemical modification when SNPs were formed. It can be observed that all samples presented characteristic peaks at 3300 cm^{-1}, 2900 cm^{-1}, 1720 cm^{-1} and 1600 cm^{-1}. The peak at 3300 cm^{-1} was due to the stretching vibration of hydroxyl groups (-OH), which indicates the degree formation of inter- and intramolecular hydrogen bridge bonds [61], peak at 2900 cm^{-1} corresponds to the stretching vibration of C-H group and peak at 1600 cm^{-1} was due to the bending vibration of the H-O-H group of water molecules absorbed into the amorphous region [62, 63]. As Abdul Hadi et al. reported when the starches were synthesized, a carbonyl stretching vibration band (C=O) with a maximum at approximately 1720 cm^{-1} was obtained, indicating that the -OH groups of the starch were replaced by acyl groups during the esterification reaction. The spectra of the native samples (also shown in the figure), where this peak is not present, also confirm this. It is also observed that this band is still present in the SNPs after nanoprecipitation, so the chemical modification does not affect their synthesis. It should also be noted that as the DS increases, so does the intensity of the band. In turn, as can be seen in the figure, for the acetylated samples the characteristic bands showed peaks around 1365 cm^{-1} and 1245 cm^{-1} and in terms of propionylated and butyrylated samples, the characteristic bands appeared in peaks 1455 cm^{-1} and 1415 cm^{-1}, which, according to other studies, are related to the bending modes of CH_2 [31]. Also, for the acetylated samples, it can be confirmed that the ester band increases at the time that the modification degree increases too, being this more noticed for the quinoa starch samples.

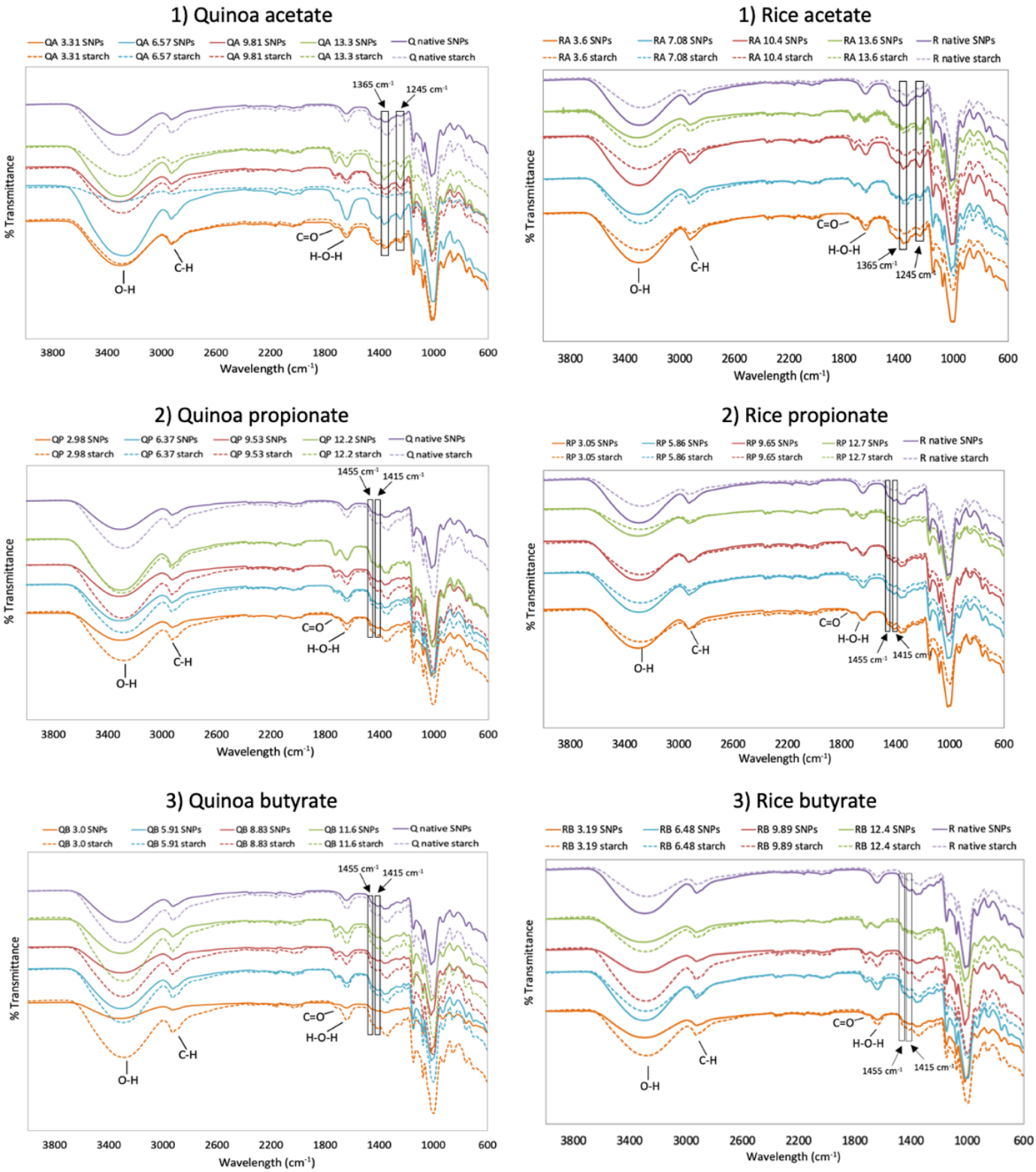

Figure 2.19. *Left column: FTIR spectra of the quinoa starch and the resulting SNPs synthesized. (a) Acetate; (b) Propionate; (c) Butyrate. Right column: FTIR spectra of the rice starch and the resulting SNPs synthesized. (a) Acetate; (b) Propionate; (c) Butyrate.*

2.4.6. Conclusions

The synthesis of controlled-size SNPs by nanoprecipitation method by using acetylated, propionylated and butyrylated quinoa and rice starches at different degrees of modification was developed. It has been demonstrated that SCFA-SNPs sizes in the range 96-170 nm can be obtained by considering the starch botanical source and the DS of the different SCFA used for modification.

Larger variations in size were observed for the SNPs prepared with the different SCFA quinoa starches, compared to rice SCFA starches that led to smaller and more similar sizes. It was proven that SCFA-SNPs with a certain controlled size can be obtained depending on the starch granules selected as raw materials for the synthesis, what offers good versatility allowing these nanoparticles to be used for different applications.

X-ray diffraction patterns showed an A-type crystalline structure for starch granules while for SNPs V-type pattern was obtained with the formation of an amylose inclusion complex with the fatty acids. FTIR spectra were similar both for the starch granules and the SNPs what demonstrated that the SNPs remained modified with the SCFA after the synthesis. Therefore, considering the health benefits of SCFA, the produced SCFA-SNPs could have a great interest for different clinical, pharmaceutical and food applications in which a specific particle size and shape is required, such could be its use as potential nanocarriers for controlled release of biocompounds or as additives or stabilizers for nutraceutical food-grade formulations.

- **References**

[1] M. A. El-Sheikh, “New technique in starch nanoparticles synthesis,” *Carbohydr Polym*, vol. 176, pp. 214–219, Nov. 2017, doi: 10.1016/j.carbpol.2017.08.033.

[2] G. Liu *et al.*, “Insights into the changes of structure and digestibility of microwave and heat moisture treated quinoa starch,” *Int J Biol Macromol*, vol. 246, p. 125681, Aug. 2023, doi: 10.1016/j.ijbiomac.2023.125681.

[3] A. P. Bonto, R. N. Tiozon, N. Sreenivasulu, and D. H. Camacho, “Impact of ultrasonic treatment on rice starch and grain functional properties: A review,” *Ultrason Sonochem*, vol. 71, p. 105383, Mar. 2021, doi: 10.1016/j.ultsonch.2020.105383.

[4] W. Berski *et al.*, "Pasting and rheological properties of oat starch and its derivatives," *Carbohydr Polym*, vol. 83, no. 2, pp. 665–671, Jan. 2011, doi: 10.1016/j.carbpol.2010.08.036.

[5] S. Punia, "Barley starch modifications: Physical, chemical and enzymatic - A review," *Int J Biol Macromol*, vol. 144, pp. 578–585, Feb. 2020, doi: 10.1016/j.ijbiomac.2019.12.088.

[6] M. Majzoobi, M. Radi, A. Farahnaky, J. Jamalian, T. Tongdang, and G. Mesbahi, "Physicochemical properties of pre-gelatinized wheat starch produced by a twin drum drier," *Journal of Agricultural Science and Technology*, vol. 13, no. 2, pp. 193–202, 2011.

[7] J.M.V. Blanshard, "Starch granule structure and function: a physicochemical approach," *Starch Properties and Potential*, pp. 16–54, 1987.

[8] R. N. Waduge, R. Hoover, T. Vasanthan, J. Gao, and J. Li, "Effect of annealing on the structure and physicochemical properties of barley starches of varying amylose content," *Food Research International*, vol. 39, no. 1, pp. 59–77, Jan. 2006, doi: 10.1016/j.foodres.2005.05.008.

[9] Jacobs H. Delcour J.A., "Hydrothermal modifications of granular starch, with retention of the granular structure," *J. Agric. Food Chem.*, pp. 2895–2905, 1998.

[10] R. Hoover and H. Manuel, "The Effect of Heat–Moisture Treatment on the Structure and Physicochemical Properties of Normal Maize, Waxy Maize, Dull Waxy Maize and Amylomaize V Starches," *J Cereal Sci*, vol. 23, no. 2, pp. 153–162, Mar. 1996, doi: 10.1006/jcrs.1996.0015.

[11] T. S. Leite, A. L. T. de Jesus, M. Schmiele, A. A. L. Tribst, and M. Cristianini, "High pressure processing (HPP) of pea starch: Effect on the gelatinization properties," *LWT - Food Science and Technology*, vol. 76, pp. 361–369, Mar. 2017, doi: 10.1016/j.lwt.2016.07.036.

[12] R. Bhat and A. A. Karim, "Impact of Radiation Processing on Starch," *Compr Rev Food Sci Food Saf*, vol. 8, no. 2, pp. 44–58, Apr. 2009, doi: 10.1111/j.1541-4337.2008.00066.x.

[13] G. Ren, D. Li, L. Wang, N. Özkan, and Z. Mao, "Morphological properties and thermoanalysis of micronized cassava starch," *Carbohydr Polym*, vol. 79, no. 1, pp. 101–105, Jan. 2010, doi: 10.1016/j.carbpol.2009.07.031.

[14] A. E. A. H. Mohamed M.E.A., "Pulsed electric fields for food processing technology," *Structure and Function of Food Engineering*, pp. 275–306, 2012.

[15] F. Zhu, "Impact of ultrasound on structure, physicochemical properties, modifications, and applications of starch," *Trends Food Sci Technol*, vol. 43, no. 1, pp. 1–17, May 2015, doi: 10.1016/j.tifs.2014.12.008.

[16] S. You and M. S. Izydorczyk, "Comparison of the physicochemical properties of barley starches after partial α-amylolysis and acid/alcohol hydrolysis," *Carbohydr Polym*, vol. 69, no. 3, pp. 489–502, Jun. 2007, doi: 10.1016/j.carbpol.2007.01.002.

[17] L. Wang and Y.-J. Wang, "Structures and Physicochemical Properties of Acid-Thinned Corn, Potato and Rice Starches," *Starch - Stärke*, vol. 53, no. 11, p. 570, Nov. 2001, doi: 10.1002/1521-379X(200111)53:11<570::AID-STAR570>3.0.CO;2-S.

[18] J. Singh, L. Kaur, and O. J. McCarthy, "Factors influencing the physico-chemical, morphological, thermal and rheological properties of some chemically modified starches for food applications-A review," *Food Hydrocolloids*, vol. 21, no. 1. pp. 1–22, Jan. 2007. doi: 10.1016/j.foodhyd.2006.02.006.

[19] S. L. M. el Halal *et al.*, "Structure, morphology and functionality of acetylated and oxidised barley starches," *Food Chem*, vol. 168, pp. 247–256, Feb. 2015, doi: 10.1016/j.foodchem.2014.07.046.

[20] L. A. Bello-Pérez, E. Agama-Acevedo, P. B. Zamudio-Flores, G. Mendez-Montealvo, and S. L. Rodriguez-Ambriz, "Effect of low and high acetylation degree in the morphological, physicochemical and structural characteristics of barley starch," *LWT - Food Science and Technology*, vol. 43, no. 9, pp. 1434–1440, Nov. 2010, doi: 10.1016/j.lwt.2010.04.003.

[21] T. Mehfooz, T. M. Ali, and A. Hasnain, "Effect of cross-linking on characteristics of succinylated and oxidized barley starch," *Journal of Food Measurement and Characterization*, vol. 13, no. 2, pp. 1058–1069, Jun. 2019, doi: 10.1007/s11694-018-00021-3.

[22] A. N. Dundar and D. Gocmen, "Effects of autoclaving temperature and storing time on resistant starch formation and its functional and physicochemical properties," *Carbohydr Polym*, vol. 97, no. 2, pp. 764–771, Sep. 2013, doi: 10.1016/j.carbpol.2013.04.083.

[23] J. N. BeMiller, "Pasting, paste, and gel properties of starch–hydrocolloid combinations," *Carbohydr Polym*, vol. 86, no. 2, pp. 386–423, Aug. 2011, doi: 10.1016/j.carbpol.2011.05.064.

[24] R. Balic, T. Miljkovic, B. Ozsisli, and S. Simsek, "Utilization of Modified Wheat and Tapioca Starches as Fat Replacements in Bread Formulation," *J Food Process Preserv*, vol. 41, no. 1, p. e12888, Feb. 2017, doi: 10.1111/jfpp.12888.

[25] O. S. Lawal, "Succinylated *Dioscorea cayenensis* starch: Effect of reaction parameters and characterisation," *Starch - Stärke*, vol. 64, no. 2, pp. 145–156, Feb. 2012, doi: 10.1002/star.201100110.

[26] H. Namazi, F. Fathi, and A. Dadkhah, "Hydrophobically modified starch using long-chain fatty acids for preparation of nanosized starch particles," *Scientia Iranica*, vol. 18, no. 3 C, pp. 439–445, 2011, doi: 10.1016/j.scient.2011.05.006.

[27] L. Boetje, X. Lan, F. Silvianti, J. van Dijken, M. Polhuis, and K. Loos, "A more efficient synthesis and properties of saturated and unsaturated starch esters," *Carbohydr Polym*, vol. 292, p. 119649, Sep. 2022, doi: 10.1016/j.carbpol.2022.119649.

[28] L. Wang *et al.*, "Effects of fatty acid chain length on properties of potato starch–fatty acid complexes under partially gelatinization," *Int J Food Prop*, vol. 21, no. 1, pp. 2121–2134, Jan. 2018, doi: 10.1080/10942912.2018.1489842.

[29] S. Pérez and E. Bertoft, "The molecular structures of starch components and their contribution to the architecture of starch granules: A comprehensive review," *Starch - Stärke*, vol. 62, no. 8, pp. 389–420, Jul. 2010, doi: 10.1002/star.201000013.

[30] Zia-ud-Din, H. Xiong, and P. Fei, "Physical and chemical modification of starches: A review," *Crit Rev Food Sci Nutr*, vol. 57, no. 12, pp. 2691–2705, Aug. 2017, doi: 10.1080/10408398.2015.1087379.

[31] A. Lopez-Rubio, J. M. Clarke, ben Scherer, D. L. Topping, and E. P. Gilbert, "Structural modifications of granular starch upon acylation with short-chain fatty acids," *Food Hydrocoll*, vol. 23, no. 7, pp. 1940–1946, Oct. 2009, doi: 10.1016/j.foodhyd.2009.01.003.

[32] A. Marinopoulou, E. Papastergiadis, S. N. Raphaelides, and M. G. Kontominas, "Structural characterization and thermal properties of amylose-fatty acid complexes prepared at different temperatures," *Food Hydrocoll*, vol. 58, pp. 224–234, Jul. 2016, doi: 10.1016/j.foodhyd.2016.02.034.

[33] S. Macfarlane and G. T. Macfarlane, "Regulation of short-chain fatty acid production," *Proceedings of the Nutrition Society*, vol. 62, no. 1, pp. 67–72, Feb. 2003, doi: 10.1079/PNS2002207.

[34] Z. Zhou, X. Cao, and J. Y. H. Zhou, "Effect of resistant starch structure on short-chain fatty acids production by human gut microbiota fermentation in vitro," *Starch - Stärke*, vol. 65, no. 5–6, pp. 509–516, May 2013, doi: 10.1002/star.201200166.

[35] H. Zeng *et al.*, "Encapsulation of propionic acid within the aqueous phase of water-in-oil emulsions: reduced thermal volatilization and enhanced gastrointestinal stability," *Food Funct*, 2023, doi: 10.1039/D2FO04076J.

[36] N. Sivapragasam, P. Thavarajah, J.-B. Ohm, J.-B. Ohm, K. Margaret, and D. Thavarajah, "Novel starch based nano scale enteric coatings from soybean meal for colon-specific delivery," *Carbohydr Polym*, vol. 111, pp. 273–279, Oct. 2014, doi: 10.1016/j.carbpol.2014.04.091.

[37] G. Annison, R. J. Illman, and D. L. Topping, "Acetylated, Propionylated or Butyrylated Starches Raise Large Bowel Short-Chain Fatty Acids Preferentially When Fed to Rats," *J Nutr*, vol. 133, no. 11, pp. 3523–3528, Nov. 2003, doi: 10.1093/jn/133.11.3523.

[38] P. A. Gill, M. C. van Zelm, J. G. Muir, and P. R. Gibson, "Review article: short chain fatty acids as potential therapeutic agents in human gastrointestinal and inflammatory disorders," *Aliment Pharmacol Ther*, vol. 48, no. 1, pp. 15–34, Jul. 2018, doi: 10.1111/apt.14689.

[39] M. Wang *et al.*, "Prebiotic effects of resistant starch nanoparticles on growth and proliferation of the probiotic Lactiplantibacillus plantarum subsp. plantarum," *LWT*, vol. 154, p. 112572, Jan. 2022, doi: 10.1016/j.lwt.2021.112572.

[40] N. Abdul Hadi, A. Marefati, M. Matos, B. Wiege, and M. Rayner, "Characterization and stability of short-chain fatty acids modified starch Pickering emulsions," *Carbohydr Polym*, vol. 240, p. 116264, Jul. 2020, doi: 10.1016/j.carbpol.2020.116264.

[41] C. Du, F. Jiang, W. Hu, W. Ge, X. Yu, and S. Du, "Comparison of properties and application of starch nanoparticles optimized prepared from different crystalline starches," *Int J Biol Macromol*, vol. 235, p. 123735, Apr. 2023, doi: 10.1016/j.ijbiomac.2023.123735.

[42] E. Alp, F. Damkaci, E. Guven, and M. Tenniswood, "Starch nanoparticles for delivery of the histone deacetylase inhibitor CG-1521 in breast cancer treatment," *Int J Nanomedicine*, vol. 14, pp. 1335–1346, 2019, doi: 10.2147/IJN.S191837.

[43] Y. Xu *et al.*, "pH-Responsive nanoparticles based on cholesterol/imidazole modified oxidized-starch for targeted anticancer drug delivery," *Carbohydr Polym*, vol. 233, Apr. 2020, doi: 10.1016/j.carbpol.2020.115858.

[44] J. Yang *et al.*, "Fabrication and characterization of hollow starch nanoparticles by gelation process for drug delivery application," *Carbohydr Polym*, vol. 173, pp. 223–232, Oct. 2017, doi: 10.1016/j.carbpol.2017.06.006.

[45] D. Morán, G. Gutiérrez, M. C. Blanco-López, A. Marefati, M. Rayner, and M. Matos, "Synthesis of Starch Nanoparticles and Their Applications for Bioactive Compound Encapsulation," *Applied Sciences*, vol. 11, no. 10, p. 4547, May 2021, doi: 10.3390/app11104547.

[46] N. Abdul Hadi, B. Wiege, S. Stabenau, A. Marefati, and M. Rayner, "Comparison of Three Methods to Determine the Degree of Substitution of Quinoa and Rice Starch Acetates, Propionates, and Butyrates: Direct Stoichiometry, FTIR, and 1H-NMR," *Foods*, vol. 9, no. 1, p. 83, Jan. 2020, doi: 10.3390/foods9010083.

[47] G. Gutiérrez, D. Morán, A. Marefati, J. Purhagen, M. Rayner, and M. Matos, "Synthesis of controlled size starch nanoparticles (SNPs)," *Carbohydr Polym*, vol. 250, Dec. 2020, doi: 10.1016/j.carbpol.2020.116938.

[48] F. G. Torres and G. E. De-la-Torre, "Synthesis, characteristics, and applications of modified starch nanoparticles: A review," *Int J Biol Macromol*, vol. 194, pp. 289–305, Jan. 2022, doi: 10.1016/j.ijbiomac.2021.11.187.

[49] L. Acevedo-Guevara, L. Nieto-Suaza, L. T. Sanchez, M. I. Pinzon, and C. C. Villa, "Development of native and modified banana starch nanoparticles as vehicles for curcumin," *Int J Biol Macromol*, vol. 111, pp. 498–504, May 2018, doi: 10.1016/j.ijbiomac.2018.01.063.

[50] S. H. Mahmoudi Najafi, M. Baghaie, and A. Ashori, "Preparation and characterization of acetylated starch nanoparticles as drug carrier: Ciprofloxacin as a model," *Int J Biol Macromol*, vol. 87, pp. 48–54, Jun. 2016, doi: 10.1016/j.ijbiomac.2016.02.030.

[51] H.-Y. Kim, S. S. Park, and S.-T. Lim, "Preparation, characterization and utilization of starch nanoparticles," *Colloids Surf B Biointerfaces*, vol. 126, pp. 607–620, Feb. 2015, doi: 10.1016/j.colsurfb.2014.11.011.

[52] A. W. Pacek, P. Ding, and A. T. Utomo, "Effect of energy density, pH and temperature on de-aggregation in nano-particles/water suspensions in high shear mixer," *Powder Technol*, vol. 173, no. 3, pp. 203–210, Apr. 2007, doi: 10.1016/j.powtec.2007.01.006.

[53] Y. Liang, N. Hilal, P. Langston, and V. Starov, "Interaction forces between colloidal particles in liquid: Theory and experiment," *Adv Colloid Interface Sci*, vol. 134–135, pp. 151–166, Oct. 2007, doi: 10.1016/j.cis.2007.04.003.

[54] F. Ye, M. Miao, K. Lu, B. Jiang, X. Li, and S. W. Cui, "Structure and physicochemical properties for modified starch-based nanoparticle from different maize varieties," *Food Hydrocoll*, vol. 67, pp. 37–44, Jun. 2017, doi: 10.1016/j.foodhyd.2016.12.041.

[55] R. H. Müller and C. Jacobs, "Buparvaquone mucoadhesive nanosuspension: preparation, optimisation and long-term stability," *Int J Pharm*, vol. 237, no. 1–2, pp. 151–161, Apr. 2002, doi: 10.1016/S0378-5173(02)00040-6.

[56] Q. Wang *et al.*, "Effects of octenyl succinylation on the properties of starches with distinct crystalline types and their Pickering emulsions," *Int J Biol Macromol*, vol. 230, p. 123183, Mar. 2023, doi: 10.1016/j.ijbiomac.2023.123183.

[57] Q. Lin *et al.*, "Fabrication of debranched starch nanoparticles via reverse emulsification for improvement of functional properties of corn starch films," *Food Hydrocoll*, vol. 104, p. 105760, Jul. 2020, doi: 10.1016/j.foodhyd.2020.105760.

[58] J. A. Putseys, L. Lamberts, and J. A. Delcour, "Amylose-inclusion complexes: Formation, identity and physico-chemical properties," *J Cereal Sci*, vol. 51, no. 3, pp. 238–247, May 2010, doi: 10.1016/j.jcs.2010.01.011.

[59] G. F. Fanta, J. A. Kenar, and F. C. Felker, "Nanoparticle formation from amylose-fatty acid inclusion complexes prepared by steam jet cooking," *Ind Crops Prod*, vol. 74, pp. 36–44, Nov. 2015, doi: 10.1016/j.indcrop.2015.04.046.

[60] H. Lu *et al.*, "Preparation and characterization of V-type starch nanoparticles by an oil-water interface method," *Food Hydrocoll*, vol. 138, p. 108455, May 2023, doi: 10.1016/j.foodhyd.2023.108455.

[61] M. Ahmad, A. Gani, ifra Hassan, Q. Huang, and H. Shabbir, "production and characterization of starch nanoparticles by mild alkali hydrolysis and ultra-sonication process," 2020, doi: 10.1038/s41598-020-60380-0.

[62] S. Liang, Y. Hong, Z. Gu, L. Cheng, C. Li, and Z. Li, "Effect of debranching on the structure and digestibility of octenyl succinic anhydride starch nanoparticles," *LWT*, vol. 141, p. 111076, Apr. 2021, doi: 10.1016/j.lwt.2021.111076.

[63] I. Dankar, A. Haddarah, F. E. L. Omar, M. Pujolà, and F. Sepulcre, "Characterization of food additive-potato starch complexes by FTIR and X-ray diffraction," *Food Chem*, vol. 260, pp. 7–12, Sep. 2018, doi: 10.1016/j.foodchem.2018.03.138.

3. STARCH NANOPARTICLES AS ANTIMICROBIAL NANOCARRIERS

CHAPTER 3 – Starch nanoparticles as antimicrobial nanocarriers

Introduction

This chapter is intended to describe the use of SNPs as nanocarriers for compounds with antimicrobial activity and is divided into two subchapters.

In the first subchapter, vanillin was selected as the compound to be encapsulated because it is widely used for antimicrobial purposes and, at the same time, is a natural compound that has no negative effects on human health. In this study, amaranth, quinoa and rice starches modified with different percentages of OSA were used and the synthesis was carried out by nanoprecipitation under optimal conditions. The SNPs were characterized by their size, shape and charge using DLS and SEM, and XRPD and FTIR were also used to analyze the structure and crystallinity of both starch granules and SNPs. Finally, native and the highest percentage OSA-modified amaranth starch were used to synthesize vanillin-loaded SNPs with slight modifications in the synthesis method. The resulting NPs were characterized by their size and shape as the previous ones, and nuclear magnetic resonance (NMR) was also used to determine the encapsulation of the vanillin. Reverse-phase high-performance liquid chromatography (RP-HPLC) was used to determine the free vanillin in the samples, and finally the antimicrobial activity of the NPs against *E. coli* was determined in tests in solid media.

The second subchapter describes the synthesis of hybrid Ag-SNPs by combining the nanoprecipitation method with an autoclaving process. AgNPs were first synthesized and then the starch was precipitated into SNPs, which acted as nanocarriers encapsulating the AgNPs. Silver is a well-known antimicrobial compound, and starch is widely used to stabilize it. However, there are no studies on the use of SNPs as a stabilizer for AgNPs and therefore this study is a novel approach in the antimicrobial field. The synthesis of the hybrid Ag-SNPs was carried out using native amaranth starch with certain modifications with respect to previous studies. Size, shape and charge were determined by DLS, SEM, TEM and high-resolution transmission electron microscopy (HR-TEM). The concentration of Ag in the formulations was determined by inductively coupled plasma mass spectroscopy (ICP-MS) and FTIR was used to determine the

encapsulation of AgNPs within the SNPs. The second part of this study deals with the evaluation of the antimicrobial activity of the formulations and was carried out in collaboration with the Packaging Research Group of the Institute of Agrochemistry and Food Technology (IATA-CSIC) in Paterna, Valencia. Antimicrobial activity tests were carried out against gram-positive and gram-negative bacteria (*S. aureus* and *E. coli*), both in liquid medium by determining log reductions and in solid medium by analyzing the inhibition zones.

3.1. Bio-based starch nanoparticles with controlled size as antimicrobial agents nanocarriers

- **Summary**

In this subchapter, OSA-modified SNPs were synthesized by nanoprecipitation. Amaranth, quinoa and rice starches were used and different percentages of OSA were compared with the native starches. The synthetized SNPs were characterized in terms of size, morphology and charge and, also, the thermal properties and crystallinity of starch granules and SNPs were compared. The molecular structure of starch granules and SNPs was also compared to determine if the OSA modification was affected by nanoprecipitation. Finally, the efficiency of using SNPs as nanocarriers was developed. Vanillin-loaded SNPs were synthesized by the same nanoprecipitation method with slight modifications, using the native and the highest % OSA-modified amaranth starch. They were characterized by shape and size and the EE, LC and LE were calculated. At the same time, it was determined whether vanillin was actually encapsulated within the SNPs or attached to their surface. On the other hand, vanillin is an organic compound known for its antimicrobial properties, so the antimicrobial activity of the vanillin-loaded SNPs against *E. coli* was also tested. The agar well diffusion method was used, and the evaluation of the inhibition zones indicated the antimicrobial activity of the formulations.

3.1.1. Introduction

Starch is one of the most abundant biopolymers in nature, which is biodegradable, biocompatible and low-cost. It is a storage carbohydrate found in all plants containing chlorophyll, such as maize, potato, rice, wheat, etc. and according to its botanical source, it presents different physico-chemical properties.

In this work, starches from three different botanical sources (amaranth, quinoa, and rice grains) were studied. Amaranth and quinoa are two pseudocereals that are widely recognized for their benefits to human health, being rich in proteins, fatty acids, vitamins or amino acids, among others [1]. Although there are several varieties of both herbs, the main component in their grains is starch. Amaranth grains contain around 65-75% of starch, while quinoa grains contain slightly less, 58.1-64.2%. The amylose content is estimated to be up to 34.4 % for amaranth [2], and up to 27.7 % for

quinoa [3] of the total starch in the grain, amylopectin being the rest. Rice is a cereal whose grain consists of 75-80% starch [4]. Its amylose content varies from 0-33% depending on the type of amylose: waxy, very low, low, intermediate, and high amylose [5].

These wide ranges of amylose content imply significant variation in the amylose/amylopectin ratio [2], affecting their macroscopic properties. For example, a starch with a high amylose content is expected to have a higher viscosity [6].

Native starches exhibit, thus, certain techno-functional limitations. In contrast, modified starches offer several benefits, including enhanced thermal stability, decreased retrogradation tendency, improved fluidity, lower gelatinization temperature, optimized gel viscosity, and better hydrophilicity or swelling characteristics [7, 8]. Consequently, the modification of starch has gained increasing attention in recent years to meet the diverse demands of various applications such as enzyme [9] or vitamin mobilization [10].

There are different types of modifications available to improve the functional properties of the starch which can be classified into physical, chemical, enzymatic, and a combination of them [11]. Among physical modifications, Kim et al. recently investigated the possibility of applying a pressure moisture treatment to tune the physico-chemical properties of starch [12]. Other physical modifications recently used are gelatinization and cold storage [13-15], high-pressure homogenization [16], high-power ultrasound treatment [17] or low-temperature plasma modification [18]. Regarding chemical modifications, acid hydrolysis [19, 20], oxidation [21], esterification [22] or etherification (where carboxymethylation stands out) [23], are some of processes reported by different authors. Chemically modified starches can also be prepared by treating the starch with different alkenyl succinic anhydrides, like, dodecyl succinic anhydride, octadecyl succinic anhydride and octenyl succinic anhydride [24].

Among those reactions, the chemical modification through esterification reactions with OSA has been frequently used in recent years. In this reaction, the starch -OH groups are replaced by OSA groups. OSA-modified starch is amphiphilic, since it combines the hydrophilic hydroxyl groups from the starch with the hydrophobic octenyl succinate groups from the OSA [25].

OSA-modified starches have a wide range of potential applications, including their use as fat replacement in the food industry [26, 27], as encapsulating agent in controlled release systems [28, 29] or as emulsifying agent in Pickering emulsions [30-32]. However, even though OSA-modified starch is a good candidate to stabilize emulsions on the macroscale (for droplet sizes of 10-50 microns), the modification also enhances its functionality as a stabilizer in the nanoscale (for droplet sizes in the 50-500 nm range). This may boost their potential applications. Therefore, using these disrupted granules as nanoparticles is one approach to improve their functionality for abovementioned purposes [33].

In recent years, SNPs have recently gained attracted attention due to their unique properties as a sustainable alternative to common nanomaterials due to their high biocompatibility, functionalization possibilities and high surface/volume ratio [34]. SNPs can be obtained by the breakdown of starch granules through different physico-chemical treatments [34-36]. The final properties of the SNPs are strongly influenced by the synthesis method. They have applications in medicine, cosmetics, biotechnology, or the food industry, among others [34, 37-44]. For certain bioapplications, it is crucial to obtain a controlled and monodispersed particle size. The nanoprecipitation method is widely used for this purpose, due to its simplicity and its capability of modulating the final size of the SNPs by controlling the synthesis parameters, as reported by Chin et al [45].

A novel application of modified SNPs that also requires controlled size particles is as sustainable immunoassay marker labels in point-of-care devices (or as detection markers in biosensors). For example, Patel et al., synthesized modified SNPs with pyrene with different degrees of substitution. Pyrene is a highly hydrophobic fluorescent dye which can be detected at very low concentrations. These pyrene-labelled SNPs were used for the detection of nitroaromatic compounds [46]. Vasileva et al. used starch-stabilized silver nanoparticles as a colorimetric sensor used in monitoring toxic metals in aquatic ecosystems. They found that the stabilized nanoparticles-based sensors had higher or at least similar sensitivity than the previously reported values for non-stabilized nanoparticles [47]. In 2018, Khachatryan and Khachatryan studied the formation of a novel biodegradable starch-based nanocomposite from cysteine, potato starch and ZnS quantum dots suitable as a sensor for Pb^{2+} and Cu^{2+} ions [48].

Moreover, there are several studies in which SNPs with controlled size (from 30 to 300 nm) were used as drug nanocarriers for cancer therapy [49-54]. They offer a wide range of possibilities to overcome the multiple physiological drug barriers that anti-tumor agents must cross, and to increase their absorption, distribution and stability in blood [55-57]. The preferential accumulation of drug-loaded nanocarriers in the tumor is favoured by the enhanced permeability and retention effect (EPR) [58]. But it can also be promoted through the functionalization of the nanoparticles with peptides, aptamers or antibodies, to recognize specific structures in cancer cells [59].

Therefore, it is important to highlight not only the size and charge control, but also the opportunities that further bioconjugation on the surface of SNPs offers for purposes such as carbodiimide chemistry for sensor detection [60] or target-specific delivery, as these functional groups allow the binding of specific ligands to their surface [61, 62].

Therefore, this work aims to produce controlled size SNPs by the nanoprecipitation method with starches from different botanical sources and with different % OSA each. The latter allows controlling the zeta potential of the SNPs' surface. The synthesized SNPs are characterized by their size, shape and charge using DLS and SEM. XRPD and FTIR are also used to analyze the structure and crystallinity of starch granules and SNPs. The thermal properties of the native starch granules and the SNPs are analyzed by thermogravimetric analysis (TGA) and differential scanning calorimetry (DSC). In addition, vanillin-loaded SNPs are prepared and characterized in terms of morphology and by NMR. The EE, LC and LE are determined and their antimicrobial activity against *E. coli* by the agar well diffusion method is assessed.

3.1.2. Materials

Milli-Q water was used to prepare the aqueous solutions and absolute ethanol (Sigma Aldrich, USA) was used as the organic phase to synthesize the SNPs and to wash the nanoparticles.

Starches from different botanical sources, amaranth, quinoa and rice, were used in this work.

Amylose content of the granules was determined using a lectin Concanavalin A assay (Megazyme International, Ireland) while lipid content was determined by Soxhlet extraction with ether as solvent. The moisture content was also determined by drying the samples at 105ºC for 30 min in a heating oven. Amaranth starch had an amylose content of 20.90%, 0.2% lipid and 9.9% moisture.

Quinoa starch had an amylose content of 20.95%, 1.2% lipid and 9.9% moisture. Finally, rice had an amylose content of 4.43%, a lipid content of 3.6% and a moisture content of 10.4%.

Besides using them in their native form, they were all modified form with different mass percentages of OSA. This modification process was performed at the Max-Rubner Institut, following the isolation and modification method described by Marefati et al. [30]. The DS was calculated based on the average number of substituted hydroxyl groups per unit of glucose in starch [25]. The protein content of the modified starch granules was also determined in this previous study using a nitrogen/protein analyzer (Flash EA 1112 Series, Thermo Scientific, USA) [30], and results are presented in Table S1. Lastly, vanillin at 99% (Sigma Aldrich, USA), an antimicrobial agent, was used as the loading compound. LB Broth with agar (Sigma Aldrich, USA) was used as nutrient agar for the antimicrobial activity tests and the *E. coli* strain (DH10b) was provided by the Dairy Research Institute of Asturias (Instituto de Productos Lácteos de Asturias, IPLA-CSIC).

3.1.3. SNPs synthesis

The nanoprecipitation method was used to synthesize the SNPs based on optimal synthesis conditions that were selected from a previous work [63]. The same experimental procedure was applied for all starches studied. Firstly, the synthesis of the SNPs was carried out for all the starches with different OSA mass percentages. Then, SNPs were washed and dried in a heater prior further characterization. All experiments were carried out at least in triplicate.

For SNPs synthesis an aqueous phase was prepared by dissolving 0.1 g of starch into 10 mL of Milli-Q water, then this starch solution was heated at 80 ºC under a 1000 rpm constant stirring for 30 min until the starch was completely dissolved. Next, to precipitate the starch in the form of nanoparticles, 1 mL of the starch solution was added dropwise with a syringe pump into an organic phase under a 4 mL/h constant injection rate. This organic phase consisted of 20 mL of absolute ethanol which was constantly stirred at 500 rpm during the injection.

Once SNPs were synthesized, samples had to be washed before characterization. Firstly, samples were centrifuged for 10 min at 15880 g (corresponding to 10000 rpm) at room temperature. The supernatant was removed, and the SNPs were obtained as pellets, and they were restored with

absolute ethanol. This washing process was repeated twice. Finally, the SNPs were dried in a heater at 80 ºC for 24 h.

3.1.4. Vanillin-loaded SNPs

Two methods can be used to produce loaded SNPs susceptible of serving as delivery vehicles. In the direct method, the synthesis and the compound loading are performed at the same time. In the indirect method, the SNPs are synthesized first and then loaded with the compound of interest [34].

In this work, the direct method was chosen. Thus, the aforementioned nanoprecipitation method was modified by adding vanillin to the organic phase (at a concentration of 50 mg/mL (C_0) in ethanol).

Once the vanillin-loaded SNPs were synthesized, the ethanol was evaporated using a rotary evaporator at reduced pressure. The film formed was rehydrated with water by rotation at 60 ºC. Samples were filtered using PES syringe filters with 0.22 µm pore diameter to separate the SNPs. The free (remaining in the liquid phase) vanillin concentration (C_{free}) was determined by RP-HPLC. EE was calculated as the concentration ratio according to equation 1:

$$EE\ (\%) = \frac{C_0 - C_{free}}{C_0} \times 100 \quad (1)$$

The amount of vanillin loaded into the SNPs was expressed as LC and calculated as the mass fraction of vanillin in the vanillin-loaded SNPs following equation 2:

$$LC\ (\%) = \frac{mg_{vai}}{mg_{vai} + mg_{SNPs}} \times 100 \quad (2)$$

(mg_{vai}: amount of vanillin; mg_{SNPs}: amount of SNPs)

Finally, LE refers to the proportion of LC that is actually successfully released. It was calculated according to equation 3:

$$LE\ (\%) = \frac{mg_{vai\ free}}{LC} \times 100 \quad (3)$$

($mg_{vai\ free}$: amount of free vanillin)

An aliquot of each sample was also washed and dried in the same way as the unloaded SNPs and characterized by SEM to check whether the process affected the SNP morphology, and by NMR to determine the presence of vanillin.

3.1.5. SNPs antimicrobial activity test

The antimicrobial activity of vanillin-loaded SNPs was tested *in vitro* on *E. coli* using the agar well diffusion method and evaluating the inhibition zones. 100 µL of bacteria inoculum was placed on Petri plates and approximately 20 mL of pre-melted nutrient agar was poured over the inoculum and allowed to solidify. Holes with approximate 1 cm of diameter were made in the plates and 100 µL of the formulations, including the starch aqueous phase as a control, were added into each hole. Then, the plates were incubated at 30 °C for 72 h. The formation of clear halos around the holes indicated the antimicrobial activity of the formulations.

3.1.6. SNPs characterization

Particle size distribution and zeta potential

DLS was used to measure the hydrodynamic size (in number) of the synthesized particles, using a Zetasizer Nano ZS equipment (Malvern Instruments Ltd, Malvern, UK). Samples were measured with the 173 °C backscatter detector in disposable low-volume cuvettes (Malvern Instruments Ltd, Malvern, UK). Zeta potential measurements were performed with the same technique in disposable folded capillary cells (DTS1070).

- **Structural analysis**

Morphology and size

The size and shape of the unloaded and vanillin-loaded SNPs were analyzed by using a JEOL JSM-5600 field emission SEM at an acceleration voltage of 20 kV. The dehydrated samples were fractured and deposited on a double-sided adhesive tape placed on a copper sample holder and coated with a gold thin film in a Balzers SCD 005 sputtering device (Bal-Tec AG, Liechtenstein) before the analysis to avoid the accumulation of electric charge under the electron beam in the

microscope. The average particle size of the SNPs was determined by random measurements using ImageJ Fiji software.

X-Ray powder diffraction

The crystalline structure of starch granules and the synthesized SNPs was determined by XRPD. Data were collected at room temperature, using CuKα1.2 radiation (λ = 1.54056 Å and 1.54439 Å) in a Bragg-Brentano reflection configuration, on a Philips Panalytical X'Pert Pro diffractometer in a 2θ range of 5-27°, with a step size of 0.08356º. The estimation of the crystalline domains of starch granules and the SNPs were determined with the FullProf program.

- **Chemical analysis**

Fourier transform infrared spectroscopy

FTIR was used to determine the molecular structure of the SNPs and starch granules, and to check whether the % OSA was affected by the synthesis method. FTIR spectra were acquired in a Fourier transform infrared spectrophotometer (Varian 620-IR, Thermo Fisher ScientificInc., U.S.A.) at room temperature. Samples of dried powder (approximately 1 mg) were directly measured, and spectra were recorded between 650–4000 cm^{-1} (medium infrared band).

Reverse-Phase High Performance Liquid Chromatography

The concentration of free vanillin was determined by analysing the samples by RP-HPLC (Agilent 1100 series chromatograph, Agilent Technologies) using a Zorbax Eclipse Plus C18 column. Milli-Q water (A) and methanol (B) in a linear gradient were used as mobile phases. The gradient started with 20% B, reached 100% B after 5 min, and was kept constant for 10 min. Flow rate was 0.8 mL/min and the vanillin concentration was measured by absorbance at λ = 280 nm. Samples were diluted 1:100 (v/v) with methanol prior to their analysis to avoid saturation of the column.

Nuclear magnetic resonance spectrometry

NMR spectrometry was used to determine whether the bioactive compound was encapsulated within the SNPs or attached to their surface. The ^{1}H NMR spectra of both vanillin-loaded SNPs

and vanillin alone were obtained using a Bruker AV400 spectrometer with a 14.0 T shielded magnet. The sample was dissolved in DMSO, and the spectra were recorded at 298 K.

Thermal analysis

The granules of the native starches and the different SNPs synthesized were analyzed by TGA and DSC to see how the physical properties of the samples would change as a function of temperature and time. TGA was performed with a TG/SDTA 851^e/1600 Mettler and DSC with a DSC 822^e/700 Mettler, in both cases following a heating program from 25 to 600 ºC at a rate of 10 ºC/min and using nitrogen as the reaction gas at a flow rate of 50 mL/min.

Statistical analysis of data

All data were expressed as mean ± standard deviation (SD) of three independent experiments and statistical analysis of data (ANOVA) was performed to analyze differences between test groups. Significant differences were determined by Fischer's LSD test using Microsoft Excel ($p < 0.05$).

3.1.7. Results and discussion

3.1.7.1. Particle size distribution, morphology, size and zeta potential

SNPs were synthesized using starches from quinoa, rice and amaranth grains, at five different OSA mass percentages. Their final size, shape and surface charge of the particles were then determined.

Sizes obtained with DLS were inconclusive (data not shown) for amaranth and quinoa starches. Particle sizes seemed to increase significantly with the % OSA, up to 500 nm, while for rice starch no signal was obtained for any of the SNPs. When SEM micrographs were analyzed (Figure 3.1), particle sizes presented an opposite trend compared to DLS results for amaranth and quinoa starch. This discrepancy can be explained by the agglomeration of the SNPs which could lead to the larger sizes determined by DLS. Furthermore, for rice starch, SNPs formation was also observed for all % OSA tested. For this reason, a customized macro of the ImageJ Fiji software was developed by the Photon Microscopy Unit of the Scientific-Technical Services of the University of Oviedo to automatically measure several SNPs from a single SEM micrograph and compute the average size. Table 3.1 shows those sizes along with the zeta potential obtained by DLS for each case.

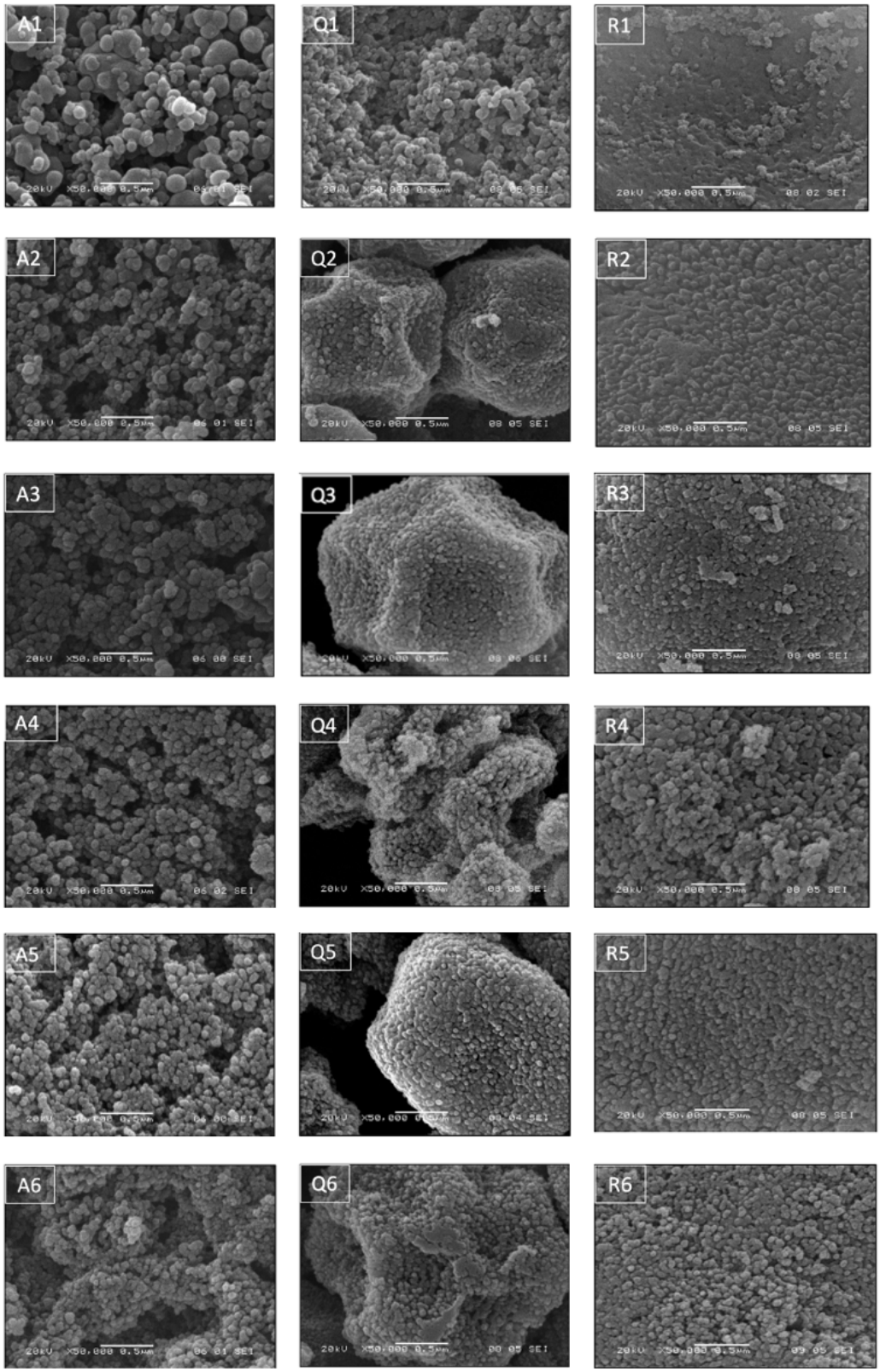

Figure 3.1. *SEM micrographs of SNPs obtained by the nanoprecipitation method using the three types of starch (AS=Amaranth Starch; QS=Quinoa Starch; RS=Rice Starch) each esterified with different amounts of OSA.*

Table 3.1. *Mean sizes of SNPs obtained by ImageJ Fiji software and zeta potential obtained by DLS for the different starches each esterified with different amounts of OSA.*

Type of starch	Sample name	% OSA	Zeta potential (mV)	Size (nm)
Amaranth	A1	0	-1.7±2.9	108±33
	A2	0.53	-8.7±2.5	94±23
	A3	1.07	-11.4±2.9	92±23
	A4	1.50	-16.3±2.6	85±19
	A5	2.06	-30.2±3.3	78±14
	A6	2.62	-27.4±3.7	75±15
Quinoa	Q1	0	-5.8±3.5	70±10
	Q2	0.58	-12.8±3.2	60±9
	Q3	1.14	-14.1±3.2	60±8
	Q4	1.67	-19.7±4.5	59±8
	Q5	2.13	-17.9±3.1	60±6
	Q6	2.59	-18.7±3.4	54±6
Rice	R1	0	-7.1±3.5	58±6
	R2	0.46	-8.8±5.2	62±9
	R3	0.97	-10.3±5.4	60±6
	R4	1.40	-9.5±4.2	63±8
	R5	1.90	-11.4±3.2	56±5
	R6	2.36	-12.9±3.9	61±7

Data are expressed as the mean±standard deviation (n=3). No significant differences between measurements ($p<0.05$).

Given the above results, for the amaranth starch, as the % OSA of the starch granules increases, the size of the synthesized SNPs decreases. The largest size was obtained for the native amaranth starch (108±33 nm) and the smallest for the amaranth starch with the highest % OSA (75±15 nm). On the other hand, as the % OSA increases, more particle agglomerates are appreciated (the individual particles become more clustered). However, in all cases the spherical shape of the particles remained. Therefore, one can conclude that for amaranth starch the % OSA affects the size of the SNPs but not their shape.

A similar behaviour was observed for quinoa starch since the particle size decreased when the % OSA increased, but to a lesser extent. However, when starch granules were modified with OSA, the spherical particles clustered into a larger particle with a polygonal morphology. This was not seen in the native starch. Despite this, spherical particles can be distinguished in most cases, although there are regions where the SNPs have not yet fully developed, i.e., for Q2 and Q6 samples.

Very different results were obtained with rice starch. For lower % OSA and for the native granules, the SNPs were not fully formed. As the % OSA increased, the particles became more spherical and monodisperse.

Although there is not much variation in size with the % OSA, these modified SNPs could find different applications as drug delivery systems, as demonstrated by Qi et al. They obtained spherical nanoparticles with excellent dispersibility and narrow size distribution, whose average diameter was only 86.69 nm. Their loading and release properties were investigated using indomethacin as a drug model, showing an increased initial release rate and total release amount when the SNPs were used [64]. On the other hand, OSA-SNPs could be a potential agent for the stabilization of oil-water systems. Jiang et al. provided a way to improve the dispersion of SNPs in polar/non-polar solvents and broaden their potential applications as a stabilizing agent. The diameters of the SNPs obtained varied from 40-60 nm for the SNPs without OSA and between 60-80 nm and 150-200 nm for the different degrees of substitution they used [65].

The zeta potential results obtained by DLS (Table 3.1), aid to explain the tendency was observed for the three types of starches studied. This parameter provides insight into the tendency of particles to form agglomerates. A zeta potential approaching zero suggests a heightened likelihood of particle agglomeration, as there is no charge repulsion between them [63], which could explain the larger sizes observed with DLS. Conversely, as the % OSA increased, the absolute value of the zeta potential also rose, leading to a reduction in particle aggregates due to enhanced charge repulsions between them.

However, for rice starch, highest % OSA resulted in less agglomerated particles. Despite this, the zeta potential results remain relatively low. This could account for the inconsistencies, as values

exceeding 30 mV are typically regarded as the minimum for considering nanoparticles stable, primarily due to electrostatic forces [66].

Similar results were previously obtained by El-Naggar et al. who synthesized cross-linked corn starch nanoparticles for medical applications using the nanoprecipitation method. They obtained a size range of 21 to 68 nm and a zeta potential ranging from -6.8 mV to -25.6 mV [49]. Qiu et al also used this nanoprecipitation method to produce EO-loaded starch nanoparticles, obtaining sizes of 84 nm when the particles were not loaded with the oil and a range of 93 to 112 nm when they were loaded with it [37].

3.1.7.2. XRPD analysis

The three types of starches used in this study and the resulting SNPs were analyzed by XRPD to determine the predominant crystalline structure. The obtained spectra are shown in Figure 3.2. All starch granules and their corresponding SNPs presented crystalline structures. The starch granules exhibited a crystalline pattern of the A-type, characterized by Bragg angle (2θ) peaks at 15º, 17º, 18º, and 23º. In contrast, a decrease in crystallinity was noted in the case of SNPs when compared to starch granules, aligning with observations from prior studies [43, 63]. They displayed V-type X-ray diffraction patterns, featuring a distinctive peak at 20º. This can be related to the formation of amylose-lipid complexes during the dissolution of starches before nanoprecipitation [65]. Earlier research has indicated that amylose within starch granules can create V-type complexes with various compounds, including fatty acids, alcohols, or emulsifiers [66].

In the case of amaranth starch, the spectra for starch granules exhibited a consistent intensity across all % OSA. However, for quinoa and rice starches, a lower intensity was observed in the native granules, while a roughly similar intensity was obtained for the subsequent % OSA. When it comes to SNPs, amaranth starch patterns indicated an increase in intensity with higher % OSA. Conversely, for quinoa and rice starches, a contrasting trend emerged, with intensity rising as the % OSA decreased. This effect was particularly pronounced for rice starch.

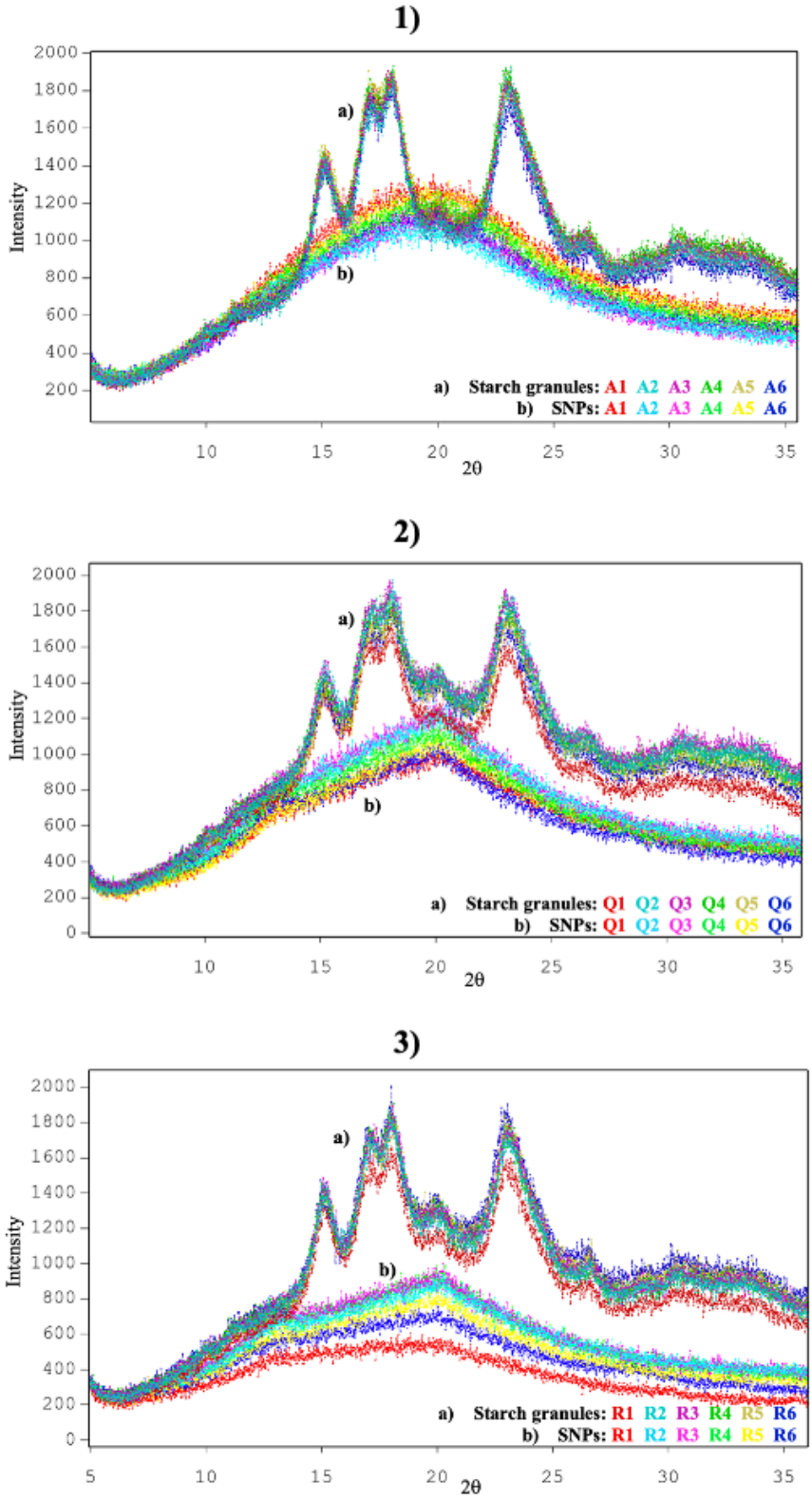

Figure 3.2. *XRPD spectra of the three starches and the resulting SNPs synthesized. 1): Amaranth starch; 2): Quinoa starch; 3): Rice starch.*

3.1.7.3. FTIR spectrometry

The type of inter- and intra-molecular bonds present in a sample can be investigated by FTIR spectrometry, offering a valuable insight on its structural features. Figure 3.3 shows the FTIR spectra of the amaranth, quinoa, and rice starch granules, respectively, and their corresponding SNPs. The spectra revealed similar characteristic bands for the SNP peaks compared to the starch granule peaks, albeit with slightly lower intensity. This suggests that the OSA modification was minimally influenced by the SNP synthesis. Additionally, only minor differences were discernible in the spectra among the three types of starch. In every case, a strong absorption peak appears at a wavelength of around 3300 cm^{-1} characteristic of the hydroxyl groups (-OH) and its intensity indicated the degree of inter- and intramolecular hydrogen bridge bonds formation [67]. Other characteristic bands were observed at a wavelength of about 2900 cm^{-1} which corresponds to the C-H stretching vibration of the glucose unit [68]. The peak at around 1600 cm^{-1} may correspond to the bending vibration of the H-O-H group of water bound in the starch [69]. By comparing OSA-modified starch granules and SNPs, with their corresponding native ones, two new absorption bands around 1720 cm^{-1} and 1540 cm^{-1} were observed. The first one was related to the stretching vibration of the carbonyl group (C=O) and the second to the stretching vibration of the carboxyl group (-COOH) introduced by the OSA [70, 71]. The appearance of these peaks indicated that the esterification reaction after OSA modification took place. In addition, according to previous works, as the % OSA increases, the intensity of these two bands increases, too [72, 73].

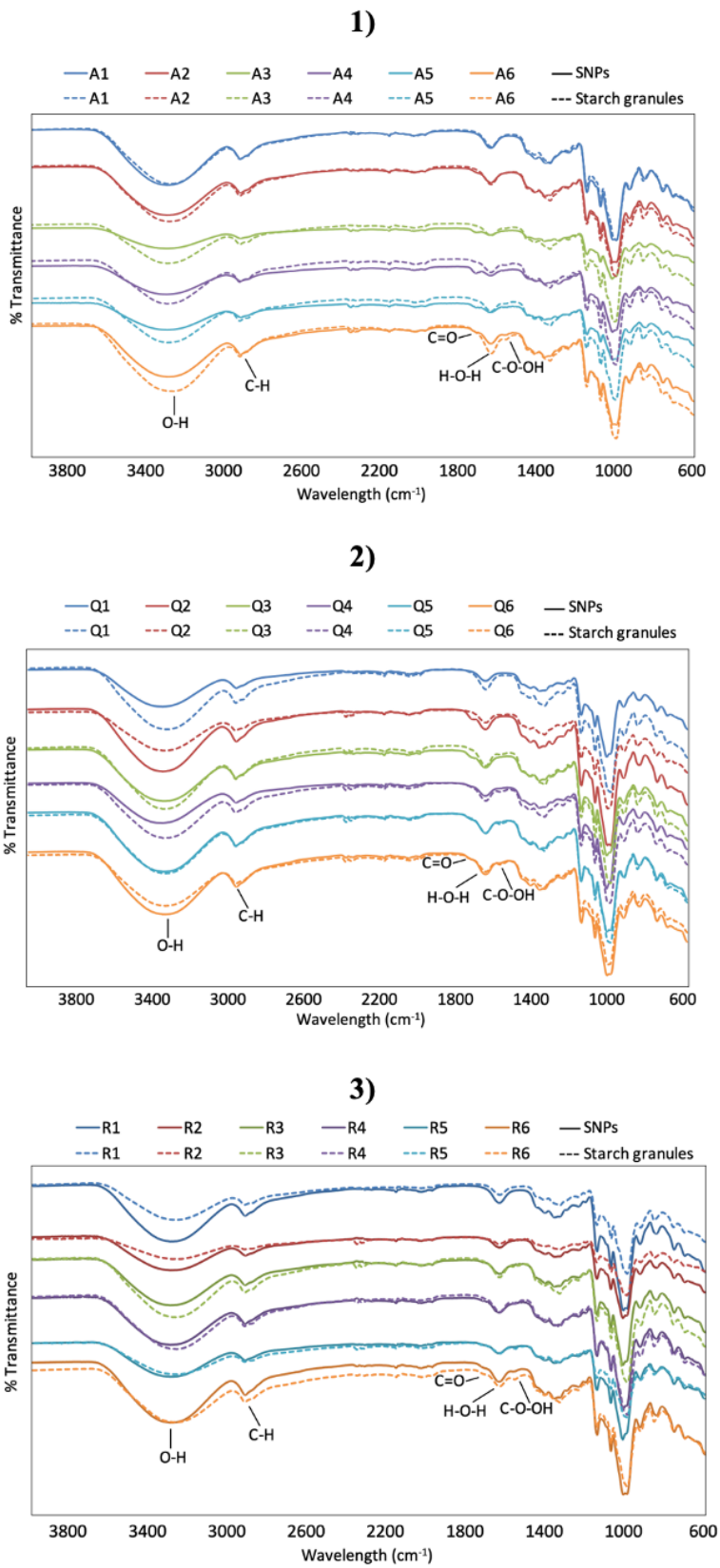

Figure 3.3. *FTIR spectra of the three starches and the resulting SNPs synthesized. 1): Amaranth starch; 2): Quinoa starch; 3): Rice starch.*

3.1.7.4. Thermal analysis

TGA and DSC were used to determine the thermal stability of SNPs and native starch granules.

For the three starches, the TGA results were similar. Both the starch granules and SNPs curves showed two stages of mass loss, the first between 25-150ºC (water loss) and the second between 260-380ºC, corresponding to the range in which the starch decomposes very rapidly. These results are in concordance with recent studies [74, 75]. Regarding the DSC curves, two endothermic bands were observed for all SNPs tested, corresponding to water lost and decomposition of the starch, which was found in each case to be around 300 ºC. TGA and DSC curves are presented in Figures S1 and S2 respectively for the three starches.

On the other hand, the percentage of water was calculated from the TGA and DSC curves. The TGA curve was used to calculate the mass loss in the first stage (25-150ºC). The first endothermic peak (corresponding to water loss) was integrated into the DSC curve, this value was compared with the value of the heat of evaporation of water (2260.4 mJ/mg) and the mg of water lost was determined. By comparing this value with the amount weighed, the percentage of water was determined.

Comparing the values obtained by TGA and DSC, the values obtained by the latter are generally slightly higher. This is because, apart from the fact that they are two different techniques, in the TGA experiments the samples are kept at 25ºC for 5 minutes, the samples have some moisture and during this isothermal time at 25ºC they lose some mass. Table S2 shows the percentage of water obtained by the two techniques and the total loss of mass by TGA.

3.1.7.5. Evaluation of vanillin-loaded SNPs antimicrobial activity

Loaded SNPs of native and highest % OSA-modified amaranth starch were used as vehicles for the controlled release of vanillin. It was intended to determine whether the % OSA could positively influence the EE since it was previously observed for peppermint flavour. The findings indicate a positive correlation between the DS and flavour retention, meaning that as the DS increased, so did the retention of flavour. However, there was a negative correlation observed between flavour release and an increase in the DS [76].

In Figure 3.4, SEM micrographs show vanillin-loaded SNPs for both native and OSA-modified amaranth starch (samples A1 and A6). In the case of native starch, the formation of spherical particles was significantly diminished, barely observable. On the other hand, for OSA-modified starch, a considerable number of spherical particles were evident. However, in comparison with the micrographs obtained for the non-loaded SNPs (Figure 1), increased agglomeration is noticeable. Nevertheless, sizes obtained in both cases remained very similar to those of the non-loaded SNPs, 110-150 nm for the smallest particles of A1 sample and 60-80 nm for A6, indicating that the vanillin loading process did not affect the final size of the SNPs but did affect their formation when native starch was used.

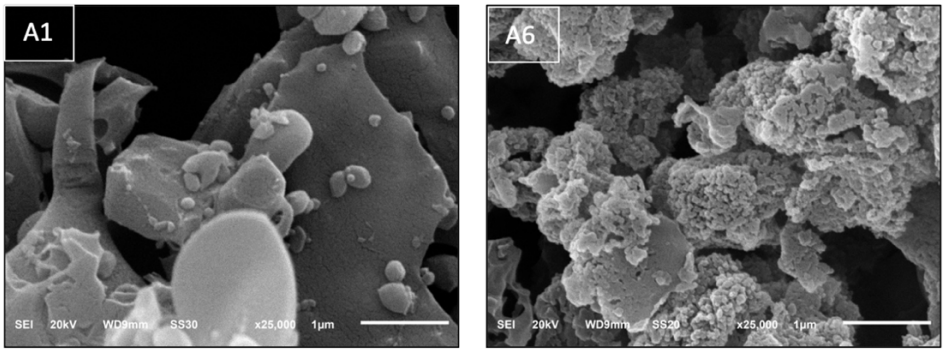

Figure 3.4. *SEM micrographs of vanillin-loaded SNPs for amaranth starch native and the highest % OSA.*

In both cases, Van der Waals forces are present between the starch and vanillin molecules, but in sample A6 the interactions between the alcohol and aldehyde groups of vanillin and the carboxyl group of OSA also formed hydrogen bonds. This strong intermolecular force allowed both the stabilization of the vanillin bond and the retention of the spherical shape of the SNPs. On the contrary, in the A1 sample, the weaker bonds formed between the starch and the vanillin could be easily broken, and therefore the spherical shape of the SNPs was lost.

Moreover, the presence of OSA enhanced the solubility of vanillin during the rehydration of the film formed with the rotary evaporator. This is evidenced by the quicker rehydration time observed for the A6 sample compared to A1, which agrees with findings from previous studies [24].

To get an idea of the effectiveness of the interaction of the modified starch with the vanillin, EE, LC and LE of vanillin-loaded SNPs were calculated. Free vanillin concentration for sample A6 was determined by RP-HPLC and an EE value of 30% was achieved while the LC achieved 60% and LE 5.8%.

Furthermore, Figure 3.5 shows the NMR spectra of the A6 sample to determine if vanillin was actually encapsulated within the SNPs or attached to their surface. The presence of vanillin is identified by its characteristic aldehyde peak (around 9.8 ppm), the aromatic ring peaks (around 7 ppm) and the one corresponding to the OMe (around 3.8 ppm) [77], none of them present in the SNPs. Vanillin is adsorbed on the surface, as evidenced by the unchanged chemical shifts compared to free vanillin. In the case of encapsulated vanillin, the absence or alterations in the position of the peaks should have been observed. Covalent binding to the particle is also ruled out, given that the aldehyde signal remains present in the spectra.

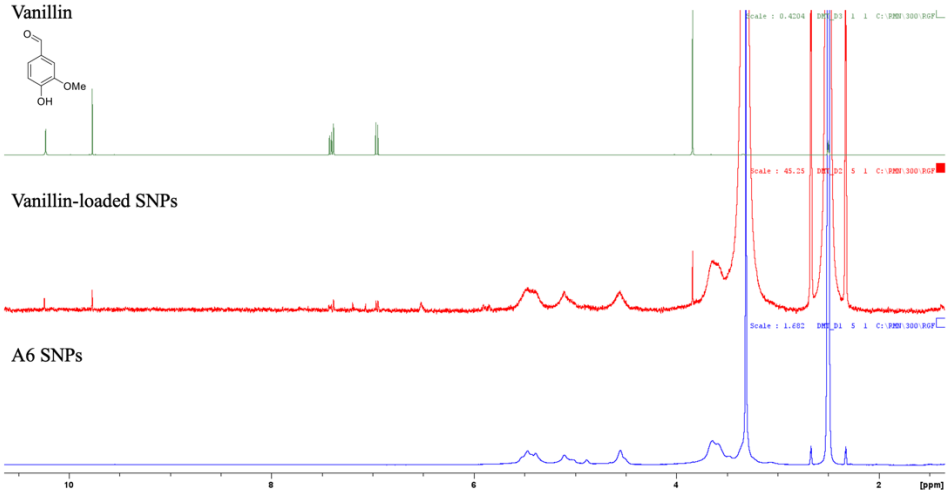

Figure 3.5. *Comparison of NMR spectra of vanillin, vanillin-loaded SNPs and unloaded SNPs.*

In the last set of experiments, the antimicrobial activity of A6 sample was determined by the agar well diffusion method. The activity against *E. coli* of vanillin-loaded SNPs, vanillin and non-loaded SNPs (A6, used as control) was compared. The antibiogram obtained is shown in Figure 3.6.

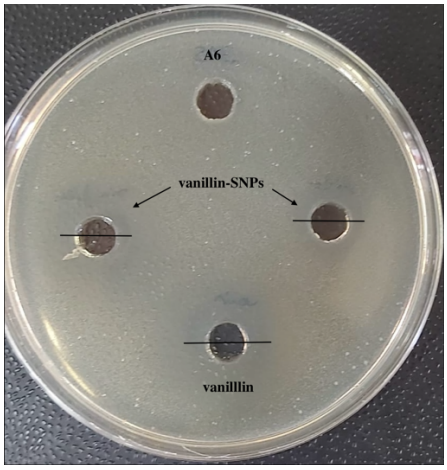

Figure 3.6. *Antimicrobial activity of vanillin-loaded SNPs against E. coli using the agar well diffusion method.*

As expected, the hole containing non-loaded SNPs (A6) has no inhibition halo, as starch alone has no antimicrobial activity. Inhibition halos can be observed in the remaining holes, both the one with vanillin and the holes containing vanillin-loaded SNPs, confirming also that vanillin has been loaded in the SNPs.

Recent studies have demonstrated the potential of starch as a nanocarrier of active ingredients to improve their properties and broaden their range of applications [78]. Therefore, it can be concluded that OSA modified SNPs are good candidates as carriers and protective agents for these compounds.

3.1.8. Conclusions

By selecting the suitable type of starch and optimizing the % OSA modification, functionalized SNPs with controlled size and charge can be synthesized through nanoprecipitation. This holds potential advantages for various bio-applications, not only due to the controlled size and charge, which are crucial for specific purposes, but also because of the opportunities for further bioconjugation on the surface of the SNPs. This opens up possibilities for applications such as target-specific delivery. Starch granules' showed A-type crystalline structure while for the SNPs V-type patterns were observed. FTIR spectra showed very similar characteristic bands in both SNPs and starch granules peaks, with slight variations in the intensity of the peaks in some samples, which could justify that the OSA molecules partially remain after the SNPs precipitation which could be an advantage for the aforementioned future applications regarding bioconjugation with

the carboxylic functional groups on the SNPs surface. SNPs showed thermal properties similar to those of starch granules.

In addition, the viability of using SNPs as nanocarriers of compounds with antimicrobial activity was demonstrated by synthesizing vanillin-loaded SNPs. NMR analysis showed the presence of vanillin adsorbed by the SNPs and an EE of 30%, LC of 60% and LE of 5.8% were obtained. Finally, their inhibitory capacity against *E. coli* was demonstrated.

- **References**

[1] S. Graziano, C. Agrimonti, N. Marmiroli, and M. Gullì, "Utilisation and limitations of pseudocereals (quinoa, amaranth, and buckwheat) in food production: A review," *Trends Food Sci Technol*, vol. 125, pp. 154–165, Jul. 2022, doi: 10.1016/j.tifs.2022.04.007.

[2] H. Corke, Y. Z. Cai, and H. X. Wu, "Amaranth: Overview," in *Reference Module in Food Science*, Elsevier, 2016. doi: 10.1016/B978-0-08-100596-5.00032-9.

[3] G. Li and F. Zhu, "Quinoa starch: Structure, properties, and applications," *Carbohydr Polym*, vol. 181, pp. 851–861, Feb. 2018, doi: 10.1016/j.carbpol.2017.11.067.

[4] D. K. Verma and P. P. Srivastav, "Proximate Composition, Mineral Content and Fatty Acids Analyses of Aromatic and Non-Aromatic Indian Rice," *Rice Sci*, vol. 24, no. 1, pp. 21–31, Jan. 2017, doi: 10.1016/j.rsci.2016.05.005.

[5] O. S. Lawal *et al.*, "Rheology and functional properties of starches isolated from five improved rice varieties from West Africa," *Food Hydrocoll*, vol. 25, no. 7, pp. 1785–1792, Oct. 2011, doi: 10.1016/j.foodhyd.2011.04.010.

[6] L. Alonso-Miravalles and J. O'Mahony, "Composition, Protein Profile and Rheological Properties of Pseudocereal-Based Protein-Rich Ingredients," *Foods*, vol. 7, no. 5, p. 73, May 2018, doi: 10.3390/foods7050073.

[7] S. Lefnaoui and N. Moulai-Mostefa, "Synthesis and evaluation of the structural and physicochemical properties of carboxymethyl pregelatinized starch as a pharmaceutical excipient,"

Saudi Pharmaceutical Journal, vol. 23, no. 6, pp. 698–711, Nov. 2015, doi: 10.1016/j.jsps.2015.01.021.

[8] D. Le Corre and H. Angellier-Coussy, "Preparation and application of starch nanoparticles for nanocomposites: A review," *React Funct Polym*, vol. 85, pp. 97–120, Dec. 2014, doi: 10.1016/j.reactfunctpolym.2014.09.020.

[9] A. Sharma, K. S. Thatai, T. Kuthiala, G. Singh, and S. K. Arya, "Employment of polysaccharides in enzyme immobilization," *React Funct Polym*, vol. 167, p. 105005, Oct. 2021, doi: 10.1016/j.reactfunctpolym.2021.105005.

[10] F. Rafiee, M. Abbaspour, and G. Mohammadi Ziarani, "Immobilization of vitamin B1 on the magnetic dialdehyde starch as an efficient carbene-type support for the copper complexation and its catalytic activity examination," *React Funct Polym*, vol. 170, p. 105106, Jan. 2022, doi: 10.1016/j.reactfunctpolym.2021.105106.

[11] A. Chávez-Salazar, C. I. Álvarez-Barreto, J. D. Hoyos-Leyva, L. A. Bello-Pérez, and F. J. Castellanos-Galeano, "Drying processes of OSA-modified plantain starch trigger changes in its functional properties and digestibility," *LWT*, vol. 154, p. 112846, Jan. 2022, doi: 10.1016/j.lwt.2021.112846.

[12] H.-Y. Kim, S.-J. Ye, and M.-Y. Baik, "Pressure moisture treatment (PMT) of starch, a new physical modification method," *Food Hydrocoll*, vol. 134, p. 108051, Jan. 2023, doi: 10.1016/j.foodhyd.2022.108051.

[13] Y. Luo, Y. Li, L. Li, and X. Xie, "Physical modification of maize starch by gelatinizations and cold storage," *Int J Biol Macromol*, vol. 217, pp. 291–302, Sep. 2022, doi: 10.1016/j.ijbiomac.2022.07.010.

[14] C. Zhang and S.-T. Lim, "Physical modification of various starches by partial gelatinization and freeze-thawing with xanthan gum," *Food Hydrocoll*, vol. 111, p. 106210, Feb. 2021, doi: 10.1016/j.foodhyd.2020.106210.

[15] J. Zhang *et al.*, "Physical modification of waxy maize starch: Combining SDS and freezing/thawing treatments to modify starch structure and functionality," *Food Structure*, vol. 32, p. 100263, Apr. 2022, doi: 10.1016/j.foostr.2022.100263.

[16] M. Shahbazi, M. Majzoobi, and A. Farahnaky, "Physical modification of starch by high-pressure homogenization for improving functional properties of κ-carrageenan/starch blend film," *Food Hydrocoll*, vol. 85, pp. 204–214, Dec. 2018, doi: 10.1016/j.foodhyd.2018.07.017.

[17] J. Wang *et al.*, "Modification in structural, physicochemical, functional, and in vitro digestive properties of kiwi starch by high-power ultrasound treatment," *Ultrason Sonochem*, vol. 86, p. 106004, May 2022, doi: 10.1016/j.ultsonch.2022.106004.

[18] Y. Guo, Y. Cui, M. Cheng, X. Wang, S. Guo, and R. Zhang, "Effects of low-temperature plasma modification on properties of CEO-SBA-15/potato starch film," *Ind Crops Prod*, vol. 187, p. 115440, Nov. 2022, doi: 10.1016/j.indcrop.2022.115440.

[19] A. Dey and N. Sit, "Modification of foxtail millet starch by combining physical, chemical and enzymatic methods," *Int J Biol Macromol*, vol. 95, pp. 314–320, Feb. 2017, doi: 10.1016/j.ijbiomac.2016.11.067.

[20] M. M. Cruz-Benítez, C. A. Gómez-Aldapa, J. Castro-Rosas, E. Hernández-Hernández, E. Gómez-Hernández, and H. A. Fonseca-Florido, "Effect of amylose content and chemical modification of cassava starch on the microencapsulation of Lactobacillus pentosus," *LWT*, vol. 105, pp. 110–117, May 2019, doi: 10.1016/j.lwt.2019.01.069.

[21] K. Sangseethong, N. Termvejsayanon, and K. Sriroth, "Characterization of physicochemical properties of hypochlorite- and peroxide-oxidized cassava starches," *Carbohydr Polym*, vol. 82, no. 2, pp. 446–453, Sep. 2010, doi: 10.1016/j.carbpol.2010.05.003.

[22] Z. Wang, P. Mhaske, A. Farahnaky, S. Kasapis, and M. Majzoobi, "Cassava starch: Chemical modification and its impact on functional properties and digestibility, a review," *Food Hydrocoll*, vol. 129, p. 107542, Aug. 2022, doi: 10.1016/j.foodhyd.2022.107542.

[23] N. Masina *et al.*, "A review of the chemical modification techniques of starch," *Carbohydr Polym*, vol. 157, pp. 1226–1236, Feb. 2017, doi: 10.1016/j.carbpol.2016.09.094.

[24] R. Bhosale and R. Singhal, "Process optimization for the synthesis of octenyl succinyl derivative of waxy corn and amaranth starches," *Carbohydr Polym*, vol. 66, no. 4, pp. 521–527, Nov. 2006, doi: 10.1016/j.carbpol.2006.04.007.

[25] Q. Lin, R. Liang, F. Zhong, A. Ye, and H. Singh, "Interactions between octenyl-succinic-anhydride-modified starches and calcium in oil-in-water emulsions," *Food Hydrocoll*, vol. 77, pp. 30–39, Apr. 2018, doi: 10.1016/j.foodhyd.2017.08.034.

[26] P. Chivero, S. Gohtani, H. Yoshii, and A. Nakamura, "Assessment of soy soluble polysaccharide, gum arabic and OSA-Starch as emulsifiers for mayonnaise-like emulsions," *LWT - Food Science and Technology*, vol. 69, pp. 59–66, Jun. 2016, doi: 10.1016/j.lwt.2015.12.064.

[27] R. Bajaj, N. Singh, and A. Kaur, "Properties of octenyl succinic anhydride (OSA) modified starches and their application in low fat mayonnaise," *Int J Biol Macromol*, vol. 131, pp. 147–157, Jun. 2019, doi: 10.1016/j.ijbiomac.2019.03.054.

[28] S. Y. Cheuk *et al.*, "Nano-encapsulation of coenzyme Q10 using octenyl succinic anhydride modified starch," *Food Chem*, vol. 174, pp. 585–590, May 2015, doi: 10.1016/j.foodchem.2014.11.031.

[29] N. Chiu, A. Tarrega, C. Parmenter, L. Hewson, B. Wolf, and I. D. Fisk, "Optimisation of octinyl succinic anhydride starch stablised w 1 /o/w 2 emulsions for oral destablisation of encapsulated salt and enhanced saltiness," *Food Hydrocoll*, vol. 69, pp. 450–458, Aug. 2017, doi: 10.1016/j.foodhyd.2017.03.002.

[30] A. Marefati, B. Wiege, N. U. Haase, M. Matos, and M. Rayner, "Pickering emulsifiers based on hydrophobically modified small granular starches – Part I: Manufacturing and physico-chemical characterization," *Carbohydr Polym*, vol. 175, pp. 473–483, Nov. 2017, doi: 10.1016/j.carbpol.2017.07.044.

[31] A. Marefati, M. Matos, B. Wiege, N. U. Haase, and M. Rayner, "Pickering emulsifiers based on hydrophobically modified small granular starches Part II – Effects of modification on emulsifying capacity," *Carbohydr Polym*, vol. 201, pp. 416–424, Dec. 2018, doi: 10.1016/j.carbpol.2018.08.049.

[32] F. Ye, M. Miao, B. Jiang, O. H. Campanella, Z. Jin, and T. Zhang, "Elucidation of stabilizing oil-in-water Pickering emulsion with different modified maize starch-based nanoparticles," *Food Chem*, vol. 229, pp. 152–158, Aug. 2017, doi: 10.1016/j.foodchem.2017.02.062.

[33] E. Agama-Acevedo and L. A. Bello-Perez, "Starch as an emulsions stability: the case of octenyl succinic anhydride (OSA) starch," *Curr Opin Food Sci*, vol. 13, pp. 78–83, Feb. 2017, doi: 10.1016/j.cofs.2017.02.014.

[34] D. Morán, G. Gutiérrez, M. C. Blanco-López, A. Marefati, M. Rayner, and M. Matos, "Synthesis of Starch Nanoparticles and Their Applications for Bioactive Compound Encapsulation," *Applied Sciences*, vol. 11, no. 10, p. 4547, May 2021, doi: 10.3390/app11104547.

[35] H. Y. Kim, S. S. Park, and S. T. Lim, "Preparation, characterization and utilization of starch nanoparticles," *Colloids and Surfaces B: Biointerfaces*, vol. 126. Elsevier, pp. 607–620, Feb. 01, 2015. doi: 10.1016/j.colsurfb.2014.11.011.

[36] C. Qiu, C. Wang, C. Gong, D. J. McClements, Z. Jin, and J. Wang, "Advances in research on preparation, characterization, interaction with proteins, digestion and delivery systems of starch-based nanoparticles," *International Journal of Biological Macromolecules*, vol. 152. Elsevier B.V., pp. 117–125, Jun. 01, 2020. doi: 10.1016/j.ijbiomac.2020.02.156.

[37] C. Qiu *et al.*, "Preparation and characterization of essential oil-loaded starch nanoparticles formed by short glucan chains," *Food Chem*, vol. 221, pp. 1426–1433, Apr. 2017, doi: 10.1016/j.foodchem.2016.11.009.

[38] S. H. Mahmoudi Najafi, M. Baghaie, and A. Ashori, "Preparation and characterization of acetylated starch nanoparticles as drug carrier: Ciprofloxacin as a model," *Int J Biol Macromol*, vol. 87, pp. 48–54, Jun. 2016, doi: 10.1016/j.ijbiomac.2016.02.030.

[39] L. Nieto-Suaza, L. Acevedo-Guevara, L. T. Sánchez, M. I. Pinzón, and C. C. Villa, "Characterization of Aloe vera-banana starch composite films reinforced with curcumin-loaded starch nanoparticles," *Food Structure*, vol. 22, p. 100131, Oct. 2019, doi: 10.1016/j.foostr.2019.100131.

[40] L. Nieto-Suaza, L. Acevedo-Guevara, L. T. Sánchez, M. I. Pinzón, and C. C. Villa, "Characterization of Aloe vera-banana starch composite films reinforced with curcumin-loaded starch nanoparticles," *Food Structure*, vol. 22, Oct. 2019, doi: 10.1016/j.foostr.2019.100131.

[41] Y. Fu, J. Yang, L. Jiang, L. Ren, and J. Zhou, "Encapsulation of Lutein into Starch Nanoparticles to Improve Its Dispersity in Water and Enhance Stability of Chemical Oxidation," *Starch/Staerke*, vol. 71, no. 5–6, May 2019, doi: 10.1002/star.201800248.

[42] C. Liu *et al.*, "Adsorption mechanism of polyphenols onto starch nanoparticles and enhanced antioxidant activity under adverse conditions," *J Funct Foods*, vol. 26, pp. 632–644, Oct. 2016, doi: 10.1016/j.jff.2016.08.036.

[43] Y. Ding, Q. Lin, and J. Kan, "Development and characteristics nanoscale retrograded starch as an encapsulating agent for colon-specific drug delivery," *Colloids Surf B Biointerfaces*, vol. 171, pp. 656–667, Nov. 2018, doi: 10.1016/j.colsurfb.2018.08.007.

[44] M. Ahmad, P. Mudgil, A. Gani, F. Hamed, F. A. Masoodi, and S. Maqsood, "Nano-encapsulation of catechin in starch nanoparticles: Characterization, release behavior and bioactivity retention during simulated in-vitro digestion," *Food Chem*, vol. 270, pp. 95–104, Jan. 2019, doi: 10.1016/j.foodchem.2018.07.024.

[45] S. F. Chin, S. C. Pang, and S. H. Tay, "Size controlled synthesis of starch nanoparticles by a simple nanoprecipitation method," *Carbohydr Polym*, vol. 86, no. 4, pp. 1817–1819, Oct. 2011, doi: 10.1016/j.carbpol.2011.07.012.

[46] S. Patel, J. Seet, L. Li, and J. Duhamel, "Detection of Nitroaromatics by Pyrene-Labeled Starch Nanoparticles," *Langmuir*, vol. 35, no. 40, pp. 13145–13156, Oct. 2019, doi: 10.1021/acs.langmuir.9b02371.

[47] P. Vasileva, T. Alexandrova, and I. Karadjova, "Application of Starch-Stabilized Silver Nanoparticles as a Colorimetric Sensor for Mercury(II) in 0.005 mol/L Nitric Acid," *J Chem*, vol. 2017, pp. 1–9, 2017, doi: 10.1155/2017/6897960.

[48] G. Khachatryan and K. Khachatryan, "Starch based nanocomposites as sensors for heavy metals – detection of Cu2+ and Pb2+ ions," *Int Agrophys*, vol. 33, no. 1, pp. 121–126, Feb. 2019, doi: 10.31545/intagr/104414.

[49] M. E. El-Naggar, M. H. El-Rafie, M. A. El-sheikh, G. S. El-Feky, and A. Hebeish, "Synthesis, characterization, release kinetics and toxicity profile of drug-loaded starch nanoparticles," *Int J Biol Macromol*, vol. 81, pp. 718–729, Nov. 2015, doi: 10.1016/j.ijbiomac.2015.09.005.

[50] P. Dandekar *et al.*, "A Hydrophobic Starch Polymer for Nanoparticle-Mediated Delivery of Docetaxel," *Macromol Biosci*, vol. 12, no. 2, pp. 184–194, Feb. 2012, doi: 10.1002/mabi.201100244.

[51] E. Alp, F. Damkaci, E. Guven, and M. Tenniswood, "Starch nanoparticles for delivery of the histone deacetylase inhibitor CG-1521 in breast cancer treatment," *Int J Nanomedicine*, vol. 14, pp. 1335–1346, 2019, doi: 10.2147/ijn.S191837.

[52] Y. Xu *et al.*, "pH-Responsive nanoparticles based on cholesterol/imidazole modified oxidized-starch for targeted anticancer drug delivery," *Carbohydr Polym*, vol. 233, Apr. 2020, doi: 10.1016/j.carbpol.2020.115858.

[53] J. Yang *et al.*, "Fabrication and characterization of hollow starch nanoparticles by gelation process for drug delivery application," *Carbohydr Polym*, vol. 173, pp. 223–232, Oct. 2017, doi: 10.1016/j.carbpol.2017.06.006.

[54] L. Wang *et al.*, "Loading paclitaxel into porous starch in the form of nanoparticles to improve its dissolution and bioavailability," *Int J Biol Macromol*, vol. 138, pp. 207–214, Oct. 2019, doi: 10.1016/j.ijbiomac.2019.07.083.

[55] Ó. Estupiñán *et al.*, "Nano-Encapsulation of Mithramycin in Transfersomes and Polymeric Micelles for the Treatment of Sarcomas," *J Clin Med*, vol. 10, no. 7, p. 1358, Mar. 2021, doi: 10.3390/jcm10071358.

[56] R. Awasthi, A. Roseblade, P. M. Hansbro, M. J. Rathbone, K. Dua, and M. Bebawy, "Nanoparticles in Cancer Treatment: Opportunities and Obstacles," *Curr Drug Targets*, vol. 19, no. 14, pp. 1696–1709, Sep. 2018, doi: 10.2174/1389450119666180326122831.

[57] B. Bahrami *et al.*, "Nanoparticles and targeted drug delivery in cancer therapy," *Immunol Lett*, vol. 190, pp. 64–83, Oct. 2017, doi: 10.1016/j.imlet.2017.07.015.

[58] S. K. Golombek *et al.*, "Tumor targeting via EPR: Strategies to enhance patient responses," *Adv Drug Deliv Rev*, vol. 130, pp. 17–38, May 2018, doi: 10.1016/j.addr.2018.07.007.

[59] F. Asghari, R. Khademi, F. Esmaeili Ranjbar, Z. Veisi Malekshahi, and R. Faridi Majidi, "Application of Nanotechnology in Targeting of Cancer Stem Cells: A Review," *Int J Stem Cells*, vol. 12, no. 2, pp. 227–239, Jul. 2019, doi: 10.15283/ijsc19006.

[60] M. Yüce and H. Kurt, "How to make nanobiosensors: surface modification and characterisation of nanomaterials for biosensing applications," *RSC Adv.*, vol. 7, no. 78, pp. 49386–49403, 2017, doi: 10.1039/C7RA10479K.

[61] M. J. Santander-Ortega *et al.*, "Nanoparticles made from novel starch derivatives for transdermal drug delivery," *Journal of Controlled Release*, vol. 141, no. 1, pp. 85–92, Jan. 2010, doi: 10.1016/j.jconrel.2009.08.012.

[62] J. Yang *et al.*, "Conjugated linoleic acid loaded starch-based emulsion nanoparticles: In vivo gastrointestinal controlled release," *Food Hydrocoll*, vol. 101, Apr. 2020, doi: 10.1016/j.foodhyd.2019.105477.

[63] G. Gutiérrez, D. Morán, A. Marefati, J. Purhagen, M. Rayner, and M. Matos, "Synthesis of controlled size starch nanoparticles (SNPs)," *Carbohydr Polym*, vol. 250, Dec. 2020, doi: 10.1016/j.carbpol.2020.116938.

[64] L. Qi, G. Ji, Z. Luo, Z. Xiao, and Q. Yang, "Characterization and Drug Delivery Properties of OSA Starch-Based Nanoparticles Prepared in [C $_3$ OHmim]Ac-in-Oil Microemulsions System," *ACS Sustain Chem Eng*, vol. 5, no. 10, pp. 9517–9526, Oct. 2017, doi: 10.1021/acssuschemeng.7b02727.

[65] S. Jiang, L. Dai, Y. Qin, L. Xiong, and Q. Sun, "Preparation and Characterization of Octenyl Succinic Anhydride Modified Taro Starch Nanoparticles," *PLoS One*, vol. 11, no. 2, p. e0150043, Feb. 2016, doi: 10.1371/journal.pone.0150043.

[66] Q. Wang *et al.*, "Effects of octenyl succinylation on the properties of starches with distinct crystalline types and their Pickering emulsions," *Int J Biol Macromol*, vol. 230, p. 123183, Mar. 2023, doi: 10.1016/j.ijbiomac.2023.123183.

[67] M. Ahmad, A. Gani, ifra Hassan, Q. Huang, and H. Shabbir, "production and characterization of starch nanoparticles by mild alkali hydrolysis and ultra-sonication process," 2020, doi: 10.1038/s41598-020-60380-0.

[68] B. Zhang, Q. Huang, F. X. Luo, X. Fu, H. Jiang, and J. L. Jane, "Effects of octenylsuccinylation on the structure and properties of high-amylose maize starch," *Carbohydr Polym*, vol. 84, no. 4, pp. 1276–1281, Apr. 2011, doi: 10.1016/j.carbpol.2011.01.020.

[69] S. Liang, Y. Hong, Z. Gu, L. Cheng, C. Li, and Z. Li, "Effect of debranching on the structure and digestibility of octenyl succinic anhydride starch nanoparticles," *LWT*, vol. 141, p. 111076, Apr. 2021, doi: 10.1016/j.lwt.2021.111076.

[70] W. Wang *et al.*, "Properties of OSA-modified starch and emulsion prepared with different materials: Glutinous rice starch, japonica rice starch, and indica rice starch," *Food Research International*, vol. 161, p. 111845, Nov. 2022, doi: 10.1016/j.foodres.2022.111845.

[71] Y. Zhao, N. Khalid, G. Shu, M. A. Neves, I. Kobayashi, and M. Nakajima, "Complex coacervates from gelatin and octenyl succinic anhydride modified kudzu starch: Insights of formulation and characterization," *Food Hydrocoll*, vol. 86, pp. 70–77, Jan. 2019, doi: 10.1016/j.foodhyd.2018.01.040.

[72] W. Zheng, L. Ren, W. Hao, L. Wang, C. Liu, and L. Zheng, "Encapsulation of indole-3-carbinol in Pickering emulsions stabilized by OSA-modified high amylose corn starch: Preparation, characterization and storage stability properties," *Food Chem*, vol. 386, p. 132846, Aug. 2022, doi: 10.1016/j.foodchem.2022.132846.

[73] Q. Lin, R. Liang, F. Zhong, A. Ye, and H. Singh, "Interactions between octenyl-succinic-anhydride-modified starches and calcium in oil-in-water emulsions," *Food Hydrocoll*, vol. 77, pp. 30–39, Apr. 2018, doi: 10.1016/j.foodhyd.2017.08.034.

[74] E. Apostolidis *et al.*, "Production of nanoparticles from resistant starch via a simple three-step physical treatment," *Food Hydrocoll*, vol. 137, p. 108412, Apr. 2023, doi: 10.1016/j.foodhyd.2022.108412.

[75] C. Zhong, S. Luo, R. Xiong, C. Liu, and J. Ye, "A new green self-assembly strategy for preparing curcumin-loaded starch nanoparticles based on natural deep eutectic solvent: Development, characterization and stability," *Food Hydrocoll*, vol. 151, p. 109878, Jun. 2024, doi: 10.1016/j.foodhyd.2024.109878.

[76] K. Wang, L. Cheng, Z. Li, C. Li, Y. Hong, and Z. Gu, "The degree of substitution of OSA-modified starch affects the retention and release of encapsulated mint flavour," *Carbohydr Polym*, vol. 294, p. 119781, Oct. 2022, doi: 10.1016/j.carbpol.2022.119781.

[77] F. Kayaci and T. Uyar, "Solid Inclusion Complexes of Vanillin with Cyclodextrins: Their Formation, Characterization, and High-Temperature Stability," *J Agric Food Chem*, vol. 59, no. 21, pp. 11772–11778, Nov. 2011, doi: 10.1021/jf202915c.

[78] D. F. Montoya-Yepes, A. A. Jiménez-Rodríguez, A. E. Aldana-Porras, L. F. Velásquez-Holguin, J. J. Méndez-Arteaga, and W. Murillo-Arango, "Starches in the encapsulation of plant active ingredients: state of the art and research trends," *Polymer Bulletin*, Feb. 2023, doi: 10.1007/s00289-023-04724-6.

Supplementary material

Table S1. *Protein content of starch granules.*

Type of starch	Sample name	% protein content
Amaranth	A1	0.112±0.030
	A2	0.036±0.001
	A3	0.033±0.001
	A4	0.032±0.001
	A5	0.032±0.004
	A6	0.032±0.004
Quinoa	Q1	0.687±0.001
	Q2	0.570±0.006
	Q3	0.548±0.003
	Q4	0.538±0.004
	Q5	0.547±0.002
	Q6	0.539±0.025
Rice	R1	0.328±0.000
	R2	0.278±0.000
	R3	0.274±0.005
	R4	0.272±0.005
	R5	0.274±0.001
	R6	0.271±0.001

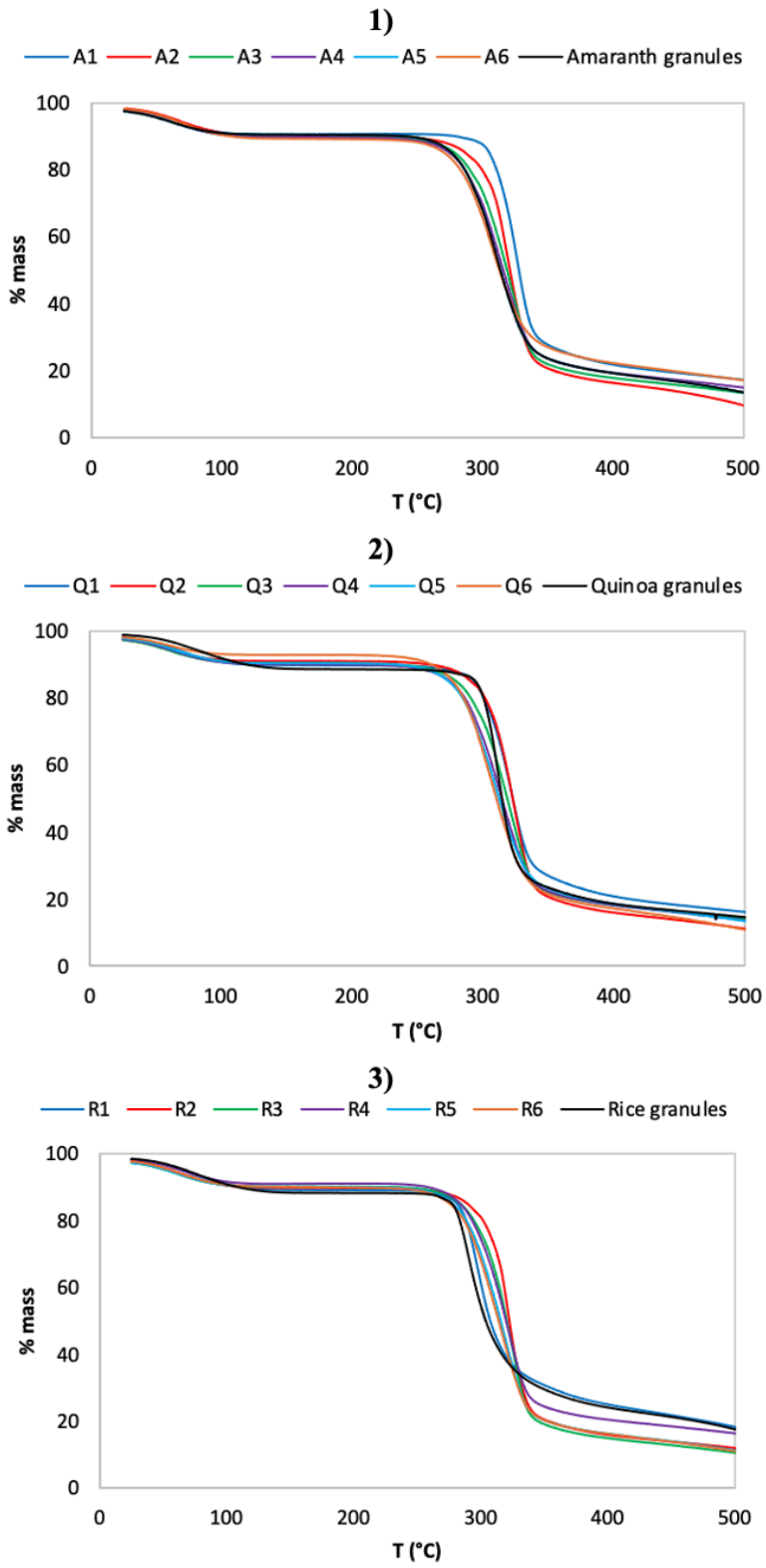

Figure S1. *TGA curves of the three starches and the resulting SNPs synthesized. 1): Amaranth starch; 2): Quinoa starch; 3): Rice starch.*

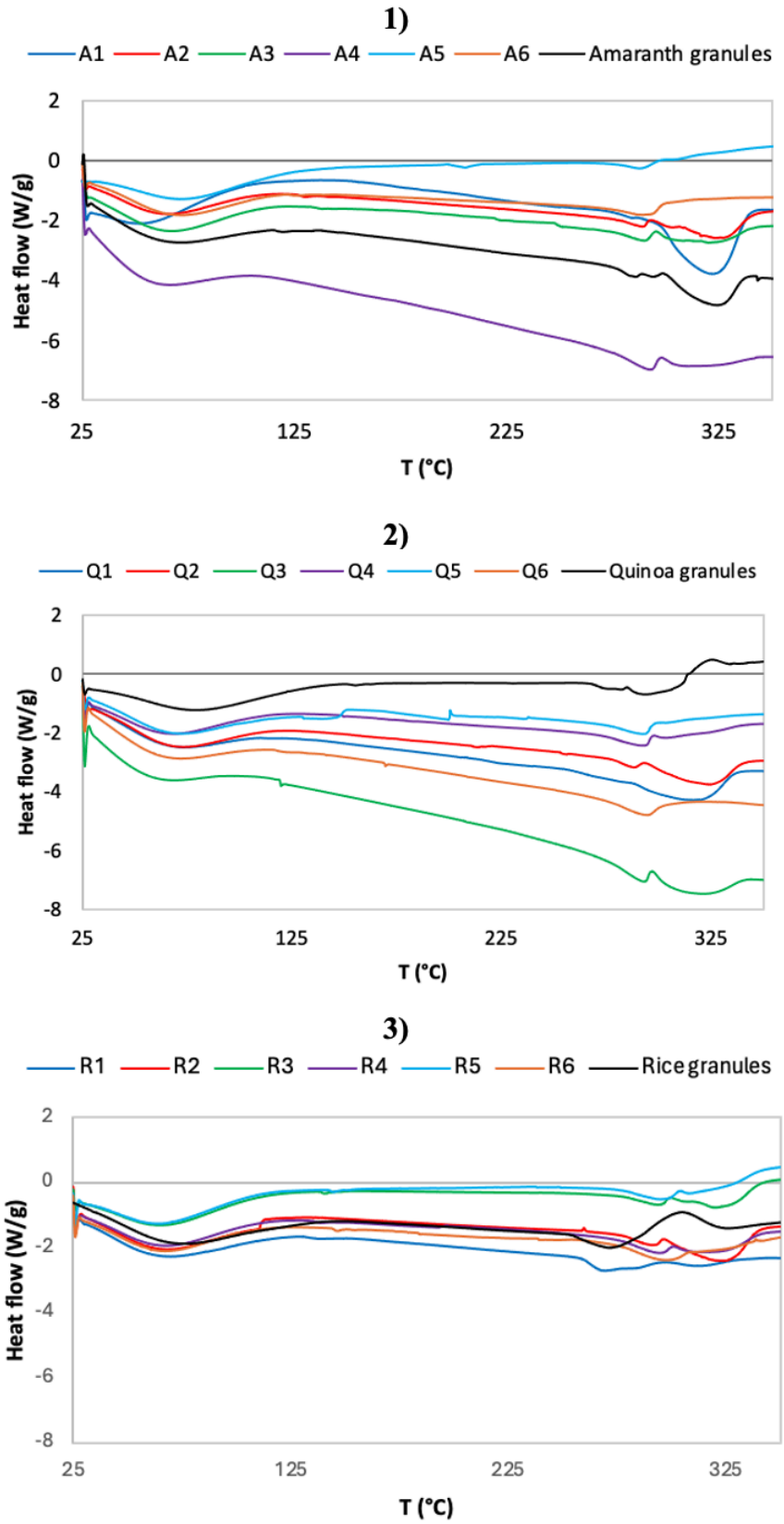

Figure S2. *DSC curves of the three starches and the resulting SNPs synthesized. 1): Amaranth starch; 2): Quinoa starch; 3): Rice starch.*

Table S2. *% of water and mass loss by TGA and DSC for the three starches and the resulting SNPs synthesized.*

Sample name	TGA		DSC
	% H_2O	**% mass**	**% H_2O**
Amaranth granules	7.6	91.6	9.5
A1	7.3	85.9	6.8
A2	8.2	96.1	9.2
A3	8.0	90.4	9.8
A4	7.8	87.7	9.0
A5	6.9	91.4	8.6
A6	9.0	84.9	9.4
Quinoa granules	10	90.1	11.5
Q1	8.1	86.8	9.6
Q2	6.4	94.2	8.7
Q3	6.9	88.8	8.0
Q4	7.4	89.8	9.0
Q5	7.3	90.3	8.3
Q6	5.2	96.0	8.7
Rice granules	10	91.8	12.2
R1	9.0	88.8	9.31
R2	7.8	91.1	12.1
R3	7.0	93.5	9.3
R4	7.2	87.2	8.6
R5	7.1	93.7	8.6
R6	7.5	93.6	8.9

3.2. Starch-silver hybrid nanoparticles: a novel antimicrobial approach

- **Summary**

Starch-silver hybrid nanoparticles were synthesized by a method combining nanoprecipitation and autoclaving. SNPs were used as matrix and stabilising agent for the AgNPs by using native starches from different botanical sources. The hybrid Ag-SNPs were characterized in terms of size, charge, morphology and molecular structure. Quantitative analysis of Ag was also carried out. Spherical SNPs were obtained with all starches with sizes ranging from 82 to 90 nm and neutral charge (zeta potentials around -1 mV). HR-TEM micrographs demonstrated the presence of AgNPs of 5 - 10 nm. FTIR showed AgNPs encapsulation within the SNPs. The antimicrobial activity of the formulations was demonstrated against *E. coli* and *S. aureus* both in solid medium by the diffusion method and in microdilution method. Slightly higher antibacterial activity against *E. coli* was observed. Hybrid amaranth Ag-SNPs with 0.0005 M and 0.001 M of $AgNO_3$ showed log reductions of 4.21 and 4.35 respectively for *S. aureus* and bactericide effect against *E. coli*. Therefore, these hybrid NPs can be considered as sustainable promising nanomaterial with antimicrobial activity.

3.2.1. Introduction

Microbial resistance to antibiotics has become a serious health problem. It is known that more than 70% of bacterial infections show resistance to one or more of the antibiotics commonly used to combat them [1]. In 2019, antimicrobial resistance was declared one of the top 10 public health threats by the World Health Organisation (WHO). Subsequently, in 2022, the Commission and Member States declared it as one of the top three priority health threats. The latest data predict a significant increase in the number of deaths and infections caused by antimicrobial resistance, particularly in healthcare settings [2]. The 2019 annual epidemiological report, based on data reported to the European Antimicrobial Resistance Surveillance Network (EARS-Net), revealed that the most reported bacterial species were *E. coli* (44.2%), followed by *S. aureus* (20.6%), *K. pneumoniae* (11.3%), *E. faecalis* (6.8%), *P. aeruginosa* (5.6%), *S. pneumoniae* (5.3%), *E. faecium* (4.5%) and *Acinetobacter* (1.7%) [3]. In this regard, there is a need to develop and design advanced

materials that allow a more effective use of antibiotics or active ingredients needed to treat different diseases caused by different pathogens.

In recent decades, noble metal-based nanomaterials have been explored for their use in antibacterial applications due to their physicochemical properties [4]. The antimicrobial activity of metals is thought to be due to the ability of metal cations to inhibit enzymes, cause damage to cell membranes and prevent the uptake of vital trace elements by microorganisms [5].

In this sense, the use of AgNPs as antibacterial agents stands out, as they have a high surface-to-volume ratio and exhibit remarkable antimicrobial capacity, even at low concentrations. On the other hand, they are also low cost and exhibit low cytotoxicity and immune response [6].

Although, it has been demonstrated that AgNPs of sizes smaller than 15 nm present antimicrobial activity [7, 8] some authors consider essential the presence of ionic silver on the surface of nanoparticles to obtain their antimicrobial effect. The mechanism of action of these AgNPs as antimicrobial is due to cell membrane adhesion phenomena, but they can also act as Ag ion delivery agents, penetrating inside the bacteria and releasing them over time [9]. These released ions can stop bacteria growth by binding to the proteins in their membranes and walls, also making these membranes more permeable and damaging their bacterial envelope [10].

Nevertheless, one of the most worrying factors in the use of AgNPs in bio-applications is the toxicological effect they may have on human health. This is because, due to their small size, they are able to cross the defence barriers of microorganisms and can induce toxic effects due to their accumulation [11]. On the other hand, considering that another of their applications may be their inclusion in dermo-cosmetic formulations or even in surgical prostheses, these AgNPs may be susceptible to penetrate the skin barrier and have possible toxicological effects [12].

In this respect, a coating of AgNPs could have a positive effect on their toxicity, reducing or even preventing their cytotoxic effects and, in turn, increasing their antimicrobial capacity [11]. The use of polymeric matrices as coating agents is highlighted because they can be easily designed according to the required application. For this purpose, the use of different polymers such as chitosan, cyclodextrins or starch has been reported, as their hydroxyl groups can form complexes with metal ions and allow control over the size, shape and dispersion of the nanoparticles [13, 14].

Recent studies have reported the use of starch as a stabilizing agent in the synthesis of AgNPs [15-17]. However, the use of native starch is limited due to its high retrogradation tendency [18], low solubility in cold water or low emulsifying ability [19]. Therefore, nanometric modification of starch would combine both the advantages of starch (low cost, bioavailability, environmentally friendly) and those of nanoparticles (unique surface area or reactivity and controlled size and shape) [20]. In this context, the use of SNPs as biocomposite bulking agents is well known [21].

To our knowledge, there are no studies on the use of SNPs as loading agents for AgNPs, therefore this work aims to report on the use, characterization and analyses of antimicrobial properties of SNPs as stabilizing and carrier matrix for AgNPs.

The hybrid Ag-SNPs were characterised in terms of size, shape and charge and the concentration of Ag in the formulations was determined. Their molecular structure was also evaluated, and the encapsulation of the AgNPs within the SNPs was also confirmed. Finally, the antimicrobial activity of the formulations was tested by the agar diffusion method and in liquid growth media against *E. coli* and *S. aureus,* both pathogens, to compare the Ag-SNPs effectiveness against gram-positive and gram-negative bacteria.

3.2.2. Materials

Native starches from different botanical sources (amaranth, quinoa and rice grains, with 20.90%, 20.95% and 4.43% amylose content, respectively) were used in this work as reductor agent. They were isolated according to a previous study [22]. Silver nitrate ($AgNO_3$) at 99% (Sigma Aldrich, USA), was used as the precursor for the AgNPs. Milli-Q water was used to prepare the aqueous solutions and absolute ethanol (Sigma Aldrich, USA) was used as the organic phase to synthesize the SNPs and to wash the hybrid NPs. *E. coli* (CECT 434, ATCC 25922) and *S. aureus* (CECT 86, ATCC 12600) strains were provided by the Spanish Type Culture Collection (Valencia, Spain) and were stored in Tryptone Soy Broth (TSB) (Scharlab, Spain) with 20% glycerol at -80 ºC until needed. The stock culture was maintained by regular subculture at 4ºC on Tryptone Soy Agar (TSA) (Scharlab, Spain). For the antimicrobial activity test by the agar diffusion method, LB Broth with agar (Scharlab, Spain) was used for *E. coli* and Mueller-Hinton Agar (MHA) (Scharlab, Spain) for *S. aureus*. For the experiments in liquid medium Mueller-Hinton Broth (MHB)

(Scharlab, Spain) and MHA were used for both strains. Peptone water was also used in both antimicrobial experiments. Culture media were purchased by Scharlab (Spain).

3.2.3. Synthesis of hybrid Ag-SNPs

The synthesis of the hybrid NPs was performed in two steps. First, the synthesis of the AgNPs was carried out following a process similar to that reported by Mohanty et al. [14]. An aqueous phase was prepared by injecting 1 mL of a 2.52 M $AgNO_3$ solution into a 1% starch solution (0.05 g of starch in 5 mL of Milli-Q water, which was dissolved at 80°C for 30 min with constant stirring at 1000 rpm). This aqueous phase was autoclaved at 1.5 bar pressure, 121 °C for 15 min. The solution turned brownish indicating the formation of AgNPs.

Next, the synthesis of the Ag-SNPs was carried out according to the study carried out by Gutiérrez et al. [23] with slight variations, 3 mL of this aqueous phase was injected in 20 mL of absolute ethanol (at 12 mL/h) to precipitate the starch in the form of nanoparticles obtaining this way the hybrid Ag-SNPs. This process is schematized in Figure 3.7.

Once the hybrid Ag-SNPs were synthesized, they were washed before characterization. First, the samples were centrifuged for 10 min at 15880 g at room temperature. The supernatant was removed, the Ag-SNPs were obtained as pellets and restored with absolute ethanol. This washing process was repeated twice. Finally, the NPs were dried in a heater at 80 °C for 24 h.

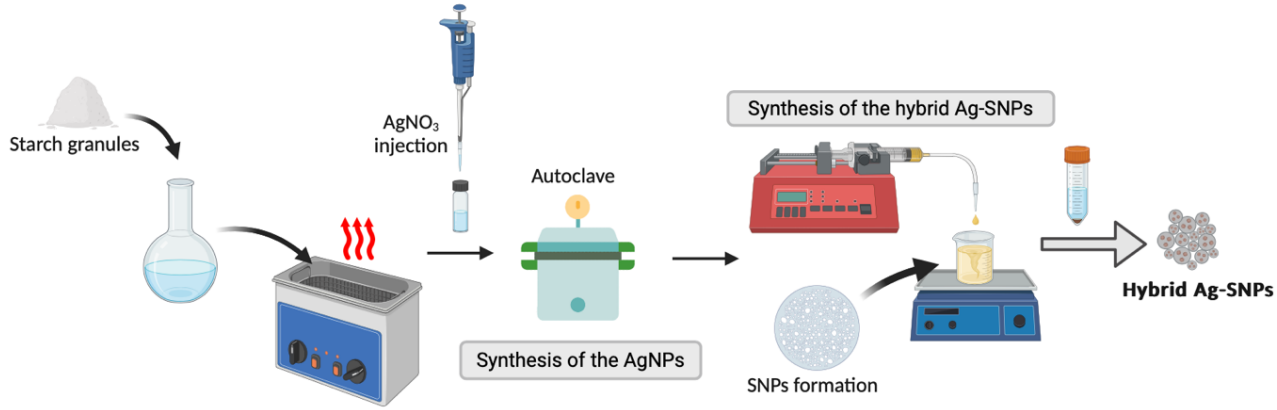

Figure 3.7. *Schematic representation of hybrid Ag-SNPs synthesis. Created with BioRender.com*

3.2.4. Hybrid NPs characterization

The size distribution and zeta potential of the hybrid NPs were determined by DLS using a Zetasizer Nano ZS instrument (Malvern Instruments Ltd, Malvern, UK).

The morphology was analyzed using a JEOL JSM-5600 field emission SEM with Energy dispersive X-Ray (EDX) microanalysis, determining qualitatively the presence of Ag in the samples. The samples were coated with a gold layer in a Balzers SCD 005 sputtering device (Bal-Tec AG, Liechtenstein) prior to analysis to avoid electrical charge accumulation under the electron beam in the microscope.

The morphology of the samples was also analyzed by TEM with negative staining using a JEOL 1011 TEM and a HR-TEM (JEOL-JEM 2100F). In both cases, the samples were placed on grids covered with carbon paper and dyed with a phosphotungstic acid (2% w/v) aqueous solution to obtain negative contrast and correct visualization.

FTIR was used to determine the molecular structure of the hybrid Ag-SNPs and to determine whether the AgNPs were encapsulated within the SNPs. Spectra were acquired on a Fourier transform infrared spectrophotometer (Varian 620-IR) at room temperature and recorded between 650-4000 cm^{-1} (mid-infrared band).

Finally, quantitative analysis of Ag was performed by ICP-MS using a quadrupole mass spectrometer with collision cell (Agilent HP 7500c). Previously, the solid samples were digested in a microwave oven equipped with Teflon containers (Ethos One).

3.2.5. Antimicrobial activity test in solid medium

A modification of Kirby-Bauer antibiotic testing or disk diffusion antibiotic was employed to determine the antimicrobial activity of hybrid Ag-SNPs against *E. coli* and *S. aureus* [24]. Prior to the start antimicrobial analyses, a loopful of each strain was transferred to tubes with 10 mL of TSB and incubated overnight at 37ºC to obtain a fresh culture (10^8 colony forming units/mL). Bacterial inoculum (100 µL) was spread on Petri dishes with approximately 15 mL of solidified nutrient LB agar for *E. coli* and MHA for *S. aureus*. Formulations (25 µL, at a $AgNO_3$ concentration of 0.001 M), including only SNPs dissolved in water as negative control and only 0.001 M $AgNO_3$ as positive control, were added and allowed to dry. Petri dishes were incubated

at 37 °C overnight. After incubation time, the diameter of the resulting inhibition zones was measured. The experiment was carried out in triplicate.

3.2.6. Antimicrobial activity test in liquid growth medium

Amaranth starch-hybrid Ag-SNPs antimicrobial activity was also tested in liquid medium against *E. coli* and *S. aureus*. Quinoa and rice starch-hybrid Ag-SNPs were not tested as their low solubility prevented their complete dissolution and therefore their use in these experiments. Bacterial inoculum (100 µL) incubated at 37 ºC overnight was placed on 10 mL of temperate TSB and was kept at 37 °C until reach the exponential growth phase (absorbance of 0.18 at 595 nm). Afterward, 10 µL of bacteria were inoculated into each well of a sterile 96-well microplate containing 290 µL of the native amaranth starch (NAS) hybrid NPs dissolved in MHB (at a concentration of 0.0005 M and 0.001 M) and MHB without NPs was also used as a control. Samples were incubated at 37 ºC overnight. Serial dilutions with peptone water were made and 100 µL of each was plated on Petri dishes with approximately 15 mL of MHA culture medium. Colonies were counted after incubation at 37 ºC overnight. Experiments were performed in triplicate and results are presented as log reduction.

3.2.7. Results and discussion

3.2.7.1. Hybrid Ag-SNPs characterization

Hybrid Ag-SNPs were synthesized using native starches from amaranth, quinoa and rice grains and their final size, shape and surface charge were determined. The stability of the AgNPs was determined beforehand and as mentioned above, a colour change in the solution into brownish indicates their formation. Figure 3.8 (A) shows a comparison of the AgNPs obtained with the three starches immediately after being autoclaved. The AgNPs have indeed been synthesized and further stabilized by starch by comparing to the Ag precipitate that appeared after the same process in the absence of starch.

On the other hand, Figure 3.8 (B) shows the same samples after being precipitated in ethanol to produce the hybrid Ag-SNPs. It can also be seen that the AgNPs are still stable, although they have lost some of their brownish colour, presumably being encapsulated by the SNPs.

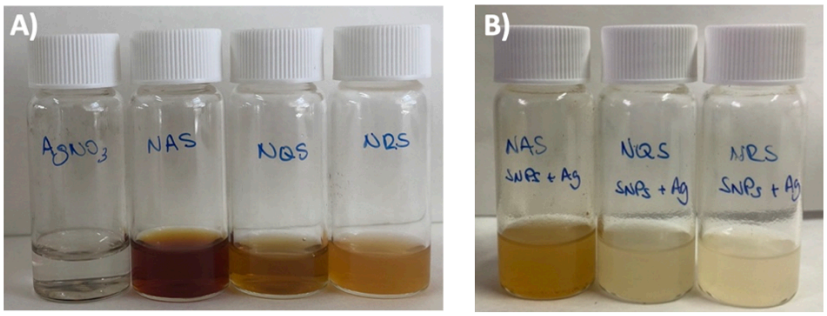

Figure 3.8. *Stability of AgNPs with the three starches before and after Ag-SNPs precipitation.*

The average size of the hybrid NPs synthesized with amaranth starch was 82.8±15.1 nm with a size range between 62.5 nm and 128.6 nm, with quinoa starch the average size was 89.8±17.9 nm with a size range between 62.5 nm and 140.2 nm and with rice starch the average size was 82.3±13.9 nm with a size range between 61.9 nm and 120.5 nm. Zeta potential values of hybrid materials were -1.23 mV, -1.46 mV and -1.81 mV for amaranth, quinoa and rice complexes respectively. These neutral zeta potential values indicates that the AgNPs were entrapped in the SNPs as the zeta potential value of the AgNPs is around -50 mV and the fact that it was reduced to almost -1 mV in all cases would indicate that there is something coating the AgNPs.

SEM micrographs showed the spherical shape of the particles in each case (Figure 3.9). At the same time, EDX microanalysis revealed the peaks corresponding to Ag, demonstrating its presence in the samples. However, this semi-quantitative analysis showed more Ag in the amaranth starch than in the quinoa and rice starches. The final concentration of Ag in the samples was determined quantitative and precisely by ICP-MS, giving a final concentration of $6.1x10^6$ ppb for amaranth starch, $5.5x10^6$ ppb for quinoa starch and $4.5x10^6$ ppb for rice starch. These low values are expected because of the washing procedure after the synthesis. However, this washing step is essential to remove unreacted dissolved starch and free Ag so as not to interfere with the results of subsequent characterisation, although there is always a risk of losing some of the synthesized particles along with the remaining starch and Ag.

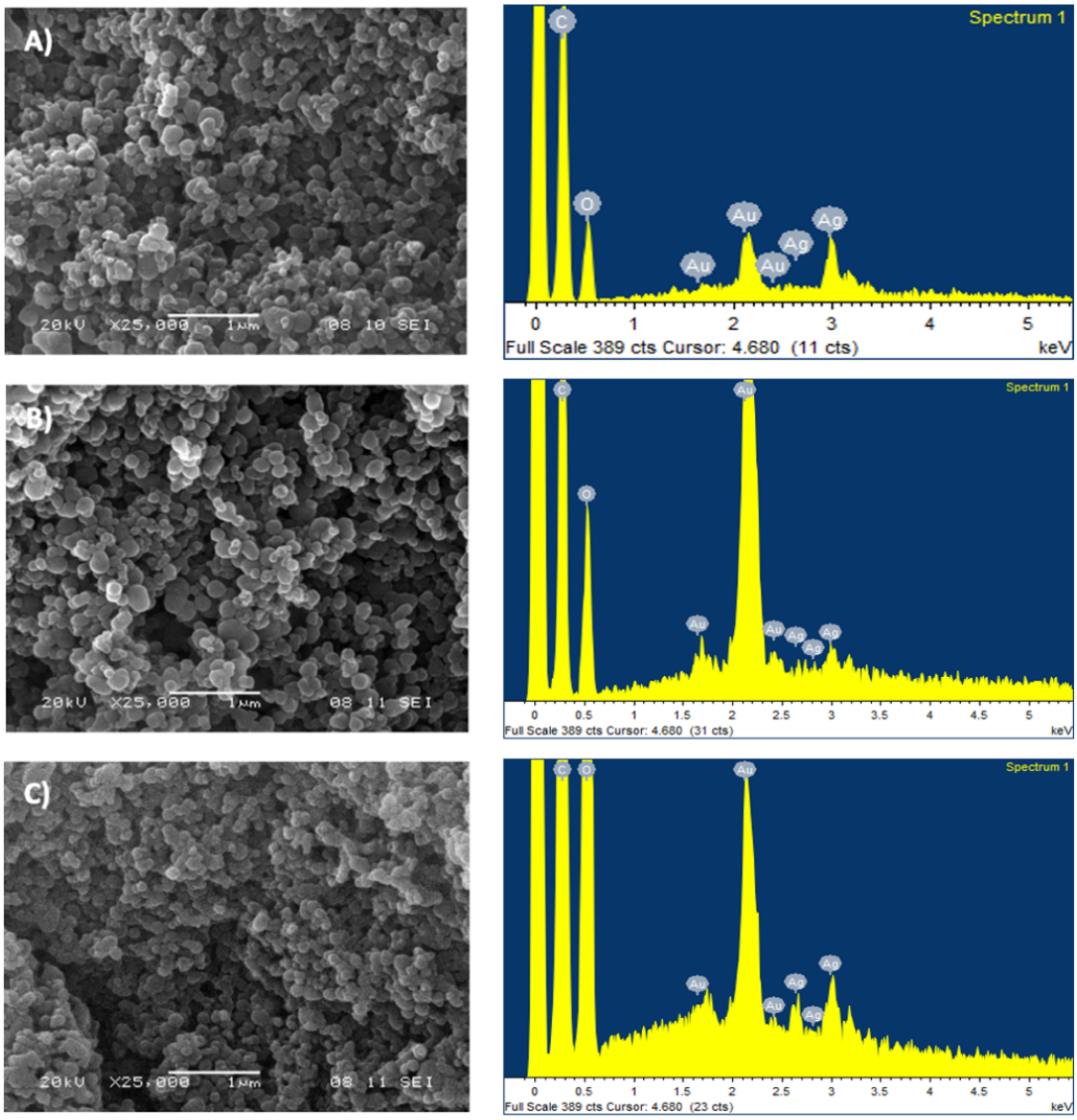

Figure 3.9. *SEM micrographs and EDX microanalysis spectra of the hybrid Ag-SNPs with the three starches: (A) amaranth, (B) quinoa and (C) rice starch.*

TEM micrographs confirmed spherical Ag-SNPs over a wide size range (Figure 3.10-1). Compared to previous studies [25], the dark color of the SNPs observed can be produced by the presence of Ag encapsulated. On the other hand, as AgNPs cannot be easily identified due to their small size at maximum TEM magnification, HR-TEM was successfully used for this purpose (Figure 3.10-2). Small AgNPs were clearly identified with mean sizes of around 5-10 nm.

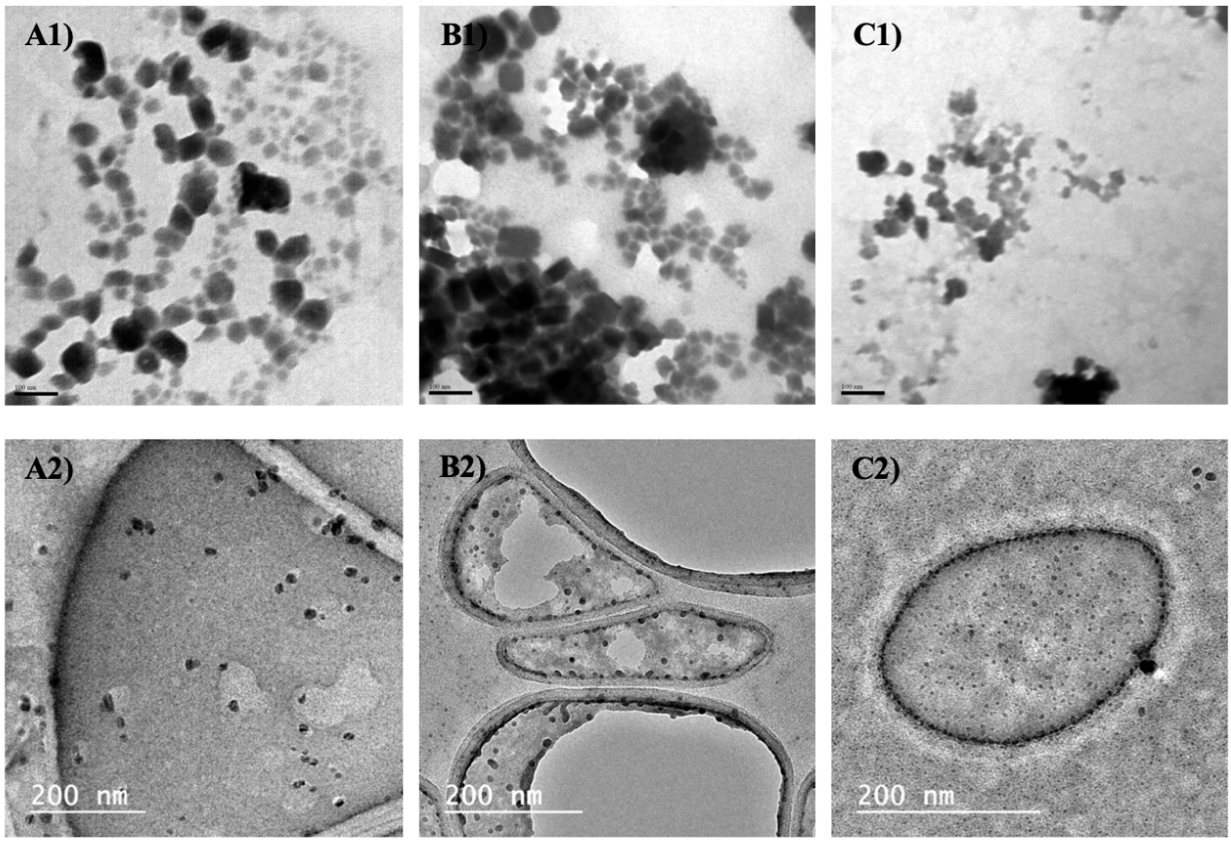

Figure 3.10. *TEM and HR-TEM micrographs of the hybrid Ag-SNPs with the three starches: (A) amaranth, (B) quinoa and (C) rice starch.*

Figure 3.11 below shows FTIR spectra of the samples. The spectra of the precipitated Ag^0 in the absence of starch after autoclave showed an intense absorption band around 1290 cm^{-1}, which is characteristic of the nitrate ion, precursor of the synthesized AgNPs [26]. On the other hand, the spectra of the SNPs and the hybrid Ag-SNPs are practically identical, confirming that the Ag was encapsulated. In both spectra, the characteristic peaks of starch were observed, at 3300 cm^{-1}, 2900 cm^{-1} and 1600 cm^{-1}, according to previous studies [27].

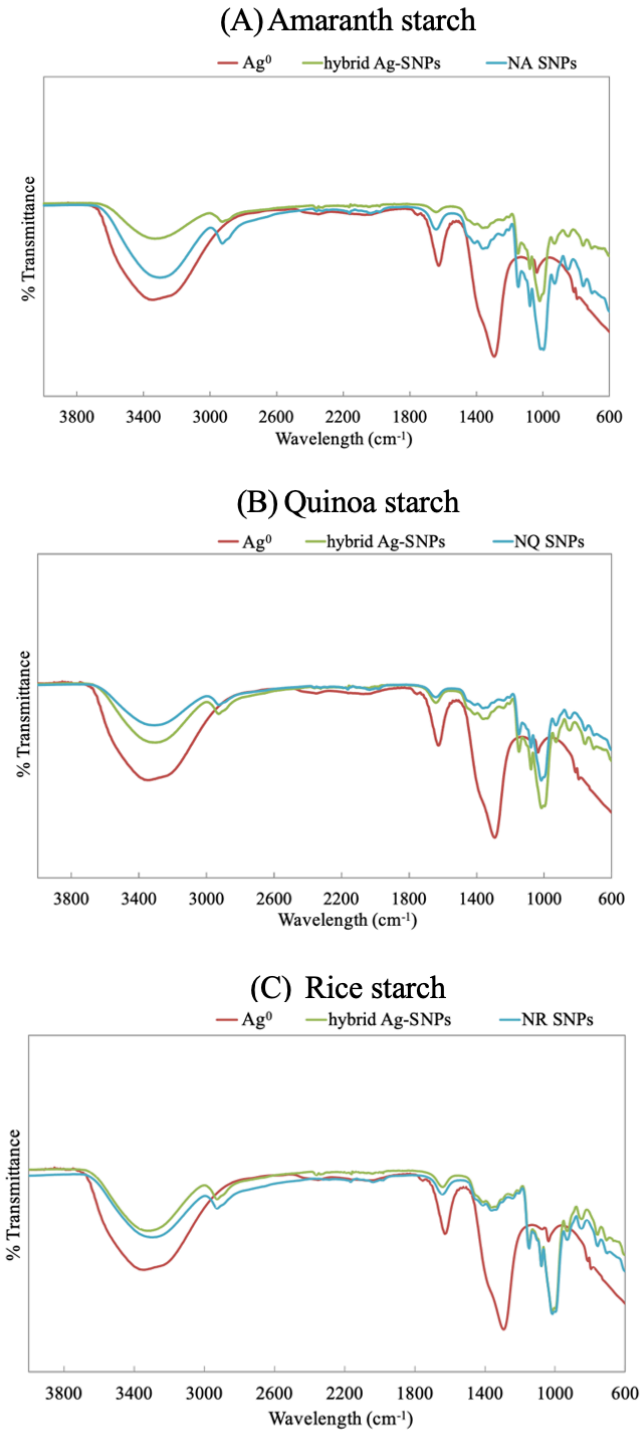

Figure 3.11. *FTIR spectra of Ag0, SNPs and the hybrid Ag-SNPs with the three starches: (A) amaranth, (B) quinoa and (C) rice starch.*

3.2.7.2. Evaluation of antimicrobial activity in solid medium

The antimicrobial activity of the hybrid Ag-SNPs against *E. coli* (gram-negative) and *S. aureus* (gram-positive) was determined by the agar diffusion method. The activity of the hybrid Ag-SNPs

synthesized using NAS, native quinoa starch (NQS) and native rice starch (NRS) at 0.001 M concentration, 0.001 M $AgNO_3$ used as positive control and SNPs used as negative control were compared. Antibiograms obtained for both microorganisms are shown in Figure 3.12.

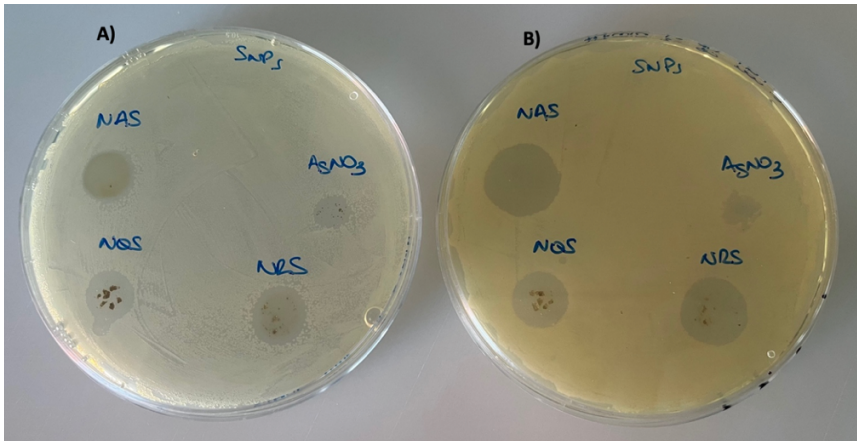

Figure 3.12. *Antimicrobial activity of hybrid Ag-SNPs against A) S. aureus and B) E. coli by agar diffusion method at 0.001 M concentration.*

As it can be seen, the zone where the SNPs were placed has no inhibition halo in any of the cases, as the starch on its one has no antimicrobial activity. The other areas showed clear inhibition zones, both those with $AgNO_3$ and those with hybrid Ag-SNPs but greater inhibition halos were clearly obtained with the last ones. The diameter of the halos has been measured and they are shown in Table 3.2.

Table 3.2. *Diameter of inhibitory zones of the formulations against E. coli and S. aureus by the agar diffusion method.*

Formulation	*S. aureus* (cm)	*E. coli* (cm)
SNPs	-	-
$AgNO_3$	0.9	0.9
NAS	1.2	1.8
NQS	1.1	1.3
NRS	1.2	1.5

It can be noted that all formulations had slightly higher antibacterial activity against *E. coli* than against *S. aureus*. This can be due to the difference in the structure of both microorganisms. *S. aureus* presents a more effective defense system than *E. coli* as the cell walls of gram-positive

bacteria have a thicker peptidoglycan layer than gram-negative bacteria, and this layer would therefore have a greater capacity to protect the cell against the penetration of Ag ions and AgNPs [9, 28].

3.2.7.3. Evaluation of antimicrobial activity in liquid growth medium

Antimicrobial activity in liquid medium was also tested against *E. coli* and *S. aureus* with NAS hybrid NPs. NQS and NRS were not tested because their solubility was not high enough to dissolve completely and therefore cannot be used in these experiments. Table 3.3 shows the antimicrobial activity of amaranth hybrid Ag-SNPs against both bacteria at 0.0005 M and 0.001 M concentrations.

Table 3.3. *Amaranth hybrid Ag-SNPs antimicrobial activity against E. coli and S. aureus at 0.0005 M and 0.001 M concentrations in liquid growth medium.*

	bacterial count (log CFU/mL)	
	E. coli	*S. aureus*
control	9.38±0.08	8.94±0.10[a]
0.0005 M	-	4.73±0.32[b]
0.001 M	-	4.59±0.16[b]

**Values within a column followed by a different lower-case letter are significantly different from each other (Tukey's adjusted analysis of variance P < 0.05).*

Again, antimicrobial activity was higher for *E. coli* than for *S. aureus*. For *S. aureus* NAS hybrid Ag-SNPs showed log reductions of 4.21 and 4.35 log for 0.0005 M and 0.001 M concentrations, respectively, while for *E. coli* the colony count was zero at both concentrations which indicated an antimicrobial activity of 100%. Therefore, this suggests that these hybrid Ag-SNPs have inhibitory activity against *S. aureus* and bactericidal activity against *E. coli*.

3.2.8. Conclusions

Hybrid Ag-SNPs were successfully synthesized using native amaranth, quinoa and rice starches by a simple method combining nanoprecipitation and autoclaving. The SNPs played a key role in

stabilizing the AgNPs, demonstrating their versatility as matrix and bulking agents. FTIR analysis revealed the presence of AgNPs encapsulated within the SNPs.

The antimicrobial capacity of the formulations in solid and liquid media was demonstrated against *E. coli* and *S. aureus*, with higher efficacy against the former in both cases. Nevertheless, the formulations studied can be considered as a promising material for antibacterial applications both against gram-positive bacteria, as inhibitory agents, and against gram-negative bacteria, as bactericidal agents.

Therefore, these hybrid Ag-SNPs could be novel sustainable nanomaterials susceptible to be used as part of antimicrobial formulations for personal care products, as well as to create antimicrobial surfaces or for food packaging purposes.

- **References**

[1] S. M. Dizaj, F. Lotfipour, M. Barzegar-Jalali, M. H. Zarrintan, and K. Adibkia, "Antimicrobial activity of the metals and metal oxide nanoparticles," *Materials Science and Engineering: C*, vol. 44, pp. 278–284, Nov. 2014, doi: 10.1016/j.msec.2014.08.031.

[2] European Commission, "EU Action on Antimicrobial Resistance." Accessed: May 23, 2024. [Online]. Available: https://health.ec.europa.eu/antimicrobial-resistance/eu-action-antimicrobial-resistance_en#documents

[3] European Centre for Disease Prevention and Control, "Antimicrobial resistance in the EU/EEA (EARS-Net) - Annual Epidemiological Report for 2019." Accessed: May 23, 2024. [Online]. Available: https://www.ecdc.europa.eu/en/publications-data/surveillance-antimicrobial-resistance-europe-2019

[4] Z. Qin *et al.*, "Versatile roles of silver in Ag-based nanoalloys for antibacterial applications," *Coord Chem Rev*, vol. 449, p. 214218, Dec. 2021, doi: 10.1016/j.ccr.2021.214218.

[5] M. Belcheva, G. Georgiev, B. Tsyntsarski, U. Szeluga, and L. Kabaivanova, "Antibacterial properties of metal nanoparticles–incorporated activated carbon composites produced from waste biomass precursor," *Diam Relat Mater*, vol. 141, p. 110545, Jan. 2024, doi: 10.1016/j.diamond.2023.110545.

[6] I. X. Yin, J. Zhang, I. S. Zhao, M. L. Mei, Q. Li, and C. H. Chu, " The Antibacterial Mechanism of Silver Nanoparticles and Its Application in Dentistry ," *Int J Nanomedicine*, vol. Volume 15, pp. 2555–2562, Apr. 2020, doi: 10.2147/IJN.S246764.

[7] J. S. Kim *et al.*, "Antimicrobial effects of silver nanoparticles," *Nanomedicine*, vol. 3, no. 1, pp. 95–101, Mar. 2007, doi: 10.1016/j.nano.2006.12.001.

[8] I. Sondi and B. Salopek-Sondi, "Silver nanoparticles as antimicrobial agent: a case study on E. coli as a model for Gram-negative bacteria," *J Colloid Interface Sci*, vol. 275, no. 1, pp. 177–182, Jul. 2004, doi: 10.1016/j.jcis.2004.02.012.

[9] G. López-Carballo, L. Higueras, R. Gavara, and P. Hernández-Muñoz, "Silver Ions Release from Antibacterial Chitosan Films Containing in Situ Generated Silver Nanoparticles," *J Agric Food Chem*, vol. 61, no. 1, pp. 260–267, Jan. 2013, doi: 10.1021/jf304006y.

[10] B. Tessema, G. Gonfa, S. Mekuria Hailegiorgis, G. A. Workneh, and T. Getachew Tadesse, "Synthesis and evaluation of the anti-bacterial effect of modified silica gel supported silver nanoparticles on E. coli and S. aureus," *Results Chem*, vol. 7, p. 101471, Jan. 2024, doi: 10.1016/j.rechem.2024.101471.

[11] T. Bruna, F. Maldonado-Bravo, P. Jara, and N. Caro, "Silver Nanoparticles and Their Antibacterial Applications," *Int J Mol Sci*, vol. 22, no. 13, p. 7202, Jul. 2021, doi: 10.3390/ijms22137202.

[12] C. Saweres-Argüelles, I. Ramírez-Novillo, M. Vergara-Barberán, E. J. Carrasco-Correa, M. J. Lerma-García, and E. F. Simó-Alfonso, "Skin absorption of inorganic nanoparticles and their toxicity: A review," *European Journal of Pharmaceutics and Biopharmaceutics*, vol. 182, pp. 128–140, Jan. 2023, doi: 10.1016/j.ejpb.2022.12.010.

[13] O. Velgosová, S. Dolinská, and A. Mražíková, "Synergic effect of sodium alginate and Citrus lemon extract on the in-situ synthesis of AgNPs in a polymeric matrix," *Nano-Structures & Nano-Objects*, vol. 28, p. 100795, Oct. 2021, doi: 10.1016/j.nanoso.2021.100795.

[14] S. Mohanty, S. Mishra, P. Jena, B. Jacob, B. Sarkar, and A. Sonawane, "An investigation on the antibacterial, cytotoxic, and antibiofilm efficacy of starch-stabilized silver nanoparticles," *Nanomedicine*, vol. 8, no. 6, pp. 916–924, Aug. 2012, doi: 10.1016/j.nano.2011.11.007.

[15] S. V. Kumar, A. P. Bafana, P. Pawar, A. Rahman, S. A. Dahoumane, and C. S. Jeffryes, "High conversion synthesis of <10 nm starch-stabilized silver nanoparticles using microwave technology," *Sci Rep*, vol. 8, no. 1, p. 5106, Mar. 2018, doi: 10.1038/s41598-018-23480-6.

[16] J. Jung, G. M. Raghavendra, D. Kim, and J. Seo, "One-step synthesis of starch-silver nanoparticle solution and its application to antibacterial paper coating," *Int J Biol Macromol*, vol. 107, pp. 2285–2290, Feb. 2018, doi: 10.1016/j.ijbiomac.2017.10.108.

[17] W. Sapyen, S. Toonchue, N. Praphairaksit, and A. Imyim, "Selective colorimetric detection of Cr(VI) using starch-stabilized silver nanoparticles and application for chromium speciation," *Spectrochim Acta A Mol Biomol Spectrosc*, vol. 274, p. 121094, Jun. 2022, doi: 10.1016/j.saa.2022.121094.

[18] W. Berski *et al.*, "Pasting and rheological properties of oat starch and its derivatives," *Carbohydr Polym*, vol. 83, no. 2, pp. 665–671, Jan. 2011, doi: 10.1016/j.carbpol.2010.08.036.

[19] F. Jiang, C. Du, N. Zhao, W. Jiang, X. Yu, and S. Du, "Preparation and characterization of quinoa starch nanoparticles as quercetin carriers," *Food Chem*, vol. 369, p. 130895, Feb. 2022, doi: 10.1016/j.foodchem.2021.130895.

[20] C. Du, F. Jiang, W. Hu, W. Ge, X. Yu, and S. Du, "Comparison of properties and application of starch nanoparticles optimized prepared from different crystalline starches," *Int J Biol Macromol*, vol. 235, p. 123735, Apr. 2023, doi: 10.1016/j.ijbiomac.2023.123735.

[21] D. Morán, G. Gutiérrez, M. C. Blanco-López, A. Marefati, M. Rayner, and M. Matos, "Synthesis of Starch Nanoparticles and Their Applications for Bioactive Compound

Encapsulation," *Applied Sciences*, vol. 11, no. 10, p. 4547, May 2021, doi: 10.3390/app11104547.

[22] A. Marefati, B. Wiege, N. U. Haase, M. Matos, and M. Rayner, "Pickering emulsifiers based on hydrophobically modified small granular starches – Part I: Manufacturing and physico-chemical characterization," *Carbohydr Polym*, vol. 175, pp. 473–483, Nov. 2017, doi: 10.1016/ j.carbpol.2017.07.044.

[23] G. Gutiérrez, D. Morán, A. Marefati, J. Purhagen, M. Rayner, and M. Matos, "Synthesis of controlled size starch nanoparticles (SNPs)," *Carbohydr Polym*, vol. 250, Dec. 2020, doi: 10.1016/j.carbpol.2020.116938.

[24] A. W. Bauer, W. M. Kirby, J. C. Sherris, and M. Turck, "Antibiotic susceptibility testing by a standardized single disk method.," *Tech Bull Regist Med Technol*, vol. 36, no. 3, pp. 49–52, Mar. 1966.

[25] S. M. Ali Razavi and A. M. Amini, "Starch nanomaterials: a state-of-the-art review and future trends," in *Novel Approaches of Nanotechnology in Food*, Elsevier, 2016, pp. 237–269. doi: 10.1016/B978-0-12-804308-0.00008-X.

[26] E. Ronquillo-de Jesús *et al.*, "Synthesis of silver nanoparticles using aqueous tejocote extracts as reducing and passivating agent," *Ingeniería Agrícola y Biosistemas*, vol. 10, no. 2, pp. 67–75, Dec. 2018, doi: 10.5154/r.inagbi.2017.12.018.

[27] D. Morán, N. Abdul Hadi, M. Schmidt, M. Rayner, G. Gutiérrez, and M. Matos, "Synthesis and characterization of controlled-size starch nanoparticles modified with Short Chain Fatty Acids," *Food Biosci*, vol. 56, p. 103381, Dec. 2023, doi: 10.1016/j.fbio.2023.103381.

[28] M. Rai, A. Yadav, and A. Gade, "Silver nanoparticles as a new generation of antimicrobials," *Biotechnol Adv*, vol. 27, no. 1, pp. 76–83, Jan. 2009, doi: 10.1016/j.biotechadv.2008.09.002.

4. CONCLUSIONES / CONCLUSIONS

CAPÍTULO 4 – Conclusiones

Por tanto, de esta tesis se pueden extraer las siguientes conclusiones:

Síntesis de nanopartículas de almidón

- Tanto el método de nanoprecipitación como el de ME fueron capaces de producir SNPs, pero este último dio un rango más amplio de tamaños. Los tamaños más pequeños se obtuvieron cuando se utilizó almidón de maíz con alto contenido en amilopectina. El tipo de aceite utilizado en el método de ME no influyó en el tamaño final, mientras que el tipo de tensioactivo utilizado fue determinante, ya que se obtuvieron tamaños más pequeños cuando se utilizaron tensioactivos muy hidrofílicos.
- Las SNPs de tamaño controlado se obtuvieron controlando los parámetros clave que afectaban a la formulación de la microemulsión utilizada para el método de síntesis: proporción y composición de los sistemas de microemulsión y el agente precipitante. La versatilidad del método de ME quedó demostrada al sintetizar de manera simultánea SNPs de óxido de hierro con tamaño controlado y propiedades superparamagnéticas.
- Se utilizaron almidones de quinoa y arroz acetilados, propionilados y butirilados con diferentes grados de modificación para sintetizar SNPs de tamaño controlado. Teniendo en cuenta la fuente botánica del almidón y el DS de los diferentes SCFA, se obtuvieron SNPs que oscilaban entre 96 y 170 nm, aunque las SNPs con almidón de arroz dieron lugar a un rango de tamaño más estrecho que las de quinoa. Al mismo tiempo, la modificación de los SCFA no se vio afectada por el método de síntesis. Teniendo en cuenta los beneficios que los SCFA pueden aportar a la salud humana, estas SCFA-SNPs podrían ser de gran interés en muchas aplicaciones en las que se requiere un tamaño y una forma controlados.

Nanopartículas de almidón como nanotransportadores antimicrobianos

- Se sintetizaron SNPs de tamaño y carga controlados mediante el método de nanoprecipitación con almidones de amaranto, quinoa y arroz y con el % óptimo de modificación OSA. Esto puede tener muchas ventajas en diferentes campos e incluso para la posterior bioconjugación en la superficie de las SNPs.

Se sintetizaron con éxito SNPs cargadas de vainillina, lo que confirma la viabilidad del uso de SNPs como nanotransportadores. Además, se demostró la capacidad inhibidora de las formulaciones frente a *E. coli*.

- Las Ag-SNPs híbridas se obtuvieron eficazmente combinando el método de nanoprecipitación con un proceso de autoclave utilizando almidones nativos de amaranto, quinoa y arroz. Se demostró la versatilidad del uso de las SNPs como matriz, ya que actuaron como agentes estabilizadores de las AgNPs.

También se demostró la actividad antimicrobiana de las formulaciones en medios sólidos y líquidos frente a *E. coli* y *S. aureus* con resultados satisfactorios. Las formulaciones pueden utilizarse como inhibidores contra bacterias grampositivas y con fines bactericidas contra bacterias gramnegativas.

CHAPTER 4 – Conclusions

Therefore, the following conclusions can be drawn from this thesis:

Synthesis of starch nanoparticles

- Both nanoprecipitation and ME methods were able to produce SNPs, but the latter gave a wider range of sizes. The smaller sizes were also obtained when waxy maize starch was used. The type of oil used in the ME method did not influence the final size, whereas the type of surfactant used was determinant, as smaller sizes were obtained when very hydrophilic surfactants were used.
- Size-controlled SNPs were obtained by controlling the key parameters that affected the formulation of the microemulsion used for the synthesis method: ratio and composition of the microemulsion systems and the precipitating agent. The versatility of the ME method was demonstrated by the simultaneous synthesis of iron oxide SNPs with controlled size and superparamagnetic properties.
- Acetylated, propionylated and butyrylated quinoa and rice starches with different degrees of modification were used to synthesize size-controlled SNPs. Considering the botanical source of starch and the DS of the different SCFA, SNPs ranging from 96-170 nm were obtained, although SNPs with rice starch resulted in a narrower size range than quinoa. At the same time, the modification of SCFA was not affected by the synthesis method. Considering the benefits that SCFA can provide to human health, these SCFA-SNPs could be of great interest in many applications where a controlled size and shape is required.

Starch nanoparticles as antimicrobial nanocarriers

- SNPs of controlled size and charge were synthesized using the nanoprecipitation method with starches from amaranth, quinoa and rice and with the optimal % OSA modification. This may have many advantages in different fields and even for subsequent bioconjugation on the surface of SNPs.

  Vanillin-loaded SNPs were successfully synthesized, confirming the feasibility of using SNPs as nanocarriers. Furthermore, the inhibitory capacity of the formulations against *E. coli* was demonstrated.

- Hybrid Ag-SNPs were effectively obtained by combining the nanoprecipitation method with an autoclaving process using native starches from amaranth, quinoa and rice. The versatility of using SNPs as matrix agents was demonstrated, as they acted as stabilizing agents for the AgNPs.

  The antimicrobial activity of the formulations was also demonstrated in both solid and liquid media against *E. coli* and *S. aureus* with satisfactory results. The formulations can be used as inhibitors against gram-positive bacteria and for bactericidal purposes against gram-negative bacteria.

5. BIBLIOGRAPHY

Bibliography

A. A. Escobar-Puentes, A. García-Gurrola, S. Rincón, A. Zepeda, and F. Martínez-Bustos, "Effect of amylose/amylopectin content and succinylation on properties of corn starch nanoparticles as encapsulants of anthocyanins," *Carbohydr Polym*, vol. 250, Dec. 2020, doi: 10.1016/j.carbpol.2020.116972.

A. Buléon, P. Colonna, V. Planchot, and S. Ball, "Starch granules: structure and biosynthesis," *Int J Biol Macromol*, vol. 23, no. 2, pp. 85–112, Aug. 1998, doi: 10.1016/S0141-8130(98)00040-3.

A. C. C. Sousa *et al.*, "Starch-based magnetic nanocomposite for targeted delivery of hydrophilic bioactives as anticancer strategy," *Carbohydr Polym*, vol. 264, p. 118017, Jul. 2021, doi: 10.1016/j.carbpol.2021.118017.

A. C. F. Ip, T. H. Tsai, I. Khimji, P. J. J. Huang, and J. Liu, "Degradable starch nanoparticle assisted ethanol precipitation of DNA," *Carbohydr Polym*, vol. 110, pp. 354–359, Sep. 2014, doi: 10.1016/j.carbpol.2014.04.007.

A. Caldonazo, S. L. Almeida, A. F. Bonetti, R. E. L. Lazo, M. Mengarda, and F. S. Murakami, "Pharmaceutical applications of starch nanoparticles: A scoping review," *International Journal of Biological Macromolecules*, vol. 181. Elsevier B.V., pp. 697–704, Jun. 30, 2021. doi: 10.1016/j.ijbiomac.2021.03.061.

A. Chávez-Salazar, C. I. Álvarez-Barreto, J. D. Hoyos-Leyva, L. A. Bello-Pérez, and F. J. Castellanos-Galeano, "Drying processes of OSA-modified plantain starch trigger changes in its functional properties and digestibility," *LWT*, vol. 154, p. 112846, Jan. 2022, doi: 10.1016/j.lwt.2021.112846.

A. Dey and N. Sit, "Modification of foxtail millet starch by combining physical, chemical and enzymatic methods," *Int J Biol Macromol*, vol. 95, pp. 314–320, Feb. 2017, doi: 10.1016/j.ijbiomac.2016.11.067.

A. E. A. H. Mohamed M.E.A., "Pulsed electric fields for food processing technology," *Structure and Function of Food Engineering*, pp. 275–306, 2012.

A. F. K. Minakawa, P. C. S. Faria-Tischer, and S. Mali, "Simple ultrasound method to obtain starch micro- and nanoparticles from cassava, corn and yam starches," *Food Chem*, vol. 283, pp. 11–18, Jun. 2019, doi: 10.1016/j.foodchem.2019.01.015.

A. H. Hashem, M. E. El-Naggar, A. M. Abdelaziz, S. Abdelbary, Y. R. Hassan, and M. S. Hasanin, "Bio-based antimicrobial food packaging films based on hydroxypropyl starch/polyvinyl alcohol loaded with the biosynthesized zinc oxide nanoparticles," *Int J Biol Macromol*, vol. 249, p. 126011, Sep. 2023, doi: 10.1016/j.ijbiomac.2023.126011.

A. Jayakumar *et al.*, "Starch-PVA composite films with zinc-oxide nanoparticles and phytochemicals as intelligent pH sensing wraps for food packaging application," *Int J Biol Macromol*, vol. 136, pp. 395–403, Sep. 2019, doi: 10.1016/j.ijbiomac.2019.06.018.

A. K. Bajpai and R. Gupta, "Magnetically mediated release of ciprofloxacin from polyvinyl alcohol based superparamagnetic nanocomposites," *J Mater Sci Mater Med*, vol. 22, no. 2, pp. 357–369, Feb. 2011, doi: 10.1007/s10856-010-4214-2.

A. K. Jain, R. K. Khar, F. J. Ahmed, and P. V. Diwan, "Effective insulin delivery using starch nanoparticles as a potential trans-nasal mucoadhesive carrier," *European Journal of Pharmaceutics and Biopharmaceutics*, vol. 69, no. 2, pp. 426–435, Jun. 2008, doi: 10.1016/j.ejpb.2007.12.001.

A. Lopez-Rubio, J. M. Clarke, ben Scherer, D. L. Topping, and E. P. Gilbert, "Structural modifications of granular starch upon acylation with short-chain fatty acids," *Food Hydrocoll*, vol. 23, no. 7, pp. 1940–1946, Oct. 2009, doi: 10.1016/j.foodhyd.2009.01.003.

A. M. Shi, D. Li, L. J. Wang, B. Z. Li, and B. Adhikari, "Preparation of starch-based nanoparticles through high-pressure homogenization and miniemulsion cross-linking: Influence of various process parameters on particle size and stability," *Carbohydr Polym*, vol. 83, no. 4, pp. 1604–1610, Feb. 2011, doi: 10.1016/j.carbpol.2010.10.011.

A. Marefati, B. Wiege, N. U. Haase, M. Matos, and M. Rayner, "Pickering emulsifiers based on hydrophobically modified small granular starches – Part I: Manufacturing and physico-chemical characterization," *Carbohydr Polym*, vol. 175, pp. 473–483, Nov. 2017, doi: 10.1016/j.carbpol.2017.07.044.

A. Marefati, M. Matos, B. Wiege, N. U. Haase, and M. Rayner, "Pickering emulsifiers based on hydrophobically modified small granular starches Part II – Effects of modification on emulsifying capacity," *Carbohydr Polym*, vol. 201, pp. 416–424, Dec. 2018, doi: 10.1016/ j.carbpol.2018.08.049.

A. Marinopoulou, E. Papastergiadis, S. N. Raphaelides, and M. G. Kontominas, "Structural characterization and thermal properties of amylose-fatty acid complexes prepared at different temperatures," *Food Hydrocoll*, vol. 58, pp. 224–234, Jul. 2016, doi: 10.1016/j.foodhyd.2016.02.034.

A. N. Dundar and D. Gocmen, "Effects of autoclaving temperature and storing time on resistant starch formation and its functional and physicochemical properties," *Carbohydr Polym*, vol. 97, no. 2, pp. 764–771, Sep. 2013, doi: 10.1016/j.carbpol.2013.04.083.

A. P. Bonto, R. N. Tiozon, N. Sreenivasulu, and D. H. Camacho, "Impact of ultrasonic treatment on rice starch and grain functional properties: A review," *Ultrason Sonochem*, vol. 71, p. 105383, Mar. 2021, doi: 10.1016/j.ultsonch.2020.105383.

A. P. Mathew and A. Dufresne, "Morphological Investigation of Nanocomposites from Sorbitol Plasticized Starch and Tunicin Whiskers," *Biomacromolecules*, vol. 3, no. 3, pp. 609–617, May 2002, doi: 10.1021/bm0101769.

A. Sharma, K. S. Thatai, T. Kuthiala, G. Singh, and S. K. Arya, "Employment of polysaccharides in enzyme immobilization," *React Funct Polym*, vol. 167, p. 105005, Oct. 2021, doi: 10.1016/j.reactfunctpolym.2021.105005.

A. Shi, D. Li, H. Liu, B. Adhikari, and Q. Wang, "Effect of drying and loading methods on the release behavior of ciprofloxacin from starch nanoparticles," *Int J Biol Macromol*, vol. 87, pp. 55–61, Jun. 2016, doi: 10.1016/j.ijbiomac.2016.02.038.

A. W. Bauer, W. M. Kirby, J. C. Sherris, and M. Turck, "Antibiotic susceptibility testing by a standardized single disk method.," *Tech Bull Regist Med Technol*, vol. 36, no. 3, pp. 49–52, Mar. 1966.

A. W. Pacek, P. Ding, and A. T. Utomo, "Effect of energy density, pH and temperature on de-aggregation in nano-particles/water suspensions in high shear mixer," *Powder Technol*, vol. 173, no. 3, pp. 203–210, Apr. 2007, doi: 10.1016/j.powtec.2007.01.006.

A. Yusoff and B. S. Murray, "Modified starch granules as particle-stabilizers of oil-in-water emulsions," *Food Hydrocoll*, vol. 25, no. 1, pp. 42–55, Jan. 2011, doi: 10.1016/j.foodhyd.2010.05.004.

B. Avvaru, M. N. Patil, P. R. Gogate, and A. B. Pandit, "Ultrasonic atomization: Effect of liquid phase properties," *Ultrasonics*, vol. 44, no. 2, pp. 146–158, Feb. 2006, doi: 10.1016/j.ultras.2005.09.003.

B. Bahrami *et al.*, "Nanoparticles and targeted drug delivery in cancer therapy," *Immunol Lett*, vol. 190, pp. 64–83, Oct. 2017, doi: 10.1016/j.imlet.2017.07.015.

B. P. Binks and C. P. Whitby, "Silica Particle-Stabilized Emulsions of Silicone Oil and Water: Aspects of Emulsification," *Langmuir*, vol. 20, no. 4, pp. 1130–1137, Feb. 2004, doi: 10.1021/la0303557.

B. Tessema, G. Gonfa, S. Mekuria Hailegiorgis, G. A. Workneh, and T. Getachew Tadesse, "Synthesis and evaluation of the anti-bacterial effect of modified silica gel supported silver nanoparticles on E. coli and S. aureus," *Results Chem*, vol. 7, p. 101471, Jan. 2024, doi: 10.1016/j.rechem.2024.101471.

B. Zhang, Q. Huang, F. X. Luo, X. Fu, H. Jiang, and J. L. Jane, "Effects of octenylsuccinylation on the structure and properties of high-amylose maize starch," *Carbohydr Polym*, vol. 84, no. 4, pp. 1276–1281, Apr. 2011, doi: 10.1016/ j.carbpol.2011.01.020.

C. Abbati De Assis *et al.*, "Techno-Economic Assessment, Scalability, and Applications of Aerosol Lignin Micro- and Nanoparticles," *ACS Sustain Chem Eng*, vol. 6, no. 9, pp. 11853–11868, Sep. 2018, doi: 10.1021/acssuschemeng.8b02151.

C. Carboni Martins, R. C. Rodrigues, G. Domeneghini Mercali, and E. Rodrigues, "New insights into non-extractable phenolic compounds analysis," *Food Research International*, vol. 157, p. 111487, Jul. 2022, doi: 10.1016/j.foodres.2022.111487.

C. Du, F. Jiang, W. Hu, W. Ge, X. Yu, and S. Du, "Comparison of properties and application of starch nanoparticles optimized prepared from different crystalline starches," *Int J Biol Macromol*, vol. 235, p. 123735, Apr. 2023, doi: 10.1016/j.ijbiomac.2023.123735.

C. Guida, A. C. Aguiar, and R. L. Cunha, "Green techniques for starch modification to stabilize Pickering emulsions: a current review and future perspectives," *Current Opinion in Food Science*, vol. 38. Elsevier Ltd, pp. 52–61, Apr. 01, 2021. doi: 10.1016/j.cofs.2020.10.017.

C. Li, Y. Li, P. Sun, and C. Yang, "Starch nanocrystals as particle stabilisers of oil-in-water emulsions," *J Sci Food Agric*, vol. 94, no. 9, pp. 1802–1807, Jul. 2014, doi: 10.1002/jsfa.6495.

C. Liu *et al.*, "Adsorption mechanism of polyphenols onto starch nanoparticles and enhanced antioxidant activity under adverse conditions," *J Funct Foods*, vol. 26, pp. 632–644, Oct. 2016, doi: 10.1016/j.jff.2016.08.036.

C. Liu, K. Li, X. Li, M. Zhang, and J. Li, "Formation and structural evolution of starch nanocrystals from waxy maize starch and waxy potato starch," *Int J Biol Macromol*, vol. 180, pp. 625–632, Jun. 2021, doi: 10.1016/j.ijbiomac.2021.03.115.

C. Manach, A. Scalbert, C. Morand, C. Rémésy, and L. Jiménez, "Polyphenols: food sources and bioavailability," *Am J Clin Nutr*, vol. 79, no. 5, pp. 727–747, May 2004, doi: 10.1093/ajcn/79.5.727.

C. Qiu, C. Wang, C. Gong, D. J. McClements, Z. Jin, and J. Wang, "Advances in research on preparation, characterization, interaction with proteins, digestion and delivery systems of starch-based nanoparticles," *International Journal of Biological Macromolecules*, vol. 152. Elsevier B.V., pp. 117–125, Jun. 01, 2020. doi: 10.1016/j.ijbiomac.2020.02.156.

C. Qiu *et al.*, "A review of green techniques for the synthesis of size-controlled starch-based nanoparticles and their applications as nanodelivery systems," *Trends in Food Science and Technology*, vol. 92. Elsevier Ltd, pp. 138–151, Oct. 01, 2019. doi: 10.1016/j.tifs.2019.08.007.

C. Qiu *et al.*, "Preparation and characterization of essential oil-loaded starch nanoparticles formed by short glucan chains," *Food Chem*, vol. 221, pp. 1426–1433, Apr. 2017, doi: 10.1016/j.foodchem.2016.11.009.

C. Qiu, Y. Qin, S. Zhang, L. Xiong, and Q. Sun, "A comparative study of size-controlled worm-like amylopectin nanoparticles and spherical amylose nanoparticles: Their characteristics and the adsorption properties of polyphenols," *Food Chem*, vol. 213, pp. 579–587, Dec. 2016, doi: 10.1016/j.foodchem.2016.07.023.

C. Saweres-Argüelles, I. Ramírez-Novillo, M. Vergara-Barberán, E. J. Carrasco-Correa, M. J. Lerma-García, and E. F. Simó-Alfonso, "Skin absorption of inorganic nanoparticles and their toxicity: A review," *European Journal of Pharmaceutics and Biopharmaceutics*, vol. 182, pp. 128–140, Jan. 2023, doi: 10.1016/j.ejpb.2022.12.010.

C. Zhang and S.-T. Lim, "Physical modification of various starches by partial gelatinization and freeze-thawing with xanthan gum," *Food Hydrocoll*, vol. 111, p. 106210, Feb. 2021, doi: 10.1016/j.foodhyd.2020.106210.

C. Zhong, S. Luo, R. Xiong, C. Liu, and J. Ye, "A new green self-assembly strategy for preparing curcumin-loaded starch nanoparticles based on natural deep eutectic solvent: Development,

characterization and stability," *Food Hydrocoll*, vol. 151, p. 109878, Jun. 2024, doi: 10.1016/j.foodhyd.2024.109878.

D. C. Aldao, E. Šárka, P. Ulbrich, and E. Menšiková, "Starch nanoparticles – Two ways of their preparation," *Czech Journal of Food Sciences*, vol. 36, no. 2, pp. 133–138, 2018, doi: 10.17221/371/2017-CJFS.

D. F. Montoya-Yepes, A. A. Jiménez-Rodríguez, A. E. Aldana-Porras, L. F. Velásquez-Holguin, J. J. Méndez-Arteaga, and W. Murillo-Arango, "Starches in the encapsulation of plant active ingredients: state of the art and research trends," *Polymer Bulletin*, Feb. 2023, doi: 10.1007/s00289-023-04724-6.

D. F. Pancu *et al.*, "Antibiotics: Conventional Therapy and Natural Compounds with Antibacterial Activity—A Pharmaco-Toxicological Screening," *Antibiotics*, vol. 10, no. 4, p. 401, Apr. 2021, doi: 10.3390/antibiotics10040401.

D. K. Verma and P. P. Srivastav, "Proximate Composition, Mineral Content and Fatty Acids Analyses of Aromatic and Non-Aromatic Indian Rice," *Rice Sci*, vol. 24, no. 1, pp. 21–31, Jan. 2017, doi: 10.1016/j.rsci.2016.05.005.

D. LeCorre, E. Vahanian, A. Dufresne, and J. Bras, "Enzymatic Pretreatment for Preparing Starch Nanocrystals," *Biomacromolecules*, vol. 13, no. 1, pp. 132–137, Jan. 2012, doi: 10.1021/bm201333k.

D. Le Corre and H. Angellier-Coussy, "Preparation and application of starch nanoparticles for nanocomposites: A review," *React Funct Polym*, vol. 85, pp. 97–120, Dec. 2014, doi: 10.1016/j.reactfunctpolym.2014.09.020.

D. Le Corre, J. Bras, and A. Dufresne, "Starch nanoparticles: A review," *Biomacromolecules*, vol. 11, no. 5. pp. 1139–1153, May 10, 2010. doi: 10.1021/bm901428y.

D. Liu, Q. Wu, H. Chen, and P. R. Chang, "Transitional properties of starch colloid with particle size reduction from micro- to nanometer," *J Colloid Interface Sci*, vol. 339, no. 1, pp. 117–124, Nov. 2009, doi: 10.1016/j.jcis.2009.07.035.

D. Morán, G. Gutiérrez, M. C. Blanco-López, A. Marefati, M. Rayner, and M. Matos, "Synthesis of Starch Nanoparticles and Their Applications for Bioactive Compound Encapsulation," *Applied Sciences*, vol. 11, no. 10, p. 4547, May 2021, doi: 10.3390/app11104547.

D. Morán, N. Abdul Hadi, M. Schmidt, M. Rayner, G. Gutiérrez, and M. Matos, "Synthesis and characterization of controlled-size starch nanoparticles modified with Short Chain Fatty Acids," *Food Biosci*, vol. 56, p. 103381, Dec. 2023, doi: 10.1016/j.fbio.2023.103381.

D. Morán *et al.*, "Bio-based starch nanoparticles with controlled size as antimicrobial agents nanocarriers," *React Funct Polym*, vol. 198, p. 105881, May 2024, doi: 10.1016/j.reactfunctpolym.2024.105881.

D. Morán *et al.*, "Sustainable antibiofilm self-assembled colloidal systems," *Frontiers in Soft Matter*, vol. 2, Nov. 2022, doi: 10.3389/frsfm.2022.1041881.

D. Song, Y. S. Thio, and Y. Deng, "Starch nanoparticle formation via reactive extrusion and related mechanism study," *Carbohydr Polym*, vol. 85, no. 1, pp. 208–214, Apr. 2011, doi: 10.1016/j.carbpol.2011.02.016.

E. Agama-Acevedo and L. A. Bello-Perez, "Starch as an emulsions stability: the case of octenyl succinic anhydride (OSA) starch," *Curr Opin Food Sci*, vol. 13, pp. 78–83, Feb. 2017, doi: 10.1016/j.cofs.2017.02.014.

E. Alp, F. Damkaci, E. Guven, and M. Tenniswood, "Starch nanoparticles for delivery of the histone deacetylase inhibitor CG-1521 in breast cancer treatment," *Int J Nanomedicine*, vol. 14, pp. 1335–1346, 2019, doi: 10.2147/IJN.S191837.

E. Apostolidis *et al.*, "Production of nanoparticles from resistant starch via a simple three-step physical treatment," *Food Hydrocoll*, vol. 137, p. 108412, Apr. 2023, doi: 10.1016/j.foodhyd.2022.108412.

E. Aytunga, A. Arık Kibar, İ. Gönenç, and F. Us, "Gelatinization of waxy, normal and high amylose corn starches" *the journal of food*, May 2009.

E. Kristo and C. Biliaderis, "Physical properties of starch nanocrystal-reinforced pullulan films," *Carbohydr Polym*, vol. 68, no. 1, pp. 146–158, Mar. 2007, doi: 10.1016/j.carbpol.2006.07.021.

E. M. Materón *et al.*, "Magnetic nanoparticles in biomedical applications: A review," *Applied Surface Science Advances*, vol. 6, p. 100163, Dec. 2021, doi: 10.1016/j.apsadv.2021.100163.

E. Medeiros, A. Dufresne, and W. Orts, "Starch-based nanocomposites," in *Starches*, CRC Press, 2009, pp. 205–251. doi: 10.1201/9781420080247-c9.

E. Ronquillo-de Jesús *et al.*, "Synthesis of silver nanoparticles using aqueous tejocote extracts as reducing and passivating agent," *Ingeniería Agrícola y Biosistemas*, vol. 10, no. 2, pp. 67–75, Dec. 2018, doi: 10.5154/r.inagbi.2017.12.018.

European Centre for Disease Prevention and Control, "Antimicrobial resistance in the EU/EEA (EARS-Net) - Annual Epidemiological Report for 2019." Accessed: May 23, 2024. [Online]. Available: https://www.ecdc.europa.eu/en/publications-data/surveillance-antimicrobial-resistance-europe-2019

European Commission, "EU Action on Antimicrobial Resistance." Accessed: May 23, 2024. [Online]. Available: https://health.ec.europa.eu/antimicrobial-resistance/eu-action-antimicrobial-resistance_en#documents

F. A. Santos *et al.*, "Systematic review of antiprotozoal potential of antimicrobial peptides," *Acta Trop*, vol. 236, p. 106675, Dec. 2022, doi: 10.1016/j.actatropica.2022.106675.

F. Asghari, R. Khademi, F. Esmaeili Ranjbar, Z. Veisi Malekshahi, and R. Faridi Majidi, "Application of Nanotechnology in Targeting of Cancer Stem Cells: A Review," *Int J Stem Cells*, vol. 12, no. 2, pp. 227–239, Jul. 2019, doi: 10.15283/ijsc19006.

F. Barreras, H. Amaveda, and A. Lozano, "Transient high-frequency ultrasonic water atomization," *Exp Fluids*, vol. 33, no. 3, pp. 405–413, 2002, doi: 10.1007/s00348-002-0456-1.

F. G. Torres and G. E. De-la-Torre, "Synthesis, characteristics, and applications of modified starch nanoparticles: A review," *Int J Biol Macromol*, vol. 194, pp. 289–305, Jan. 2022, doi: 10.1016/j.ijbiomac.2021.11.187.

F. Jiang, C. Du, N. Zhao, W. Jiang, X. Yu, and S. Du, "Preparation and characterization of quinoa starch nanoparticles as quercetin carriers," *Food Chem*, vol. 369, p. 130895, Feb. 2022, doi: 10.1016/j.foodchem.2021.130895.

F. Kayaci and T. Uyar, "Solid Inclusion Complexes of Vanillin with Cyclodextrins: Their Formation, Characterization, and High-Temperature Stability," *J Agric Food Chem*, vol. 59, no. 21, pp. 11772–11778, Nov. 2011, doi: 10.1021/jf202915c.

F. Rafiee, M. Abbaspour, and G. Mohammadi Ziarani, "Immobilization of vitamin B1 on the magnetic dialdehyde starch as an efficient carbene-type support for the copper complexation and its catalytic activity examination," *React Funct Polym*, vol. 170, p. 105106, Jan. 2022, doi: 10.1016/j.reactfunctpolym.2021.105106.

F. Saeed, M. Afzaal, T. Tufail, and A. Ahmad, "Use of Natural Antimicrobial Agents: A Safe Preservation Approach," in *Active Antimicrobial Food Packaging*, IntechOpen, 2019. doi: 10.5772/intechopen.80869.

F. Ye, M. Miao, B. Jiang, O. H. Campanella, Z. Jin, and T. Zhang, "Elucidation of stabilizing oil-in-water Pickering emulsion with different modified maize starch-based nanoparticles," *Food Chem*, vol. 229, pp. 152–158, Aug. 2017, doi: 10.1016/j.foodchem.2017.02.062.

F. Ye, M. Miao, K. Lu, B. Jiang, X. Li, and S. W. Cui, "Structure and physicochemical properties for modified starch-based nanoparticle from different maize varieties," *Food Hydrocoll*, vol. 67, pp. 37–44, Jun. 2017, doi: 10.1016/j.foodhyd.2016.12.041.

F. Zhu, "Impact of ultrasound on structure, physicochemical properties, modifications, and applications of starch," *Trends Food Sci Technol*, vol. 43, no. 1, pp. 1–17, May 2015, doi: 10.1016/j.tifs.2014.12.008.

G. Annison, R. J. Illman, and D. L. Topping, "Acetylated, Propionylated or Butyrylated Starches Raise Large Bowel Short-Chain Fatty Acids Preferentially When Fed to Rats," *J Nutr*, vol. 133, no. 11, pp. 3523–3528, Nov. 2003, doi: 10.1093/jn/133.11.3523.

G. F. Fanta, J. A. Kenar, and F. C. Felker, "Nanoparticle formation from amylose-fatty acid inclusion complexes prepared by steam jet cooking," *Ind Crops Prod*, vol. 74, pp. 36–44, Nov. 2015, doi: 10.1016/j.indcrop.2015.04.046.

G. Gutiérrez, D. Morán, A. Marefati, J. Purhagen, M. Rayner, and M. Matos, "Synthesis of controlled size starch nanoparticles (SNPs)," *Carbohydr Polym*, vol. 250, Dec. 2020, doi: 10.1016/j.carbpol.2020.116938.

G. Khachatryan and K. Khachatryan, "Starch based nanocomposites as sensors for heavy metals – detection of Cu2+ and Pb2+ ions," *Int Agrophys*, vol. 33, no. 1, pp. 121–126, Feb. 2019, doi: 10.31545/intagr/104414.

G. Li and F. Zhu, "Quinoa starch: Structure, properties, and applications," *Carbohydr Polym*, vol. 181, pp. 851–861, Feb. 2018, doi: 10.1016/j.carbpol.2017.11.067.

G. Liu *et al.*, "Insights into the changes of structure and digestibility of microwave and heat moisture treated quinoa starch," *Int J Biol Macromol*, vol. 246, p. 125681, Aug. 2023, doi: 10.1016/j.ijbiomac.2023.125681.

G. López-Carballo, L. Higueras, R. Gavara, and P. Hernández-Muñoz, "Silver Ions Release from Antibacterial Chitosan Films Containing in Situ Generated Silver Nanoparticles," *J Agric Food Chem*, vol. 61, no. 1, pp. 260–267, Jan. 2013, doi: 10.1021/jf304006y.

G. Maróti, A. Kereszt, É. Kondorosi, and P. Mergaert, "Natural roles of antimicrobial peptides in microbes, plants and animals," *Res Microbiol*, vol. 162, no. 4, pp. 363–374, May 2011, doi: 10.1016/j.resmic.2011.02.005.

G. Ren, D. Li, L. Wang, N. Özkan, and Z. Mao, "Morphological properties and thermoanalysis of micronized cassava starch," *Carbohydr Polym*, vol. 79, no. 1, pp. 101–105, Jan. 2010, doi: 10.1016/j.carbpol.2009.07.031.

G. W. C., "Calculation of HLB values of non-ionic surfactants," *Am Perfumer Essent Oil Rev*, vol. 65, pp. 26–29, 1955, Accessed: May 14, 2024. [Online]. Available: https://cir.nii.ac.jp/crid/1572261549150924416.bib?lang=ja

G. Zhou, Z. Luo, and X. Fu, "Preparation and characterization of starch nanoparticles in ionic liquid-in-oil microemulsions system," *Ind Crops Prod*, vol. 52, pp. 105–110, Jan. 2014, doi: 10.1016/j.indcrop.2013.10.019.

H. Angellier, J.-L. Putaux, S. Molina-Boisseau, D. Dupeyre, and A. Dufresne, "Starch Nanocrystal Fillers in an Acrylic Polymer Matrix," *Macromol Symp*, vol. 221, no. 1, pp. 95–104, Jan. 2005, doi: https://doi.org/10.1002/masy.200550310.

H. Bouwmeester, P. Brandhoff, H. J. P. Marvin, S. Weigel, and R. J. B. Peters, "State of the safety assessment and current use of nanomaterials in food and food production," *Trends Food Sci Technol*, vol. 40, no. 2, pp. 200–210, Dec. 2014, doi: 10.1016/j.tifs.2014.08.009.

H. Corke, Y. Z. Cai, and H. X. Wu, "Amaranth: Overview," in *Reference Module in Food Science*, Elsevier, 2016. doi: 10.1016/B978-0-08-100596-5.00032-9.

H. Jin, C. Zha, and L. Gu, "Direct dissolution of cellulose in NaOH/thiourea/urea aqueous solution," *Carbohydr Res*, vol. 342, no. 6, pp. 851–858, May 2007, doi: 10.1016/j.carres.2006.12.023.

H. Lin, L. Z. Qin, H. Hong, and Q. Li, "Preparation of Starch Nanoparticles via High-Energy Ball Milling," *Journal of Nano Research*, vol. 40, pp. 174–179, 2016, doi: 10.4028/www.scientific.net/JNanoR.40.174.

H. Lu *et al.*, "Preparation and characterization of V-type starch nanoparticles by an oil-water interface method," *Food Hydrocoll*, vol. 138, p. 108455, May 2023, doi: 10.1016/j.foodhyd.2023.108455.

H. Lundqvist, "Binding of hexadecyltrimethylammonium bromide to starch polysaccharides. Part I. Surface tension measurements," *Carbohydr Polym*, vol. 49, no. 1, pp. 43–55, Jul. 2002, doi: 10.1016/S0144-8617(01)00299-5.

H. Lundqvist, A.-C. Eliasson, and G. Olofsson, "Binding of hexadecyltrimethylammonium bromide to starch polysaccharides. Part II. Calorimetric study," *Carbohydr Polym*, vol. 49, no. 2, pp. 109–120, Aug. 2002, doi: 10.1016/S0144-8617(01)00326-5.

H. Ma, W. Qin, B. Guo, and P. Li, "Effect of plant tannin and glycerol on thermoplastic starch: Mechanical, structural, antimicrobial and biodegradable properties," *Carbohydr Polym*, vol. 295, p. 119869, Nov. 2022, doi: 10.1016/j.carbpol.2022.119869.

H. Mubarak Aldawsari *et al.*, "Development and evaluation of quercetin enriched bentonite-reinforced starch-gelatin based bioplastic with antimicrobial property," *Saudi Pharmaceutical Journal*, vol. 31, no. 12, p. 101861, Dec. 2023, doi: 10.1016/j.jsps.2023.101861.

H. Namazi, F. Fathi, and A. Dadkhah, "Hydrophobically modified starch using long-chain fatty acids for preparation of nanosized starch particles," *Scientia Iranica*, vol. 18, no. 3 C, pp. 439–445, 2011, doi: 10.1016/j.scient.2011.05.006.

H. Saari, C. Fuentes, M. Sjöö, M. Rayner, and M. Wahlgren, "Production of starch nanoparticles by dissolution and non-solvent precipitation for use in food-grade Pickering emulsions," *Carbohydr Polym*, vol. 157, pp. 558–566, Feb. 2017, doi: 10.1016/ j.carbpol.2016.10.003.

H. Siddiqui *et al.*, "Solanum tuberosum tuber-driven starch-mediated green-hydrothermal synthesis of cerium oxide nanoparticles for efficient photocatalysis and antimicrobial activities," *Chemosphere*, vol. 352, p. 141418, Mar. 2024, doi: 10.1016/j.chemosphere.2024.141418.

H. Ullah and S. Ali, "Classification of Anti-Bacterial Agents and Their Functions," in *Antibacterial Agents*, InTech, 2017. doi: 10.5772/intechopen.68695.

H. Vaghari *et al.*, "Application of magnetic nanoparticles in smart enzyme immobilization," *Biotechnol Lett*, vol. 38, no. 2, pp. 223–233, 2016, doi: 10.1007/s10529-015-1977-z.

H.-Y. Kim, D. J. Park, J.-Y. Kim, and S.-T. Lim, “Preparation of crystalline starch nanoparticles using cold acid hydrolysis and ultrasonication,” *Carbohydr Polym*, vol. 98, no. 1, pp. 295–301, Oct. 2013, doi: 10.1016/j.carbpol.2013.05.085.

H.-Y. Kim, J.-A. Han, D.-K. Kweon, J.-D. Park, and S.-T. Lim, “Effect of ultrasonic treatments on nanoparticle preparation of acid-hydrolyzed waxy maize starch,” *Carbohydr Polym*, vol. 93, no. 2, pp. 582–588, Apr. 2013, doi: 10.1016/j.carbpol.2012.12.050.

H.-Y. Kim, S.-J. Ye, and M.-Y. Baik, “Pressure moisture treatment (PMT) of starch, a new physical modification method,” *Food Hydrocoll*, vol. 134, p. 108051, Jan. 2023, doi: 10.1016/j.foodhyd.2022.108051.

H. Y. Kim, S. S. Park, and S. T. Lim, “Preparation, characterization and utilization of starch nanoparticles,” *Colloids and Surfaces B: Biointerfaces*, vol. 126. Elsevier, pp. 607–620, Feb. 01, 2015. doi: 10.1016/j.colsurfb.2014.11.011.

H. Zeng *et al.*, “Encapsulation of propionic acid within the aqueous phase of water-in-oil emulsions: reduced thermal volatilization and enhanced gastrointestinal stability,” *Food Funct*, 2023, doi: 10.1039/D2FO04076J.

H. Zhang, D. Zeng, and Z. Liu, “The law of approach to saturation in ferromagnets originating from the magnetocrystalline anisotropy,” *J Magn Magn Mater*, vol. 322, no. 16, pp. 2375–2380, Aug. 2010, doi: 10.1016/j.jmmm.2010.02.040.

I. Dankar, A. Haddarah, F. E. L. Omar, M. Pujolà, and F. Sepulcre, “Characterization of food additive-potato starch complexes by FTIR and X-ray diffraction,” *Food Chem*, vol. 260, pp. 7–12, Sep. 2018, doi: 10.1016/j.foodchem.2018.03.138.

I. Delsarte, F. Delattre, C. Rafin, and E. Veignie, “Investigations of benzo[a]pyrene encapsulation and Fenton degradation by starch nanoparticles,” *Carbohydr Polym*, vol. 186, pp. 344–349, Apr. 2018, doi: 10.1016/j.carbpol.2018.01.037.

I. Sondi and B. Salopek-Sondi, “Silver nanoparticles as antimicrobial agent: a case study on E. coli as a model for Gram-negative bacteria,” *J Colloid Interface Sci*, vol. 275, no. 1, pp. 177–182, Jul. 2004, doi: 10.1016/j.jcis.2004.02.012.

I. X. Yin, J. Zhang, I. S. Zhao, M. L. Mei, Q. Li, and C. H. Chu, “ The Antibacterial Mechanism of Silver Nanoparticles and Its Application in Dentistry ,” *Int J Nanomedicine*, vol. Volume 15, pp. 2555–2562, Apr. 2020, doi: 10.2147/IJN.S246764.

J. A. Han and S. T. Lim, “Structural changes in corn starches during alkaline dissolution by vortexing,” *Carbohydr Polym*, vol. 55, no. 2, pp. 193–199, Jan. 2004, doi: 10.1016/ j.carbpol.2003.09.006.

J. A. Putseys, L. Lamberts, and J. A. Delcour, “Amylose-inclusion complexes: Formation, identity and physico-chemical properties,” *J Cereal Sci*, vol. 51, no. 3, pp. 238–247, May 2010, doi: 10.1016/j.jcs.2010.01.011.

J. Acar, "Broad- and narrow-spectrum antibiotics: an unhelpful categorization," *Clinical Microbiology and Infection*, vol. 3, no. 4, pp. 395–396, Aug. 1997, doi: 10.1111/j.1469-0691.1997.tb00274.x.

Jacobs H. Delcour J.A., "Hydrothermal modifications of granular starch, with retention of the granular structure," *J. Agric. Food Chem.*, pp. 2895–2905, 1998.

J. B. Pires *et al.*, "Starch extraction from avocado by-product and its use for encapsulation of ginger essential oil by electrospinning," *Int J Biol Macromol*, vol. 254, p. 127617, Jan. 2024, doi: 10.1016/j.ijbiomac.2023.127617.

J. Hu, M. Chen, X. Fang, and L. Wu, "Fabrication and application of inorganic hollow spheres," *Chem Soc Rev*, vol. 40, no. 11, pp. 5472–5491, 2011, doi: 10.1039/C1CS15103G.

J. Jung, G. M. Raghavendra, D. Kim, and J. Seo, "One-step synthesis of starch-silver nanoparticle solution and its application to antibacterial paper coating," *Int J Biol Macromol*, vol. 107, pp. 2285–2290, Feb. 2018, doi: 10.1016/j.ijbiomac.2017.10.108.

J. Kim, D. Park, and S. Lim, "Fragmentation of Waxy Rice Starch Granules by Enzymatic Hydrolysis," *Cereal Chem*, vol. 85, no. 2, pp. 182–187, Mar. 2008, doi: 10.1094/cchem-85-2-0182.

J.-L. Putaux, S. Molina-Boisseau, T. Momaur, and A. Dufresne, "Platelet Nanocrystals Resulting from the Disruption of Waxy Maize Starch Granules by Acid Hydrolysis," *Biomacromolecules*, vol. 4, no. 5, pp. 1198–1202, Sep. 2003, doi: 10.1021/bm0340422.

J.M.V. Blanshard, "Starch granule structure and function: a physicochemical approach," *Starch Properties and Potential*, pp. 16–54, 1987.

J. N. BeMiller, "Pasting, paste, and gel properties of starch–hydrocolloid combinations," *Carbohydr Polym*, vol. 86, no. 2, pp. 386–423, Aug. 2011, doi: 10.1016/j.carbpol.2011.05.064.

J. N. Putro, S. Ismadji, C. Gunarto, F. E. Soetaredjo, and Y. H. Ju, "A study of anionic, cationic, and nonionic surfactants modified starch nanoparticles for hydrophobic drug loading and release," *J Mol Liq*, vol. 298, Jan. 2020, doi: 10.1016/j.molliq.2019.112034.

J. P. Rao and K. E. Geckeler, "Polymer nanoparticles: Preparation techniques and size-control parameters," *Progress in Polymer Science (Oxford)*, vol. 36, no. 7. Elsevier Ltd, pp. 887–913, 2011. doi: 10.1016/j.progpolymsci.2011.01.001.

J. Qi *et al.*, "Multi-shelled hollow micro-/nanostructures," *Chem Soc Rev*, vol. 44, no. 19, pp. 6749–6773, 2015, doi: 10.1039/C5CS00344J.

J. Qiao, Y. Dong, C. Chen, and J. Xie, "Development and characterization of starch/PVA antimicrobial active films with controlled release property by utilizing electrostatic interactions between nanocellulose and lauroyl arginate ethyl ester," *Int J Biol Macromol*, vol. 261, p. 129415, Mar. 2024, doi: 10.1016/j.ijbiomac.2024.129415.

J. S. Kim *et al.*, "Antimicrobial effects of silver nanoparticles," *Nanomedicine*, vol. 3, no. 1, pp. 95–101, Mar. 2007, doi: 10.1016/j.nano.2006.12.001.

J. Salonen *et al.*, "Mesoporous silicon microparticles for oral drug delivery: Loading and release of five model drugs," *Journal of Controlled Release*, vol. 108, no. 2–3, pp. 362–374, Nov. 2005, doi: 10.1016/j.jconrel.2005.08.017.

J. Singh, L. Kaur, and O. J. McCarthy, "Factors influencing the physico-chemical, morphological, thermal and rheological properties of some chemically modified starches for food applications-A review," *Food Hydrocolloids*, vol. 21, no. 1. pp. 1–22, Jan. 2007. doi: 10.1016/j.foodhyd.2006.02.006.

J. Wang *et al.*, "Modification in structural, physicochemical, functional, and in vitro digestive properties of kiwi starch by high-power ultrasound treatment," *Ultrason Sonochem*, vol. 86, p. 106004, May 2022, doi: 10.1016/j.ultsonch.2022.106004.

J. Yang *et al.*, "Conjugated linoleic acid loaded starch-based emulsion nanoparticles: In vivo gastrointestinal controlled release," *Food Hydrocoll*, vol. 101, Apr. 2020, doi: 10.1016/j.foodhyd.2019.105477.

J. Yang *et al.*, "Fabrication and characterization of hollow starch nanoparticles by gelation process for drug delivery application," *Carbohydr Polym*, vol. 173, pp. 223–232, Oct. 2017, doi: 10.1016/j.carbpol.2017.06.006.

J. Yang *et al.*, "The inhibition effect of starch nanoparticles on tyrosinase activity and its mechanism," *Food Funct*, vol. 7, no. 12, pp. 4804–4815, 2016, doi: 10.1039/C6FO01228K.

J. Yang, Y. Huang, C. Gao, M. Liu, and X. Zhang, "Fabrication and evaluation of the novel reduction-sensitive starch nanoparticles for controlled drug release," *Colloids Surf B Biointerfaces*, vol. 115, pp. 368–376, Mar. 2014, doi: 10.1016/j.colsurfb.2013.12.007.

J. Zhang *et al.*, "Physical modification of waxy maize starch: Combining SDS and freezing/thawing treatments to modify starch structure and functionality," *Food Structure*, vol. 32, p. 100263, Apr. 2022, doi: 10.1016/j.foostr.2022.100263.

K. A. Ramisetty, A. B. Pandit, and P. R. Gogate, "Investigations into ultrasound induced atomization," *Ultrason Sonochem*, vol. 20, no. 1, pp. 254–264, 2013, doi: 10.1016/j.ultsonch.2012.05.001.

K. M. Percival, "Antibiotic Classification and Indication Review for the Infusion Nurse," *Journal of Infusion Nursing*, vol. 40, no. 1, pp. 55–63, Jan. 2017, doi: 10.1097/NAN.0000000000000207.

K. R. Rajisha, H. J. Maria, L. A. Pothan, Z. Ahmad, and S. Thomas, "Preparation and characterization of potato starch nanocrystal reinforced natural rubber nanocomposites," *Int J Biol Macromol*, vol. 67, pp. 147–153, Jun. 2014, doi: 10.1016/j.ijbiomac.2014.03.013.

K. Ramadhan and T. J. Foster, "Effects of ball milling on the structural, thermal, and rheological properties of oat bran protein flour," *J Food Eng*, vol. 229, pp. 50–56, Jul. 2018, doi: 10.1016/j.jfoodeng.2017.10.024.

K. Sangseethong, N. Termvejsayanon, and K. Sriroth, "Characterization of physicochemical properties of hypochlorite- and peroxide-oxidized cassava starches," *Carbohydr Polym*, vol. 82, no. 2, pp. 446–453, Sep. 2010, doi: 10.1016/j.carbpol.2010.05.003.

K. Saravanakumar *et al.*, "Synthesis, characterization, and cytotoxicity of starch-encapsulated biogenic silver nanoparticle and its improved anti-bacterial activity," *Int J Biol Macromol*, vol. 182, pp. 1409–1418, Jul. 2021, doi: 10.1016/j.ijbiomac.2021.05.036.

K. Wang, L. Cheng, Z. Li, C. Li, Y. Hong, and Z. Gu, "The degree of substitution of OSA-modified starch affects the retention and release of encapsulated mint flavour," *Carbohydr Polym*, vol. 294, p. 119781, Oct. 2022, doi: 10.1016/j.carbpol.2022.119781.

L. A. Bello-Pérez, E. Agama-Acevedo, P. B. Zamudio-Flores, G. Mendez-Montealvo, and S. L. Rodriguez-Ambriz, "Effect of low and high acetylation degree in the morphological, physicochemical and structural characteristics of barley starch," *LWT - Food Science and Technology*, vol. 43, no. 9, pp. 1434–1440, Nov. 2010, doi: 10.1016/j.lwt.2010.04.003.

L. Acevedo-Guevara, L. Nieto-Suaza, L. T. Sanchez, M. I. Pinzon, and C. C. Villa, "Development of native and modified banana starch nanoparticles as vehicles for curcumin," *Int J Biol Macromol*, vol. 111, pp. 498–504, May 2018, doi: 10.1016/j.ijbiomac.2018.01.063.

L. Alonso-Miravalles and J. O'Mahony, "Composition, Protein Profile and Rheological Properties of Pseudocereal-Based Protein-Rich Ingredients," *Foods*, vol. 7, no. 5, p. 73, May 2018, doi: 10.3390/foods7050073.

L. Boetje, X. Lan, F. Silvianti, J. van Dijken, M. Polhuis, and K. Loos, "A more efficient synthesis and properties of saturated and unsaturated starch esters," *Carbohydr Polym*, vol. 292, p. 119649, Sep. 2022, doi: 10.1016/j.carbpol.2022.119649.

L. Chen *et al.*, "Encapsulation of tea polyphenols into high amylose corn starch composite nanofibrous film for active antimicrobial packaging," *Int J Biol Macromol*, vol. 245, p. 125245, Aug. 2023, doi: 10.1016/j.ijbiomac.2023.125245.

L. Chronopoulou, I. Fratoddi, C. Palocci, I. Venditti, and M. V. Russo, "Osmosis based method drives the self-assembly of polymeric chains into micro-and nanostructures," *Langmuir*, vol. 25, no. 19, pp. 11940–11946, Oct. 2009, doi: 10.1021/la9016382.

L. Dai, C. Li, J. Zhang, and F. Cheng, "Preparation and characterization of starch nanocrystals combining ball milling with acid hydrolysis," *Carbohydr Polym*, vol. 180, pp. 122–127, Jan. 2018, doi: 10.1016/j.carbpol.2017.10.015.

L. Nieto-Suaza, L. Acevedo-Guevara, L. T. Sánchez, M. I. Pinzón, and C. C. Villa, "Characterization of Aloe vera-banana starch composite films reinforced with curcumin-loaded starch nanoparticles," *Food Structure*, vol. 22, Oct. 2019, doi: 10.1016/j.foostr.2019.100131.

L. Protesescu, S. Yakunin, O. Nazarenko, D. N. Dirin, and M. V. Kovalenko, "Low-Cost Synthesis of Highly Luminescent Colloidal Lead Halide Perovskite Nanocrystals by Wet Ball Milling," *ACS Appl Nano Mater*, vol. 1, no. 3, pp. 1300–1308, Mar. 2018, doi: 10.1021/acsanm.8b00038.

L. Qi, G. Ji, Z. Luo, Z. Xiao, and Q. Yang, "Characterization and Drug Delivery Properties of OSA Starch-Based Nanoparticles Prepared in [C_3OHmim]Ac-in-Oil Microemulsions System," *ACS Sustain Chem Eng*, vol. 5, no. 10, pp. 9517–9526, Oct. 2017, doi: 10.1021/acssuschemeng.7b02727.

L. Wang and Y.-J. Wang, "Structures and Physicochemical Properties of Acid-Thinned Corn, Potato and Rice Starches," *Starch - Stärke*, vol. 53, no. 11, p. 570, Nov. 2001, doi: 10.1002/1521-379X(200111)53:11<570::AID-STAR570>3.0.CO;2-S.

L. Wang *et al.*, "Effects of fatty acid chain length on properties of potato starch–fatty acid complexes under partially gelatinization," *Int J Food Prop*, vol. 21, no. 1, pp. 2121–2134, Jan. 2018, doi: 10.1080/10942912.2018.1489842.

L. Wang *et al.*, "Loading paclitaxel into porous starch in the form of nanoparticles to improve its dissolution and bioavailability," *Int J Biol Macromol*, vol. 138, pp. 207–214, Oct. 2019, doi: 10.1016/j.ijbiomac.2019.07.083.

L. Zhu, H. Luo, Z.-W. Shi, C. Lin, and J. Chen, "Preparation, characterization, and antibacterial effect of bio-based modified starch films," *Food Chem X*, vol. 17, p. 100602, Mar. 2023, doi: 10.1016/j.fochx.2023.100602.

M. A. El-Sheikh, "New technique in starch nanoparticles synthesis," *Carbohydr Polym*, vol. 176, pp. 214–219, Nov. 2017, doi: 10.1016/j.carbpol.2017.08.033.

M. Ahmad and A. Gani, "Ultrasonicated resveratrol loaded starch nanocapsules: Characterization, bioactivity and release behaviour under in-vitro digestion," *Carbohydr Polym*, vol. 251, Jan. 2021, doi: 10.1016/j.carbpol.2020.117111.

M. Ahmad, A. Gani, F. A. Masoodi, and S. H. Rizvi, "Influence of ball milling on the production of starch nanoparticles and its effect on structural, thermal and functional properties," *Int J Biol Macromol*, vol. 151, pp. 85–91, May 2020, doi: 10.1016/j.ijbiomac.2020.02.139.

M. Ahmad, A. Gani, ifra Hassan, Q. Huang, and H. Shabbir, "production and characterization of starch nanoparticles by mild alkali hydrolysis and ultra-sonication process," 2020, doi: 10.1038/s41598-020-60380-0.

M. A. El-Sheikh, "New technique in starch nanoparticles synthesis," *Carbohydr Polym*, vol. 176, pp. 214–219, Nov. 2017, doi: 10.1016/j.carbpol.2017.08.033.

M. Ahmad, P. Mudgil, A. Gani, F. Hamed, F. A. Masoodi, and S. Maqsood, "Nano-encapsulation of catechin in starch nanoparticles: Characterization, release behavior and bioactivity retention during simulated in-vitro digestion," *Food Chem*, vol. 270, pp. 95–104, Jan. 2019, doi: 10.1016/j.foodchem.2018.07.024.

M. Amrani, S. Pourshamohammad, M. Tabibiazar, H. Hamishehkar, and M. Mahmoudzadeh, "Antimicrobial activity and stability of Satureja khuzestanica essential oil pickering emulsions stabilized by starch nanocrystals and bacterial cellulose nanofibers," *Food Biosci*, vol. 55, p. 103016, Oct. 2023, doi: 10.1016/j.fbio.2023.103016.

M. Babaee, F. Garavand, A. Rehman, S. Jafarazadeh, E. Amini, and I. Cacciotti, "Biodegradability, physical, mechanical and antimicrobial attributes of starch nanocomposites containing chitosan nanoparticles," *Int J Biol Macromol*, vol. 195, pp. 49–58, Jan. 2022, doi: 10.1016/j.ijbiomac.2021.11.162.

M. Belcheva, G. Georgiev, B. Tsyntsarski, U. Szeluga, and L. Kabaivanova, "Antibacterial properties of metal nanoparticles–incorporated activated carbon composites produced from waste biomass precursor," *Diam Relat Mater*, vol. 141, p. 110545, Jan. 2024, doi: 10.1016/j.diamond.2023.110545.

M. Bhatia and S. Rohilla, "Formulation and optimization of quinoa starch nanoparticles: Quality by design approach for solubility enhancement of piroxicam," *Saudi Pharmaceutical Journal*, vol. 28, no. 8, pp. 927–935, Aug. 2020, doi: 10.1016/j.jsps.2020.06.013.

M. Borgogna, B. Bellich, L. Zorzin, R. Lapasin, and A. Cesàro, "Food microencapsulation of bioactive compounds: Rheological and thermal characterisation of non-conventional gelling system," *Food Chem*, vol. 122, no. 2, pp. 416–423, Sep. 2010, doi: 10.1016/j.foodchem.2009.07.043.

M. Darroudi, M. Hakimi, E. Goodarzi, and R. Kazemi Oskuee, "Superparamagnetic iron oxide nanoparticles (SPIONs): Green preparation, characterization and their cytotoxicity effects," *Ceram Int*, vol. 40, no. 9, pp. 14641–14645, Nov. 2014, doi: 10.1016/j.ceramint.2014.06.051.

M. E. El-Naggar, M. H. El-Rafie, M. A. El-sheikh, G. S. El-Feky, and A. Hebeish, "Synthesis, characterization, release kinetics and toxicity profile of drug-loaded starch nanoparticles," *Int J Biol Macromol*, vol. 81, pp. 718–729, Nov. 2015, doi: 10.1016/j.ijbiomac.2015.09.005.

M. G. Carrión, M. A. R. Corripio, J. V. H. Contreras, M. R. Marrón, G. M. Olán, and A. S. H. Cázares, "Optimization and characterization of taro starch, nisin, and sodium alginate-based biodegradable films: antimicrobial effect in chicken meat," *Poult Sci*, vol. 102, no. 12, p. 103100, Dec. 2023, doi: 10.1016/j.psj.2023.103100.

M. J. dos Santos Alves *et al.*, "Starch nanoparticles containing phenolic compounds from green propolis: Characterization and evaluation of antioxidant, antimicrobial and digestibility properties," *Int J Biol Macromol*, vol. 255, p. 128079, Jan. 2024, doi: 10.1016/j.ijbiomac.2023.128079.

M. J. Santander-Ortega *et al.*, "Nanoparticles made from novel starch derivatives for transdermal drug delivery," *Journal of Controlled Release*, vol. 141, no. 1, pp. 85–92, Jan. 2010, doi: 10.1016/j.jconrel.2009.08.012.

M. K. Remanan and F. Zhu, "Encapsulation of rutin using quinoa and maize starch nanoparticles," *Food Chem*, 2020, doi: 10.1016/j.foodchem.2020.128534.

M. Labet, W. Thielemans, and A. Dufresne, "Polymer Grafting onto Starch Nanocrystals," *Biomacromolecules*, vol. 8, no. 9, pp. 2916–2927, Sep. 2007, doi: 10.1021/bm700468f.

M. M. Cruz-Benítez, C. A. Gómez-Aldapa, J. Castro-Rosas, E. Hernández-Hernández, E. Gómez-Hernández, and H. A. Fonseca-Florido, "Effect of amylose content and chemical modification of cassava starch on the microencapsulation of Lactobacillus pentosus," *LWT*, vol. 105, pp. 110–117, May 2019, doi: 10.1016/j.lwt.2019.01.069.

M. M. Vuolo, V. S. Lima, and M. R. Maróstica Junior, "Phenolic Compounds," in *Bioactive Compounds*, Elsevier, 2019, pp. 33–50. doi: 10.1016/B978-0-12-814774-0.00002-5.

M. Majzoobi, M. Radi, A. Farahnaky, J. Jamalian, T. Tongdang, and G. Mesbahi, "Physicochemical properties of pre-gelatinized wheat starch produced by a twin drum drier," *Journal of Agricultural Science and Technology*, vol. 13, no. 2, pp. 193–202, 2011.

M. N. Tahir *et al.*, "Facile synthesis and characterization of monocrystalline cubic ZrO2 nanoparticles," *Solid State Sci*, vol. 9, no. 12, pp. 1105–1109, Dec. 2007, doi: 10.1016/j.solidstatesciences.2007.07.033.

M. N. Z. Abidin *et al.*, "Highly adsorptive oxidized starch nanoparticles for efficient urea removal," *Carbohydr Polym*, vol. 201, pp. 257–263, Dec. 2018, doi: 10.1016/j.carbpol.2018.08.069.

M. Rai, A. Yadav, and A. Gade, "Silver nanoparticles as a new generation of antimicrobials," *Biotechnol Adv*, vol. 27, no. 1, pp. 76–83, Jan. 2009, doi: 10.1016/j.biotechadv.2008.09.002.

M. S. Hernández, L. N. Ludueña, and S. K. Flores, "Citric acid, chitosan and oregano essential oil impact on physical and antimicrobial properties of cassava starch films," *Carbohydrate Polymer Technologies and Applications*, vol. 5, p. 100307, Jun. 2023, doi: 10.1016/j.carpta.2023.100307.

M. Salvador, G. Gutiérrez, S. Noriega, A. Moyano, M. C. Blanco-López, and M. Matos, "Microemulsion synthesis of superparamagnetic nanoparticles for bioapplications," *Int J Mol Sci*, vol. 22, no. 1, pp. 1–17, Jan. 2021, doi: 10.3390/ijms22010427.

M. Shahbazi, M. Majzoobi, and A. Farahnaky, "Physical modification of starch by high-pressure homogenization for improving functional properties of κ-carrageenan/starch blend film," *Food Hydrocoll*, vol. 85, pp. 204–214, Dec. 2018, doi: 10.1016/j.foodhyd.2018.07.017.

M. V. Tzoumaki, T. Moschakis, and C. G. Biliaderis, "Mixed aqueous chitin nanocrystal–whey protein dispersions: Microstructure and rheological behaviour," *Food Hydrocoll*, vol. 25, no. 5, pp. 935–942, Jul. 2011, doi: 10.1016/j.foodhyd.2010.09.004.

M. Wang *et al.*, "Prebiotic effects of resistant starch nanoparticles on growth and proliferation of the probiotic Lactiplantibacillus plantarum subsp. plantarum," *LWT*, vol. 154, p. 112572, Jan. 2022, doi: 10.1016/j.lwt.2021.112572.

M. Yüce and H. Kurt, "How to make nanobiosensors: surface modification and characterisation of nanomaterials for biosensing applications," *RSC Adv.*, vol. 7, no. 78, pp. 49386–49403, 2017, doi: 10.1039/C7RA10479K.

M. Zanetti *et al.*, "Use of encapsulated natural compounds as antimicrobial additives in food packaging: A brief review," *Trends Food Sci Technol*, vol. 81, pp. 51–60, Nov. 2018, doi: 10.1016/j.tifs.2018.09.003.

N. Abdul Hadi, A. Marefati, M. Matos, B. Wiege, and M. Rayner, "Characterization and stability of short-chain fatty acids modified starch Pickering emulsions," *Carbohydr Polym*, vol. 240, p. 116264, Jul. 2020, doi: 10.1016/j.carbpol.2020.116264.

N. Abdul Hadi, B. Wiege, S. Stabenau, A. Marefati, and M. Rayner, "Comparison of Three Methods to Determine the Degree of Substitution of Quinoa and Rice Starch Acetates, Propionates, and Butyrates: Direct Stoichiometry, FTIR, and 1H-NMR," *Foods*, vol. 9, no. 1, p. 83, Jan. 2020, doi: 10.3390/foods9010083.

N. Chiu, A. Tarrega, C. Parmenter, L. Hewson, B. Wolf, and I. D. Fisk, "Optimisation of octinyl succinic anhydride starch stablised w 1 /o/w 2 emulsions for oral destablisation of encapsulated salt and enhanced saltiness," *Food Hydrocoll*, vol. 69, pp. 450–458, Aug. 2017, doi: 10.1016/j.foodhyd.2017.03.002.

N. El Hachlafi *et al.*, "Tetraclinis articulata (Vahl) Mast. essential oil as a promising source of bioactive compounds with antimicrobial, antioxidant, anti-inflammatory and dermatoprotective properties: In vitro and in silico evidence," *Heliyon*, vol. 10, no. 1, p. e23084, Jan. 2024, doi: 10.1016/j.heliyon.2023.e23084.

N. K. Monych and R. J. Turner, "Multiple Compounds Secreted by *Pseudomonas aeruginosa* Increase the Tolerance of *Staphylococcus aureus* to the Antimicrobial Metals Copper and Silver," *mSystems*, vol. 5, no. 5, Oct. 2020, doi: 10.1128/mSystems.00746-20.

N. Li, M. Niu, B. Zhang, S. Zhao, S. Xiong, and F. Xie, "Effects of concurrent ball milling and octenyl succinylation on structure and physicochemical properties of starch," *Carbohydr Polym*, vol. 155, pp. 109–116, Jan. 2017, doi: 10.1016/j.carbpol.2016.08.063.

N. M. C. Da Silva, P. R. C. Correia, J. I. Druzian, F. M. Fakhouri, R. L. L. Fialho, and E. C. M. C. De Albuquerque, "PBAT/TPS Composite Films Reinforced with Starch Nanoparticles Produced by Ultrasound," *Int J Polym Sci*, vol. 2017, 2017, doi: 10.1155/2017/4308261.

N. Malhotra *et al.*, "Potential Toxicity of Iron Oxide Magnetic Nanoparticles: A Review," *Molecules*, vol. 25, no. 14, 2020, doi: 10.3390/molecules25143159.

N. Masina *et al.*, "A review of the chemical modification techniques of starch," *Carbohydr Polym*, vol. 157, pp. 1226–1236, Feb. 2017, doi: 10.1016/j.carbpol.2016.09.094.

N. Nakagiri, M. H. Manghnani, L. C. Ming, and S. Kimura, "Crystal structure of magnetite under pressure," *Phys Chem Miner*, vol. 13, no. 4, pp. 238–244, Jul. 1986, doi: 10.1007/BF00308275.

N. S. Ismail and S. C. B. Gopinath, "Enhanced antibacterial effect by antibiotic loaded starch nanoparticle," *Journal of the Association of Arab Universities for Basic and Applied Sciences*, vol. 24, no. 1, pp. 136–140, Oct. 2017, doi: 10.1016/j.jaubas.2016.10.005.

N. Shahgholian and G. Rajabzadeh, "Preparation of BSA nanoparticles and its binary compounds via ultrasonic piezoelectric oscillator for curcumin encapsulation," *J Drug Deliv Sci Technol*, vol. 54, Dec. 2019, doi: 10.1016/j.jddst.2019.101323.

N. Sivapragasam, P. Thavarajah, J.-B. Ohm, J.-B. Ohm, K. Margaret, and D. Thavarajah, "Novel starch based nano scale enteric coatings from soybean meal for colon-specific delivery," *Carbohydr Polym*, vol. 111, pp. 273–279, Oct. 2014, doi: 10.1016/j.carbpol.2014.04.091.

N. Thajai *et al.*, "Antimicrobial thermoplastic starch reactive blend with chlorhexidine gluconate and epoxy resin," *Carbohydr Polym*, vol. 301, p. 120328, Feb. 2023, doi: 10.1016/j.carbpol.2022.120328.

N. Zidan *et al.*, "Active and smart antimicrobial food packaging film composed of date palm kernels extract loaded carboxymethyl chitosan and carboxymethyl starch composite for prohibiting foodborne pathogens during fruits preservation," *Eur Polym J*, vol. 197, p. 112353, Oct. 2023, doi: 10.1016/j.eurpolymj.2023.112353.

Ó. Estupiñán *et al.*, "Nano-Encapsulation of Mithramycin in Transfersomes and Polymeric Micelles for the Treatment of Sarcomas," *J Clin Med*, vol. 10, no. 7, p. 1358, Mar. 2021, doi: 10.3390/jcm10071358.

O. Franssen and W. E. Hennink, "A novel preparation method for polymeric microparticles without the use of organic solvents," 1998.

O. S. Lawal, "Succinylated *Dioscorea cayenensis* starch: Effect of reaction parameters and characterisation," *Starch - Stärke*, vol. 64, no. 2, pp. 145–156, Feb. 2012, doi: 10.1002/star.201100110.

O. S. Lawal *et al.*, "Rheology and functional properties of starches isolated from five improved rice varieties from West Africa," *Food Hydrocoll*, vol. 25, no. 7, pp. 1785–1792, Oct. 2011, doi: 10.1016/j.foodhyd.2011.04.010.

O. Velgosová, S. Dolinská, and A. Mražíková, "Synergic effect of sodium alginate and Citrus lemon extract on the in-situ synthesis of AgNPs in a polymeric matrix," *Nano-Structures & Nano-Objects*, vol. 28, p. 100795, Oct. 2021, doi: 10.1016/j.nanoso.2021.100795.

P. A. Gill, M. C. van Zelm, J. G. Muir, and P. R. Gibson, "Review article: short chain fatty acids as potential therapeutic agents in human gastrointestinal and inflammatory disorders," *Aliment Pharmacol Ther*, vol. 48, no. 1, pp. 15–34, Jul. 2018, doi: 10.1111/apt.14689.

P. Chivero, S. Gohtani, H. Yoshii, and A. Nakamura, "Assessment of soy soluble polysaccharide, gum arabic and OSA-Starch as emulsifiers for mayonnaise-like emulsions," *LWT - Food Science and Technology*, vol. 69, pp. 59–66, Jun. 2016, doi: 10.1016/j.lwt.2015.12.064.

P. Dandekar *et al.*, "A Hydrophobic Starch Polymer for Nanoparticle-Mediated Delivery of Docetaxel," *Macromol Biosci*, vol. 12, no. 2, pp. 184–194, Feb. 2012, doi: 10.1002/mabi.201100244.

P. H. Campelo, A. S. Sant'Ana, and M. T. Pedrosa Silva Clerici, "Starch nanoparticles: production methods, structure, and properties for food applications," *Current Opinion in Food Science*, vol. 33. Elsevier Ltd, pp. 136–140, Jun. 01, 2020. doi: 10.1016/j.cofs.2020.04.007.

P. I. P. Soares *et al.*, "Iron oxide nanoparticles stabilized with a bilayer of oleic acid for magnetic hyperthermia and MRI applications," *Appl Surf Sci*, vol. 383, pp. 240–247, Oct. 2016, doi: 10.1016/j.apsusc.2016.04.181.

P. Nallasamy, T. Ramalingam, T. Nooruddin, R. Shanmuganathan, P. Arivalagan, and S. Natarajan, "Polyherbal drug loaded starch nanoparticles as promising drug delivery system: Antimicrobial, antibiofilm and neuroprotective studies," *Process Biochemistry*, vol. 92, pp. 355–364, May 2020, doi: 10.1016/j.procbio.2020.01.026.

P. Sufi-Maragheh, N. Nikfarjam, Y. Deng, and N. Taheri-Qazvini, "Pickering emulsion stabilized by amphiphilic pH-sensitive starch nanoparticles as therapeutic containers," *Colloids Surf B Biointerfaces*, vol. 181, pp. 244–251, Sep. 2019, doi: 10.1016/j.colsurfb.2019.05.046.

P. Vasileva, T. Alexandrova, and I. Karadjova, "Application of Starch-Stabilized Silver Nanoparticles as a Colorimetric Sensor for Mercury(II) in 0.005 mol/L Nitric Acid," *J Chem*, vol. 2017, pp. 1–9, 2017, doi: 10.1155/2017/6897960.

Q. Lin *et al.*, "Fabrication of debranched starch nanoparticles via reverse emulsification for improvement of functional properties of corn starch films," *Food Hydrocoll*, vol. 104, p. 105760, Jul. 2020, doi: 10.1016/j.foodhyd.2020.105760.

Q. Lin, R. Liang, F. Zhong, A. Ye, and H. Singh, "Interactions between octenyl-succinic-anhydride-modified starches and calcium in oil-in-water emulsions," *Food Hydrocoll*, vol. 77, pp. 30–39, Apr. 2018, doi: 10.1016/j.foodhyd.2017.08.034.

Q. Sun, H. Fan, and L. Xiong, "Preparation and characterization of starch nanoparticles through ultrasonic-assisted oxidation methods," *Carbohydr Polym*, vol. 106, pp. 359–364, Jun. 2014, doi: 10.1016/j.carbpol.2014.02.067.

Q. Wang *et al.*, "Effects of octenyl succinylation on the properties of starches with distinct crystalline types and their Pickering emulsions," *Int J Biol Macromol*, vol. 230, p. 123183, Mar. 2023, doi: 10.1016/j.ijbiomac.2023.123183.

R. Awasthi, A. Roseblade, P. M. Hansbro, M. J. Rathbone, K. Dua, and M. Bebawy, "Nanoparticles in Cancer Treatment: Opportunities and Obstacles," *Curr Drug Targets*, vol. 19, no. 14, pp. 1696–1709, Sep. 2018, doi: 10.2174/1389450119666180326122831.

R. Bajaj, N. Singh, and A. Kaur, "Properties of octenyl succinic anhydride (OSA) modified starches and their application in low fat mayonnaise," *Int J Biol Macromol*, vol. 131, pp. 147–157, Jun. 2019, doi: 10.1016/j.ijbiomac.2019.03.054.

R. Balic, T. Miljkovic, B. Ozsisli, and S. Simsek, "Utilization of Modified Wheat and Tapioca Starches as Fat Replacements in Bread Formulation," *J Food Process Preserv*, vol. 41, no. 1, p. e12888, Feb. 2017, doi: 10.1111/jfpp.12888.

R. Bhat and A. A. Karim, "Impact of Radiation Processing on Starch," *Compr Rev Food Sci Food Saf*, vol. 8, no. 2, pp. 44–58, Apr. 2009, doi: 10.1111/j.1541-4337.2008.00066.x.

R. Bhosale and R. Singhal, "Process optimization for the synthesis of octenyl succinyl derivative of waxy corn and amaranth starches," *Carbohydr Polym*, vol. 66, no. 4, pp. 521–527, Nov. 2006, doi: 10.1016/j.carbpol.2006.04.007.

R. Chang *et al.*, "Fabrication and characterization of hollow starch nanoparticles by heterogeneous crystallization of debranched starch in a nanoemulsion system," *Food Chem*, vol. 323, p. 126851, Sep. 2020, doi: 10.1016/j.foodchem.2020.126851.

R. Chang *et al.*, "Green preparation and characterization of starch nanoparticles using a vacuum cold plasma process combined with ultrasonication treatment," *Ultrason Sonochem*, vol. 58, p. 104660, Nov. 2019, doi: 10.1016/j.ultsonch.2019.104660.

R. de Sousa Victor, A. Marcelo da Cunha Santos, B. Viana de Sousa, G. de Araújo Neves, L. Navarro de Lima Santana, and R. Rodrigues Menezes, "A Review on Chitosan's Uses as Biomaterial: Tissue Engineering, Drug Delivery Systems and Cancer Treatment," *Materials*, vol. 13, no. 21, p. 4995, Nov. 2020, doi: 10.3390/ma13214995.

R. H. Müller and C. Jacobs, "Buparvaquone mucoadhesive nanosuspension: preparation, optimisation and long-term stability," *Int J Pharm*, vol. 237, no. 1–2, pp. 151–161, Apr. 2002, doi: 10.1016/S0378-5173(02)00040-6.

R. Hoover and H. Manuel, "The Effect of Heat–Moisture Treatment on the Structure and Physicochemical Properties of Normal Maize, Waxy Maize, Dull Waxy Maize and Amylomaize V Starches," *J Cereal Sci*, vol. 23, no. 2, pp. 153–162, Mar. 1996, doi: 10.1006/jcrs.1996.0015.

R. Jain *et al.*, "Enhanced cellular delivery of idarubicin by surface modification of propyl starch nanoparticles employing pteroic acid conjugated polyvinyl alcohol," *Int J Pharm*, vol. 420, no. 1, pp. 147–155, Nov. 2011, doi: 10.1016/j.ijpharm.2011.08.030.

R. K. Maheshwari, A. K. Singh, J. Gaddipati, and R. C. Srimal, "Multiple biological activities of curcumin: A short review," in *Life Sciences*, Mar. 2006, pp. 2081–2087. doi: 10.1016/j.lfs.2005.12.007.

R. L. Rebodos and P. J. Vikesland, "Effects of Oxidation on the Magnetization of Nanoparticulate Magnetite," *Langmuir*, vol. 26, no. 22, pp. 16745–16753, Nov. 2010, doi: 10.1021/la102461z.

R. N. Waduge, R. Hoover, T. Vasanthan, J. Gao, and J. Li, "Effect of annealing on the structure and physicochemical properties of barley starches of varying amylose content," *Food Research International*, vol. 39, no. 1, pp. 59–77, Jan. 2006, doi: 10.1016/j.foodres.2005.05.008.

R. Sarder *et al.*, “Copolymers of starch, a sustainable template for biomedical applications: A review,” *Carbohydr Polym*, vol. 278, p. 118973, Feb. 2022, doi: 10.1016/j.carbpol.2021.118973.

R. Singh, “Nanotechnology based therapeutic application in cancer diagnosis and therapy,” *3 Biotech*, vol. 9, p. 415, 1940, doi: 10.1007/s13205-019-1940-0.

R. Wang, “The chemistry of nanomaterials - C. N. R. Rao, A. M□ller, A. K. Cheetham (eds), WILEY-VCH Verlag GmbH & Co. KGaA, Weinheim 2004. ISBN 3-527-30686-2, 741 pages,” *Colloid Polym Sci*, vol. 283, no. 2, pp. 234–234, Dec. 2004, doi: 10.1007/s00396-004-1140-1.

S. A. Kheradvar, J. Nourmohammadi, H. Tabesh, and B. Bagheri, “Starch nanoparticle as a vitamin E-TPGS carrier loaded in silk fibroin-poly(vinyl alcohol)-Aloe vera nanofibrous dressing,” *Colloids Surf B Biointerfaces*, vol. 166, pp. 9–16, Jun. 2018, doi: 10.1016/j.colsurfb.2018.03.004.

S. A. Varghese, H. Pulikkalparambil, S. M. Rangappa, J. Parameswaranpillai, and S. Siengchin, “Antimicrobial active packaging based on PVA/Starch films incorporating basil leaf extracts,” *Mater Today Proc*, vol. 72, pp. 3056–3062, 2023, doi: 10.1016/j.matpr.2022.09.062.

S. Asgari, A. H. Saberi, D. J. McClements, and M. Lin, “Microemulsions as nanoreactors for synthesis of biopolymer nanoparticles,” *Trends Food Sci Technol*, vol. 86, pp. 118–130, Apr. 2019, doi: 10.1016/J.TIFS.2019.02.008.

S. B. Sant, “Nanoparticles: From Theory to Applications,” *Materials and Manufacturing Processes*, vol. 27, no. 12, pp. 1462–1463, Dec. 2012, doi: 10.1080/10426914.2012.663137.

S. Bel Haaj, A. Magnin, C. Pétrier, and S. Boufi, “Starch nanoparticles formation via high power ultrasonication,” *Carbohydr Polym*, vol. 92, no. 2, pp. 1625–1632, Feb. 2013, doi: 10.1016/j.carbpol.2012.11.022.

S. D. Steichen, M. Caldorera-Moore, and N. A. Peppas, “A review of current nanoparticle and targeting moieties for the delivery of cancer therapeutics,” *European Journal of Pharmaceutical Sciences*, vol. 48, no. 3. Elsevier B.V., pp. 416–427, Feb. 14, 2013. doi: 10.1016/j.ejps.2012.12.006.

S. D. Todorov and L. M. T. Dicks, “Bacteriocin production by Pediococcus pentosaceus isolated from marula (Scerocarya birrea),” *Int J Food Microbiol*, vol. 132, no. 2–3, pp. 117–126, Jun. 2009, doi: 10.1016/j.ijfoodmicro.2009.04.010.

S. Deng, R. Huang, M. Zhou, F. Chen, and Q. Fu, “Hydrophobic cellulose films with excellent strength and toughness via ball milling activated acylation of microfibrillated cellulose,” *Carbohydr Polym*, vol. 154, pp. 129–138, Dec. 2016, doi: 10.1016/j.carbpol.2016.07.101.

S. F. Chin, A. Azman, and S. C. Pang, “Size controlled synthesis of starch nanoparticles by a microemulsion method,” *J Nanomater*, vol. 2014, 2014, doi: 10.1155/2014/763736.

S. F. Chin, S. C. Pang, and S. H. Tay, “Size controlled synthesis of starch nanoparticles by a simple nanoprecipitation method,” *Carbohydr Polym*, vol. 86, no. 4, pp. 1817–1819, Oct. 2011, doi: 10.1016/j.carbpol.2011.07.012.

S. F. Chin, S. N. A. Mohd Yazid, and S. C. Pang, "Preparation and Characterization of Starch Nanoparticles for Controlled Release of Curcumin," *Int J Polym Sci*, vol. 2014, pp. 1–8, 2014, doi: 10.1155/2014/340121.

S. F. Medeiros *et al.*, "Synthesis and characterization of stable aqueous dispersion of functionalized double-coated iron oxide nanoparticles," *Mater Lett*, vol. 160, pp. 522–525, Dec. 2015, doi: 10.1016/j.matlet.2015.08.026.

S. Gao *et al.*, "Starch/poly (butylene adipate-co-terephthalate) blown films contained the quaternary ammonium salts with different N-alkyl chain lengths as antimicrobials," *Food Chem*, vol. 436, p. 137650, Mar. 2024, doi: 10.1016/j.foodchem.2023.137650.

S. Gao, X. Zhang, J. Jiang, W. Wang, and H. Hou, "Starch/poly(butylene adipate-co-terephthalate) blown antimicrobial films based on ε-polylysine hydrochloride and different nanomontmorillonites," *Int J Biol Macromol*, vol. 253, p. 126609, Dec. 2023, doi: 10.1016/j.ijbiomac.2023.126609.

S. Graziano, C. Agrimonti, N. Marmiroli, and M. Gullì, "Utilisation and limitations of pseudocereals (quinoa, amaranth, and buckwheat) in food production: A review," *Trends Food Sci Technol*, vol. 125, pp. 154–165, Jul. 2022, doi: 10.1016/j.tifs.2022.04.007.

S. H. Mahmoudi Najafi, M. Baghaie, and A. Ashori, "Preparation and characterization of acetylated starch nanoparticles as drug carrier: Ciprofloxacin as a model," *Int J Biol Macromol*, vol. 87, pp. 48–54, Jun. 2016, doi: 10.1016/j.ijbiomac.2016.02.030.

S. Jiang, L. Dai, Y. Qin, L. Xiong, and Q. Sun, "Preparation and Characterization of Octenyl Succinic Anhydride Modified Taro Starch Nanoparticles," *PLoS One*, vol. 11, no. 2, p. e0150043, Feb. 2016, doi: 10.1371/journal.pone.0150043.

S. K. Golombek *et al.*, "Tumor targeting via EPR: Strategies to enhance patient responses," *Adv Drug Deliv Rev*, vol. 130, pp. 17–38, May 2018, doi: 10.1016/j.addr.2018.07.007.

S. Kanth, Y. Malgar Puttaiahgowda, and A. Kulal, "Synthesis, characterization, and antimicrobial activities of a starch-based polymer," *Carbohydr Res*, vol. 532, p. 108900, Oct. 2023, doi: 10.1016/j.carres.2023.108900.

S. Kumari, B. S. Yadav, and R. B. Yadav, "Synthesis and modification approaches for starch nanoparticles for their emerging food industrial applications: A review," *Food Research International*, vol. 128, p. 108765, Feb. 2020, doi: 10.1016/j.foodres.2019.108765.

S. L. M. el Halal *et al.*, "Structure, morphology and functionality of acetylated and oxidised barley starches," *Food Chem*, vol. 168, pp. 247–256, Feb. 2015, doi: 10.1016/j.foodchem.2014.07.046.

S. Lefnaoui and N. Moulai-Mostefa, "Synthesis and evaluation of the structural and physicochemical properties of carboxymethyl pregelatinized starch as a pharmaceutical excipient," *Saudi Pharmaceutical Journal*, vol. 23, no. 6, pp. 698–711, Nov. 2015, doi: 10.1016/j.jsps.2015.01.021.

S. Liang, Y. Hong, Z. Gu, L. Cheng, C. Li, and Z. Li, "Effect of debranching on the structure and digestibility of octenyl succinic anhydride starch nanoparticles," *LWT*, vol. 141, p. 111076, Apr. 2021, doi: 10.1016/j.lwt.2021.111076.

S. Likhitkar and A. K. Bajpai, "Magnetically controlled release of cisplatin from superparamagnetic starch nanoparticles," *Carbohydr Polym*, vol. 87, no. 1, pp. 300–308, Jan. 2012, doi: 10.1016/j.carbpol.2011.07.053.

S. M. Ali Razavi and A. M. Amini, "Starch nanomaterials: a state-of-the-art review and future trends," in *Novel Approaches of Nanotechnology in Food*, Elsevier, 2016, pp. 237–269. doi: 10.1016/B978-0-12-804308-0.00008-X.

S. M. Dizaj, F. Lotfipour, M. Barzegar-Jalali, M. H. Zarrintan, and K. Adibkia, "Antimicrobial activity of the metals and metal oxide nanoparticles," *Materials Science and Engineering: C*, vol. 44, pp. 278–284, Nov. 2014, doi: 10.1016/j.msec.2014.08.031.

S. Macfarlane and G. T. Macfarlane, "Regulation of short-chain fatty acid production," *Proceedings of the Nutrition Society*, vol. 62, no. 1, pp. 67–72, Feb. 2003, doi: 10.1079/PNS2002207.

S. Mohanty, S. Mishra, P. Jena, B. Jacob, B. Sarkar, and A. Sonawane, "An investigation on the antibacterial, cytotoxic, and antibiofilm efficacy of starch-stabilized silver nanoparticles," *Nanomedicine*, vol. 8, no. 6, pp. 916–924, Aug. 2012, doi: 10.1016/j.nano.2011.11.007.

S. Patel, J. Seet, L. Li, and J. Duhamel, "Detection of Nitroaromatics by Pyrene-Labeled Starch Nanoparticles," *Langmuir*, vol. 35, no. 40, pp. 13145–13156, Oct. 2019, doi: 10.1021/acs.langmuir.9b02371.

S. Pérez and E. Bertoft, "The molecular structures of starch components and their contribution to the architecture of starch granules: A comprehensive review," *Starch - Stärke*, vol. 62, no. 8, pp. 389–420, Jul. 2010, doi: 10.1002/star.201000013.

S. Punia, "Barley starch modifications: Physical, chemical and enzymatic - A review," *Int J Biol Macromol*, vol. 144, pp. 578–585, Feb. 2020, doi: 10.1016/j.ijbiomac.2019.12.088.

S. Ramos-Inza, D. Plano, and C. Sanmartín, "Metal-based compounds containing selenium: An appealing approach towards novel therapeutic drugs with anticancer and antimicrobial effects," *Eur J Med Chem*, vol. 244, p. 114834, Dec. 2022, doi: 10.1016/j.ejmech.2022.114834.

S. Shabana, R. Prasansha, I. Kalinina, I. Potoroko, U. Bagale, and S. H. Shirish, "Ultrasound assisted acid hydrolyzed structure modification and loading of antioxidants on potato starch nanoparticles," *Ultrason Sonochem*, vol. 51, pp. 444–450, Mar. 2019, doi: 10.1016/j.ultsonch.2018.07.023.

S. V. Kumar, A. P. Bafana, P. Pawar, A. Rahman, S. A. Dahoumane, and C. S. Jeffryes, "High conversion synthesis of <10 nm starch-stabilized silver nanoparticles using microwave technology," *Sci Rep*, vol. 8, no. 1, p. 5106, Mar. 2018, doi: 10.1038/s41598-018-23480-6.

S. Varahan, V. S. Iyer, W. T. Moore, and L. E. Hancock, "Eep Confers Lysozyme Resistance to Enterococcus faecalis via the Activation of the Extracytoplasmic Function Sigma Factor SigV," *J Bacteriol*, vol. 195, no. 14, pp. 3125–3134, Jul. 2013, doi: 10.1128/JB.00291-13.

S. Vijay, and S. Lalit, "Various techniques for the modification of starch and the applications of its derivatives" 2012.

S.-W. Choi, H.-Y. Kwon, W.-S. Kim, and J.-H. Kim, "Thermodynamic parameters on poly(D,L-lactide-co-glycolide) particle size in emulsification-diffusion process," 2002. [Online]. Available: www.elsevier.com/locate/colsurfa

S. Xiao *et al.*, "Preparation of folate-conjugated starch nanoparticles and its application to tumor-targeted drug delivery vector," *Chinese Science Bulletin*, vol. 51, no. 14, pp. 1693–1697, Jul. 2006, doi: 10.1007/s11434-006-2039-7.

S. Y. Cheuk *et al.*, "Nano-encapsulation of coenzyme Q10 using octenyl succinic anhydride modified starch," *Food Chem*, vol. 174, pp. 585–590, May 2015, doi: 10.1016/j.foodchem.2014.11.031.

S. You and M. S. Izydorczyk, "Comparison of the physicochemical properties of barley starches after partial α-amylolysis and acid/alcohol hydrolysis," *Carbohydr Polym*, vol. 69, no. 3, pp. 489–502, Jun. 2007, doi: 10.1016/j.carbpol.2007.01.002.

T. A. Tari and R. S. Singhal, "Starch-based spherical aggregates: stability of a model flavouring compound, vanillin entrapped therein," *Carbohydr Polym*, vol. 50, no. 4, pp. 417–421, Dec. 2002, doi: 10.1016/S0144-8617(02)00055-3.

T. Bruna, F. Maldonado-Bravo, P. Jara, and N. Caro, "Silver Nanoparticles and Their Antibacterial Applications," *Int J Mol Sci*, vol. 22, no. 13, p. 7202, Jul. 2021, doi: 10.3390/ijms22137202.

T. M. T. Vo *et al.*, "Rice starch coated iron oxide nanoparticles: A theranostic probe for photoacoustic imaging-guided photothermal cancer therapy," *Int J Biol Macromol*, vol. 183, pp. 55–67, Jul. 2021, doi: 10.1016/j.ijbiomac.2021.04.053.

T. Mehfooz, T. M. Ali, and A. Hasnain, "Effect of cross-linking on characteristics of succinylated and oxidized barley starch," *Journal of Food Measurement and Characterization*, vol. 13, no. 2, pp. 1058–1069, Jun. 2019, doi: 10.1007/s11694-018-00021-3.

T. Nakashima and N. Kimizuka, "Interfacial synthesis of hollow TiO2 microspheres in ionic liquids," *J Am Chem Soc*, vol. 125, no. 21, pp. 6386–6387, May 2003, doi: 10.1021/ja034954b.

T. S. Leite, A. L. T. de Jesus, M. Schmiele, A. A. L. Tribst, and M. Cristianini, "High pressure processing (HPP) of pea starch: Effect on the gelatinization properties," *LWT - Food Science and Technology*, vol. 76, pp. 361–369, Mar. 2017, doi: 10.1016/j.lwt.2016.07.036.

T. Silvetti, S. Morandi, M. Hintersteiner, and M. Brasca, "Use of Hen Egg White Lysozyme in the Food Industry," in *Egg Innovations and Strategies for Improvements*, Elsevier, 2017, pp. 233–242. doi: 10.1016/B978-0-12-800879-9.00022-6.

V. Pitpisutkul and J. Prachayawarakorn, "Porous antimicrobial crosslinked film of hydroxypropyl methylcellulose/carboxymethyl starch incorporating gallic acid for wound dressing application," *Int J Biol Macromol*, vol. 256, p. 128231, Jan. 2024, doi: 10.1016/j.ijbiomac.2023.128231.

V. Srivastava, S. Singh, and D. Das, "Rice husk fiber-reinforced starch antimicrobial biocomposite film for active food packaging," *J Clean Prod*, vol. 421, p. 138525, Oct. 2023, doi: 10.1016/j.jclepro.2023.138525.

V. Valdiglesias *et al.*, "Are iron oxide nanoparticles safe? Current knowledge and future perspectives," *Journal of Trace Elements in Medicine and Biology*, vol. 38, pp. 53–63, Dec. 2016, doi: 10.1016/j.jtemb.2016.03.017.

W. Berski *et al.*, "Pasting and rheological properties of oat starch and its derivatives," *Carbohydr Polym*, vol. 83, no. 2, pp. 665–671, Jan. 2011, doi: 10.1016/j.carbpol.2010.08.036.

W. Sapyen, S. Toonchue, N. Praphairaksit, and A. Imyim, "Selective colorimetric detection of Cr(VI) using starch-stabilized silver nanoparticles and application for chromium speciation," *Spectrochim Acta A Mol Biomol Spectrosc*, vol. 274, p. 121094, Jun. 2022, doi: 10.1016/j.saa.2022.121094.

W. Thielemans, M. N. Belgacem, and A. Dufresne, "Starch Nanocrystals with Large Chain Surface Modifications," *Langmuir*, vol. 22, no. 10, pp. 4804–4810, May 2006, doi: 10.1021/la053394m.

W. Wang *et al.*, "Properties of OSA-modified starch and emulsion prepared with different materials: Glutinous rice starch, japonica rice starch, and indica rice starch," *Food Research International*, vol. 161, p. 111845, Nov. 2022, doi: 10.1016/j.foodres.2022.111845.

W. Xia, B. Zheng, T. Li, F. Lian, Y. Lin, and R. Liu, "Fabrication, characterization and evaluation of myricetin adsorption onto starch nanoparticles," *Carbohydr Polym*, vol. 250, Dec. 2020, doi: 10.1016/j.carbpol.2020.116848.

W. Zheng, L. Ren, W. Hao, L. Wang, C. Liu, and L. Zheng, "Encapsulation of indole-3-carbinol in Pickering emulsions stabilized by OSA-modified high amylose corn starch: Preparation, characterization and storage stability properties," *Food Chem*, vol. 386, p. 132846, Aug. 2022, doi: 10.1016/j.foodchem.2022.132846.

X. Hou, H. Wang, Y. Shi, and Z. Yue, "Recent advances of antibacterial starch-based materials," *Carbohydr Polym*, vol. 302, p. 120392, Feb. 2023, doi: 10.1016/j.carbpol.2022.120392.

X. Lin, S. Sun, B. Wang, B. Zheng, and Z. Guo, "Structural and physicochemical properties of lotus seed starch nanoparticles," *Int J Biol Macromol*, vol. 157, pp. 240–246, Aug. 2020, doi: 10.1016/j.ijbiomac.2020.04.155.

X. Ma, R. Jian, P. R. Chang, and J. Yu, "Fabrication and characterization of citric acid-modified starch nanoparticles/plasticized-starch composites," *Biomacromolecules*, vol. 9, no. 11, pp. 3314–3320, Nov. 2008, doi: 10.1021/bm800987c.

X. Sun, J. Liu, and Y. Li, "Use of Carbonaceous Polysaccharide Microspheres as Templates for Fabricating Metal Oxide Hollow Spheres," *Chemistry – A European Journal*, vol. 12, no. 7, pp. 2039–2047, Feb. 2006, doi: https://doi.org/10.1002/chem.200500660.

X. Wang, H. Chen, Z. Luo, and X. Fu, "Preparation of starch nanoparticles in water in oil microemulsion system and their drug delivery properties," *Carbohydr Polym*, vol. 138, pp. 192–200, Mar. 2016, doi: 10.1016/j.carbpol.2015.11.006.

X. Zhang, H. Ma, W. Qin, B. Guo, and P. Li, "Antimicrobial and improved performance of biodegradable thermoplastic starch by using natural rosin to replace part of glycerol," *Ind Crops Prod*, vol. 178, p. 114613, Apr. 2022, doi: 10.1016/j.indcrop.2022.114613.

Y. Chang, X. Yan, Q. Wang, L. Ren, J. Tong, and J. Zhou, "High efficiency and low cost preparation of size controlled starch nanoparticles through ultrasonic treatment and precipitation," *Food Chem*, vol. 227, pp. 369–375, Jul. 2017, doi: 10.1016/j.foodchem.2017.01.111.

Y. Chen, X. Cao, P. R. Chang, and M. A. Huneault, "Comparative study on the films of poly(vinyl alcohol)/pea starch nanocrystals and poly(vinyl alcohol)/native pea starch," *Carbohydr Polym*, vol. 73, no. 1, pp. 8–17, Jul. 2008, doi: 10.1016/j.carbpol.2007.10.015.

Y. Ding, Q. Lin, and J. Kan, "Development and characteristics nanoscale retrograded starch as an encapsulating agent for colon-specific drug delivery," *Colloids Surf B Biointerfaces*, vol. 171, pp. 656–667, Nov. 2018, doi: 10.1016/j.colsurfb.2018.08.007.

Y. Fang, J. Fu, C. Tao, P. Liu, and B. Cui, "Mechanical properties and antibacterial activities of novel starch-based composite films incorporated with salicylic acid," *Int J Biol Macromol*, vol. 155, pp. 1350–1358, Jul. 2020, doi: 10.1016/j.ijbiomac.2019.11.110.

Y. Fu, J. Yang, L. Jiang, L. Ren, and J. Zhou, "Encapsulation of Lutein into Starch Nanoparticles to Improve Its Dispersity in Water and Enhance Stability of Chemical Oxidation," *Starch/Staerke*, vol. 71, no. 5–6, May 2019, doi: 10.1002/star.201800248.

Y. Guo, Y. Cui, M. Cheng, X. Wang, S. Guo, and R. Zhang, "Effects of low-temperature plasma modification on properties of CEO-SBA-15/potato starch film," *Ind Crops Prod*, vol. 187, p. 115440, Nov. 2022, doi: 10.1016/j.indcrop.2022.115440.

Y. Hu, Y. Qin, C. Qiu, X. Xu, Z. Jin, and J. Wang, "Ultrasound-assisted self-assembly of β-cyclodextrin/debranched starch nanoparticles as promising carriers of tangeretin," *Food Hydrocoll*, vol. 108, Nov. 2020, doi: 10.1016/j.foodhyd.2020.106021.

Y. L. P. López, R. Torres-Rosas, and L. Argueta-Figueroa, "Mecanismos de acción de los probióticos en la inhibición de microorganismos cariogénicos," *Revista Médica Clínica Las Condes*, vol. 34, no. 3, pp. 216–223, May 2023, doi: 10.1016/j.rmclc.2023.03.010.

Y. Li *et al.*, "Antimicrobial packaging materials of PLA/starch composites functionalized by pomegranate peel," *J Taiwan Inst Chem Eng*, vol. 156, p. 105371, Mar. 2024, doi: 10.1016/j.jtice.2024.105371.

Y. Liang, N. Hilal, P. Langston, and V. Starov, "Interaction forces between colloidal particles in liquid: Theory and experiment," *Adv Colloid Interface Sci*, vol. 134–135, pp. 151–166, Oct. 2007, doi: 10.1016/j.cis.2007.04.003.

Y. Luo, Y. Li, L. Li, and X. Xie, "Physical modification of maize starch by gelatinizations and cold storage," *Int J Biol Macromol*, vol. 217, pp. 291–302, Sep. 2022, doi: 10.1016/j.ijbiomac.2022.07.010.

Y. Rojas-Aguirre, K. Aguado-Castrejón, and I. González-Méndez, "La nanomedicina y los sistemas de liberación de fármacos: ¿la (r)evolución de la terapia contra el cáncer?," *Educación Química*, vol. 27, no. 4, pp. 286–291, Oct. 2016, doi: 10.1016/j.eq.2016.07.002.

Y. Tan, K. Xu, L. Li, C. Liu, C. Song, and P. Wang, "Fabrication of Size-Controlled Starch-Based Nanospheres by Nanoprecipitation," *ACS Appl Mater Interfaces*, vol. 1, no. 4, pp. 956–959, Apr. 2009, doi: 10.1021/am900054f.

Y. Tian, Q. Lei, F. Yang, J. Xie, and C. Chen, "Development of cinnamon essential oil-loaded PBAT/thermoplastic starch active packaging films with different release behavior and antimicrobial activity," *Int J Biol Macromol*, vol. 263, p. 130048, Apr. 2024, doi: 10.1016/j.ijbiomac.2024.130048.

Y. Xu *et al.*, "pH-Responsive nanoparticles based on cholesterol/imidazole modified oxidized-starch for targeted anticancer drug delivery," *Carbohydr Polym*, vol. 233, Apr. 2020, doi: 10.1016/j.carbpol.2020.115858.

Y. Yin, Y. Lu, B. Gates, and Y. Xia, "Template-assisted self-assembly: A practical route to complex aggregates of monodispersed colloids with well-defined sizes, shapes, and structures," *J Am Chem Soc*, vol. 123, no. 36, pp. 8718–8729, Sep. 2001, doi: 10.1021/ja011048v.

Y. yuan Fang *et al.*, "Preparation of crosslinked starch microspheres and their drug loading and releasing properties," *Carbohydr Polym*, vol. 74, no. 3, pp. 379–384, Nov. 2008, doi: 10.1016/j.carbpol.2008.03.005.

Y. Zhao, N. Khalid, G. Shu, M. A. Neves, I. Kobayashi, and M. Nakajima, "Complex coacervates from gelatin and octenyl succinic anhydride modified kudzu starch: Insights of formulation and characterization," *Food Hydrocoll*, vol. 86, pp. 70–77, Jan. 2019, doi: 10.1016/j.foodhyd.2018.01.040.

Z. Qin *et al.*, "Versatile roles of silver in Ag-based nanoalloys for antibacterial applications," *Coord Chem Rev*, vol. 449, p. 214218, Dec. 2021, doi: 10.1016/j.ccr.2021.214218.

Z. Wang, P. Mhaske, A. Farahnaky, S. Kasapis, and M. Majzoobi, "Cassava starch: Chemical modification and its impact on functional properties and digestibility, a review," *Food Hydrocoll*, vol. 129, p. 107542, Aug. 2022, doi: 10.1016/j.foodhyd.2022.107542.

Z. Zhou, X. Cao, and J. Y. H. Zhou, "Effect of resistant starch structure on short-chain fatty acids production by human gut microbiota fermentation in vitro," *Starch - Stärke*, vol. 65, no. 5–6, pp. 509–516, May 2013, doi: 10.1002/star.201200166.

Zia-ud-Din, H. Xiong, and P. Fei, “Physical and chemical modification of starches: A review,” *Crit Rev Food Sci Nutr*, vol. 57, no. 12, pp. 2691–2705, Aug. 2017, doi: 10.1080/10408398.2015.1087379.

6. APPENDIX

A.1. List of figures

Supplementary material

A.2. List of tables

Supplementary material

A.3. List of abbreviations

- 5-ASA 5-Aminosalicylic acid
- 5-FU 5-fluorouracil
- Ag-SNPs Hybrid starch-silver nanoparticles
- AgNPs Silver nanoparticles
- AML12 Normal liver cells
- ANOVA Analysis of variance
- ATCC American Type Culture Collection
- BaP Benzo[a]pyrene
- BS Butane sultone
- BSA Bovine serum albumin
- CAC Critical aggregation concentration
- CECT Colección Española de Cultivos Tipo
- CEO Cinnamon essential oil
- Cho-Imi-OS Oxidized starch modified with cholesterol and imidazole
- CLA Conjugated linoleic acid
- CTAB Cetyl Trimethyl Ammonium Bromide
- DDSA Dodecenyl succinic anhydride
- DLS Dynamic light scattering
- DMSO Dimethyl sulfoxide
- DOX-HCl Doxorubicin hydrochloride
- DFS Diclofenac sodium
- DS Degree of substitution
- DSC Differential scanning calorimetry
- EARS-Net European Antimicrobial Resistance Surveillance Network
- EDX Energy dispersive X-Ray
- EE Encapsulation efficiency
- EO Essential oil
- EPR Permeability and retention effect

- EU European Union
- FTIR Fourier transform infrared spectroscopy
- HepG2 Hepatocellular liver cells
- HLB Hydrophilic-lipophilic balance
- HNPs Hollow nanoparticles
- HP/CMS Hydroxypropylmethylcellulose / carboxymethylstarch
- HPLC High-performance liquid chromatography
- HR-TEM High-resolution transmission electron microscopy
- ICP-MS Inductively coupled plasma mass spectroscopy
- IONPs Iron oxide nanoparticles
- LAB Lactic acid bacteria
- LAE Ethyl lauroyl arginate
- LC Loading capacity
- LE Loading efficiency
- LSD Least significant difference
- OSA Octenyl Succinic Anhydride
- Oxy-SNPs Oxidized starch nanoparticles
- MBAA N,N'-methylenediacrylamide
- ME Microemulsion method
- MHA Mueller-Hinton agar
- MHB Mueller-Hinton broth
- MRS agar Man-Rogosa-Sharpe agar
- MTT assay Colorimetric assay for assessing cell metabolic activity
- MW Molecular weigh
- NAS Native amaranth starch
- NMR Nuclear magnetic resonance
- NPs Nanoparticles
- NQS Native quinoa starch
- NRS Native rice starch
- OMMT Organically modified nanomontmorillonites

- PBAT Poly(butylene adipate-co-terephthalate)
- PBS Phosphate buffer solution
- PdI Polydispersity index
- PGP Pomegranate peel
- PLA Polylactic acid
- PVA Polyvinyl alcohol
- RP-HPLC Reverse-phase high-performance liquid chromatography
- Rpm Revolutions per minute
- RS Retrograded starch
- SCFA Short Chain Fatty Acids
- SD Standard deviation
- SDS Sodium dodecyl sulphate
- SEM Scanning Electron Microscopy
- SIF Simulated intestinal fluids
- SIG Simulated gastric fluids
- SNPs Starch nanoparticles / nanopartículas de almidón
- Span 60 Sorbitan Monostearate
- STPP Sodium tripolyphosphate
- TEM Transmission Electron Microscopy
- TGA Thermogravimetric analysis
- TP Tea polyphenols
- TSA Tryptone soy agar
- TSB Tryptone soy broth
- TVC Total viable count
- Tween 20 Polysorbate 20
- Tween 80 Polysorbate 80
- UV-vis Ultraviolet-visible
- VSM Vibrating sample magnetometer
- W/O Water in Oil
- w/v weigh/volume relation

- WHO World Health Organisation
- XG Xanthan gum
- XRPD X-ray powder diffraction